DOT-HS-805-874
DOT-TSC-NHTSA-81-12

Closed Loop Control of Automotive Engines

J. David Powell
Itshak Glaser
Kent Randall
Rick Hosey

Stanford University
Guidance and Control Laboratory
Stanford CA 94305

December 1981
Final Report

U.S. Department of Transportation
National Highway Traffic Safety Administration

Office of Research and Development
Washington DC 20590

Technical Report Documentation Page

1. Report No.	2. Government Accession No.	3. Recipient's Catalog No.
DOT-HS-805-874		PB82 164088

4. Title and Subtitle
CLOSED LOOP CONTROL OF AUTOMOTIVE ENGINES

5. Report Date
December 1981

6. Performing Organization Code
DTS-323 043046

7. Author(s)
Itshak Glaser, K. Randall, R. Hosey & J.D. Powell

8. Performing Organization Report No.
DOT-TSC-NHTSA-81-12

9. Performing Organization Name and Address
Stanford University*
Guidance and Control Laboratory
Stanford CA 94305

10. Work Unit No. (TRAIS)
HS273/R2410

11. Contract or Grant No.
DOT-TSC-1466

12. Sponsoring Agency Name and Address
U.S. Department of Transportation
National Highway Traffic Safety Administration
Office of Research & Development
Washington DC 20590

13. Type of Report and Period Covered
Final Report
Feb 1978 through June 1980

14. Sponsoring Agency Code
NRD-13

15. Supplementary Notes
*Under contract to: U.S. Department of Transportation
Research and Special Programs Administration
Transportation Systems Center
Cambridge, MA 02142

16. Abstract Internal combustion engine economy and emissions are known to be sensitive to changes in engine control variables. Two of the most important variables are fuel/air ratio (f/a) and spark advance. These variables are affected by environmental changes, manufacturing tolerances, and time degradation. The combined effect of all these changes can cause as much as a 15% loss in economy and a 30% increase in emissions.

This research concerns the application of optimization theory to develop control laws for use in closed loop control strategies to minimize the effect of the variables discussed above. The report describes the automated dynamometer facility developed for the acquisition of engine mapping data. The facility was completed during the contract period and used to acquire a map of a 2.3L, 4 cylinder engine. This data was used to develop analytical functions describing the fuel consumption and emissions at each of 10 torque/RPM points. The functions were used by an optimization procedure to arrive at control strategies and driving cycle predictions of fuel consumption and emissions.

The optimum schedules were then used to determine a closed-loop control strategy. This control was evaluated for driving cycle conditions and found to yield a 2% improvement in fuel economy over the open-loop control when the relative humidity was 75% at 90°F. It was also found that the closed-loop spark advance control based on cylinder pressure was more difficult to implement under conditions of heavy spark retard for emissions reduction.

17. Key Words
Closed-loop control; spark advance control
engine modelling; internal combustion engine control; automated dynamometer, pressure sensor

18. Distribution Statement
DOCUMENT IS AVAILABLE TO THE PUBLIC THROUGH THE NATIONAL TECHNICAL INFORMATION SERVICE, SPRINGFIELD, VIRGINIA 22161

19. Security Classif. (of this report)	20. Security Classif. (of this page)	21. No. of Pages	22. Price
Unclassified	Unclassified	322	

Form DOT F 1700.7 (8-72) Reproduction of completed page authorized

METRIC CONVERSION FACTORS

Approximate Conversions to Metric Measures

Symbol	When You Know	Multiply by	To Find	Symbol
	LENGTH			
in	inches	*2.5	centimeters	cm
ft	feet	30	centimeters	cm
yd	yards	0.9	meters	m
mi	miles	1.6	kilometers	km
	AREA			
in^2	square inches	6.5	square centimeters	cm^2
ft^2	square feet	0.09	square meters	m^2
yd^2	square yards	0.8	square meters	m^2
mi^2	square miles	2.6	square kilometers	km^2
	acres	0.4	hectares	ha
	MASS (weight)			
oz	ounces	28	grams	g
lb	pounds	0.45	kilograms	kg
	short tons (2000 lb)	0.9	tonnes	t
	VOLUME			
tsp	teaspoons	5	milliliters	ml
Tbsp	tablespoons	15	milliliters	ml
fl oz	fluid ounces	30	milliliters	ml
c	cups	0.24	liters	l
pt	pints	0.47	liters	l
qt	quarts	0.95	liters	l
gal	gallons	3.8	liters	l
ft^3	cubic feet	0.03	cubic meters	m^3
yd^3	cubic yards	0.76	cubic meters	m^3
	TEMPERATURE (exact)			
°F	Fahrenheit temperature	5/9 (after subtracting 32)	Celsius temperature	°C

*1 in = 2.54 (exactly). For other exact conversions and more detailed tables, see NBS Misc. Publ. 286, Units of Weights and Measures, Price $2.25, SD Catalog No. C13.10:286.

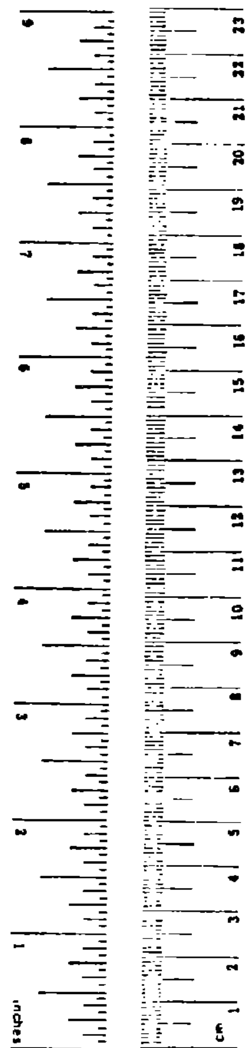

Approximate Conversions from Metric Measures

Symbol	When You Know	Multiply by	To Find	Symbol
	LENGTH			
mm	millimeters	0.04	inches	in
cm	centimeters	0.4	inches	in
m	meters	3.3	feet	ft
m	meters	1.1	yards	yd
km	kilometers	0.6	miles	mi
	AREA			
cm^2	square centimeters	0.16	square inches	in^2
m^2	square meters	1.2	square yards	yd^2
km^2	square kilometers	0.4	square miles	mi^2
ha	hectares (10,000 m^2)	2.5	acres	
	MASS (weight)			
g	grams	0.035	ounces	oz
kg	kilograms	2.2	pounds	lb
t	tonnes (1000 kg)	1.1	short tons	
	VOLUME			
ml	milliliters	0.03	fluid ounces	fl oz
l	liters	2.1	pints	pt
l	liters	1.06	quarts	qt
l	liters	0.26	gallons	gal
m^3	cubic meters	35	cubic feet	ft^3
m^3	cubic meters	1.3	cubic yards	yd^3
	TEMPERATURE (exact)			
°C	Celsius temperature	9/5 (then add 32)	Fahrenheit temperature	°F

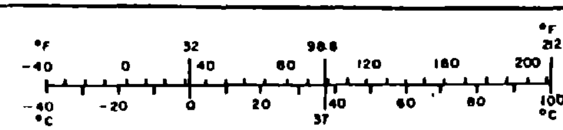

PREFACE

The economy and emissions of automotive internal combustion engines depend on many operating variables. These variables are not always maintained at the best possible values, partly due to the inability to design and manufacture to these values, partly because the initial design did not account for all of these values, and partly due to degradation with time. The need for more accurate fuel/air ratio has been particularly acute for acceptable operation of three-way catalysts. However, there are other incentives for more accurate engine control. It has been reported that fuel economy degrades as much as 14% in 12,000 miles and that changes in the fuel/air ratio and spark timing are the major sources of the efficiency loss. Even larger deterioration has been reported for emissions. Environmental effects and fuel characteristics have similar impacts.

In present day engines, fuel control and spark timing are done by open-loop devices that are based on engine speed, throttle setting, and perhaps temperature. Closed loop control is based on engine measurements that are more directly related to the quantity being controlled and hence, are more accurate and less sensitive to disturbances.

The objectives of this research are:

1. To develop an automated dynamometer facility for mapping and optimization studies of typical automotive engines.
2. To design a particular closed-loop control system which will maintain optimal operation of the engine over a wide torque and speed range regardless of mechanical degradation or external disturbances. The technique used is to maintain cylinder peak pressure near its optimum value by controlling spark advance in a closed-loop system.
3. To generate trade-off curves between optimum fuel economy, evaluated for a given emissions level, and various levels of emission constraints.
4. To investigate appropriate engine models.

The dynamometer facility was completed and used to acquire engine data at 730 test points. These data were used to generate analytical functions describing the fuel consumption and emissions at each of 10 torque/speed points using least square fitting procedures. It was found in the process of arriving at these functions that individual fits to data at each torque/speed point were superior to a single global fit valid at all torque/speed points. The functions were used by an optimization procedure to arrive at control strategies and driving cycle predictions of fuel consumption and emissions over a wide range of emission levels.

The optimum schedules were then used to determine a closed-loop control strategy. This control was evaluated for driving cycle conditions and found to yield a 2% improvement in fuel economy over the open-loop control when the relative humidity was 75% at 90°F. It was also found that the closed-loop spark advance control based on cylinder pressure was more difficult to implement under conditions of heavy spark retard for emissions reduction.

Results of the research have been presented at technical conferences attended by automotive industry representatives. Because of the proprietary nature of development efforts within the industry, it is not possible to determine the extent to which these results are being utilized. However, the Holley Carburetor Division of Colt Industries Operating Corp. has obtained license rights to the spark advance controller from Stanford University, indicating a serious interest in this aspect of the research. Further, the introduction by the industry of closed-loop air/fuel ratio systems and the knock adaption by Buick is an additional indication of the importance to the automotive industry of closed-loop control concepts.

The research has demonstrated the benefits of closed-loop spark control under nominal and off-nominal humidity conditions for a 4 cylinder automotive engine. Other effects such as manufacturing tolerances, time degradation, altitude, and air/fuel ratio will likely have similar effects than humidity. It is estimated that fleetwide average benefits will probably be on the order of 2% or 3% for spark control alone and on the order of 5% for a complete closed-loop control system for spark, fuel, and exhaust gas recirculation.

CONTENTS

CONTENTS (Cont.)

CONTENTS (Cont.)

LIST OF ILLUSTRATIONS

LIST OF ILLUSTRATIONS (Cont.)

LIST OF TABLES

LIST OF TABLES (Cont.)

LIST OF SYMBOLS

ENGLISH

a_i Ch. III	Regression coefficient
a_i Ch. IV	Emission constraint coefficient
a App. A	Number of Moles of dry air per mole of gasoline
AIR	Air mass flow through the carburetor (lb/hr)
AIRP	Air pump mass flow (lb/hr)
AF	Air/fuel ratio based on direct measurement
AFE	Air/fuel ratio based on emissions measurement
b_i Ch. III	Regression coefficient
b_i Ch. IV	Emission constraint coefficient
C	Sensor capacitance (PF)
C_L	Coaxial cable capacitance (PF)
C_U^i	Urban coefficient of the i^{th} load speed point (sec)
C_H^i	Highway coefficient of the i^{th} load/speed point (sec)
C_e	Volumetric fraction of emissions in the exhaust gas
E	Emission mass flow (gm/sec)
E_0	Desired emission constraint
ED	Moles of dry exhaust per moles of fuel
EW	Moles of wet exhaust at the engine outlet per mole of gas.
F	Fuel consumption (gallons/mile)
$\dot{F}$	Fuel mass flow lb/hr
F_H	Amount of fuel consumed in the highway portion of the EPA cycle (lb)
F_U	Amount of fuel consumed in the urban portion of the EPA cycle
F_1	Amount of fuel consumed in 55 urban miles
F_2	Amount of fuel consumed in 45 highway miles
f	Frequency (Hz)

ENGLISH (Cont.)

$\dot{G}_a$	Inlet air mass flow to the carburetor (lb/sec)
$\dot{G}_{ex}$	Total exhaust mass flow (lb/sec)
$\dot{G}_f$	Fuel mass flow (lb/sec)
$\dot{G}_p$	Air pump mass flow to the exhaust (lb/sec)
H_d	Total highway driving schedule (miles)
$(HC)_D$	Hydrocarbon volumetric concentration in the exhaust gases measured on dry basis
$(HC)_W$	Hydrocarbon volumetric concentration in the exhaust gases measured on wet basis
(H_2O)	Water vapor volumetric concentration in the exhaust gases
i	Index
J	Cost function
J_0	Cost function at the optimum
k	Number of terms in the regression equation
K_H	Humidity correction factor
l	Number of carbon atoms assumed in one hydrocarbon gas molecule generated by the engine
M	Molecular weight
M_e	Emission molecular weight
M_{ex}	Exhaust gases molecular weight
m Ch. III	Index
m App. A	Number of hydrogen atoms assumed in one hydrocarbon gas molecule generated by the engine
N	Number of constant load/speed points
n Ch. III	Index
n Ch. IV	Number of Measurements
n App. A	Ratio of the number of atoms of hydrogen to the number of carbon atoms in a fuel molecule

ENGLISH (Cont.)

p(x,y)	Probability density function
P_{air}	Air pump pressure (in Hg)
P_{ex}	Exhaust gases pressure (in Hg)
R	Electric resistance (ohms)
RPM	Engine speed (rev/min)
S	Variable following the χ^2 distribution
Torque-T	Torque (ft lb)
U	Independent random variable with χ^2 distribution
U_d	Urban driving schedule (miles)
V	Independent random variable with χ^2 distribution
V_{CO}	Voltage produced by the sensor (volts)
V_0	Output voltage of sensor circuit (volts)
V_1	Peak detector output voltage (Volts)
$\dot{V}_{ex}$	Exhaust gases volumetric flow (ft^3/sec)
x	Independent variable
X	Independent variables matrix
x App. A	Molar ratio of recirculated exhaust gas to total exhaust flow
y_i	Measurement at data point i
$\bar{y}$	Average of measurements
$\hat{y}_i$	Predicted value at data point i
Y	Measurements vector
$\hat{Y}$	Predicted values vector
Y_i	Marginal contribution to R-square from the i^{th} term
z_i	Independent variable

GREEK

α Ch. III	Level of confidence
α Ch. IV	Peak pressure angle measured from TDC
α App. A	Moles of air injected by the pump per moles of gasoline
η	Catalyst efficiency
θ_{pp}	Peak pressure angle
θ_{pp}^{opt}	Optimal peak pressure angle
λ	Lagrange multiplier
μ_i	A sequence of mutually independent variables
ν	Degrees of freedom
ρ_a	Air density (lb/ft^3)
ρ_F	Fuel density (lb/ft^3)
ρ_e	Emission density (gm/ft^3)
ρ_{ex}	Exhaust density (gm/ft^3)
Σ	Summation
τ	Engine revolution time (msec)
τ_1	Time between TDC and peak pressure (msec)
ω Ch. III	Weighing function
ω Ch. V	Angular velocity (rad/sec)
ω_0	Sensor circuit break point (rad/sec)
ω_1	Filter circuit break point (rad/sec)

SUBSCRIPTS

cold/hot	cold/hot driving cycle
choc	cold hot cycle with oxidizing catalyst
chtc	cold/hot cycle with three-way catalyst
hot	hot driving cycle
H	High range of the independent variables
i	Measurement at the i^{th} load/speed point
L	Low range of the independent variables
meas	Value measured at actual torque and speed
Nom	Value assumed to be at nominal torque and speed

SUPERSCRIPTS

T	Transpose matrix
$\cdot$	Time derivative
$-$ Ch. III	Average value
$-$ Appendices	Normalized value
$\hat{}$ Ch. III	Predicted value
$\hat{}$ Ch. IV	Weighted average

LIST OF ABBREVIATIONS

ATDC	After top dead center
BTDC	Before top dead center
CO	Carbon monoxide
CO_2	Carbon dioxide
deg	Degrees
D/A	Digital-to-analog
E	Emissions
EGR	Exhaust gas recirculation
EGT	Exhaust gas temperature (^oF)
EGRDP	Exhaust gas recirculation pressure drop (in water)
EPA	Environmental Protection Agency
F	Degrees farheneit
FID	Flame ionization detector
HC	Hydrocarbon
HUM	Humidity (grains water/kg dry air)
IAT	Inlet air temperature (^oF)
IMP	Intake manifold pressure (absolute psi)
LAG	Lagrange multiplier
MBT	Minimum spark advance for best torque
NO-NOx	Nitrogen oxides
N_2	Molecular nitrogen
NC	Non-catalyst
NDIR	Non-dispersive infrared
NHTSA	National Highway Traffic Safety Administration
O_2	Molecular Oxygen
OC	Oxidizing Catalyst

ABBREVIATIONS (Cont.)

OT	Oil temperature (OF)
P_i	Legendre polynomial of order i
PPM	Part per million
PRESS	Ambient pressure (in Hg)
psi	Pounds per square inch
R^2-RSQ	R-square
RESPAV	Residual percentage average
RMS	Root mean square
RMSP	RMS percentage of the average measurement
rpm	Revolutions per minute
SA-SPKADV	Spark advance (deg from TDC)
SCFM	Specific cubic feet per minute
TEMP	Ambient temperature (°F)
TDC-TC	Top dead center
TWC	Three-way catalyst
USE FAC	Usage factor of the NOVA
WT	Engine coolant water temperature (°F)
ZOS	Zirconia oxygen sensor

COMPUTER PROGRAMS

BMDP2R	Stepwise regression program of the BMD package
CLOCK	Clock task synchronizing control and data collection of the engine
CONTROLLER	Task controlling the engine
DACOL	Task collecting data from the engine
DDSUPER	Task supervising various tasks
DDTTOUT	Task outputting data to the console
DSP	Data sorting program - prepares raw data to be processed by BMDP2R
ETSMS	Engine test stand monitor software
NS	A program linking NOVA to IBM
OPT	Optimization program

I. INTRODUCTION

A. BACKGROUND AND RELATED WORKS

Fuel consumption and emissions levels are known to deteriorate in time due to mechanical wear and external disturbances. An idea of the size of the deterioration can be obtained from a few recent surveys. A survey done by NHTSA [B-4] found that fuel consumption, HC (hydrocarbons), and CO (carbon monoxides) can go down as much as 11%, 22% and 12% respectively after a tune-up.

Higher improvement in HC and CO of 45% and 60% respectively was stated in [W-1]. It was found that 40% of one year old cars do not meet HC requirements, and 50% do not meet CO requirements, with these numbers deteriorating quite fast for older cars [C-3]. Changes in ambient conditions and manufacturing tolerances also cause deterioration in engine performance. Wrausmann and Smith [WR-1] report a 259% increase in CO, 45% increase in HC, and 22% decrease in nitrogen oxides (NOx) emissions when an automobile calibrated for sea level atmospheric pressure was driven to Denver.

Ostrouchov [O-1] reports the effect of very cold inlet air ($-4^{o}F$) on engine emissions and fuel consumption. Depending on the emission devices that were installed on the engine, HC could go up as much as 4 times, whereas CO could go up 3 times and NOx could double. Fuel consumption could increase by 10%. Similarly an increase in ambient humidity also raises fuel consumption [PO-5].

The emissions constraints imposed by the federal authorities have been continually tightened. For example, the 1975 requirements of HC/CO/NO of 1.5/15/3.1 gm/mile will be replaced by the 1983 requirements of 0.41/3.4/0.4 gm/mile. Therefore there is a great potential for improvement if feedback methods can be employed to control engine operation to maintain optimal condition.

Most of the spark ignited internal combustion engines of today's vehicles are controlled in an open loop fashion. The controlled variables are the spark timing (SA), air/fuel ratio (AF) and the portion of the exhaust gases recirculated through the intake manifold (EGR). Spark timing is determined by engine speed and inlet manifold pressure. Air fuel ratio is determined by the throttle setting and the inlet manifold pressure. Whereas the level of EGR is determined by the exhaust pressure and the intake manifold pressure. This calibration cannot compensate for any deviation from a nominal scheduling. A closed loop system based on engine measurements which are more directly related to the controlled variables is likely to reduce these effects.

A few closed loop systems have been installed recently on vehicle engines. Draper and Li [DR-1] applied their theory of "optimalizing" (peak holding) control using dither spark control of a single cylinder internal combustion engine. Schweitzer, et al. [SC-1, SC-2, SC-3, SC-4], applied the above theory to the design of peak holding controllers for spark advance and for flow rate for a multicylinder engine. A knock detection system using an accelerometer on the engine head as the sensor was installed on Buick engines [C-2]. Spark was retarded when knock was detected and then returned to the nominal setting. A closed loop carburetor which maintains the air/fuel ratio around stochiometry for the best three-way catalyst efficiency was introduced by Ford [M-3], and is used also in a number of GM models. An oxygen sensor in the exhaust line provides the signal. A closed loop system keeping the engine operating on the lean side where both fuel consumption and emissions are low was developed [L-1].

The angle that corresponds to cylinder peak pressure (θ_{pp}) was used in [PO-2, PO-3 , PO-4, PO-5, H-3] as a feedback signal to keep the engine at best fuel economy for various engine operating conditions and in the presence of external disturbances. Maintaining the engine at best fuel economy could be achieved by keeping θ_{pp} at 15^{o}ATDC by changing the spark timing as required. The pressure trace was used as the feedback signal in a closed loop knock detection system developed by R. Hosey [H-4]. Spark was retarded when knock was detected to the point of incipient knock until it was optimal to retard from that point.

Engine modelling and optimization solutions, together with the appropriate feedback signals can provide the required closed loop engine calibration. A few optimization works evaluating best fuel economy for given emission constraints have been done in the last ten years. Rishavy et al. [R-1] used an integer programming technique over a set of points approximating the EPA cycle to solve a steady state warmed up fuel economy optimization, subject to emission constraints. A model of a catalytic converter efficiency as a function of air/fuel ratio was included. A steady state engine mapping was required.

Cassidy [C-1] reduced the data acquisition time by using an online approach. The online real time computer controlled and monitored engine performance as it was seeking out the optimum calibrations. Lagrange multipliers were used to replace the constrained optimization problem by a set of unconstrained problems in points of constant torque and speed. Only steady state warmed-up engine data were considered. This approach did not require any engine mapping. Auiler et al. [A-1] used dynamic programming to find the optimal way with respect to fuel economy, to allocate total allowable mass emissions among the various points of constant speed and torque. Only warmed-up steady state engine data was considered. An engine model developed by Baker and Daby [B-2] was used.

Dohner [D-2] considered drivability by adding a constraint relating the coefficient of variation of the indicated mean effective pressure to the engine surge. The cold-hot cycle as well as transients were considered. The emission constrained optimization problem was solved by applying the Maximum Principle to a terminal control problem over the EPA cycle. No mapping was required. Rao et al. [R-2] solved a nonlinear programming problem with equality and inequality constraints to find best fuel economy for a given emissions level. The Lagrange Multipliers method converted the constrained problem into a set of unconstrained problems at points of constant torque and speed. Only warmed-up engine data was considered. A relationship between the engine controls and engine speed and intake manifold pressure at the optimum point was established.

Trella [T-2] used dynamic programming to find an optimal way with respect to fuel economy of allocating total allowable emissions among points of constant torque and speed representing the EPA cycle. The effect of the number of these points on the optimization was checked by carrying out the analysis for both a 12 point grid and a 41 point grid. The finer grid yielded better fuel economy especially when emissions tightened. Only warmed-up steady state engine data was considered.

Some of the optimization works discussed above were based on engine modelling. Baker [B-2] developed a method of representing the EPA cycle by running the engine for various time lengths at a finite number of constant torque and speed points. Fuel and emissions were correlated with the control variables at any of these points. A similar approach was taken by Rishavy et al. [R-1]. Vora [V-1] correlated the engine outputs, fuel and emissions, with the 3 control variables, air/fuel ratio, spark advance and the portion of the exhaust gases recirculated through the intake manifold as well as with engine speed and torque. Data acquisition time was shortened by sweeping through a range of spark advance, while keeping all the other variables constant, and by taking data at fixed time intervals. As the sweep was slow, there was no need to wait for thermal equilibrium. Rao et al. [R-3] modelled the engine over a wider load-speed range than is required by the EPA cycle. The engine was taken through sequences of speed load points in quick successions for various levels of air/fuel ratio, spark advance and EGR. Engine outputs, fuel and emissions, were correlated with engine speed, fuel injection pulse width, inlet manifold pressure, exhaust gas recirculation and combustion chamber metal temperature. Trella [T-2] also used a five parameter model in which fuel and emissions were correlated with AF, SA, EGR, RPM and Torque.

B. SUMMARY

The objectives of this research are as follows:

1. To design a particular closed loop control system which will maintain optimal operation of the engine over a wide torque and speed range regardless of mechanical degradation or external disturbances. The technique used is to maintain cylinder peak pressure near its optimum value by controlling spark advance in a closed-loop system.
2. To generate trade-off curves between optimal fuel economy, evaluated for a given emissions level, and various levels of emission constraints.
3. To investigate appropriate engine models.

The angle that corresponds to cylinder peak pressure is sensed and used as the feedback signal to keep the engine operating optimally. Optimally operating is to consume minimum amount of fuel for given emissions level over a wide torque/speed range. The optimal operating of the engine can be done by finding a relationship between the angle and some engine parameters that vary with engine speed and load, given an optimally tuned engine. The relationship will provide the reference value of the closed loop system for various speed-load points. The optimal closed loop scheme together with the optimization program, are evaluated over the EPA cycle which is approximated by running the engine for various time lengths at points of constant torque and speed [B-2]. Data were collected for various settings of air/fuel ratio, spark advance timing, and the portion of exhaust gases recirculated through the intake manifold, at the points of constant torque/speed approximating the EPA cycle. Analytic expressions can be fit to fuel consumption and emissions level as a function of the control variables. Once analytic expressions have been derived, the optimization problem of minimizing fuel consumption for given emissions constraints can be formulated and solved. Trade-off curves relating optimal fuel consumption to various emissions constraints can be generated by repeating the optimization solution for various emissions levels.

The optimization solutions also provide the values of the controls, AF, SA and EGR at the points of constant torque and speed as well as the value of the feedback signal θ_{pp}^{opt} which is the angle that corresponds to peak pressure. A relationship between θ_{pp}^{opt} measured at the points of constant torque and speed and engine power was found. This relationship provides the updated reference value for the closed loop control system.

C. SUMMARY BY CHAPTERS

Chapter II:

This chapter describes the engine test facility which consists of a 2.3 litre four cylinder Ford engine directly coupled to a speed controlled dynamometer. The simulation of an EPA cycle required running the engine at points of constant torque and speed. Therefore, a torque controller was developed. The controls, air/fuel ratio, spark timing and the EGR system, were modified to be compatible with the data acquisition procedure. Various control tasks were done by a NOVA minicomputer which also collected data from the various sensors. This chapter briefly describes the software and hardware of the test facility. A more detailed description is contained in Appendix J.

Chapter III:

This chapter describes the procedure of fitting functions to the engine outputs, fuel and emissions levels. Some statistical terms, such as R-square. RMS, F-statistics, which evaluate the quality of fit are discussed. The existence of a theoretical relationship between engine outputs and the controls justifies the function fitting approach. These relationships are described in this chapter. A single function relating either fuel consumption or emissions level to the control variables can be fit to the entire data base with the controls AF, SA, EGR as well as RPM and TORQUE as the independent variables. Or engine outputs can be correlated with the controls for any of the points of constant torque and speed. The advantages and drawbacks of each method are discussed in this chapter. It concludes with a fit procedure error.

Chapter IV:

The optimization problem of minimizing fuel consumption subject to emissions constraints over the EPA cycle can be formulated with the aid of the models derived in Chapter III. The composite fuel and emissions levels over the EPA cycle are evaluated by combining fuel and emissions levels for the 10 points of constant torque and speed with different weighting coefficients.

The adjoining of the emission constraints to the fuel function using Lagrange Multipliers converts the original constrained problems to a set of unconstrained problems each depending only on the controls of one torque/speed point. Trade-off curves between optimum fuel and various emission levels were generated by solving the optimization problem for various emission constraints.

Chapter V:

A closed loop scheme that maintains the engine operating optimally regardless of external disturbances or mechanical degradation over a wide torque/rpm range is desired. It is presented in [H-3] that if the angle of cylinder peak pressure is kept constant at 15^{o}ATDC, the best fuel economy target for various engine operating conditions is maintained. This angle can be used as a feedback signal to keep the engine at optimum fuel economy for given emissions levels over a wide torque/speed range. The reasoning for using the signal is given in this chapter. Piezoelectric sensors installed between the spark plugs and the engine head convert the pressure changes into electric signals. The electronics required to process the signal and to detect the peak pressure angle is described. It was found that the optimal angle is a function of engine power. Therefore, this function will provide the updated reference value with the spark advance timing which changes as required to control θ_{pp}. Humidity was introduced into the inlet air stream simulating an external disturbance. With only open loop control, fuel consumption increased by 4% and NOx level decreased by 30%, whereas with the closed loop system, fuel consumption went up 2% and NOx decreased by 20%.

D. CONTRIBUTIONS OF THIS RESEARCH

1. Design of a closed loop scheme for an internal combustion engine that minimizes fuel consumption subject to a limitation on emissions over a prescribed driving cycle.

2. Generation of detailed trade-off curves relating optimal fuel consumption to various levels of emission constraints for the engine configuration tested. The average values of the control variables, AF, SA, EGR, over the E PA cycle for the various optimal solutions taking into account the various catalysts are also displayed.

3. Comparison of the quality of fit of global and individual fits. Global fit is the estimate of the function for all measurements, whereas local fit refers to a fit at a specific torque/speed point.

II. MULTICYLINDER ENGINE TEST FACILITY

A. INTRODUCTION

Optimizing fuel consumption for given emission constraints requires a detailed engine mapping. An automated engine test facility can shorten the data acquisition time considerably. The engine was run at points of constant torque and speed which were used to approximate the EPA cycle. Therefore a speed controller as well as a torque controller were required. This chapter describes these control systems. In addition, the controls--air/fuel ratio, spark timing and the portion of exhaust gases recirculated through the intake manifold, had to be modified to be compatible with the mapping requirement.

Sensors were installed to measure engine inputs and outputs and to collect some reference data. A NOVA minicomputer was introduced to perform various control tasks and to collect and process data. This chapter describes the required hardware and software.

B. ENGINE AND DYNAMOMETER SET-UP

Data was collected from a 2.3L 4-cylinder 1975 Ford engine. The engine was connected to a dynamometer by a manual transmission with the fourth gear engaged; therefore, the engine and the dynamometer turned at the same speed.

An automatic speed controller was installed on the dynamometer. The tachometer is a digital counting device yielding a resolution of 1 rpm. The speed is controlled by the dynamometer field current. The speed controller can accept both local commands and computer commands. Only a few seconds are required to obtain a steady state error of ± 2 rpm for a step in commanded speed. Figure 2.2 is a schematic diagram of the system. The dynamometer settling time is much shorter than the elapsed time between two measurements. Therefore it did not have any impact on

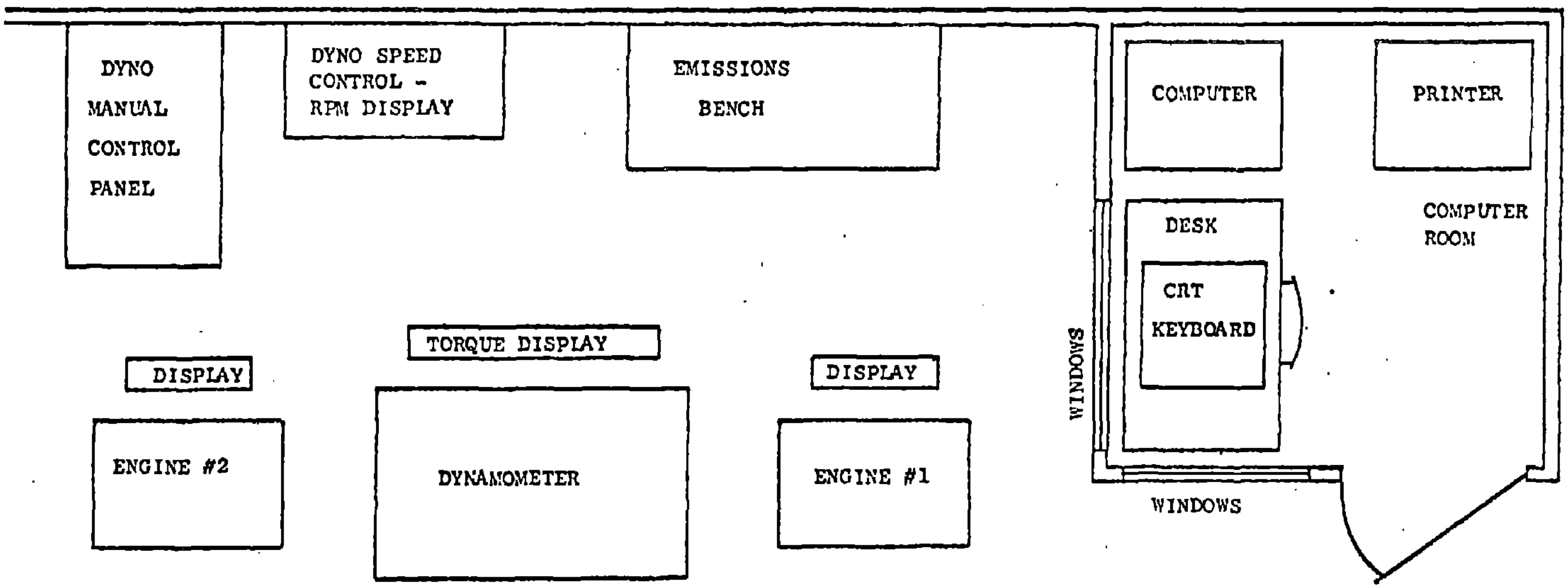

Fig. 2-1 Dynamometer Facility Layout

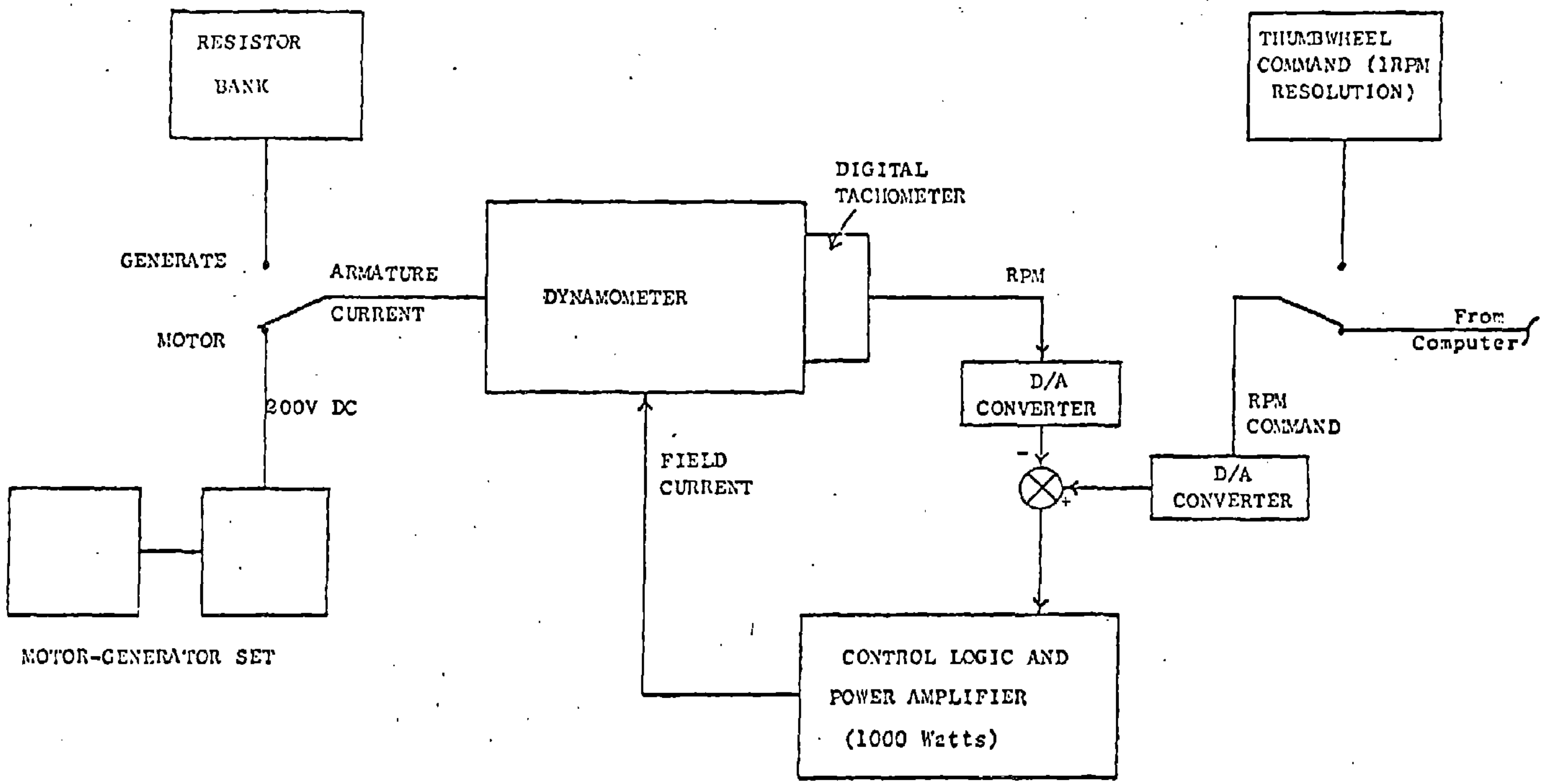

Fig. 2-2 Speed Controller Schematic Diagram

the steady state data acquisition procedure. The dynamometer was used only for a steady state mapping because it was not capable of tracking any arbitrary change in load and speed.

C. ENGINE MODIFICATION AND INSTRUMENTATION

A few engine changes and measuring instruments were introduced for the following reasons:

1. Arbitrary setting of air/fuel ratio, spark timing and the amount of EGR.
2. Controlling engine torque .
3. Measuring fuel and inlet air flow, emissions concentration, pressures and temperatures in various parts of the engine.

The following systems were changed or added to meet the above requirements:

1. Carburetor.
2. EGR line and valve.
3. Fuel system.
4. Spark advance.
5. Torque controller.
6. Emission cabinet measuring CO, CO_2, O_2, NOx, HC.
7. Inlet air flow meter.
8. Temperature gauges measuring:
   a. water temperature,
   b. inlet air temperature,
   c. engine oil temperature,
   d. exhaust gas temperature.
9. Inlet manifold pressure transducer.

The Carburetor:

The original 1975, 2bbl Holley 5200 carburetor could not accommodate any external mixture changes; therefore, it was replaced by the latest model 2bbl Holley 6500 which includes a vacuum activated fuel enrichment system. The vacuum is applied externally providing an easy means of changing the fuel mixture. The vacuum activates a piston which closes a secondary passage from the float chamber to the main well; thus higher vacuums leanout the mixture. The vacuum ranged between 0 to 5 in Hg under atmospheric pressure. Air/fuel ratio varied from 11 to 16 for low and medium air/flow levels and went up slightly to 12-17.5 for the higher air/flow points. As a leaner AF range was desired, it was decided to change the jets that affect the mixture. Air/fuel ratio is determined by 4 jets, each of which dominates the mixture at a different air/flow level. Therefore it was quite easy to tailor the mixture pattern to our needs.

One idle jet and one main jet are installed in the primary and in the secondary bowls. The idle primary jet dominates the mixture at speeds lower than 1000 rpm. The main primary jet dominates the mixture above that level up to a throttle opening of 40° above which the idle secondary jet has only a slight effect and the main secondary jet takes over. The sizes of the original and the replacement jets are given in Table 2.1. The modified mixture range as a function of air flow and the vacuum level applied to the carburetor leaning port is given in Fig. 2.3.

	IDLE		MAIN	
	Primary	Secondary	Primary	Secondary
Original	0.90	0.50	1.26	1.10
Replaced	0.72	0.90	1.22	1.30

TABLE 2.1 Original and modified carburetor jet sizes (size in mm)

Fig. 2-3

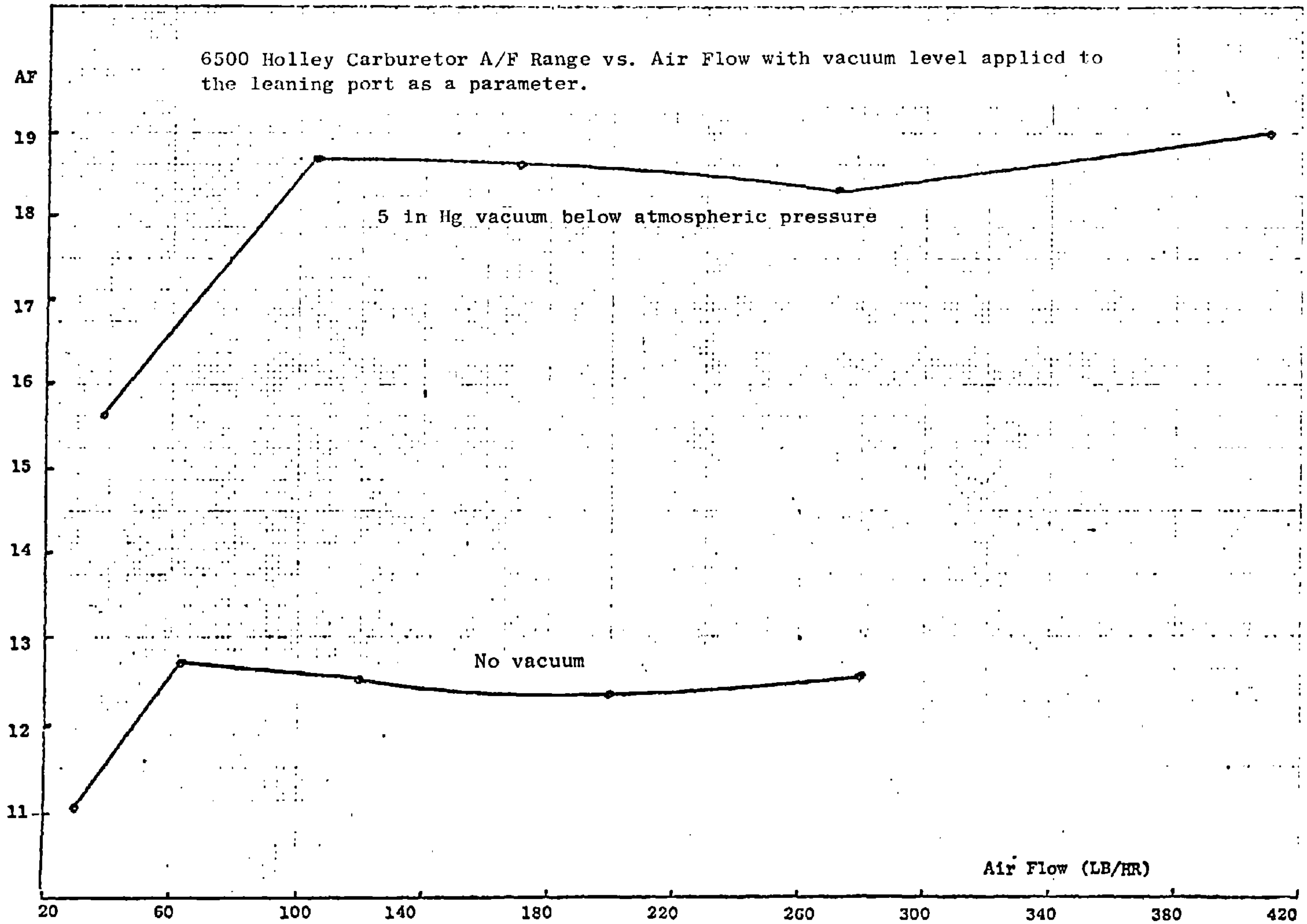
6500 Holley Carburetor A/F Range vs. Air Flow with vacuum level applied to the leaning port as a parameter.
AF
19
18
17
16
15
14
13
12
11
5 in Hg vacuum below atmospheric pressure
No vacuum
Air Flow (LB/HR)
20
60
100
140
180
220
260
300
340
380
420

EGR System:

The original EGR system was modified for two reasons:

1. to enable an arbitrary setting of EGR flow over the normal engine operating range;
2. to provide means for mass flow measurement.

The EGR valve as well as the EGR line were modified to meet these two requirements. Usually the EGR valve is activated by a diaphragm which responds to a vacuum signal from the carburetor venturi. The diaphragm was replaced by a threaded shaft which was connected to the EGR valve. This shaft was mounted in a nut; therefore, the valve could be advanced by rotating the shaft. Approximately 9 turns are required to fully open the valve. Each turn advances the shaft 1/16" which gives a reasonable resolution.

The EGR flow was determined by introducing an on-line orifice with pressure taps on both sides. The design of this orifice complied with ASME Power Test Code 19.5, 4-1959. The line configuration had to be altered because straight portions of a minimum length are required in the upstream and downstream parts of the line. The modified EGR line was calibrated on a test bench. The discharge coefficient was determined by recording both pressure drop across the orifice and the volumetric flow which was measured by a highly accurate swirl meter. The EGR mass flow can also be evaluated by considering the air density at the orifice. The air density is determined by the pressure on the inlet side of the orifice and by the exhaust gas temperature. These measurements were recorded.

Fuel Measurement System:

Fuel flow was measured by an Electronic Mass Flow Transmitter of Flo-Tron, Inc. Measurement is achieved by arranging 4 orifices and a constant volume pump in a "Wheatstone Bridge" network. The total mass flow is proportional to the pressure difference across the pump, thus one gets a simple and direct measurement. This device was calibrated by measuring the time required to pump a known amount of gasoline. Error never exceeded 1/2% over a wide range of low levels.

Emission Instruments:

The engine emissions are measured by an instrumentation bench which was designed to measure the molal concentrations of CO, CO_2, O_2,C (hydrocarbons) and NO. The design of the system was carried out so that the gas sample flow rate was held constant, thereby reducing the error of the individual instrument to flow variations. Large sample flow rates are used to assure rapid system response to changing emissions. The bench includes the following instruments:

1. CO - Olson Horiba Mexa 200 (NDIR);
2. CO_2 - Olson Horiba Mexa 204 (NDIR);
3. C in HC - Olson Horiba FID-1 (FID);
4. O_2 - Applied Electrochemistry S3A (Zirconia Electrochemical);
5. NO-NOx - Thermo Electron Model 44 (CHGM illuminescent).

Of the instruments listed, all except the FID require a dry and filtered sample to protect internal components and reduce interference from water vapor and particulates. The HC analyzer can accept hot, high humidity samples resulting in the elimination of condensation of heavier hydrocarbons in the sample line that could take place had the exhaust gases been allowed to cool. This condensation could introduce a measurement error.

The emission cabinet incorporates the necessary plumbing to provide these sample conditions to the instruments. The sample gas drawn from the engine passes through a controlled electrically heated line that maintains the desired sample line temperature to avoid condensation.

The output signal of all the emission instruments is also directed to an external port that can be connected to the NOVA minicomputer. In addition, all the instruments except the oxygen analyzer are multirange devices. The status bit is also available on the external ports for the NOVA. Therefore the physical measurement is obtained on the NOVA by combining the output signal of the instrument, indicating the fraction of full scale, together with the range. The various ranges of the emission instruments are listed in Table 2.2. The multiplier increases the range by the multiplication factor. In NO for example a range of 5 and a multiplier of 100 yields a range of 500 ppm, etc. The response time of the emissions cabinet is around 10 seconds, which is the sum of the individual instruments response and the delay introduced by the sampling line having a total length of 30 ft.

Instrument	Range	Multiplier	Unit
CO	0-2, 0, 5		%
CO_2	0-5, 0-16		%
HC	0-100	1,5,10,50,100,1000	PPM
O_2	0-100		%
NO	2, 5, 10	1, 10, 100, 1000	PPM

TABLE 2.2 Emission instruments range

Air Flow Measurement:

Air flow into the engine is measured by an air flow transducer, series 100 of Autotronic Controls Corporation. Volumetric air flow is measured by counting the number of turns of a turbine that rotates as air flows by. The instrument has very high linearity over a wide range. The instrument was checked against a tank flowmeter where flow is measured by reading the pressure drop across an orifice through which the flow passes. The reading of the turbine meter was always higher than the tank meter with maximum difference of 3% probably due to some internal leakages in the tank. Air mass flow is evaluated by considering air density which is determined by inlet air temperature and ambient pressure which were both recorded.

Temperature Measurement Devices:

Temperature at four points was recorded in the experiment.

1. Water temperature in the engine water jacket.
2. Inlet air temperature near the air flow meter.
3. Oil temperature in the engine oil pan.
4. Exhaust gas temperature in the exhaust line.

Water, air and oil temperatures were measured by Fenwal Electronic thermistors. These devices change resistance as a function of temperature; resistance decreases as temperature goes up. The thermistor in series with an additional resistor are excited by a constant voltage. The voltage across the thermistor is then amplified and biased to fit the NOVA analog input range which is -10v to 10v.

The exhaust gas temperature was measured by a Conax RTD, a resistance temperature device in which resistance increases as temperature goes up. The circuitry is similar to that of the thermistors.

Air Pump Calibration:

The total exhaust mass flow is affected by an air pump which injects fresh air into the exhaust manifold to oxydize the emissions. As the total exhaust mass flow is required for converting emissions from molal concentration to mass flow, air pump mass flow level must be known at any instant. The air pump mass flow was measured on a flow bench for various speeds and back pressures is given in Fig. 2.4 and can be condensed to the expression given in (2.1).

During engine mapping the air pump back pressure was monitored and was introduced from the computer keyboard console.

Air pump mass flow is given by the following expressions:

$$\dot{G}p = \rho \cdot (0.008 \times RPM-3.3-0.667\ Pex) \text{ for } RPM < 2500 \qquad (2.1)$$

$$\dot{G}p = \rho \cdot (0.00773 \times RPM-3.75-0.645\ Pex) \text{ for } 2500 < RPM$$

where:

ρ = Air density on the air pump inlet side, ambient pressure and 110°F are assumed (lb/ft^3);

Fig. 2-4

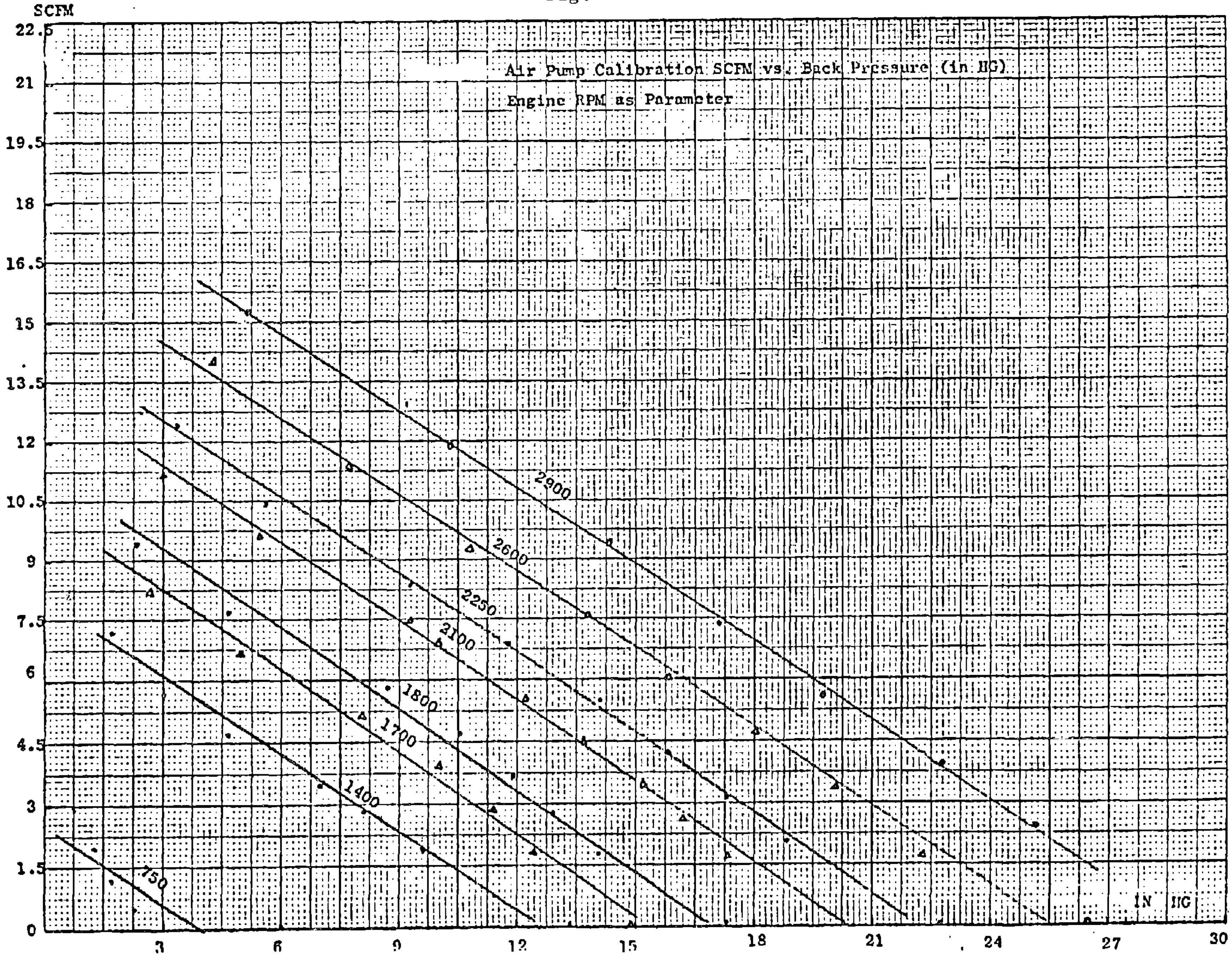

Air Pump Calibration SCFM vs. Back Pressure (in HG)
Engine RPM as Parameter
SCFM
22.5
21
19.5
18
16.5
15
13.5
12
10.5
9
7.5
6
4.5
3
1.5
0
3
6
9
12
15
18
21
24
27
30
IN HG
2900
2600
2250
2100
1800
1700
1400
750

$\dot{G}p$ = Air pump mass delivery (lb/min);

RPM = Engine speed (rpm);

Pex = Exhaust pressure (in Hg).

Exhaust Back Pressure Simulation:

The absence of any catalyst or muffler in the exhaust line of the experimental facility could change the exhaust back pressure and the engine performance. A back pressure judged to be typical of an in-use vehicle was simulated by the introduction of an orifice in the exhaust line.

D. COMPUTER SYSTEM

1. Hardware

The computer for engine/dynamometer control and data acquisition is a Data General Nova III. It has 32K words of core memory, dual diskette ("floppy") drive, paper tape reader, a 120 character/sec line printer, and a CRT/keyboard. The interface equipment consists of a 32 channel 12-bit analog to digital converter, a 64 channel digital multiplex for input or output, four channels of digital to analog conversion, and an acoustic coupler. Normal operator input/output for programming or control commands is accomplished by the CRT/keyboard while permanent records are made by the line printer. The acoustic coupler allows direct telephone access to our central campus computation center and essentially converts the NOVA system into a terminal for the campus IBM 370-168. This mode of operation was used to transfer engine data directly from the floppy disks to the campus computer where the engine modelling and optimization was carried out. Figure 2.5 is a schematic diagram of the computer system.

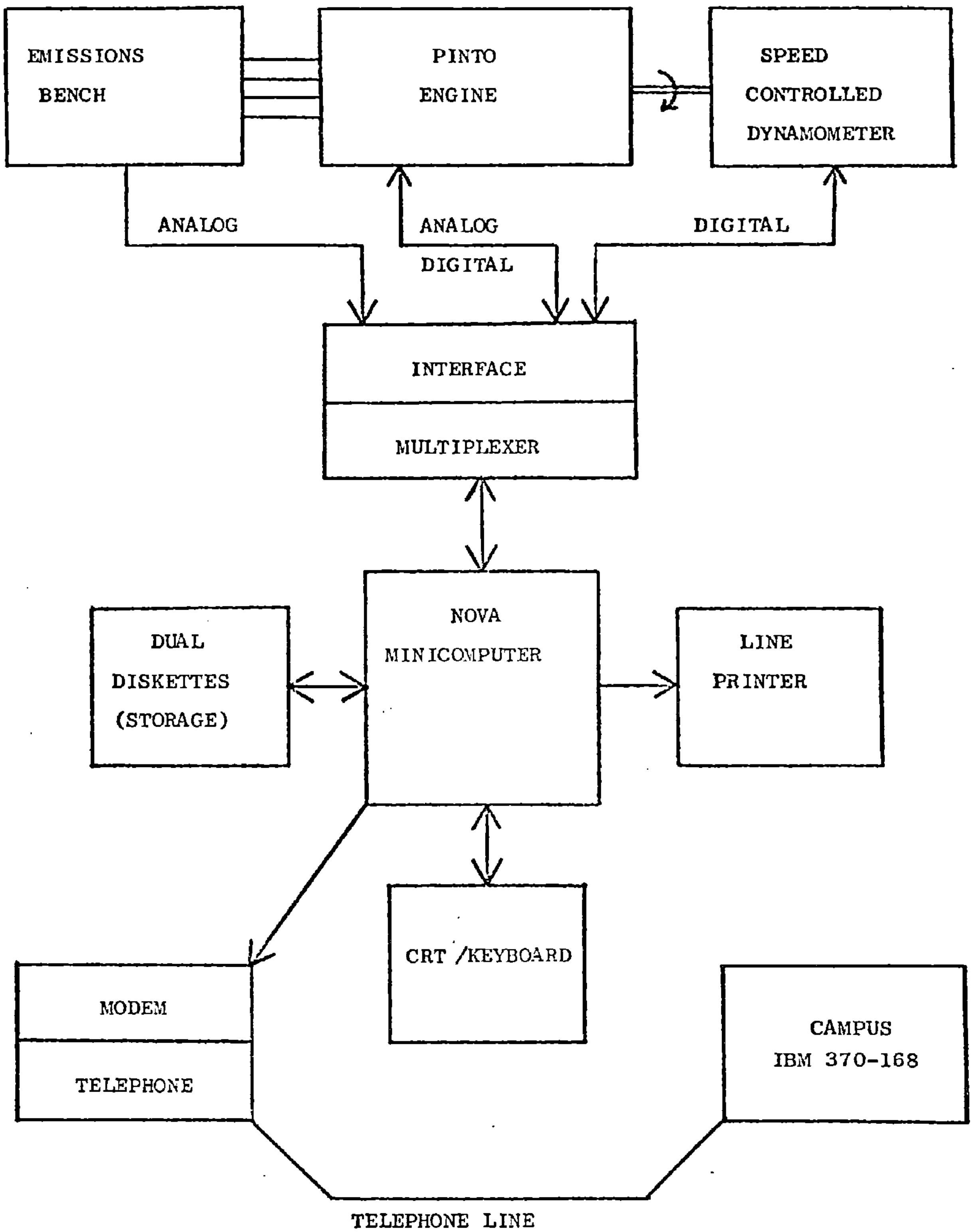

Fig. 2-5 Computer System Schematic

2. Software

Raw data that was sampled from the engine is processed by 5 consecutive programs in which the output of one serves as the input of the next in the sequence. The first three programs reside on the NOVA whereas the two others reside on the campus IBM computer.

Data is sampled by the engine test stand monitor software (ETSMS) (Appendix B) and passes to the Data Sorter Program (DSP) which picks up selected data and converts measurements to convenient units. The NOVA-SCIP[‡] (NS) program transfers the data to the IBM computer where the BMDP2R package (see Ch. III) evaluates the parameter estimates for the measurements. The estimates are the input of OPT - the optimization program (see Ch. IV) that evaluates best fuel economy for various emissions levels. The logical data flow is given in Fig. 2.6.

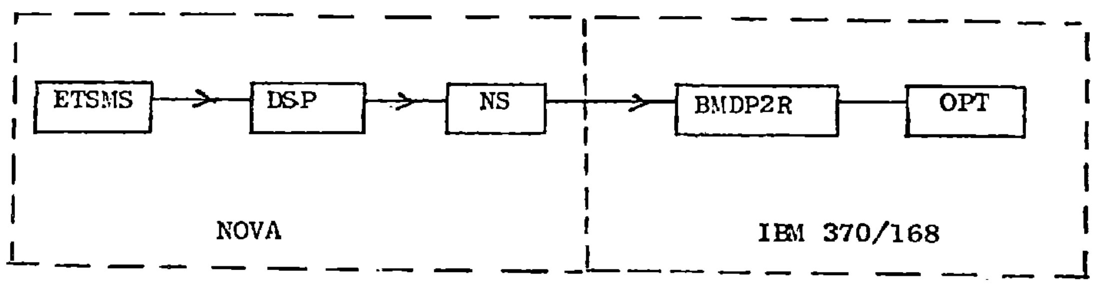

Fig. 2.6 Logical Data Flow

The BMDP2R program will be discussed in detail in Ch. III and the OPT program in Ch. IV.

a. ETSMS (Engine Test Stand Monitor Software)

The engine test stand monitor software was designed to provide the following capabilities:

1. The monitor allows continuous display on the CRT console of engine variables such as torque, RPM, air and fuel flows, spark advance, emissions, and temperatures. The CRT display

‡Stanford Center for Information Processing.

No.	SYMBOL	UNITS	PHYSICAL MEANING
1	A/F	vac. in Hg	Airfuel ratio indicator
2	EGR	valve turns	Exhaust gas recirculation
3	torque	ft. lb.	Engine torque
4	throttle	degrees	Throttle opening
5	fuel	lb/hr	Fuel flow
6	Air	CFM	Inlet air flow
7	SPK ADV	degrees	Spark Advance
8	NO_x	PPM	Equivalent NO
9	HC	PPM	Count number of C
10	CO	%	
11	CO_2	%	
12	O_2	%	
13	IAT	^oF	Inlet Air temperature
14	OT	^oF	Oil temperature
15	EGT	^oF	Exhaust gas temperature
16	WT	^oF	Water temperature
17	IMP	abs PSI	Inlet manifold pressure
18	ZOS	bits	Zirconia Oxygen sensor
19	USE FAC		Fraction of cycle time used by NOVA
20	TEMP	^oF	Ambient temperature
21	PRESS	in Hg	Ambient pressure
22	HUM	grains H_2O/lb air	Humidity
23	EGRDP	In H_2O	Pressure drop on EGR orifice
24	Pex	In Hg	Exhaust pressure
25	Pair	In Hg	Air pump back pressure

TABLE 2-3: Monitored variables

may be updated as often as once per second.

2. The operator may obtain a permanent record of engine variables by commanding a data dump to the lineprinter and/or to a disk. The disk record can be used by other data processing computer programs.

3. The desired setpoints for RPM, torque and spark advance may be input by the operator from the console. The monitor software also outputs the actual values achieved by the hardware controls for RPM and spark advance and the torque values achieved by the NOVA digital feedback loop from the load cell to the throttle angle.

25 variables are monitored (see Table 2-3). The last three variables in the list -- EGRDP (pressure drop across the EGR orifice), Pex-absolute exhaust gas pressure, and Pair-air pump back pressure are introduced manually from the console keyboard. Fuel enrichment system vacuum which indicates air/fuel ratio and EGR level (number of turns of valve) are also input manually from the console for recording purposes only.

The engine test stand monitor program consists of four tasks running in parallel (see Table 2-4). Engine control is performed by the highest priority task; therefore, the resources of the computer are always available when control functions are required. Second priority is given to the data collection task. Next priority is given to the supervisor function which provides for communication between the operator and the monitor program; thus control and data collection will continue during operator inputs. A separate task is devoted to outputting test variables to the console screen so the data collection task is not held up by the slow process of outputting the data which is has collected.

The controller task (labelled Controller in Table 2-4) controls the engine at a test point. It controls RPM, throttle setting and torque, spark advance and the angle that corresponds to peak pressure. The NOVA sets desired RPM values at the speed controller. When the NOVA is in the open loop mode it can set desired throttle setting by commanding a microprocessor system which in turn activates a stepper motor that is attached to the throttle mechanism. In the closed loop mode, torque is controlled by outputting signal to the throttle control system whenever torque deviates from the desired value. A detailed discussion of the torque controller is given in Appendix J. Similarly spark advance timing is controlled in an open loop mode and the angle that corresponds to peak pressure is controlled in the closed loop mode. Spark advance is controlled by a microprocessor as discussed in Appendix I. The controller task outputs the desired spark advance value whenever a new setting is desired. The angle that corresponds to peak pressure is controlled by closing the loop through the NOVA and outputting commands to the spark controller as necessary.

The data collection task (labelled DACOL in Table 2-4) inputs and stores data, it converts the input data to engineering units, and it reduces, formats and outputs data to the lineprinter and to the disk. The operator can input the data sampling rate. A maximum sampling rate of 10 Hz was chosen as a reasonable upper limit that would be slow enough to allow software flexibility and fast enough for good resolution of engine test data.

TASK NAME	CONTROLLER	DATA COLLECTION	SUPERVISOR	CONSOLE OUTPUT
TASK PRIORITY	1	2	3	4
TASK FUNCTION	engine control	data collection, data translation to engineering units, data reduction and data output	communication between other tasks and operator via CRT console	data output to console

TABLE 2-4 Engine Test Stand Monitor Organization

```
NOMINAL              TORQUE  RPM   SPKADV      A/F    EG
ENGINE TEST DATA             10/28/78           14:16:19
DISK DUMP             FILE #  1

NOMINAL              TORQUE  RPM   SPKADV      A/F    EGR
                     50.00 1700.00   10.00     0.00    0.00

             RPM   TORQUE THROTTLE  FUEL      AIR   SPK ADV   NOX     HC        CO
AVE       1702.16   50.21   20.99   11.78   32.95   10.00  181.83  211.30     0.57
VAR          0.66    0.40    0.05    0.06    0.11    0.00    0.93    1.10     0.01
WORST     1701.00   49.23   21.24   11.91   32.73   10.00  179.06  205.10     0.55

             CO2     O2      IAT      OT     EGT      WT      IMP     ZOS  USE FAC
AVE         11.56    3.16   75.13  197.41 1486.91  179.35   10.14    7.18     1.00
VAR          0.02    0.19    0.17    0.17    2.89    0.16    0.04    2.09     0.00
WORST       11.48    4.10   75.48  197.73 1470.15  178.43   10.37    2.00     1.00

  TEMP    PRESS    HUM    EGRDP   PEX      PAIR
   69.00   30.04   82.00    0.00    1.50    4.20

ENGINE TEST DATA             10/28/78           14:18:14
DISK DUMP             FILE #  2

NOMINAL              TORQUE  RPM   SPKADV      A/F    EGR
                     50.00 1700.00   18.00     0.00    0.00

             RPM   TORQUE THROTTLE  FUEL      AIR   SPK ADV   NOX     HC        CO
AVE       1702.40   50.00   18.43   10.66   29.76   18.00  228.39  419.95     1.26
VAR          0.66    1.00    0.06    0.06    0.08    0.00    2.61    2.63     0.03
WORST     1701.00   43.27   18.72   10.45   30.00   18.00  224.06  411.73     1.22

             CO2     O2      IAT      OT     EGT      WT      IMP     ZOS  USE FAC
AVE         11.21    3.03   74.13  199.62 1349.19  178.38    9.35    7.36     1.00
VAR          0.04    0.04    0.11    0.14    2.68    0.27    0.07    2.26     0.00
WORST       10.97    3.22   73.82  199.26 1344.45  176.57    9.83    0.00     1.00

  TEMP    PRESS    HUM    EGRDP   PEX      PAIR
   69.00   30.04   82.00    0.00    1.50    3.80

ENGINE TEST DATA             10/28/78           14:23: 0
DISK DUMP             FILE #  3

NOMINAL              TORQUE  RPM   SPKADV      A/F    EGR
                     50.00 1700.00   26.00     0.00    0.00

             RPM   TORQUE.THROTTLE  FUEL      AIR   SPK ADV   NOX     HC        CO
AVE       1702.30   49.88   17.29   10.04   28.17   26.00  420.21 1710.97     2.94
VAR          0.90    0.39    0.01    0.06    0.12    0.00    4.57   10.07     0.02
WORST     1704.00   50.59   17.37    9.86   28.36   26.00  407.34 1652.32     2.90

             CO2     O2      IAT      OT     EGT      WT      IMP     ZOS  USE FAC
AVE         10.10    2.75   77.03  203.37 1019.41  179.54    8.90   17.90     1.00
VAR          0.02    0.04    0.26    0.27    1.66    0.32    0.02    2.04     0.00
WORST       10.06    2.89   77.44  202.84 1007.88  177.35    8.98   29.00     1.00

  TEMP    PRESS    HUM    EGRDP   PEX      PAIR
   69.00   30.04   82.00    0.00    1.20    3.60
```

TABLE 2.5 Lineprinter Data Dump

An updated average of the recent 50 readings is evaluated for 18 selected variables. When a data dump is desired, the worst case, as well as the variance of the most recent 50 readings, is evaluated for these variables. Table 2-5 is a sample of a lineprinter dump. This same information is put on a disk for permanent storage. The data collection task also averages 10 selected engine variables which are displayed on the console.

The supervisor task enables the operator to select the number of input points which are averaged before being displayed. The supervisor task (labelled DDSUPER in Table 2-4) provides the communications link between the operator's console and the controller and the data collection tasks. A number of mnemonics (listed in Table 2-6) may be input from the operator's console allowing the operator to control the engine and the data collection. "C" enables the operator to change engine set points such as torque, RPM, spark timing, throttle setting and the desired peak pressure angle. "I" enables the operator to input NOx instrument calibration factor, ambient temperature, pressure and humidity, the EGR line pressures - EGRDP and PEX, exhaust back pressure-PAIR and the desired data sampling rate. "T" enables the operator to select the variables he wishes for display on the console.

COMMAND	FUNCTION
C	Operator input of engine setpoints
I	Operator input of parameters for data collection
D	Disk dump
L	Line printer dump
DL	Simultaneous line printer and disk dump
T	Operator selection of variables for console display
E	Program Termination

TABLE 2-6 Supervisor Mnemonics

The console output task (labelled DDTTOUT in the listing) is initiated by a message from the data collection task which is issued when a buffer is filled with the calculated averages for the selected variables. This organization allows the data collection task to continue uninterrupted while the console output task is occupied by the slow process of outputting the information.

The user clock subroutine (labelled CLOCK in the listing) is a real time clock interrupt driven subroutine which runs in the operating system. It provides the interface between the real time clock and the controller and data collection tasks by transmission of messages which start the tasks. The CLOCK subroutine also performs timing functions by decrementing counters with each clock interrupts until time to start a task.

b. DSP (Data Sorting Program)

The raw data generated by ETSMS and stored in the floppy disk serves as an input to this program which has two purposes:

1. It compares air/fuel ratio based on emissions (see Appendix A) to that based on direct measurements serving as a check for a proper system measurement.
2. It converts emission measurements from volumetric concentrations to mass flow by considering the exhaust mass flow together with the emission concentration. It also organizes the variables that are sent to the IBM computer in matrices. These variables are the three independent variables, AF, SA and EGR; and Fuel and emissions HC, CO and NO. Only measurements that correspond to the same torque and speed values (a set point) are entered into the same matrix. Thus DSP groups the data in 10 different matrices which can be sent later to the IBM computer.

c. NS (NOVA-SCIP)

This program transfers data from the NOVA minicomputer to the IBM computer. The matrices generated by DSP are the input. Data is transferred via an acoustic coupler and the phone line. NS is a multitask program that reads characters from the NOVA core and transfers them to the external port that connects to the IBM computer, and vice versa. It reads characters that come from the IBM computer through the acoustic coupler and displays them on the CRT. The matrices generated by the DSP program are first transferred to the core from where they are sent line by line to the external port.

E. DATA ACQUISITION PROCEDURE

The conventional emissions and fuel figures typically quoted refer to a prescribed urban and highway EPA cycle that can be simulated on the dynamometer by running the engine at a finite number (12) of torque and RPM points for various lengths of time (see Table 2-7) [B-2] and combining the results by a weighted average.

During the experiment it was found that 2 set points which are 900/2 (900 rpm and 2 ft lb) and 1250/-7.5 had to be excluded from our schedule due to the dynamometer inability to maintain constant speed for a very low torque. Their weighting factors were added to those of the neighboring points. Those of 1250/-7.5 were added to 1800/-14 and those of 900/2 to 750/15.

In addition, a full mapping was impossible at 2600/95. The engine could not maintain the desired torque level when a combination of retarded spark timing, lean mixture and EGR were applied. It was decided to redistribute the matrix in this region thus affecting the neighboring point (2900/70) and its weighting factors. As a result, the new set points were 2500/85 and 2900/72 with weighting coefficients as given in Table 2-8.

For each of these 10 points, the fuel mass flow in lb/hr and the emission levels -- HC and NOx in PPM and CO in % -- as well as some other variables (see Table 2-3) were measured for various values of the three independent variables: air/fuel ratio, spark advance and EGR. Of these three variables only SA could be changed from the console. The two others were set manually by either changing the vacuum level of the carburetor fuel enrichment system or by manually turning the EGR valve.

Approximately 80 data points were taken for each set point, 4 different values of air fuel ratio, 4 levels of EGR and 5 settings of spark advance were tried. In a few cases, at the high power points, some of the points had to be excluded due to roughness difficulties, thus reducing the total number of data points slightly. Typically they were for lean mixtures, retarded spark and some EGR. A detailed listing of the independent variables range, as well as the total number of data points, is given in Table 2-9.

TABLE 2-7 Original Weighting Coefficients as suggested in [B-2]

Vehicle Weight: 3000 lb

Axle Ratio: 3.4

Transmission: Automatic

Test Point (i)	Speed (rpm)	Torque (ft lb)	Urban Weighting Factor, C_U^i(sec)	Highway Weighting Factor, C_H^i(sec)
1	2600	38	77	297
2	2900	70	22	132
3	1400	20	317	0
4	1800	25	87	68
5	1700	50	256	24
6	2100	75	45	26
7	750	10	316	10
8	1800	-14	27	31
9	1250	- 7.5	90	17
10	900	2	125	0
11	2600	95	8	5
12	2250	50	0	152

The spark advance was the variable to be swept first. It was stepped for a certain value of EGR and air fuel ratio. When spark advance reached its limit, EGR was stepped up and the sequence was repeated. This time in the opposite direction; namely, had the spark been advanced previously it would have been retarded now. This was repeated until all 4 levels of EGR were exhausted, then EGR was set again to zero and the entire procedure was repeated for a different air fuel ratio.

TABLE 2-8 Modified Weighting Coefficients

Vehicle Weight: 3000 lb

Axle Ratio: 3.4

Transmission: Automatic

Test Point (i)	Speed (rpm)	Torque (ft. lb)	Urban Weighting Factor, C_U^i(sec)	Highway Weighting Factor, C_H^i(sec)
1	1700	50	256	24
2	1800	25	87	68
3	2100	75	45	26
4	2250	50	0	152
5	2600	38	77	297
6	1400	20	317	0
7	2500	85	6	6
8	2900	72	24	128
9	1800	-14	117	48
10	750	·15	441	10

Torque	RPM	AF Range	SA Range	EGR Range	# Points
50	1700	12.5-18.5	10-42	0-7	76
25	1800	12.8-18.5	10-42	0-7	80
75	2100	12.5-18.5	15-38	0-7	82
50	2250	12.4-18.5	15-45	0-7	80
38	2600	12.4-18.5	18-45	0-7	81
20	1400	13.0-18.5	10-45	0-7	80
85	2500	12.7-18.5	21-38	0-7	78
72	2900	13.0-18.0	24-42	0-7	73
-14	1800	12.5-18.0	10-45	0-4.5	80
15	750	11.0-15.5	10-30	0	20
					TOTAL 730

TABLE 2-9 Independent Variables Range

III. PARAMETER ESTIMATE ANALYSIS

A. INTRODUCTION

Engine performance can be described either by the solution of the corresponding thermodynamic and chemical equations, or by correlating the outputs with the inputs. The first method has not yet been able to predict engine outputs very efficiently nor very accurately ([H-1],[S-3], [Z-1]).

The second method, on the other hand, can be justified only if engine inputs and outputs are known to be theoretically correlated.

In this chapter, the theoretical as well as the experimental relationship between engine inputs and outputs are discussed. The raw data was sorted by DSP (Data Sorting Program, see Ch. II) and transferred to the 370/168 IBM computer by phone line where functions were fit to fuel and emissions measurements. Two approaches can be used in the function fit: the first one calls for fitting of functions to the measurements of each separate point of constant torque and speed, whereas the other method fits a single function to the entire range. AF, SA and EGR are the independent variables in the first case, whereas AF, SA, EGR, RPM,TORQUE are the independent variables in the second case.

Data curve fitting to engine outputs, fuel and emissions levels, was done by [B-2], [P-1], [R-1], [R-3]. The global fit which relates engine outputs to AF, SA, EGR, TORQUE, RPM was used. No attempt was made to compare these results with those of local fits.

The quality of fits, as well as the type of functions used in the fitting process is analyzed in this chapter. The parameters were estimated by the BMDP2R program whose features are given below. The chapter concludes with the presentation of one fitted function and the evaluation of its quality.

B. ENGINE INPUT/OUTPUT RELATIONSHIP

1. Background

One way of describing the engine performance is by solving the appropriate thermodynamic and chemical equations. For example, Heywood [H-1], simulated a four stroke spark ignition engine cycle to study its effect on engine performance and NO emissions. T. Singh [S-3] developed a model of the combustion process in a spark ignition engine to predict emissions, NO, CO and fuel. The solution was based on energy mass and chemical equations. Extensive computation is required to evaluate fuel and emissions at just one operating point, even for a model simplifying the complex combustion chamber geometry. Zeleznik, et al. [Z-1] developed a model of the complete Otto cycle. The model incorporates heat transfer, combustion kinetic and chemical kinetic to evaluate fuel and emissions. A number of cycles must be calculated in order to obtain steady-state conditions.

The approach used in this research is based on input/output descriptions. The theoretical relationship based on chemical and thermodynamic reasoning is given below. This relationship justifies the correlations of the outputs to the inputs.

Once analytic functions are derived, the engine outputs can be predicted for any intermediate control values. Many parameters can serve as engine inputs. A few examples of these parameters are the combustion chamber geometry, valve timing, fuel composition, intake manifold pressure, water coolant temperature, air/fuel ratio, spark timing and the portion of the exhaust gases recirculated through the intake manifold. This list can be divided into two groups with one group including parameters, such as air/fuel ratio and spark timing, that can be controlled in real time, and with the other group including parameters, such as combustion chamber geometry that are fixed for a given engine and fuel composition, that is fixed for a given operating condition.

The variables air/fuel ratio, spark timing and the portion of the exhaust recirculated through the intake manifold are easy to control. The engine output, fuel and emissions levels, is strongly affected by them. Therefore high correlation between the engine outputs and these control variables can be expected.

Fuel efficiency and emissions are determined by chemical and thermodynamic processes. The way that the control variables affect these processes determines the engine input/output relationship. Fuel efficiency strongly depends on flame speed and on the spark timing [H-2]. HC formation depends mostly on the quenching layer next to wall which is formed by a slow flame propagation caused by cool wall temperature. In addition, the slow flame breaks down the appropriate chemical kinetics. As a consequence the burning is incomplete.

NO formation depends mainly on oxygen availability and high temperature, both of which are essential to promote the reaction. CO formation also depends on the amount of oxygen. The effect of the control variables on fuel and emissions is given below.

2. Fuel Dependence on Control Variables

Fuel consumption goes up, for a given engine load, as spark timing is either retarded or advanced from a point called MBT which is minimum spark timing for best torque. When the spark is retarded, the utilization of fuel is incomplete due to lack of time for the combustion process. Cylinder pressure buildup due to combustion is counteracted by the down movement of the piston in the expansion stroke. As this counteracting phenomenon is more pronounced for retarded spark, engine efficiency goes down since it depends on the pressure buildup. When spark is advanced beyond MBT. The pressure buildup occurs in the compression stroke rather than in the expansion stroke and it might work against the upgoing piston. Therefore engine efficiency is expected to decrease at this region also.

Fuel consumption should decrease as fuel mixture becomes leaner [T-1]. Excessive oxygen, which is typical to lean mixture, reduces the amount of unutilized fuel. In addition, air specific heat is lower than that of fuel. Therefore the combined air/fuel mixture specific heat goes down as the mixture becomes leaner. The cycle heat losses go down as the mixture becomes leaner since they are proportional to the specific heat, resulting in additional increase to engine efficiency. In very lean mixtures, however, fuel efficiency degrades because of an incomplete combustion due to weaker flame.

Injection of exhaust gas into the intake manifold is expected to have a limited effect on fuel consumption. Addition of EGR dilutes the fresh charge admitted to the cylinder. It was reported in [B-5] that this effect was quite small resulting in a slight increase in fuel consumption.

3. Emissions Dependence on Control Variables

Air/fuel ratio, spark advance and exhaust gas recirculation affect emission levels as follows:

a) AF Ratio:

HC - HC concentration is proportional to the product of the quench layer thickness and the fuel concentration in that layer. The quench thickness increases for either very lean or very rich mixtures, whereas fuel concentration decreases as air/fuel mixture becomes leaner. Therefore HC concentration is expected to reach a minimum, usually at a lean mixture. A cylinder-to-cylinder variation in air/fuel ratio can shift the minimum to a point richer than stochiometry since some of the cylinders might be lean even though the average mixture of the entire engine is rich. These lean cylinders will reduce the total HC level, resulting in an overall minimum for a total average mixture.

CO - CO oxidation to CO_2 depends on the availability of oxygen. CO concentration is high in rich mixtures due to lack of oxygen and is low in lean mixtures.

NO - NO concentration strongly depends on gas temperature and the available oxygen in the combustion. NO concentration is low for both rich and lean mixtures and peaks in some intermediate value. In very rich mixtures NO concentration is low due to lack of oxygen, whereas in very lean mixtures NO concentration is low due to low combustion temperature. Therefore a maximum can be expected in some intermediate value where combustion temperature is not too low and the amount of oxygen is sufficient for the reaction.

b) SA:

HC - Retarding the spark timing decreases HC levels since it increases exhaust temperature thus promoting oxidation in the exhaust tube.

CO - The effect of spark retard on CO concentration is similar to that on HC in trend but smaller in magnitude. The higher exhaust temperature due to spark retard further oxidizes CO. At very retarded spark lack of time to complete CO oxidation results in increased CO emissions. These increased emissions are offset to some extent by reduction in CO concentration caused by increased exhaust temperature.

NO - Spark retard should decrease NO concentration since it reduces peak combustion temperature. As NO formation depends on high temperature, the drop in temperature will result in decreased NO concentration.

c) EGR:

NO - Addition of exhaust gases to the intake manifold increases the mixture dilution reducing both flame speed and maximum cycle temperature. Therefore NO concentration is expected to go down as EGR level goes up.

HC - Addition of EGR increases the mixture dilution resulting in lowering the mixture temperature. Therefore HC concentration should go up. The quench layer thickness increases as temperature decreases resulting in higher HC concentration.

d) Load Influence

The various emission concentrations change with load as follows:

HC - HC concentration is expected to go down as engine speed goes up due to increased turbulence promoting the combustion and HC oxidation.

CO - One should not expect any effect on CO concentration due to changes in load, because CO formation is determined by the chemical kinetics which is not affected by the load.

NO - Two opposing effects on the formation of NO occur as engine speed increases. The first one is an increase in NO formation due to increased turbulence, whereas the second one is a decrease in NO formation due to increase in late burning. The increased turbulence reduces the heat loss per cycle resulting in an increase in NO concentration. For a given spark timing, late burning increases engine speed. This will cause a larger portion of the combustion to occur in the expansion stroke where temperature is lower which will decrease NO levels.

For rich mixtures the first effect is dominant, where combustion is rapid; whereas for lean mixtures the second effect is dominant, where late burning increases. Therefore, NO concentration goes up with engine speed for rich mixtures and goes down for lean mixtures.

C. THEORETICAL BACKGROUND

The undetermined function is found by the least squares method which minimizes the difference between the function and the data. The quality of fit is commonly judged by the "R-square" of the fit. In addition, the level of confidence that the various terms brought into the equation differ from zero can be checked by the F-statistics. These terms are defined and discussed below.

This chapter concludes with the discussion of individual vs. global fits, specifically the advantages and disadvantages of each approach.

1. Statistical Definitions

The quality of fit, or how well the fitted functions describe the engine performance is judged according to a few criteria; the most common one being the coefficient of determination known also as R-square which gives the ratio between the variance explained by the function to the total variance as given in the following formula: (see [M-2])

$$R^2 = \frac{\sum_{i=1}^{N} (\hat{y}_i - \bar{y})^2}{\sum_{i=1}^{N} (y_i - \bar{y})^2} = 1 - \frac{\sum_{i=1}^{N} (\hat{y}_i - y_i)^2}{\sum_{i=1}^{N} (y_i - \bar{y})^2} \tag{3.1}$$

where

$\hat{y}_i$ = predicted value of point i;

$\bar{y}$ = average value of measurements;

y_i = measurement at point i;

N = number of measurements.

For a perfect fit where the function passes through all the points, R-square is 1 because $\hat{y}_i = y_i$ for each i, whereas where the function does not explain any of the variance R-square is 0. Therefore, R-square gives a qualitative nondimensional measurement for the quality of the fit.

A few more relations derived to give some idea of how the variance is spread, are RMS, RMSP and RESPAV as defined in (3.2)-(3.4). RMS is the standard deviation; RMSP is the fraction of standard deviation from the average; RESPAV is the mean of the absolute relative deviation, giving a rough idea of what the average relative error is.

$$\text{RMS} = \sqrt{\frac{\sum_{i=1}^{N} (y-y_i)^2}{N}} \tag{3.2}$$

$$\text{RMSP} = \frac{\text{RMS}}{\bar{y}} \times 100 \tag{3.3}$$

$$\text{RESPAV} = \frac{100}{N} \sum_{i=1}^{N} \frac{\text{abs}(y-\hat{y})}{y} \tag{3.4}$$

Note that RMSP may be misleading in a few cases because it can assume a value close to 100% which does not necessarily reflect large unexplained variation. When function value changes considerably through the entire region with more points on the low value sides, $\bar{y}$ can be quite small. Yet the RMS can be high due to a variation at just a few high value points.

2. The Null Hypothesis and F-Statistics

The statistical significance of the various regressor variables can be evaluated by introducing the null hypothesis which checks if the i^{th} regression coefficient is zero, or if all the regression coefficients are zero. It is desired to check if the value of the regression coefficient is due merely to a random error.

The null hypothesis is associated with some level of confidence which can be evaluated by the F-statistics. The null hypothesis and the F-statistics are explained below.

The null hypothesis is stated as:

$$Ho:bi = 0$$

which means that the coefficient bi is zero. The level of confidence associated with rejecting this hypothesis can be evaluated. If, for example, this level of confidence is 99%, the null hypothesis will be rejected in 99 out of 100 cases.

The level of confidence can be evaluated by the F-statistics, which is defined as the ratio of two independent χ^2 (chi-square) variables, each divided by their degrees of freedom. This relationship is written as:

$$F(\nu_1, \nu_2) = \frac{U/\nu_1}{V/\nu_2} \qquad (3.5)$$

where U and V are independent random variables having χ^2 distribution with ν_1 and ν_2 degrees of freedom respectively.

A χ^2 distribution is a particular case of the exponential distribution and it is most useful in studying the distribution of a variance of a sample. A sequence of mutually independent variables μ_1, μ_2, μ_ℓ having a normal distribution can define a χ^2 distribution as follows. The variable S that is defined as:

$$S = \sum_{i=1}^{\ell} \mu_i^2 \qquad (3.6)$$

follows the χ^2 distribution with ℓ degrees of freedom. Based on the variance and the degrees of freedom of two samples, the F-ratio will indicate if the samples are drawn from the same population for a given level of confidence.

We wish to check the hypothesis that the F-ratio calculated in (3.5) follows the theoretical F-distribution. This hypothesis will be rejected by a level of confidence of at least $1-\alpha$ if

$$F(\nu_1,\nu_2) > F_{tabl}(\nu_1,\nu_2,\alpha)$$

where $F(\nu_1,\nu_2)$ is based on the experiments and evaluated according to (3.5) and $F_{tabl}(\nu_1,\nu_2,\alpha)$ is a tabulated value for ν_1,ν_2 degrees of freedom with a level of confidence α.

The first null hypothesis that can be checked is if the i^{th} regression coefficient is zero. This term is assumed to be entered last into the equation. The various terms of (3.5) are:

$U = Y_i$ marginal contribution to R-square due to the i^{th} term;

$\nu_1 = 1$;

$V = 1-R^2$ the unexplained variance;

$\nu_2 = N-k-1$;

where

N = number of data points;

k = number of terms in the regression equation.

Substituting the above in (3.5) yields:

$$F(1,N-k-1) = \frac{Y_i(N-k-1)}{1-R^2} \quad . \tag{3.7}$$

As stated above the null hypothesis will be rejected by a level of confidence of at least $1-\alpha$ of the value evaluated in (3.7) is greater than the tabulated value with 1 and N-k-1 degrees of freedom for a level of confidence α.

Rejection of the null hypothesis with a level of confidence of at least $1-\alpha$ is equivalent to rejection of the assumption that the i^{th} term is zero with a level of confidence of at least $1-\alpha$.

The other null hypothesis that can be tested is whether all the regression coefficients are zero. For this case the various terms in (3.5) are:

$U = R^2$ the explained variance;

$\nu_1 = k$ number of terms in the equation;

$V = 1-R^2$ the unexplained variance;

$\nu_2 = N-k-1$.

Substituting these expressions in (3.5) yields:

$$F(k,N-k-1) = \frac{R^2(N-k-1)}{(1-R^2)k} \quad . \tag{3.8}$$

The null hypothesis will be rejected (meaning that the assumption that all the terms are zero is rejected) with a level of confidence of at least $1-\alpha$ if the value evaluated in (3.8) exceeds the tabulated F ratio for k and N-k-1 degrees of freedom for a level of confidence α.

3. Global vs. Individual Fits

Functions can be fit to measurements in two ways. A single expression for either fuel or emissions can be derived over the entire range with AF, SA, EGR, TORQUE and RPM as independent variables, or functions can be fit for all measurements having the same torque and speed. The second method generates 10 functions with AF, SA and EGR as independent variables. A global fit is superior to 10 individual functions in terms of its compactness and ability to predict fuel and emissions levels at intermediate torque and rpm points rather than only at the 10 constant TORQUE-RPM points that were mapped.

A global expression is inferior to a set of individual expressions in the quality of fit for the same degree of polynomials, since the global expression has to compromise between a few groups of data resulting in an oversll expression that is different from that of the local expressions. As it will be discussed in Section F of this chapter, typical cross sections of both local and global fits for the fuel function is shown in Fig. 3.2, which clearly demonstrates the differences between the two methods of fit.

This idea can be demonstrated in the following simplified example. Suppose that y is a function of x and z, and that all the data points can be separated into two distinct groups according to the value of z with some points having $z = z_1$ and the rest having $z = z_2$ (see Fig. 3.1). y represents the dependent measurement, x represents any of the control variables and z represents TORQUE. For simplicity, only one control variable is used, yet the comparison between local and global fits can be extended quite easily for any number of control variables. Only linear relationships between y to x and y to z are assumed. Yet any nonlinearity can be converted into a linear relationship by an appropriate transformation. Lines A_1B_1 and A_2B_2 in Fig. 3.1 represent the local fits to the two data subsets with $z = z_1$ and $z = z_2$, respectively. These lines have slopes of a_1 and a_2. A single expression for the two data subsets is of the form

$$y = a_3x + a_4z + a_5 \quad . \qquad (3.9)$$

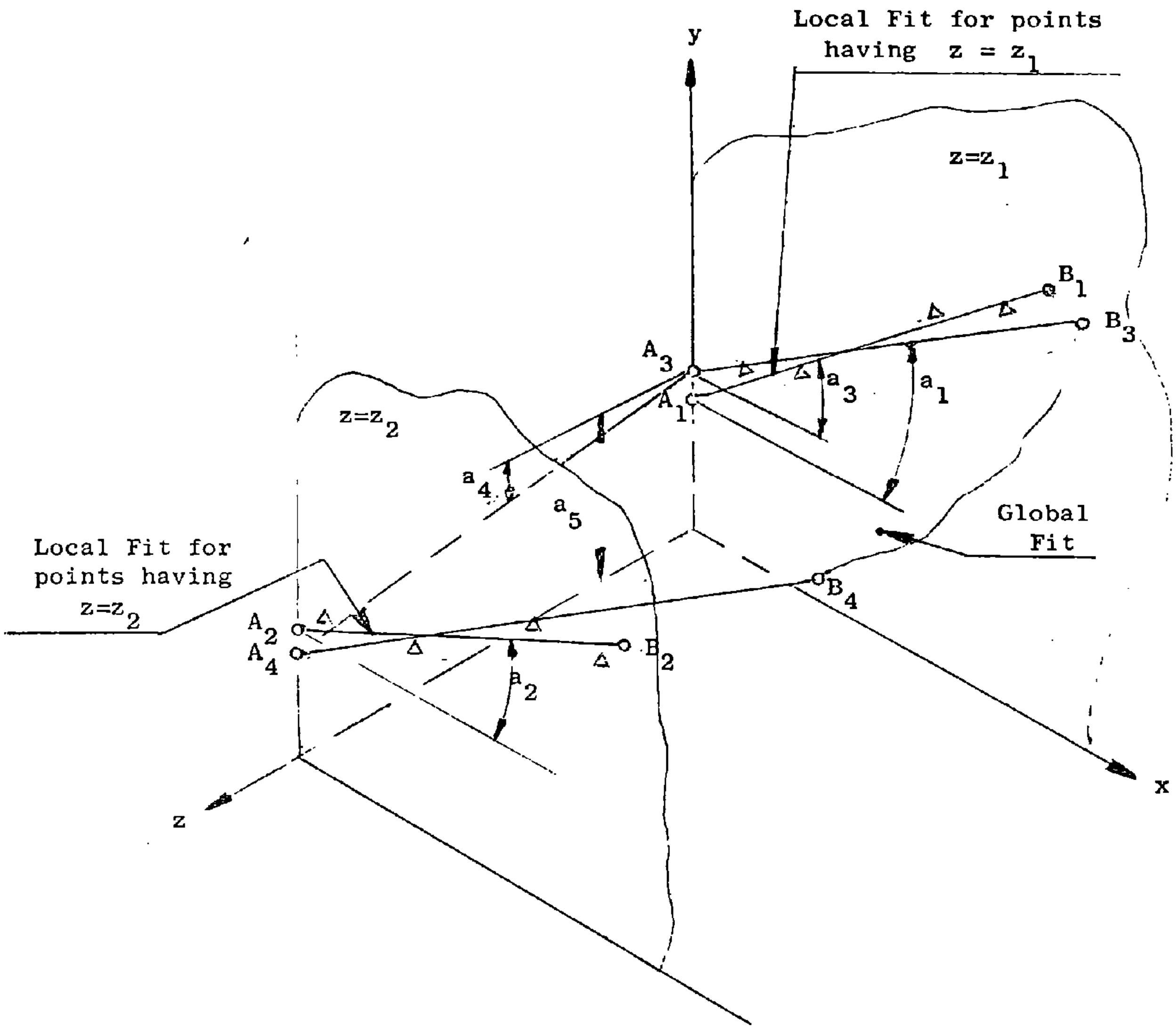

Fig. 3.1 AN ILLUSTRATION OF GLOBAL AND LOCAL FITS.

A_1B_1 and A_2B_2 are the local fits for the data subsets with $z=z_1$ and $z=z_2$ respectively, whereas $A_3B_3B_4A_4$ is the global fit for the two data subsets. The resituals of the global fit are larger than the residuals of the local fits.

The slope of the fit plane with respect to the z axis will differ from the slopes of lines A_1B_1 and A_2B_2 since it is determined so as to minimize the total residuals of both data subsets. This slope will be equal to those of A_1B_1 and A_2B_2 only if $a_1 = a_2$.

The plane $A_3B_3B_4A_4$ that is defined in (3.9) intersects the planes of $z = z_1$ and $z = z_2$ along lines A_3B_3 and A_4B_4. A_3B_3 gives a lower quality of fit to the data subset of $z = z_1$ because line A_1B_1 was found by the least squares method while considering only the data subset with $z = z_1$; therefore there cannot be any other line yielding smaller residuals. The mathematical proof will be as follows. Suppose there are n sets of measurements of the type $\{(x_{1i}, x_{2i}, \ldots, x_{ki}, y_i);\ i=1,2,\ldots,n\}$ where y_i is the observed value of the dependent variable and x_{1i} to x_{ki} are the values of the k independent variables in the i^{th} observation. Each observation satisfies the equation

$$y_i = b_0 + b_1 x_{1i} + b_k x_{ki} + e_i \quad . \tag{3.10}$$

The n observations will satisfy the following matrix equation:

$$Y = Xb + e \tag{3.11}$$

where

$$Y^T = (y_1, \ldots, y_n)$$

$$b^T = (b_0, \ldots, b_k)$$

$$X = \begin{pmatrix} 1 & x_{11} & x_{k1} \\ 1 & & \\ \vdots & \vdots & \vdots \\ 1 & x_{1n} & x_{kn} \end{pmatrix} \tag{3.12}$$

$$e^T = (e_1, \ldots, e_n) \quad .$$

b is the estimate of the parameters and e_i is the residual in the i^{th} measurement indicating the difference between the observed and the predicted value. The predicted value $\hat{Y}$ which is defined as $\hat{Y}^T = (\hat{y}_1, \ldots, \hat{y}_n)$ is evaluated as

$$\hat{Y} = Xb \quad . \tag{3.13}$$

The components of b are found by the least squares method which minimizes the residuals given by:

$$\min \sum_{i=1}^{n} e_i^2 = \min \sum_{i=1}^{n} (y_i - \hat{y}_i)^2 = \min (Y-\hat{Y})(Y-\hat{Y})^T \quad . \tag{3.14}$$

The solution is found by substituting for $\hat{Y}$ from (3.13), taking the derivative of (3.14) with respect to b and equating to zero. The final form is [W-2]

$$b = (X^T X)^{-1} X^T Y \quad . \tag{3.14}$$

The parameter estimates of the local and global fits of the simplified example given above can be found by substituting for X and Y accordingly.

The matrices X_1, Y_1, X_2, Y_2 that correspond to the data sets having $z = z_1$ and $z = z_2$ respectively are:

$$X_1 = \begin{bmatrix} 1 & x_{11} & z_1 \\ \vdots & \vdots & \vdots \\ 1 & x_{1n} & z_1 \end{bmatrix} ; \quad Y_1 = \begin{bmatrix} y_{11} \\ \vdots \\ y_{1n} \end{bmatrix} \tag{3.15}$$

$$X_2 = \begin{bmatrix} 1 & x_{21} & z_2 \\ \vdots & \vdots & \vdots \\ 1 & x_{2m} & z_2 \end{bmatrix} ; \quad Y_2 = \begin{bmatrix} y_{21} \\ \vdots \\ y_{2m} \end{bmatrix} \tag{3.16}$$

where n and m denote the number of measurements in the two data sets with $z = z_1$ and $z = z_2$, respectively. The regression coefficients vectors b_1 and b_2 of these two data sets are found by combining (3.14) with either (3.15) or with (3.16) yielding

$$b_1 = (X_1^T X_1)^{-1} X_1^T Y_1 \tag{3.17}$$

$$b_2 = (X_2^T X_2)^{-1} X_2^T Y_2 \quad . \tag{3.18}$$

The regression coefficient vector -b, of the entire data set can be evaluated by constructing the matrices X and Y of the entire data set and substituting in (3.14). X and Y are:

$$X = \begin{pmatrix} X_1 \\ ---- \\ X_2 \end{pmatrix} \quad ; \quad Y = \begin{pmatrix} Y_1 \\ ---- \\ Y_2 \end{pmatrix} \tag{3.19}$$

from which b is:

$$b = \left[(X_1^T : X_2^T) \begin{pmatrix} X_1 \\ ---- \\ X_2 \end{pmatrix} \right]^{-1} (X_1^T : X_2^T) \begin{pmatrix} Y_1 \\ ---- \\ Y_2 \end{pmatrix} \quad . \tag{3.20}$$

Carrying out the matrices' products yields:

$$b = (X_1^T X_1 + X_2^T X_2)^{-1} (X_1^T Y_1 + X_2^T Y_2) \tag{3.21}$$

solving for $X_1^T Y_1$ from (3.17) and for $X_2^T Y_2$ from (3.18) and substituting in (3.21) yields:

$$b = (X_1^T X_1 + X_2^T X_2)^{-1} (X_1^T X_1 b_1 + X_2^T X_2 b_2) \tag{3.22}$$

which means that the parameter estimate of the global fit b is a weighted average of the parameter estimates of the local fits b_1 and b_2. Only when $b_1 = b_2$ will

$$b = b_1 = b_2 \tag{3.23}$$

which means that the global fit can be equal to the local fit only if all the local fits are identical. The quality of fit of the local expressions can be compared now to that of the global expressions. R-square is defined as (using (3.12))

$$R^2 = 1 - \frac{\sum_{i=1}^{N} (y_i - \hat{y}_i)^2}{\sum_{i=1}^{N} (y_i - \bar{y})^2} = 1 - \frac{e \cdot e^T}{\sum (y_i - \bar{y})^2} \quad . \tag{3.24}$$

$\hat{y}$ was selected to minimize $e \cdot e^T$ and thereby to also maximize R^2. Therefore if any values of $\hat{y}$ other than those found in (3.13) are used, R^2 will become smaller. Therefore, if the predicted values of the global fit are used to check the quality of fit of the local data set, they will yield worse results. Only in the unique case that the regression coefficients of all local data sets are equal, will the global fit be the same as the local fit, otherwise it will be inferior. Figure 3.2 demonstrates how a global fit can produce a lower quality fit than a local fit, and even is not able to follow the general shape of the measurements.

As discussed in III.D polynomial series were used for fitting. The number of terms considered in the regression fitting for a given degree of the polynomial goes up sharply with the number of the independent variables, as shown in Table 3.1 since all the cross coupling terms are considered also.

No. of m = variables	n = degree of polynomial 2	3	4
3	10	20	35
5	21	56	126

TABLE 3.1 Number of Terms in a Polynomial of Degree n, with m Independent Variables.

Therefore for the same number of terms, the degree of the polynomial goes down as the number of the independent variables goes up. From Table 3.1 it is obvious that a fourth order polynomial of 3 independent variables has less terms than a third order polynomial of 5 independent variables. As the complexity of the expressions goes up with the number of terms, maintaining the same number of terms in the equation will result in lowering the degree of the polynomial of the local expression as compared to the global expression thus affecting the quality of fit.

D. FUNCTION SELECTION

The measurements are known to have a nonlinear dependence on the independent variables. No attempt was made to evaluate the physical functions. Instead, empirical expressions were evaluated. A power series was tried because of ease of generation. As it was not known beforehand which are the dominant terms, a fourth order polynomial of the three independent variables was tried for the individual fits, and a third order polynomial with 5 independent variables was tried for the global fits. The computer program selected the terms that best explained the variation in the measurements.

One of the disadvantages of a power series is the high correlation between many terms. For example x^2 is highly correlated with either x or x^3, etc. This eliminates many terms from the power series resulting in a lower number of terms to be introduced into the equation, thus affecting the total R-square. This drawback was overcome by using orthogonal functions which are defined as:

$$\int_a^b P_n(x)P_m(x)\omega(x)\,dx = \begin{cases} 0 & n\neq m \\ 1 & n=m \end{cases} \qquad (3.25)$$

over a range (a,b) and a weighting function $\omega(x)$. This approach is justified because of the similarity between the orthogonal functions defined in (3.25) and the correlation function defined as:

$$C(x,y) = \sum_{i=1}^{N} (x_i-\bar{x})(y-\bar{y})p(x,y) \quad , \qquad (3.26)$$

where the weighting function of (3.25) is the probability function $p(x,y)$ and the integral is replaced by a summation.

The orthogonal functions that were tried are the Legendre Polynomials which are:

$$P_0(x) = 1 \quad (3.27)$$

$$P_1(x) = x \quad (3.28)$$

$$P_2(x) = 1.5x^2 - 0.5 \quad (3.29)$$

$$P_3(x) = 2.5x^3 - 1.5x \quad (3.30)$$

$$P_4(x) = 4.375x^4 - 3.75x^2 + .375 \quad . \quad (3.31)$$

The introduction of these expressions enables the computer program to select the dominant terms from a longer list thus obtaining a higher R-square. While using a Legendre polynomial, a typical term like $AF^2 \cdot SA \cdot EGR$ will actually be $(1.5AF^2 - 0.5)SA \cdot EGR$.

An attempt to set a function for the emissions could yield negative predicted values in the low range. This is typical for functions that might vary by a few orders of magnitude over the entire range and the predicted function which can usually assume lower values than the measurements can be negative for the low valued measurements. In addition, even when no negative predicted values are obtained, the quality of fit can be degraded while trying to estimate the parameters of functions that vary considerably. These drawbacks can be eliminated by using the natural log of the emissions. This method reduces the range of the measurements and as a consequence improves the quality of fit. A complete listing of the polynomial expressions of all the cross coupling terms is given for the global fit in Appendix C and for the local fit in Appendix E.

E. BMDP2R PROGRAM

This program computes estimates of the parameters of a multiple linear regression equation in a stepwise manner using the least squares method. The BMDP2R is a part of the BMDP (BioMedical Computer Programs) P-series (B-3) and was preferred to similar statistical packages because of an easy access to the source code that made storage of the regression coefficients possible.

The subroutine that prints the regression coefficients was modified to also write them to a disk. The modified subroutine was compiled and linked with the rest of the program.

The fuel and emission measurements converted to mass flow, together with the independent variables AF,SA and EGR that were sorted by DSP(Sec. II.D.2) and stored in matrices according to the torque and speed serve as an input.

The TRANSF subroutine of the program enables us to introduce new independent variables which are functions of the original independent variables. 31 terms were added to account for all possible high power terms of the local fits. These terms describe a fourth order polynomial with 3 independent variables. 16 and 51 terms were added for the second and third order polynomials respectively for the global fit having 5 independent variables.

The stepwise regression method enters or removes independent variables according to two methods: the F method and the R method. The F method removes any variable if its F-to-remove is less than the F-to-remove limit which means that the level of confidence that the coefficient is zero is larger than a desired limit. If no variable meets this criteria, the variable with the largest F-to-enter is entered if the F-to-enter exceeds the F-to-enter limit (implying that the variables with the lowest level of confidence of being zero is entered).

The R method removes the variable with the smallest F-to-remove if its removal results in a larger multiple R than was previously obtained for the same number of variables. If no variable meets this criterion a variable is entered as for F. The R method was preferred because it gives rise to a higher R-square. It turns out that the first variables to be entered explain the variance more than the terms to be last entered. The stepwise process of bringing new terms terminates when the next variable to be introduced is correlated with the other variables above a certain value selected as 0.99.

The program printout includes statistical information at each stage about the current R-square and the regression coefficients of the already entered variables in a regular as well as in standard form. The F-ratio is also displayed.

Following the stepwise process, the program prints a stepwise summary table of the R-square obtained by considering all the terms introduced up to that step and the F-to-enter ratio of the considered terms (see Table 3-8).

F. RESULTS

Polynomials were fitted both for sets of data of the same torque/RPM points and to the entire data base the quality of fit of these two methods as well as a comparison with some other results reported recently, is given below. Probable causes for the measurements residual are discussed together with the effect of torque and speed fluctuation around the nominal values. This section concludes with the comparison of the predicted functions with the theoretical relationships that were outlined in III.B.

1. Quality of Fit and Comparison to Other Works

Forty individual functions were fit to the measurements. The associated statistics are given in Table 3-2. Functions were fit to fuel and to log of emissions, yet the statistical values were evaluated for the physical values. Thirty-five functions are described by Legendre Polynomials which usually yielded higher R-square. Only for 5 cases was it discovered that regular polynomials were preferable. R-square, RMS, RMSP and RESPAV were defined in III.C. A typical value of RMSP (RMS over average measurement) can be 2% for fuels, 35% for HC, 37% for CO and 27% for NO.

Global functions were fit to fuel measurements and to log of emissions for the entire data base. A second order polynomial as well as a third order were tried. No improvement in R-square was obtained by the usage of Legendre polynomials, therefore regular polynomials were used. The statistics associated with the physical values of the global fits as well as with the log of emissions is given in Table 3-3.

Parameter estimates of engine mapping were reported by Trella [T-2] and by Tennant [R-3]. A comparison of the global functions with the individual expressions, as well as with the results reported in [T-2] and in [R-3], is given in Table 3-4. The statistics of the 40 individual functions which appear in Table 3-2 are summarized in the first part of the table. The functions were fit to log of emissions, yet R-square was evaluated for the corresponding predicted physical values.

Each box of the first part of the table contains the range of

TORQUE	RPM	FUEL RSQ	FUEL RMS	FUEL RMSP	FUEL RESPAV	HC RSQ	HC RMS	HC RMSP	HC RESPAV
50	1700	0.959	0.229	2.289	1.805	0.875	22.915	21.630	18.903
25	1800	0.974	0.221	2.719	2.112	0.900	68.607	42.431	18.656
75	2100	0.969	0.211	1.367	1.060	0.799	23.211	31.379	26.377
50	2250	0.960	0.262	2.000	1.645	*0.864	28.329	28.525	18.986
38	2600	0.976	0.265	1.950	1.539	0.788	106.977	89.265	28.843
20	1400	0.963	0.184	3.196	2.601	0.885	45.581	32.412	22.603
85	2500	0.926	0.434	2.031	1.670	0.870	14.053	46.764	32.519
72	2900	0.959	0.253	1.193	0.968	*0.735	13.471	34.748	26.012
-14	1800	0.939	0.100	2.554	2.054	0.877	84.454	22.793	22.107
15	750	0.958	0.052	1.967	1.355	*0.365	1.200	12.456	10.832

TORQUE	RPM	CO RSQ	CO RMS	CO RMSP	CO RESPAV	NO RSQ	NO RMS	NO RMSP	NO RESPAV
50	1700	0.897	64.224	49.246	32.583	0.885	2.640	28.979	19.365
25	1800	0.884	16.548	31.649	21.818	*0.798	1.262	45.875	23.445
75	2100	0.960	83.460	32.548	24.123	0.765	9.794	24.451	23.946
50	2250	0.939	74.349	39.048	19.036	0.843	6.282	34.204	20.952
38	2600	0.835	49.531	51.949	13.620	0.803	4.994	39.699	27.429
20	1400	0.653	7.162	31.869	28.016	0.848	0.318	42.368	25.761
85	2500	0.782	159.915	49.388	33.698	0.905	7.024	14.799	13.447
72	2900	0.943	46.403	32.689	18.432	*0.827	12.205	18.849	13.154
-14	1800	0.929	0.979	11.564	8.855	0.891	0.007	14.451	10.792
15	750	0.854	9.375	50.316	50.169	0.937	0.007	11.183	9.974

TABLE 3-2

Summary Table of Residuals of the Physical Values of the Individual Fits Which Were Evaluated For Fuel and For Log (Emissions). Legendre Polynomials Were Used Except Where Regular Polynomials Were Used As Marked by * .

SUMMARY TABLE OF RESIDUALS FOR GLOBAL FIT (LOG)

SECOND ORDER

	RSQ	RMS	RMSP	RESPAV
FUEL	0.985	0.744	6.127	5.454
HC	0.763	0.661	16.361	21.636
CO	0.757	0.701	418.428	98.518
NO	0.959	0.483	31.726	58.353

THIRD ORDER

FUEL	0.994	0.454	3.738	3.944
HC	0.832	0.555	13.719	18.270
CO	0.866	0.519	13.645	45.093
NO	0.974	0.388	25.431	45.012

SUMMARY TABLE OF RESIDUALS FOR GLOBAL FIT (PHYSICAL)

SECOND ORDER

FUEL	0.985	0.744	6.127	5.454
HC	0.277	148.125	118.967	62.370
CO	0.658	145.617	109.922	64.329
NO	0.819	11.288	54.520	42.874

THIRD ORDER

FUEL	0.994	0.454	3.738	3.944
HC	0.526	119.988	96.353	51.883
CO	0.739	127.169	95.997	45.070
NO	0.886	8.950	43.226	33.801

TABLE 3-3

Summary Table of Residuals of Global Fits Evaluated For Fits of Fuel and Log (Emissions) As Well As For The Physical Measurements.

			FUEL	HC	CO	NO
INDIVIDUAL FIT		PHYSICAL VALUE	0.9279-0.9888 $\overline{RSQ}$ = 0.964 $\bar{n}$ = 10.6	0.365-0.900 $\overline{RSQ}$ = 0.796 $\bar{n}$ = 9.8	0.782-0.960 $\overline{RSQ}$ = 0.888 $\bar{n}$ = 10.5	0.765-0.937 $\overline{RSQ}$ = 0.850 $\bar{n}$ = 10.0
INDIVIDUAL FIT		LOG		0.366-0.969 $\overline{RSQ}$ = 0.858 $\bar{n}$ = 9.8	0.804-.958 $\overline{RSQ}$ = 0.909 $\bar{n}$ = 10.5	0.775-0.939 $\overline{RSQ}$ = 0.846 $\bar{n}$ = 10.0
GLOBAL FIT	2nd ORDER	PHYSICAL VALUE	0.9851 (10) 0.984 (7)	0.277	0.658	0.819
GLOBAL FIT	2nd ORDER	LOG		0.766 (17) 0.748 (10)	0.758 (13) 0.755 (9)	0.961 (18) 0.943 (6)
GLOBAL FIT	3rd ORDER	PHYSICAL VALUE	0.994 (19) 0.980 (5)	0.526	0.739	0.886
GLOBAL FIT	3rd ORDER	LOG		0.832 (16) 0.816 (11)	0.866 (13) 0.845 (9)	0.974 (17) 0.969 (4)
GLOBAL FIT	REFERENCE DATA	TRELLA'S[T-2] 121/305 CID	2nd Order 0.98/0.99	3rd Order Log 0.89/0.87	2nd Order Log 0.84/0.84	2nd Order Log 0.93/0.98
GLOBAL FIT	REFERENCE DATA	TENNANT'S[R-3] 350 CID	2nd Order 1.00	3rd Order Log 0.931	3rd Order Log 0.973	3rd Order Log 0.988

TABLE 3-4 Summary table of residuals of the individual and global fits as compared to reference data in [T-2] and in [R-3].
Log means that the residuals were evaluated for a prediction function of Log (Emissions).
Physical Value means that the residuals were evaluated for a prediction function of emissions.

$\overline{RSQ}$ is the average of the individual fits

$\bar{n}$ is the average number of terms in the individual fits
The number in parentheses denotes number of terms brought into the equation.

R-square of the individual fits, the average value for the 10 functions and the average number of terms brought into the equation.

The second part of the table lists R-square and the number of terms used in the global fits. R-square was evaluated both for log of emissions and for the predicted physical values. R-square was also evaluated both for second and third order polynomials. Some intermediate results of the stepwise regression fitting are given in the table. For example, 4 terms can explain 96% of the total variation of log(NO) when a third polynomial is fitted, whereas the next thirteen terms explain additional 0.0135 of the total variation.

The results reported in [T-2] and in [R-3] are listed for comparison. Trella's results correspond to 121 and 350 CID engines respectively, whereas Tennant's results correspond to a 350 CID engine.

The value of R-square of the fuel function is quite close to the values reported in the two other sources. The largest discrepancy was noticed for log(HC) where our fit yielded R-square of 0.83 as compared to 0.87 or 0.93 reported in [T-2] and [R-3] respectively. Log(CO) yielded inferior results to those quoted in [R-3] -- 0.86 vs. 0.97. [T-2] obtained similar R-square results for log(CO) -- 0.84, although he used second order polynomials while we used third order polynomials. Log(NO) quality of fit yielded results similar to those reported in the two other sources. The second order polynimial found in [T-2] with R-square of 0.93/0.98 is similar to our second order polynomial with R-square of 0.96, whereas the third order polynomial reported in [R-3] with R-square of 0.988 is superior to our third order polynomial having R-square of 0.974.

The quality of fit of the global function can be compared to that of the 10 individual functions by examining the residuals. The global expression depends on AF, SA, EGR, TORQUE and RPM. In the comparison of the quality of fit to that of the individual function, TORQUE and RPM assume the measured values. The statistics for how well a global function can fit to a data subset (all measurements with the same nominal torque and speed) is given in Table 3-5. As expected, the residuals and hence rms always increased as compared to the individual fits, sometimes by a few percent and sometimes by a factor of 10.

SUMMARY TABLE OF RESIDUALS FOR GLOBAL FIT

THIRD ORDER POLYNOMIALS

		FUEL				HC			
TORQUE	RPM	RSQ	RMS	RMSP	RESPAV	RSQ	RMS	RMSP	RESPAV
50	1700	0.897	0.365	3.651	2.917	0.532	44.415	41.926	30.432
25	1800	0.939	0.341	4.186	3.511	0.666	125.358	77.530	49.174
75	2100	0.907	0.306	2.369	1.922	0.203	46.180	62.431	45.694
50	2250	0.929	0.352	2.684	2.108	0.633	46.460	46.780	30.326
38	2600	0.925	0.462	3.408	2.218	0.557	154.712	129.097	67.654
20	1400	0.776	0.454	7.890	6.479	0.609	83.955	59.699	38.244
85	2500	0.799	0.726	3.394	2.534	0.568	25.609	85.223	58.679
72	2900	0.882	0.495	2.332	1.960	0.391	20.396	53.933	101.078
-14	1800	0.828	0.392	10.008	8.268	-0.332	277.638	74.930	46.862
15	750	-2.945	0.508	19.161	17.515	-22.797	7.342	76.239	60.587

		CO				NO			
TORQUE	RPM	RSQ	RMS	RMSP	RESPAV	RSQ	RMS	RMSP	RESPAV
50	1700	0.558	132.801	101.829	44.422	0.762	3.803	41.748	28.490
25	1800	0.433	36.612	70.022	28.605	0.344	2.276	82.705	27.096
75	2100	0.850	160.901	62.748	54.718	0.661	11.760	29.361	30.812
50	2250	0.660	176.230	92.557	40.252	0.685	8.904	48.484	46.818
38	2600	0.604	76.879	80.633	22.470	0.730	5.838	46.403	33.271
20	1400	0.376	14.770	65.717	35.689	0.464	0.596	79.578	28.925
85	2500	0.513	239.003	73.813	39.150	0.678	12.927	27.238	27.045
72	2900	0.708	103.585	71.793	44.450	0.647	17.923	28.058	31.582
-14	1800	-5.653	9.482	111.959	76.432	-0.604	0.025	55.515	45.412
15	750	0.289	20.681	111.001	122.112	-0.536	0.037	55.100	50.700

TABLE 3-5

Summary Table of Residuals of the Global Functions Evaluated at the Points of Constant Torque and RPM. The Residuals are Evaluated for the Physical Values of Fuel and Emissions. The Functions Fit for Fuel and Log (Emissions).

Therefore, the global function is quite similar to some of the individual expressions, but is quite far off from some other individual functions.

The R-square values listed in Table 3-5 have a different meaning than those in Table 3-2 because they were not evaluated for a least square fit. According to equation (3.1), R-square is confined to the region (0,1) when the predicted function was found by least squares method. In this case R-square was evaluated according to:

$$R^2 = 1 - \frac{\sum_{i=1}^{n} (\hat{y}_i - y_i)^2}{\sum_{i=1}^{n} (y_i - \bar{y})^2}$$

where $\hat{y}_i$ is the value predicted by the local fits.

As the predicted function was not derived by a least square method, the sum of residuals can exceed the total variance in very poor cases, thus causing R-square to be negative. Comparison of R-square of the global fit to that of any individual fit has to be done very carefully. The third order global fuel function has R-square of 0.994, while R-square of a fourth order individual fuel function with TORQUE/RPM = 85/2500 is 0.928. It is misleading to conclude that the global function is superior in that region because these two functions were evaluated with different data bases and have different number of independent variables. Actually in that region, the individual function is superior to the global fit. This idea can be demonstrated in Fig. 3.2 where the observed values for fuel at 85/2500 ft lb/rpm, as well as the predicted values of both the global and the individual fit, are displayed.

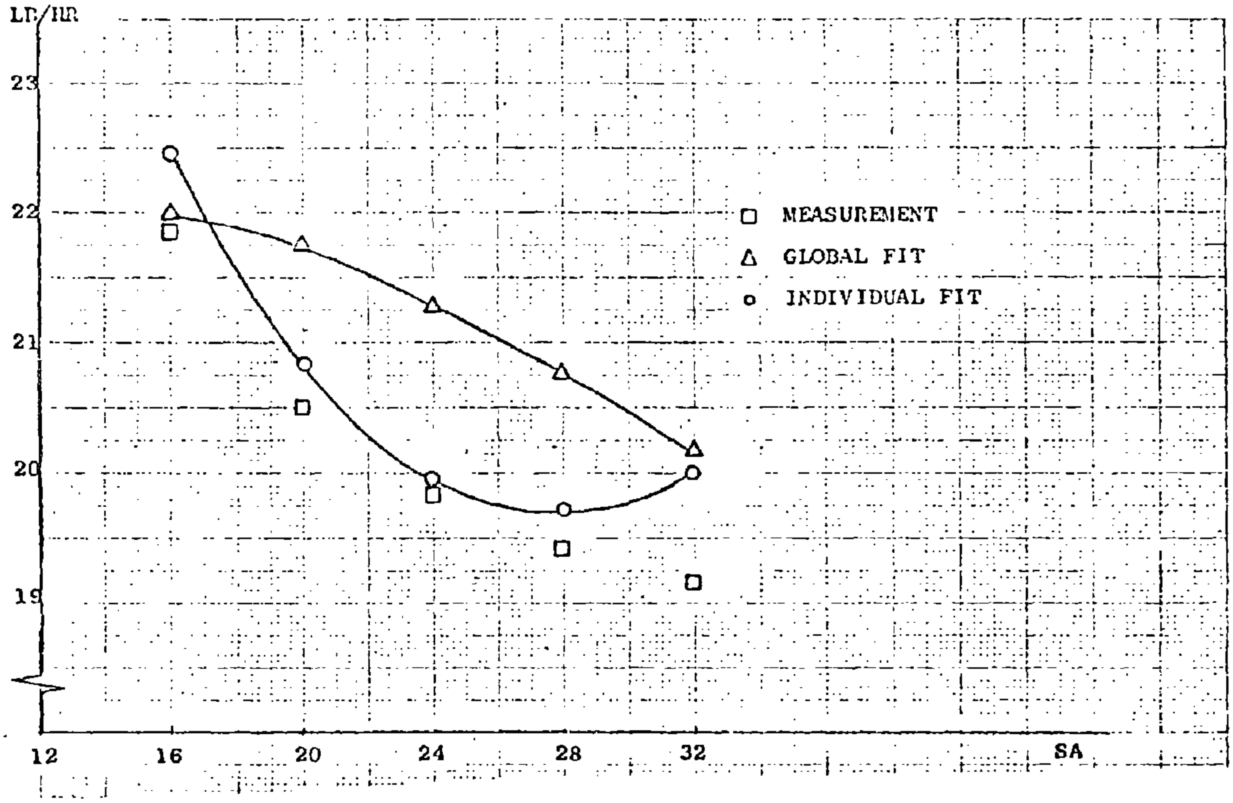

Fig. 3.2 GLOBAL AND INDIVIDUAL FITS OF FUEL WITH TORQUE/RPM = 85 lb ft/ 2500 rpm AF/EGR = 14.7/0.

The R-square of the global and local fits are 0.995 and 0.928 respectively. The global fit is not capable of tracking the general shape of the data as well as the local fit.

2. Residual Analysis

There are several possible reasons for the unexplained variation:

a) instrument noise;

b) engine fluctuations;

c) measurement schedule;

d) functions selected for the fitting process.

The emission instruments were periodically calibrated during the experiment, yet a 10% drift could be noted occasionally, especially when ambient temperature was changing.

The engine behavior is not constant and repeatable and a cycle to cycle variation occurs. Averaging the most recent 50 readings as explained in (Sec. II.D.2) reduced this effect, yet engine fluctuation effect was not entirely eliminated.

TORQUE and RPM were assumed to equal the nominal settings. As TORQUE and RPM varied, additional noise was possibly added to engine measurements. A detailed discussion of this effect is given below.

The emission measurement is somewhat related to the way the data point is approached. As discussed in II.E, some of the measurement points were approached by retarding the spark and some by advancing it, which had an impact on engine and exhaust gas temperature transients. As no thermal equilibrium was obtained due to short time intervals between measurements, a small additional error was introduced.

As it was discussed in III.D, the functions selected in the parameter estimate process have a strong influence on R-square. Only polynomials were tried. Probably more complicated functions could describe the measurements better, especially when the function value was changing abruptly. Fuel measurements have the highest R-square because of several reasons. Fuel flow measurement is very accurate with an error of less than 1% as opposed to a much larger error in the emission instruments (Sec. II.C). In addition, fuel data spread is much smaller than that of emissions. The highest to lowest fuel flow ratio for a given TORQUE and RPM point does not exceed 1.5 as compared to 100 for emissions. As the quality of fit degrades with increased data spread, fuel has a higher R-square than emissions.

3. TORQUE-RPM Fluctuations

One of the possible contributors to residuals in the individual fit is the deviations of TORQUE and RPM from their nominal settings. While fitting a function to measurements having the same TORQUE and RPM, it was assumed that TORQUE and RPM were identical for all the measured points.

As it can be seen in Table 3-6, the average values were quite close to the nominal settings with relatively small rms of 1 rpm for speed and 1 lb ft for TORQUE. The actual measurements of fuel and emissions differ slightly from those that might have been obtained had TORQUE and RPM been held exactly at the nominal value. The effect on the residuals can be found by evaluating the measurements at the nominal TORQUE and RPM settings according to the following formula:

$$F_{nom} = F_{meas} + (T_{meas} - T_{nom}) \left. \frac{\partial F_{global}}{\partial T} \right|_{\substack{T=T_{meas} \\ RPM=RPM_{meas}}} + (RPM_{meas} - RPM_{nom}) \left. \frac{\partial F_{global}}{\partial RPM} \right|_{\substack{T=T_{meas} \\ RPM=RPM_{meas}}} \qquad (3.32)$$

where nom denotes the value at the nominal TORQUE/RPM point, meas is the actual measurement and T is the load. Global indicates the single function fit over the entire range. This procedure was repeated for emissions except that it was actually done for log of emissions as the global function describing emission was fit to the log of the measurements.

The various statistical values evaluated for the original data as R-square, RMS, RMSP and RESPAV were evaluated again for the corrected data. An expedient way to get a rough estimate of how these statistical values change for the corrected data is to assume that the predicted functions are unchanged. This imposes a lower bound on R-square and an

NOMINAL RPM	AVERAGE RPM	RMS RPM	NOMINAL TORQUE	AVERAGE TORQUE	RMS TORQUE
1700.	1702.8360	1.2876	50.	45.8709	0.4181
1800.	1802.5580	1.5105	25.	24.9223	0.3527
2100.	2101.7020	1.4961	75.	74.8930	0.4678
2250.	2251.9080	1.1646	50.	50.0536	0.2970
2600.	2601.3010	1.2211	38.	37.9334	0.3068
1400.	1401.2030	1.7059	20.	20.1024	0.3399
2500.	2501.8020	0.9800	85.	84.8746	0.3660
2900.	2899.2490	1.1711	72.	71.9155	0.4431
1800.	1800.7880	1.3030	-14.	-14.0232	0.2793
750.	753.5396	1.4825	15.	14.9170	0.2692

TABLE 3-6

RPM and TORQUE Statistics

(RPM in rpm, TORQUE in lb ft)

TORQUE	RPM	FUEL RSQ	FUEL RMS	FUEL RMSP	FUEL RESPAV	HC RSQ	HC RMS	HC RMSP	HC RESPAV
50	1700	0.957	0.236	2.359	1.872	0.871	23.389	22.025	19.018
25	1800	0.974	0.222	2.725	2.128	0.898	69.704	43.043	18.731
75	2100	0.972	0.202	1.309	1.063	0.802	23.216	34.311	26.143
50	2250	0.961	0.259	1.979	1.632	0.867	28.051	28.140	18.907
38	2600	0.975	0.268	1.976	1.558	0.796	103.432	86.567	28.754
20	1400	0.965	0.179	3.126	2.568	0.885	45.775	32.468	22.758
85	2500	0.930	0.433	2.025	1.672	0.871	14.182	46.722	32.338
72	2900	0.968	0.261	1.228	0.987	0.734	13.433	34.836	26.155
-14	1800	0.988	0.103	2.637	2.065	0.873	85.873	23.232	22.067
15	750	0.967	0.046	1.750	1.244	0.363	1.222	12.651	10.965

TORQUE	RPM	CO RSQ	CO RMS	CO RMSP	CO RESPAV	NO RSQ	NO RMS	NO RMSP	NO RESPAV
50	1700	0.893	65.646	50.119	32.626	0.888	2.612	28.723	19.169
25	1800	0.883	16.675	31.900	21.943	0.793	1.275	46.217	24.015
75	2100	0.960	83.242	32.425	24.243	0.770	5.654	24.225	23.968
50	2250	0.939	74.568	39.179	19.131	0.842	6.325	34.608	21.206
38	2600	0.834	49.962	52.229	13.537	0.803	4.989	39.519	27.450
20	1400	0.856	7.122	31.747	27.969	0.853	0.310	41.752	25.954
85	2500	0.782	161.107	49.448	33.629	0.905	6.976	14.832	13.577
72	2900	0.958	39.078	26.999	17.317	0.820	12.495	19.227	13.499
-14	1800	0.929	0.974	11.503	8.876	0.883	0.007	14.841	11.042
15	750	0.855	9.397	50.363	49.932	0.930	0.008	11.779	10.199

TABLE 3-7

Summary Table of Residuals in Which Data Used in
Table 3-2 Was Corrected For RPM And TORQUE Fluctuations

Fig. 3.3 COMPARISON OF R-SQUARE OF THE INDIVIDUAL FITS AND OF THE FUNCTIONS FIT TO DATA CORRECTED FOR TORQUE AND RPM FLUCTUATIONS IN VARIOUS TORQUE/RPM POINTS.

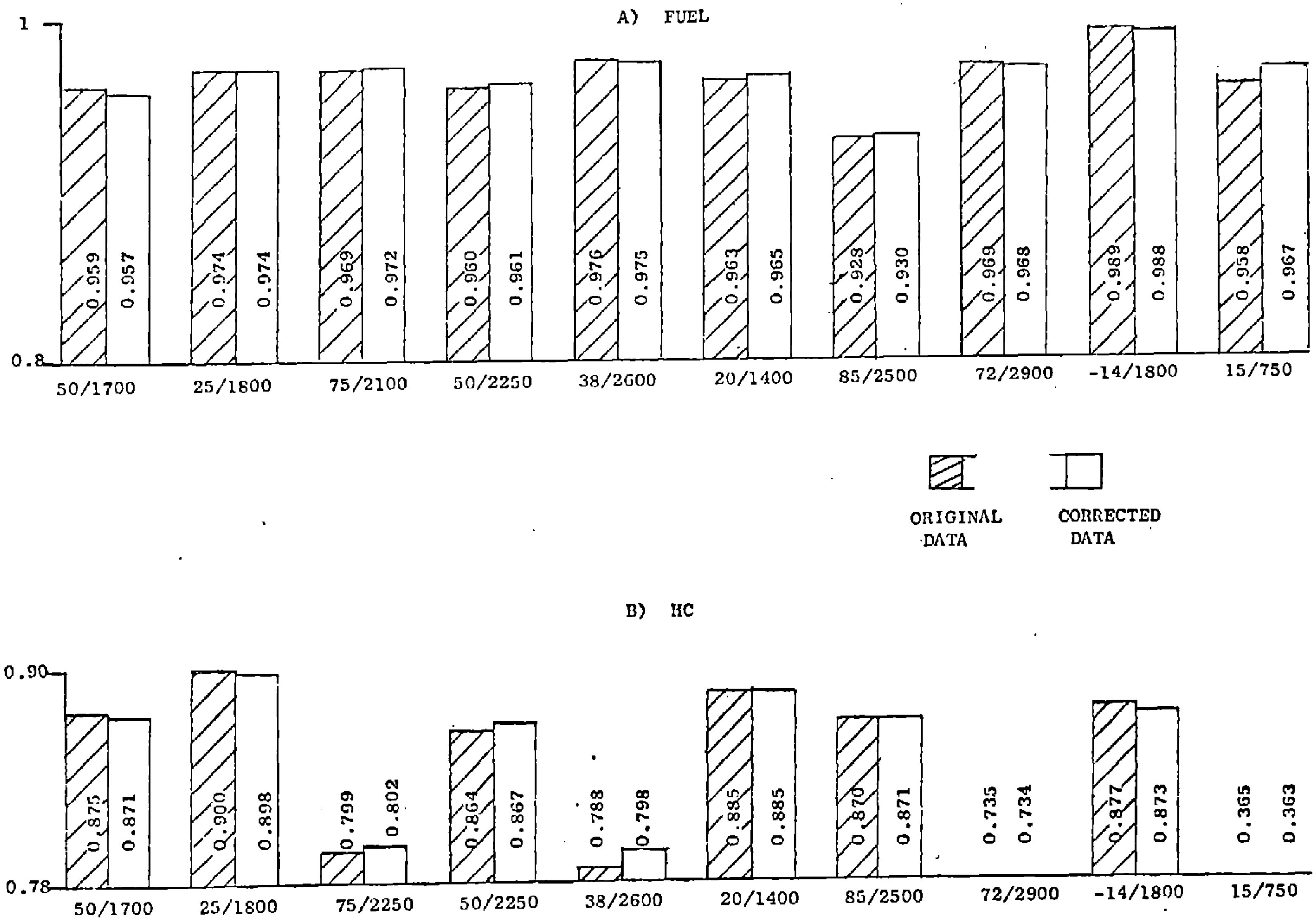

Fig. 3.3 (Cont.) COMPARISON OF R-SQUARE OF THE INDIVIDUAL FITS AND OF THE FUNCTIONS FIT TO DATA CORRECTED FOR TORQUE AND RPM FLUCTUATIONS IN VARIOUS TORQUE/RPM POINTS

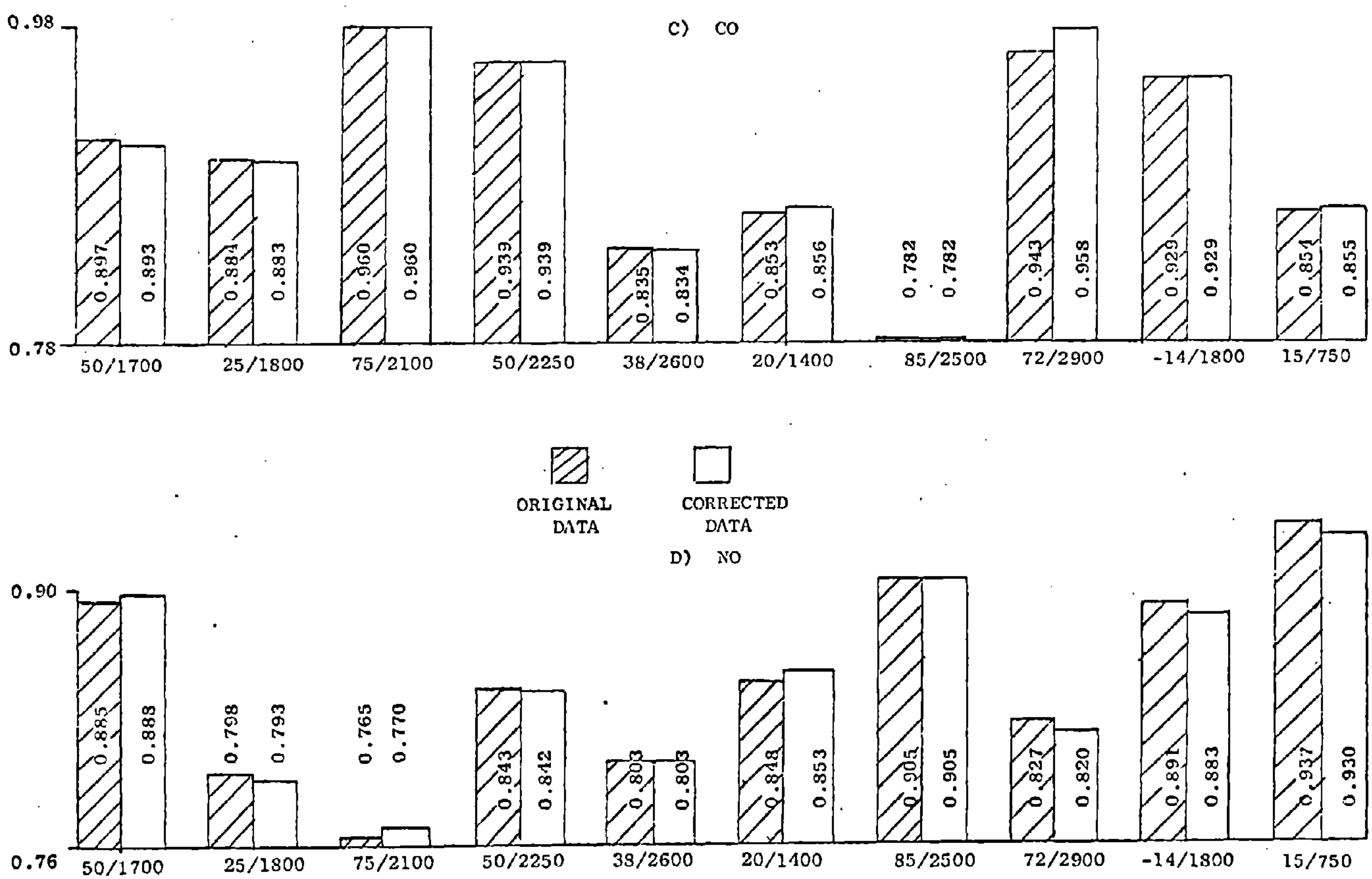

upper bound on RMS, because the quality of fit of an arbitrary function to a given data set will always be inferior to that of the function evaluated by the least squares method.

The statistics for the corrected data are given in Table 3-7 where RSQ is R-square, RMS is the root mean square, RMSP is the RMS to average measurement ratio in percents and RESPAV is the average of the absolute value of the ratio of the residual to the measurement. The predicted values of the original data were used. As seen in Table 3-7 the corrected data yielded some improvements in the quality of fit in a few cases with RMS going down by up to 5% and R-square going up by 0.03, whereas the quality of fit decreased in a few other cases due to the fact that a non-least square function was used. Comparison of R-square of the original data to that of the corrected data is displayed in Fig. 3.3 from which it can be concluded that the contribution of TORQUE and RPM fluctuations to the residuals of the individual functions is quite small.

4. Comparison of the Experimental Functions with the Theoretical Predictions

A few cross sections of some of the functions are displayed in Figs. 3.4 to 3.10. Functions having the highest and lowest R-square were selected to give an idea about the entire spectrum of R-square. The dependence of fuel and emissions measurement on the engine controls (AF, SA and EGR) can now be compared with the theoretical relationships that were discussed in III.B.

The measured fuel consumption closely follows the theoretical analysis which predicted a decrease in fuel consumption as spark advances up to the angle where additional spark advance increases fuel consumption since most of the cylinder pressure buildup occurs in the compression stroke rather than in the expansion stroke. Leaning the mixture did improve fuel consumption except for very lean mixtures where it went up again. Addition of EGR always increased fuel consumption (see Fig. 3.4).

HC concentration increased as expected when spark was advanced; the dependence on AF was not uniform at the various TORQUE/RPM points. In a few cases the minimum occurred at a lean mixture, while in a few other cases it occurred at rich mixtures. Addition of EGR usually increased HC concentration (see Figs. 3-5, 3-6).

CO concentration increased when spark was advanced for lean mixtures whereas it decreased for rich mixtures. CO concentration sharply dropped as the mixture became leaner. Addition of EGR usually increased CO level (Figs. 3-7, 3-8).

NO concentration always decreased when spark was retarded. A maximum value was obtained for air/fuel mixture leaner than the stochiometric mixture and NO concentration decreased when EGR was added (Figs. 3-9, 3-10).

On the whole, most of the fuel and emissions measurements, except for HC, followed the theoretical predictions discussed in Section B of this chapter, yielding good agreement in the values of the control variables at the optimum solutions (see Ch. IV) with some other results [A-1]. The greatest discrepancy occurred with HC dependence on air/fuel ratio where the minimum was obtained in a few cases for very rich mixtures. As it will be discussed in Ch. IV, this discrepancy caused the value of AF at the optimal points to be richer than it was reported in other sources [A-1].

From the BMDP2R output it was concluded that the contribution of the last terms to be entered to the R-square was quite small and the equations could be simplified by omitting these terms. In addition, the null hypotheses of having any single coefficient drawn from a zero population was rejected based on the F-statistics with a level of confidence larger than 99%.

The regression coefficients of the various functions are listed in Appendices D and F for the local and global expressions.

Fig. 3.4 FUEL VS. ENGINE CONTROLS AT 1700/50 rpm/ft lb

$R^2 = 0.959$

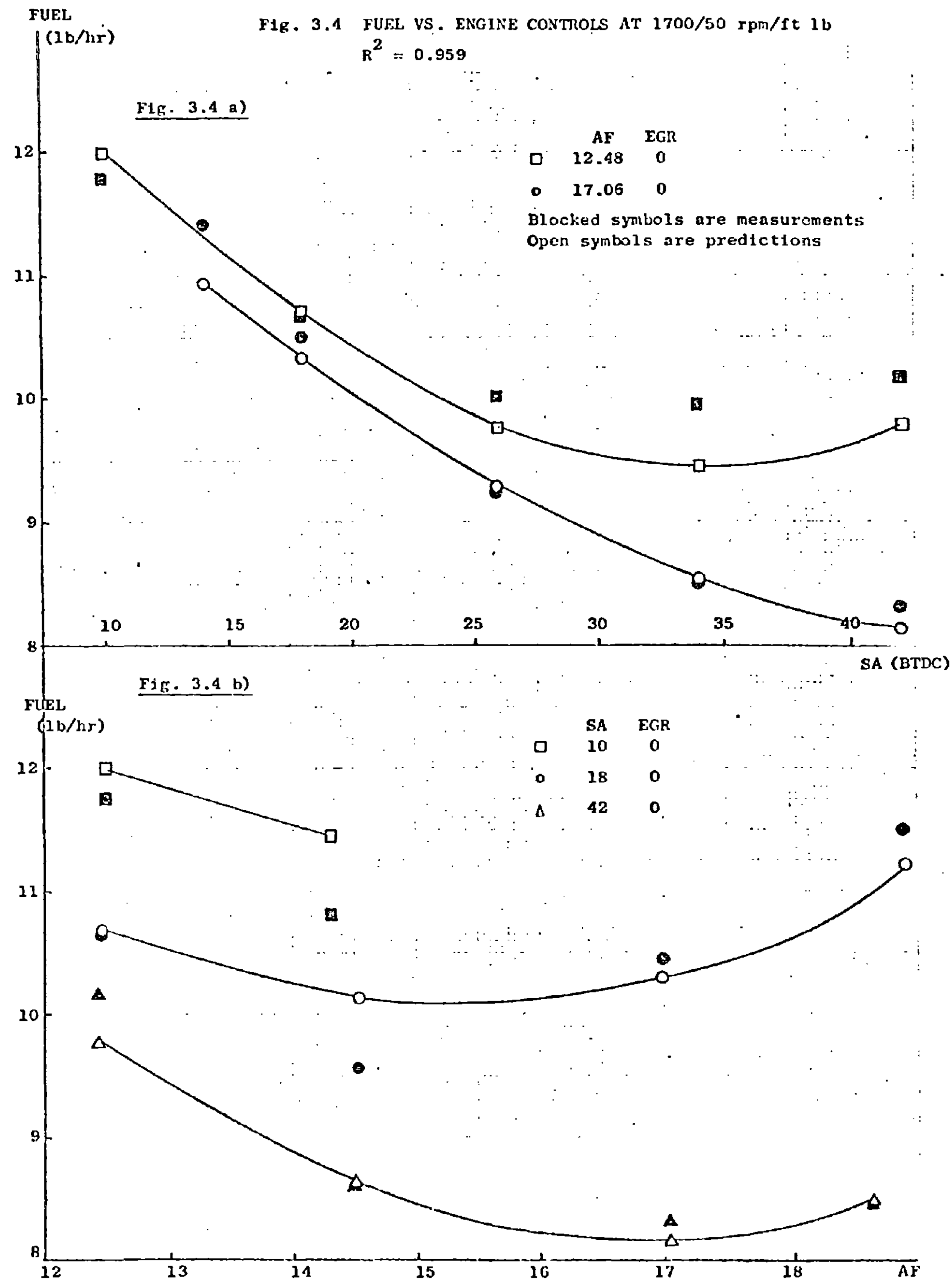

Fig. 3.4 (Cont.) FUEL VS. ENGINE CONTROLS AT 1700/50 rpm/ft lb

$R^2 = 0.959$

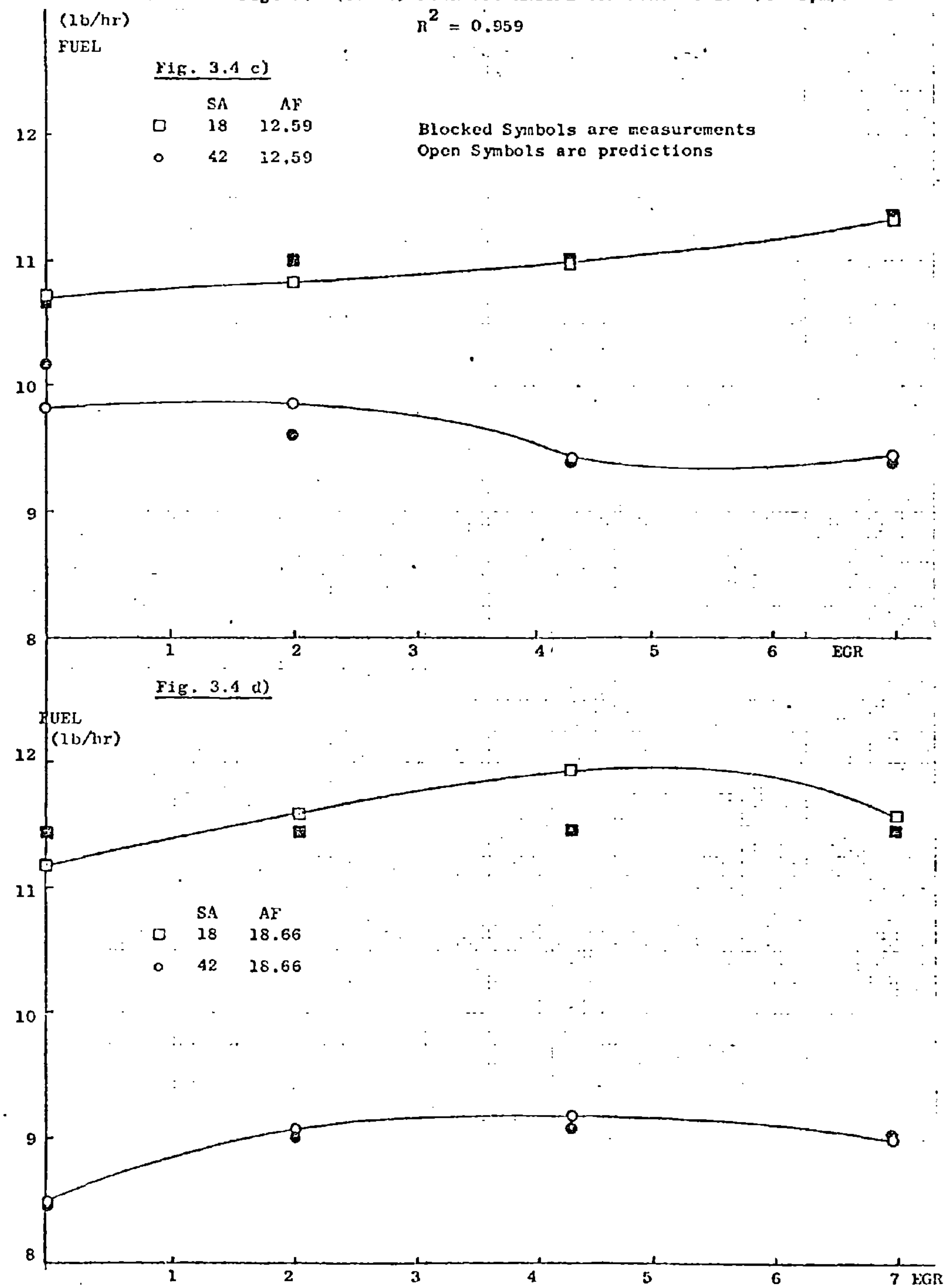

Fig. 3.5 HC VS. ENGINE CONTROLS AT 1800/25 rpm/lb ft R^2= 0.900

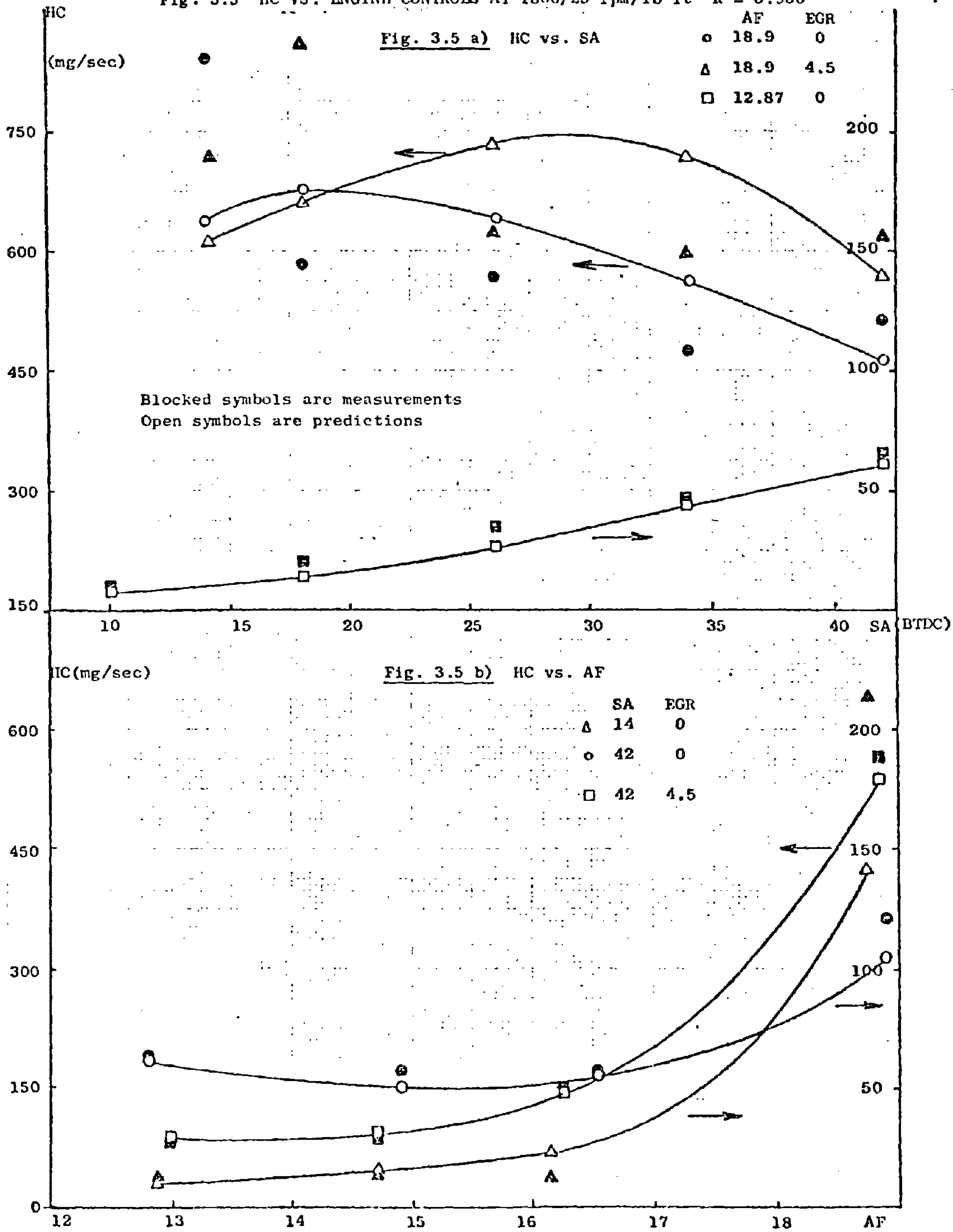

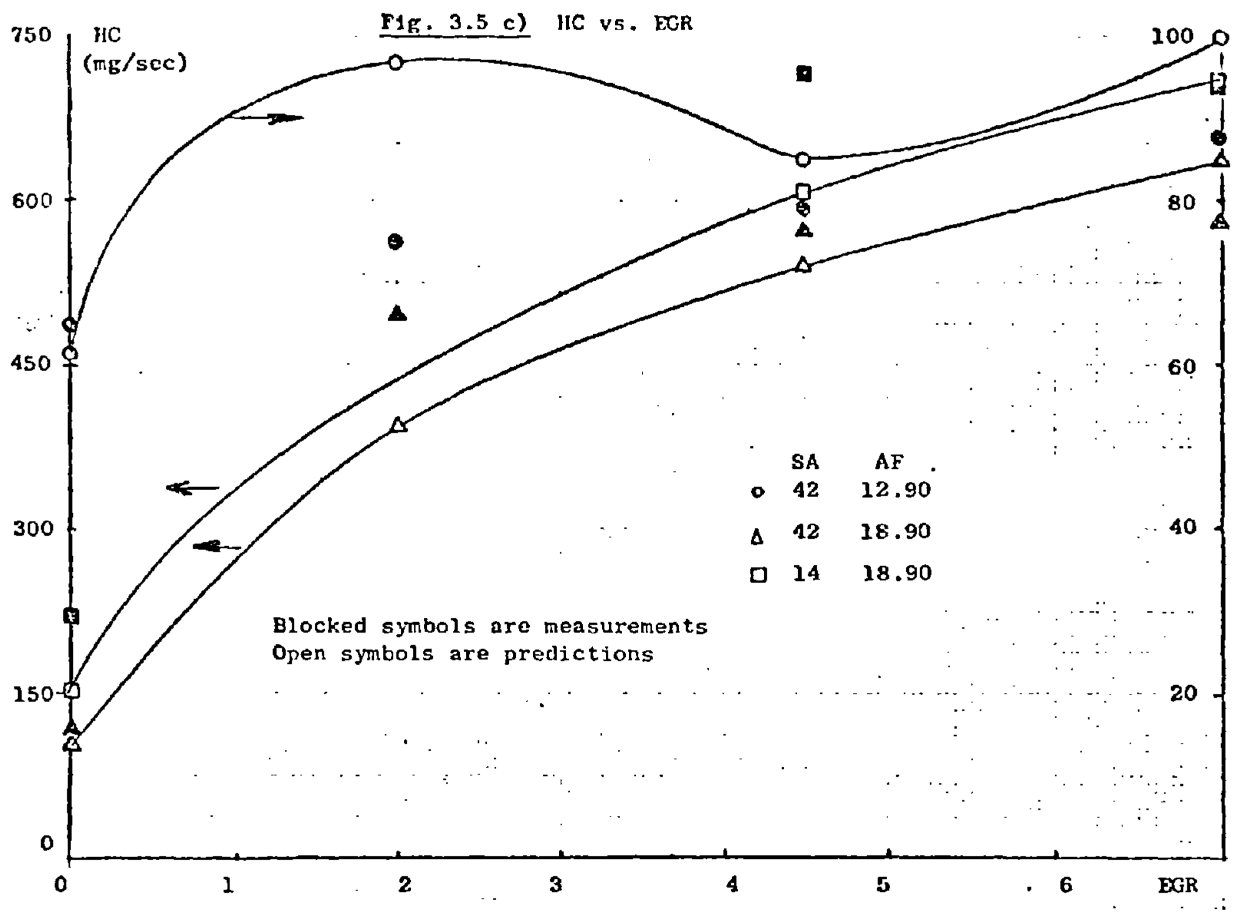

Fig. 3.5 (Cont.) HC VS ENGINE CONTROLS AT 1800/25 rpm/lb ft

$R^2 = 0.900$

Fig. 3.6 HC VS. ENGINE CONTROLS AT 2900/72 rpm/ft lb R^2=0.735

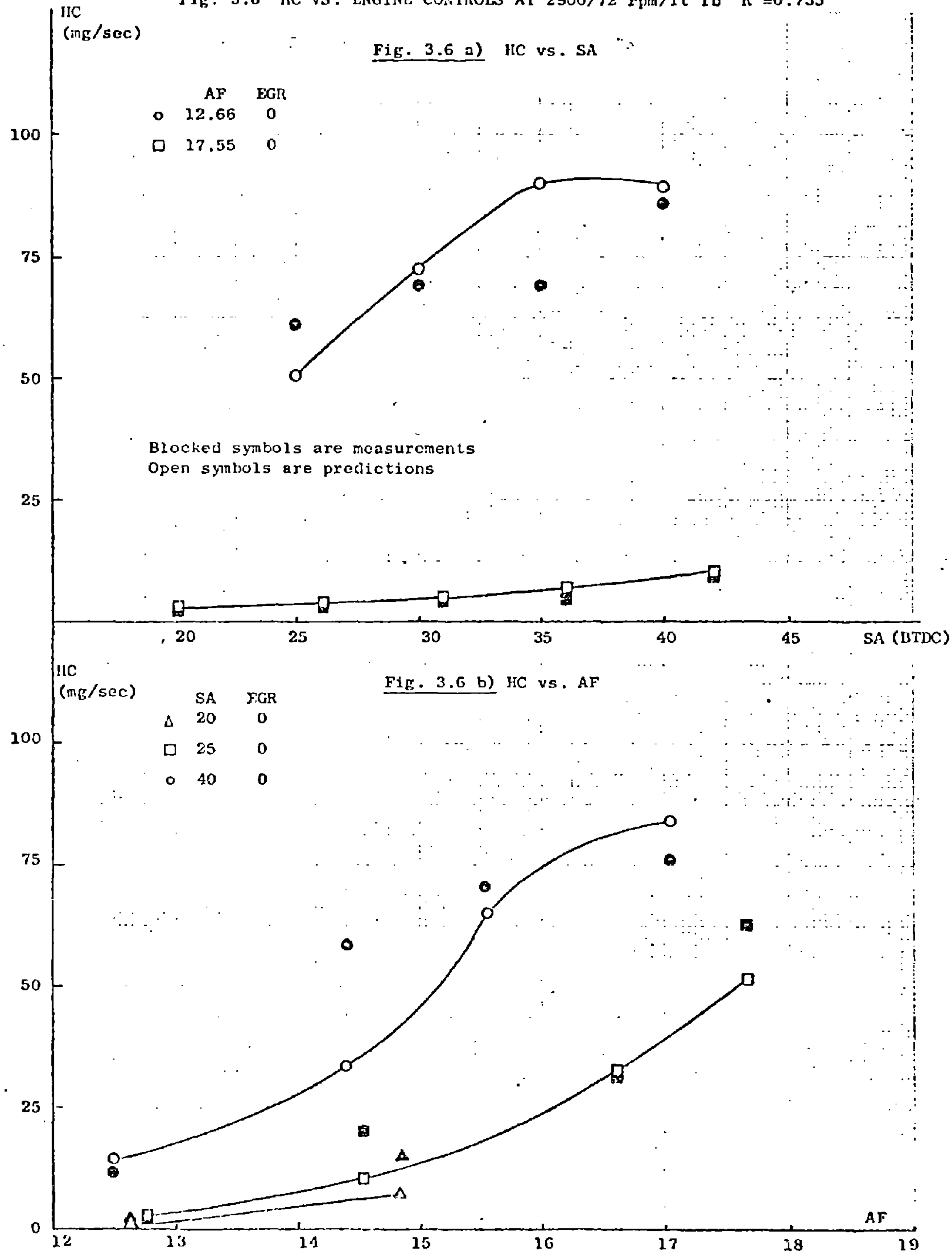

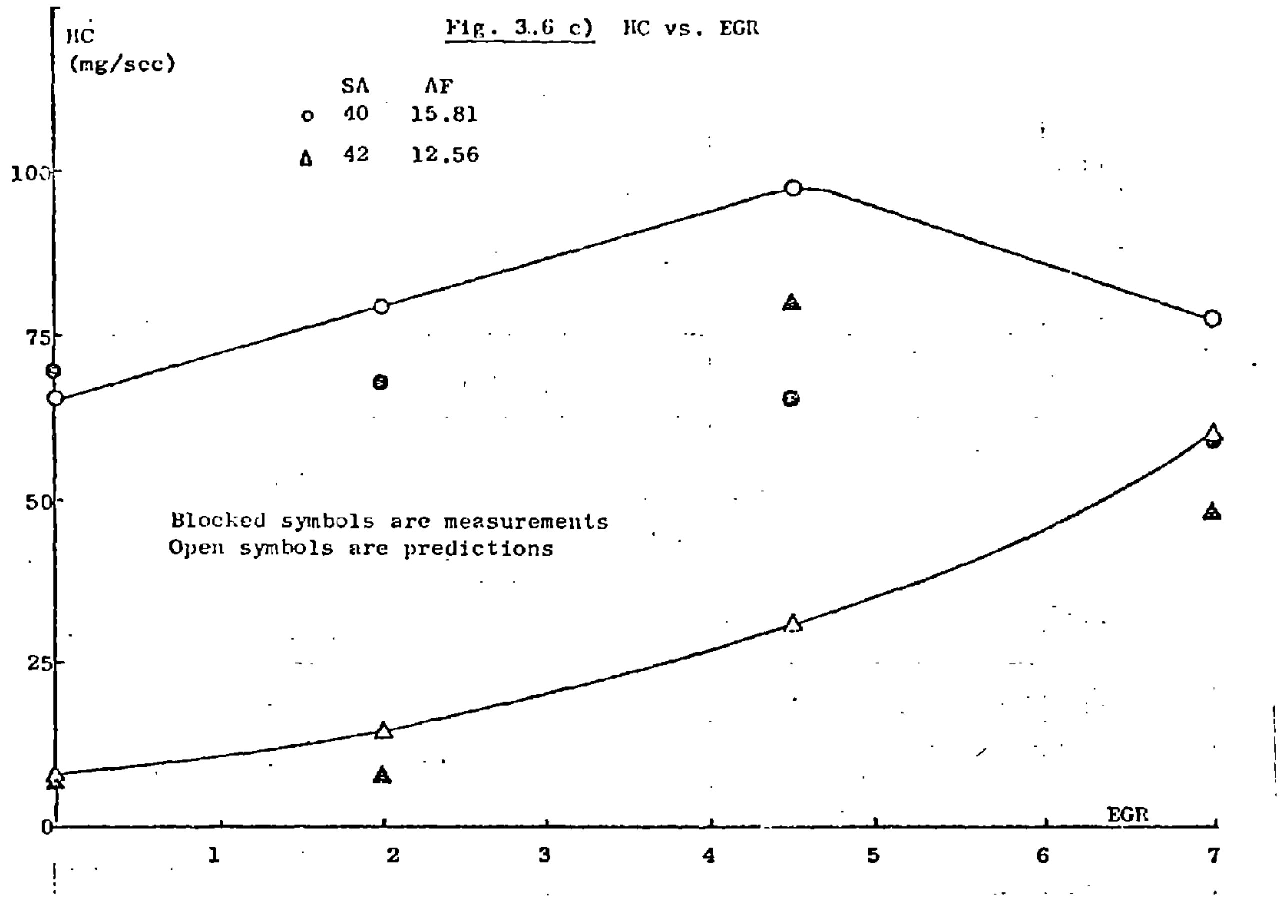

Fig. 3.6 (Cont) HC VS. ENGINE CONTROLS AT 2900/72 rpm/ft lb R^2=0.735

Fig. 3.7 CO VS. ENGINE CONTROLS AT 2100/75 rpm/ft lb

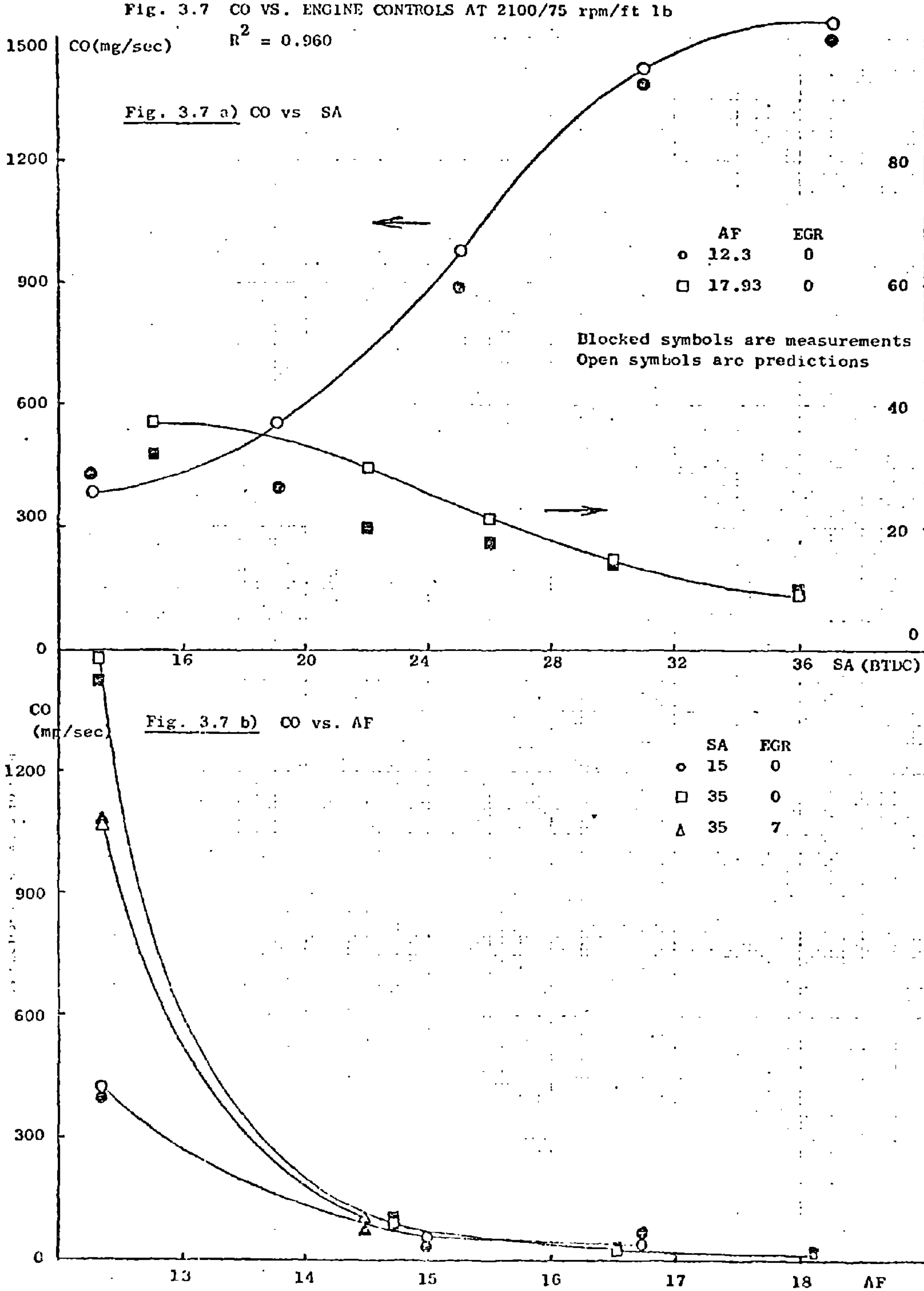

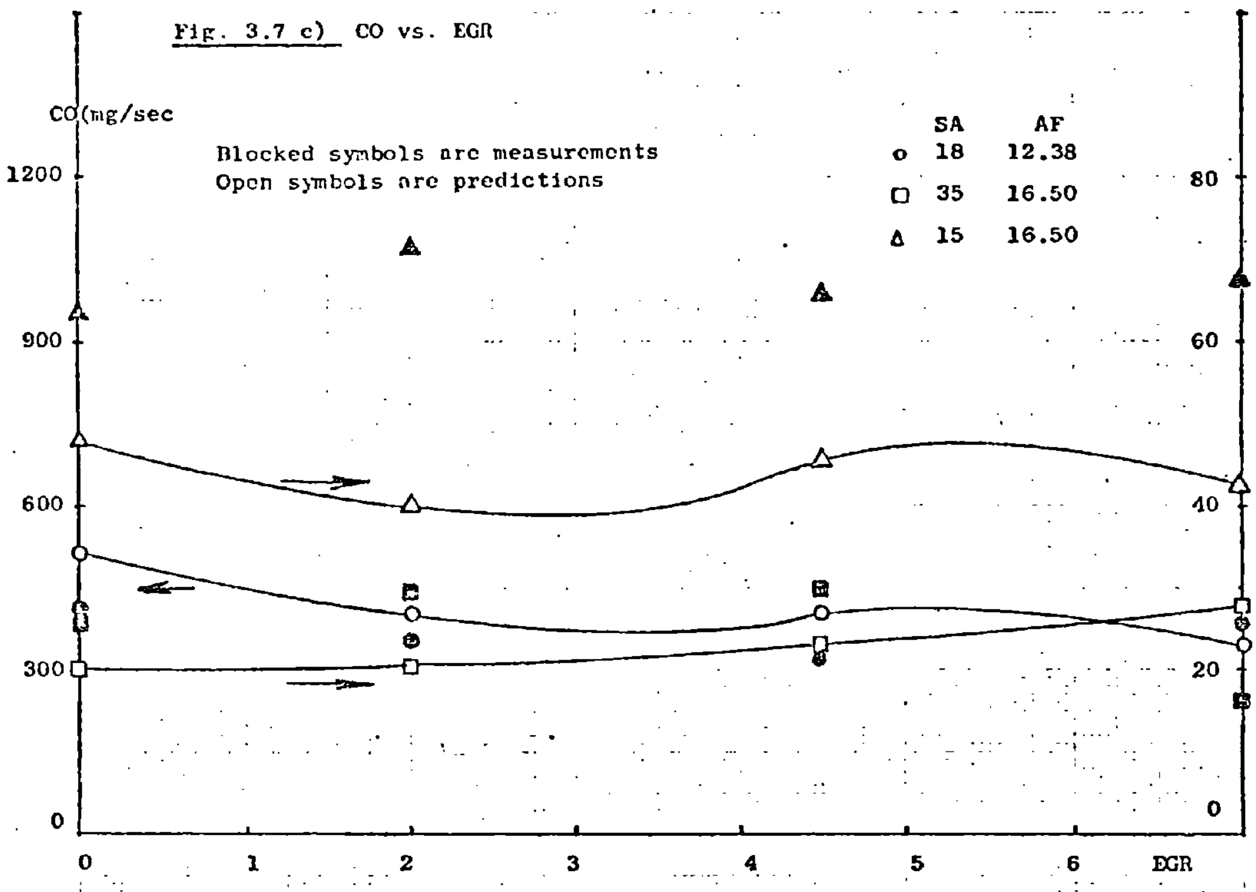

Fig. 3.7 (Cont) CO VS. ENGINE CONTROLS AT 2100/75 rpm/ft lb $R^2 = 0.960$

Fig. 3.8 CO VS. ENGINE CONTROLS AT 2500/85 rpm/ft lb $R^2 = 0.786$

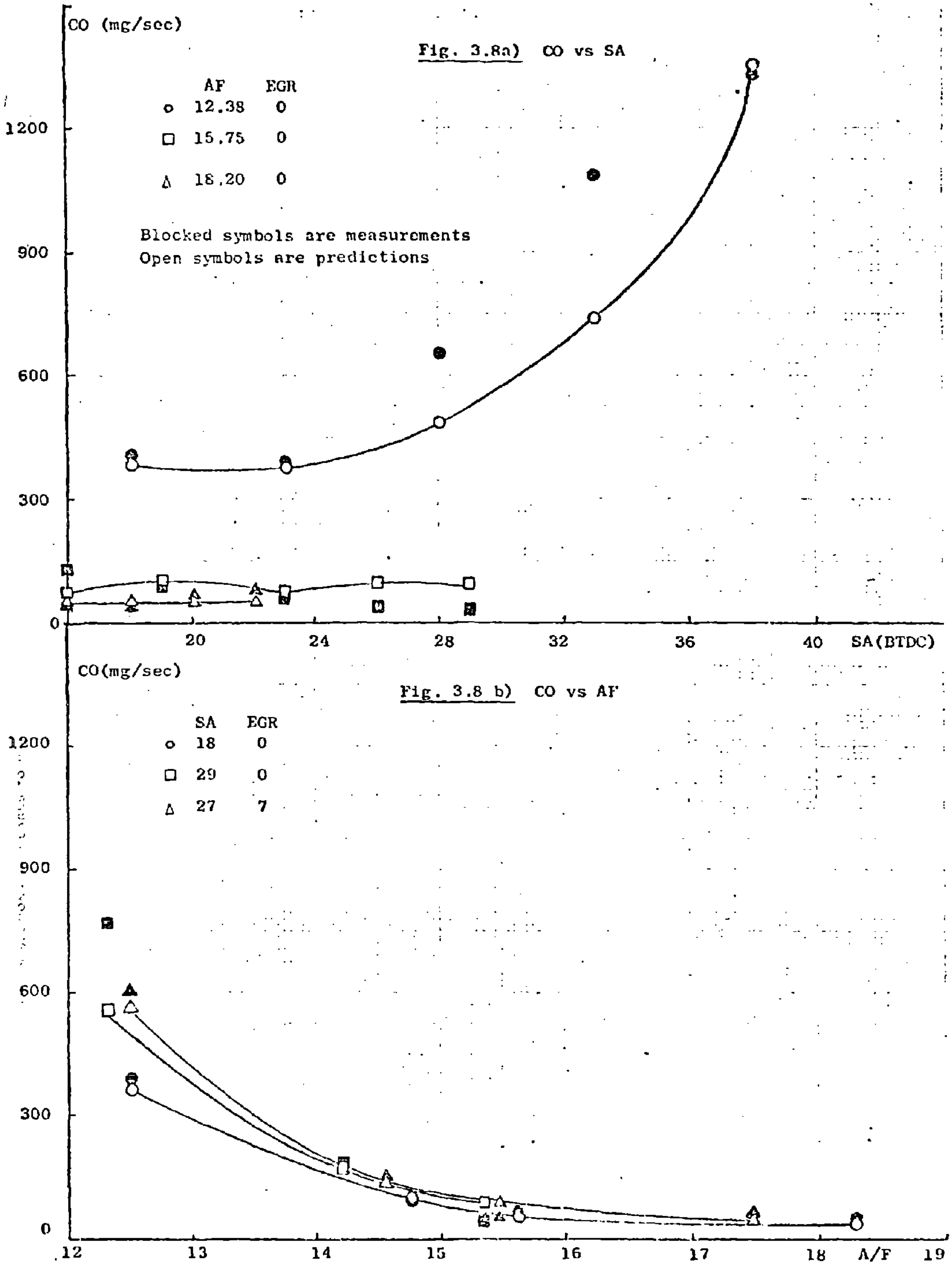

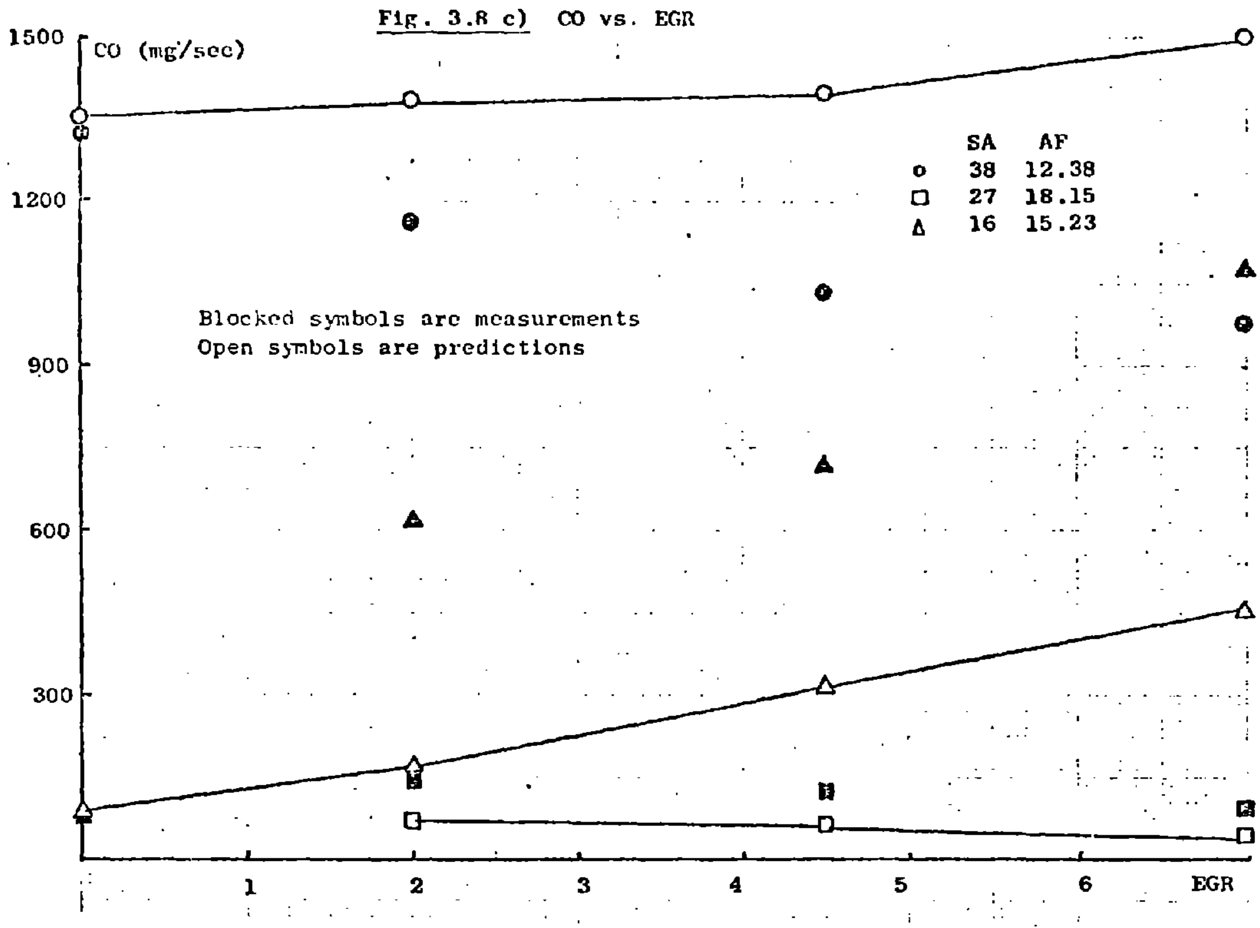

Fig. 3.8 (Cont) CO VS. ENGINE CONTROLS AT 2500/85 rpm/lb ft
$R^2 = 0.786$

Fig. 3.9 NO vs. ENGINE CONTROLS AT 1800/25 rpm/ft lb $R^2 = 0.798$

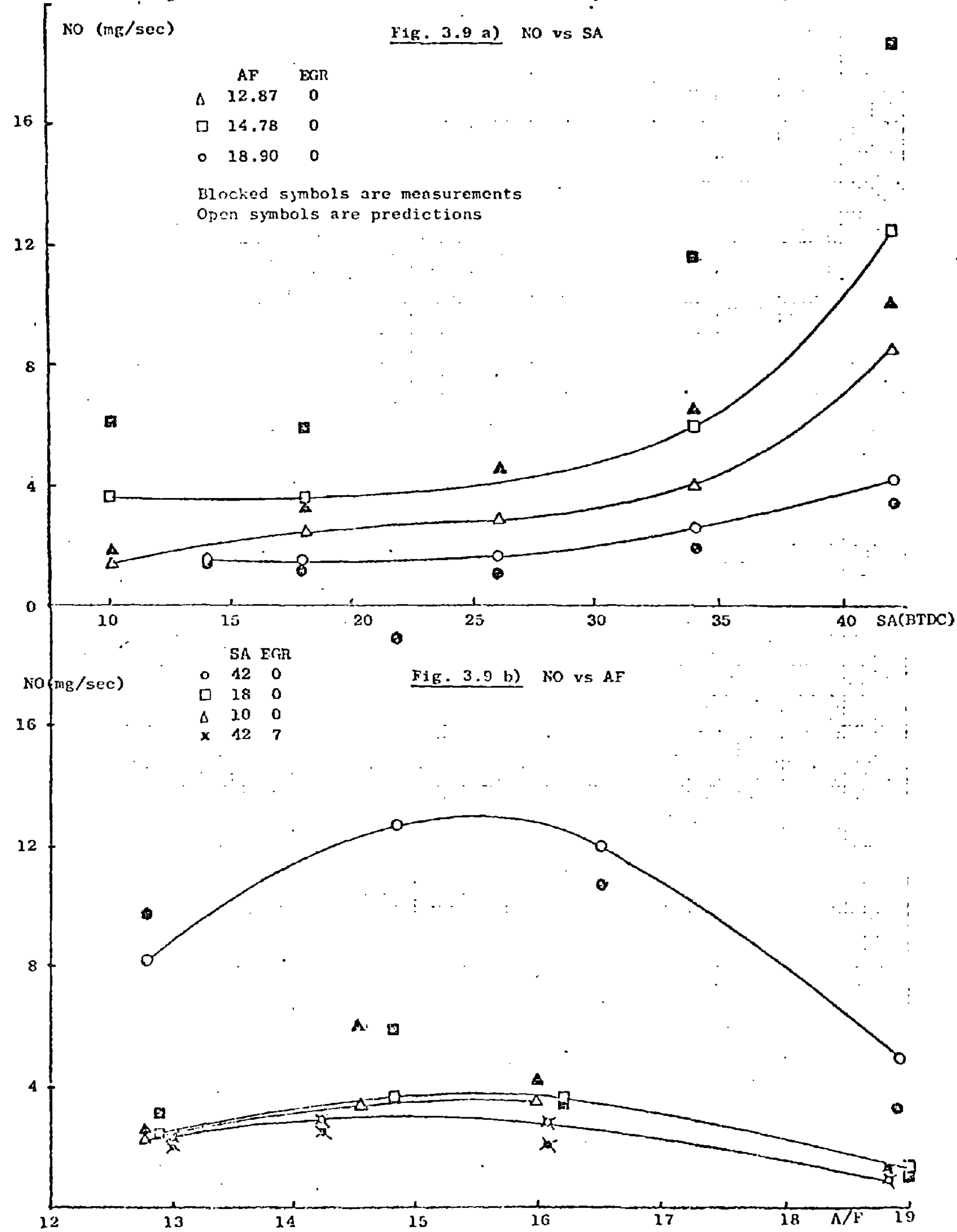

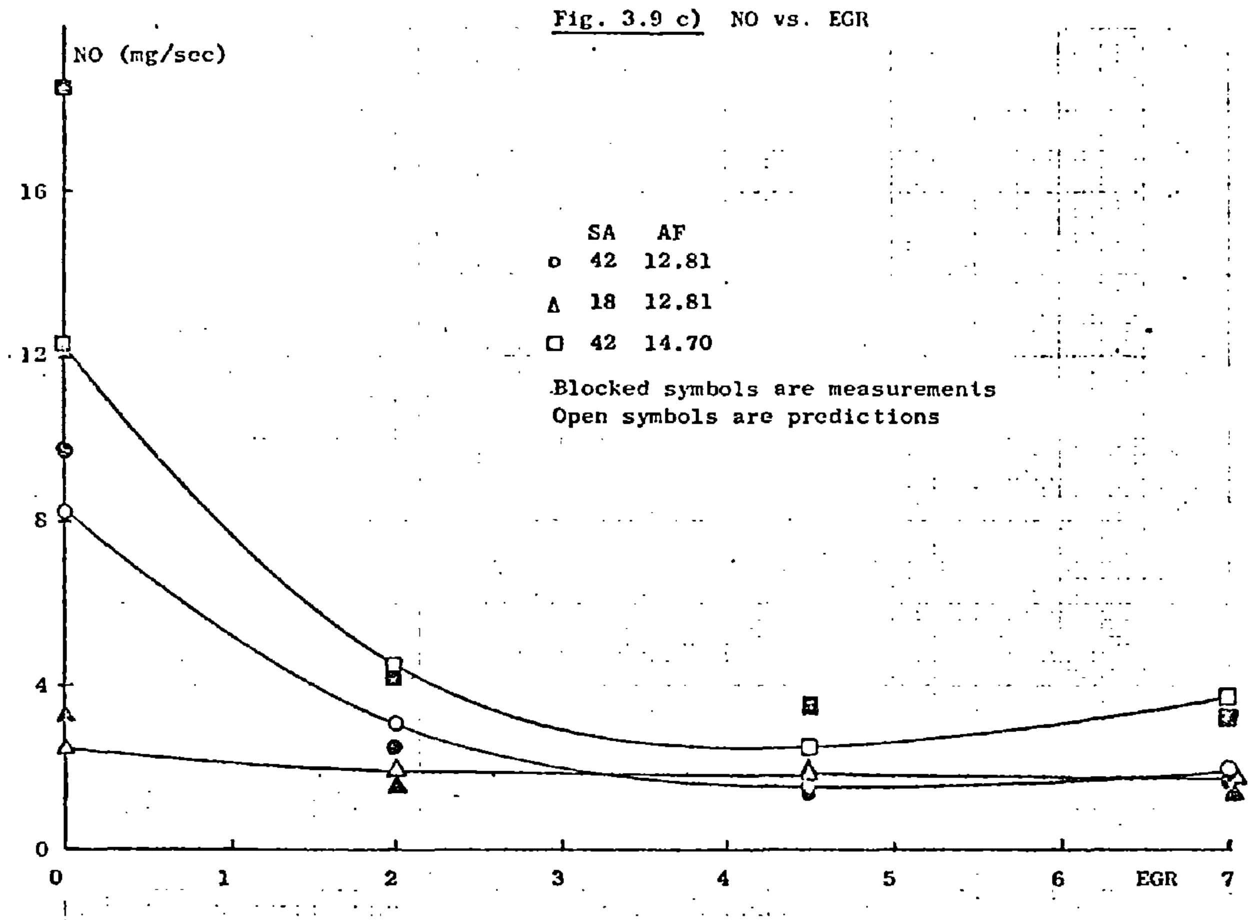

Fig. 3.9 (Cont) NO VS. ENGINE CONTROLS AT 1800/25 rpm/ft lb
$R^2 = 0.798$

Fig. 3.10 NO VS. ENGINE CONTROLS AT 2500/85 rpm/lb ft R^2 = 0.905

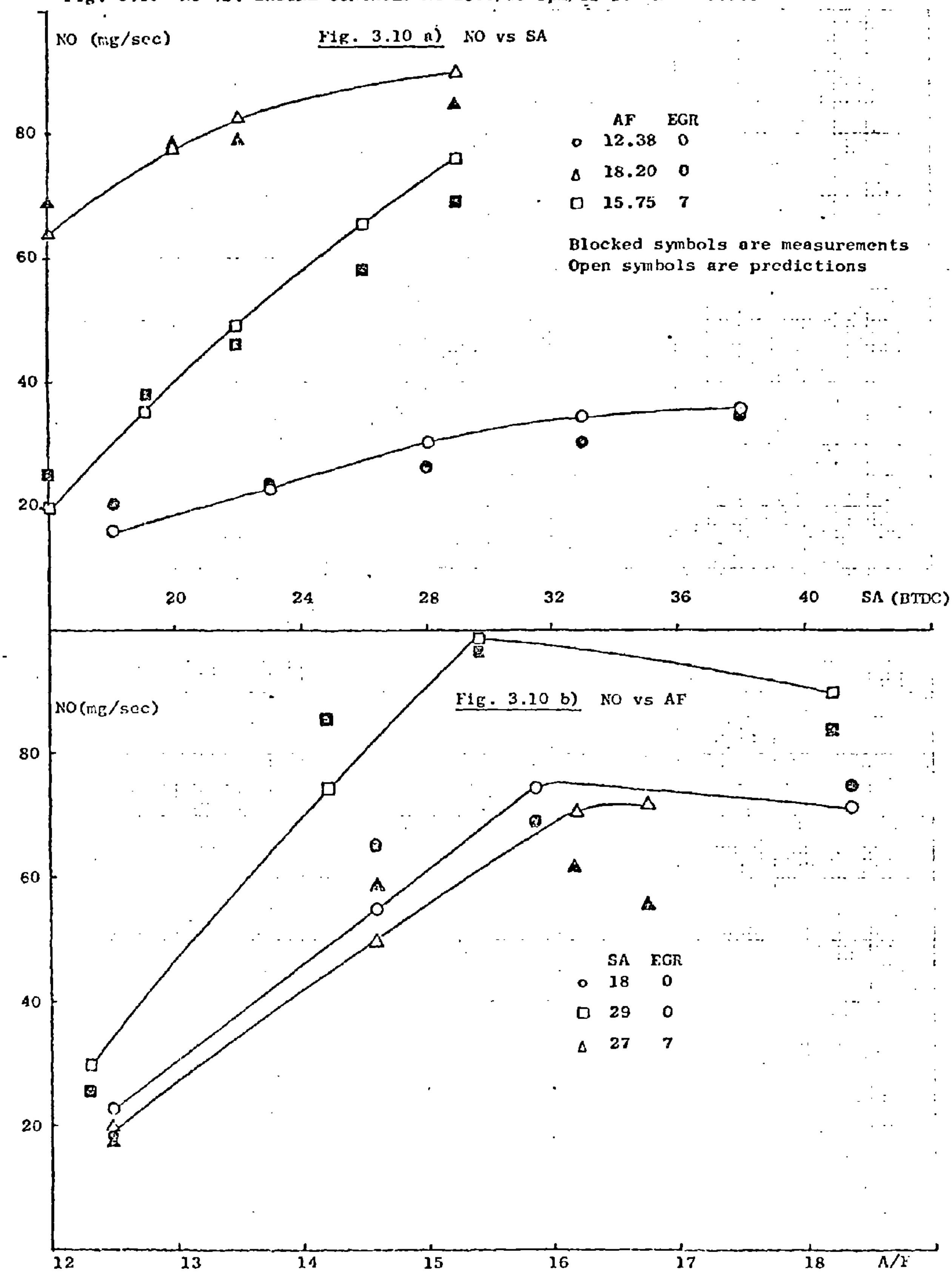

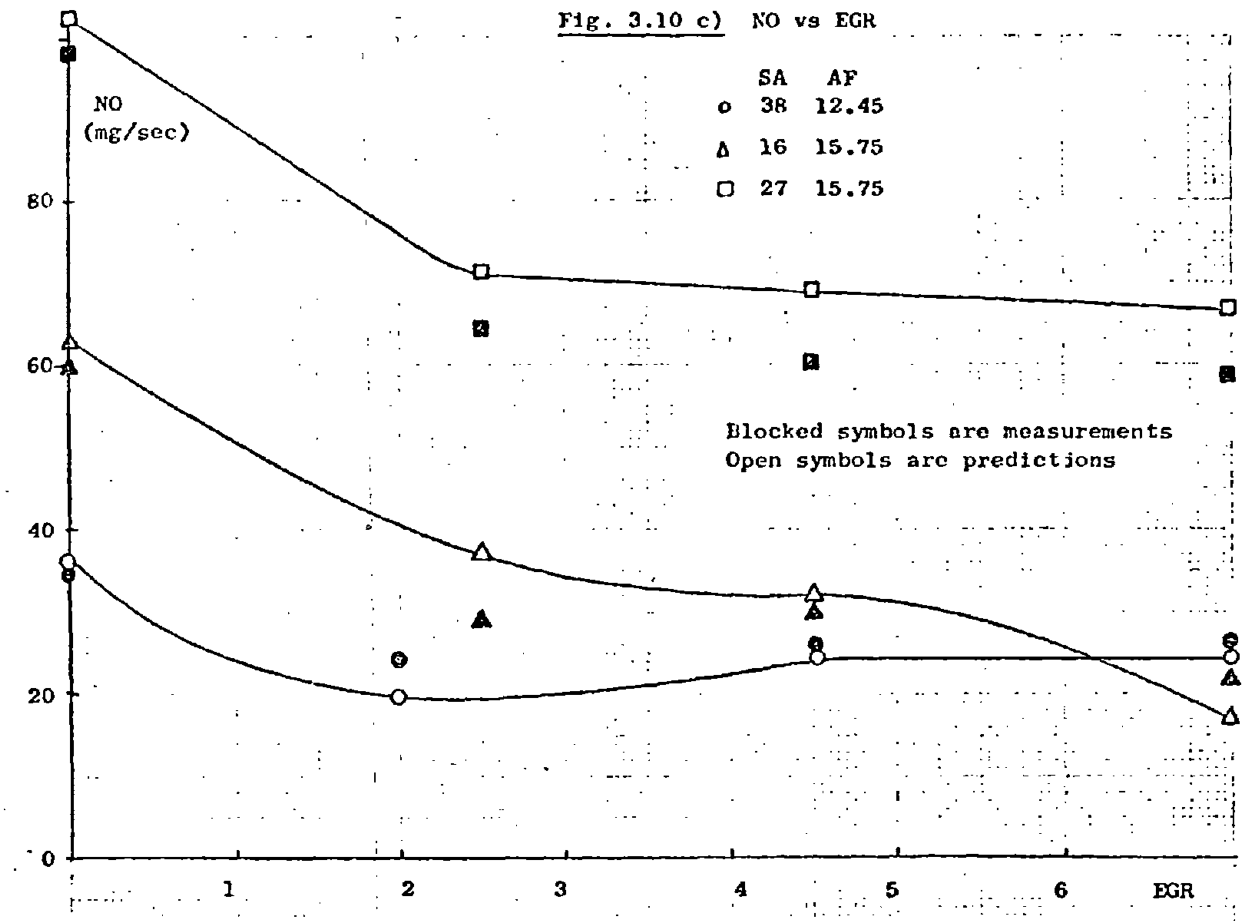

Fig. 3.10 (Cont) NO VS. ENGINE CONTROLS AT 2500/85 rpm/ft lb

$R^2 = 0.905$

G. EXAMPLE

The preceding analysis will best be demonstrated by the following example. CO level at TORQUE/RPM of 50 ft lb and 1700 rpm. Table 3-8 is a summary table of the stepwise parameter estimate. The variables entering x_2 through x_{29} are products of polynomials of AF·SA and EGR and are listed in Appendix C. The marginal contribution of the next terms to be entered to R-square is generally diminishing and steps 6-11 change R-square by 0.0008 which is really insignificant. F-to-enter gives the level of confidence in which the null hypothesis (having zero coefficients) is rejected. The lower the number the higher the probability that the coefficients are zero. For all coefficients that enter in steps 1-5 having F-to-enter 5.27 and higher, the null hypothesis is rejected in a confidence level greater than 99%, whereas the F-to-enter for steps 6-11 indicate a much lower level of confidence in rejecting the zero hypotheses.

SUMMARY TABLE

STEP NO.	VARIABLE ENTERED	VARIABLE REMOVED	MULTIPLE R	MULTIPLE RSQ	INCREASE IN RSQ	F-TO-ENTER	F-TO-REMOVE	NUMBER OF INDEPENDENT VARIABLES INCLUDED
1	2 X(2)		0.7287	0.5310	0.5310	83.7754		1
2	11 X(11)		0.9343	0.8730	0.3420	196.5506		2
3	24 X(24)		0.9456	0.8941	0.0211	14.3459		3
4	3 X(3)		0.9539	0.9099	0.0158	12.4459		4
5	16 X(16)		0.9572	0.9162	0.0063	5.2751		5
6	23 X(23)		0.9573	0.9165	0.0003	0.2260		6
7	25 X(25)		0.9574	0.9166	0.0001	0.0999		7
8	35 X(35)		0.9575	0.9168	0.0002	0.1923		8
9	33 X(33)		0.9575	0.9168	0.0000	0.0069		9
10	34 X(34)		0.9575	0.9168	0.0000	0.0004		10
11	29 X(29)		0.9576	0.9170	0.0002	0.1710		11

TABLE 3-8

A Stepwise Regression Summary Table for LOG(CO) At 1700/50 rpm/ft lb. A Sample Output of BMDP2R

IV. OPTIMIZATION ALGORITHM

A. INTRODUCTION

Once some analytic expressions that describe the engine performance have been derived, as outlined in Chapter 3, the optimization problem of minimizing fuel consumption subject to emission constraints can be formulated. The optimization problem is solved over the EPA cycle by the Lagrange multipliers method. The constrained problem is transferred into an unconstrained problem by adjoining the constraints to the fuel function. Tradeoff curves relating fuel consumption to various levels of emission constraints are of interest.

This analysis has not accurately accounted for either cold start or engine transients or catalyst efficiency effects; therefore the final results presented in the analysis should be used mainly for sensitivity analysis and trends in fuel economy as emission constraints change, rather than for establishing some absolute standards for fuel and emissions from this particular engine. The solution method, as well as discussion of results, are outlined in this chapter.

B. PROBLEM DEFINITION

The optimization problem calls for minimization of fuel consumption subject to emission constraints, which can be stated as:

$$\text{Min } F \tag{4.1}$$

subject to

$$E < E_0 \tag{4.2}$$

$$x \in X \tag{4.3}$$

where

F = fuel consumption in gallon/mile;

E = emission vector

$$E = \begin{pmatrix} HC \\ CO \\ NO \end{pmatrix} ;$$

and the inequality applies to any component.

E_0 = the vector of the desired emissions.

The other constraint $x \epsilon X$ implies that the set of independent variables x - AF, SA and EGR must be within certain bounds for proper engine operation.

The conventional data of emissions in gm/mile and the fuel economy in MPG differs from the data format that was collected; therefore, a conversion procedure which is outlined below must take place.

As explained in II.H the EPA urban and highway cycle can be approximated on the test bench by running the engine in finite number of torque and rpm points for various lengths of time. The number of points in our case is 10.

The composite fuel and emission levels based on the fitted functions derived in Section 3 for the i^{th} load and speed point, can be written as:

$$\dot{F}_i = \dot{F}_i(SA, AF, EGR) \quad (lb/hr) \tag{4.4}$$

$$\dot{HC}_i = HC_i(SA, AF, EGR) \quad (mg/sec) \tag{4.5}$$

$$\dot{NOx}_i = NOx_i(SA, AF, EGR) \quad (mg/sec) \tag{4.6}$$

$$\dot{CO}_i = CO_i(SA, AF, EGR) \quad (mg/sec) \tag{4.7}$$

The data acquired at the 10 points is modified as explained below to comply with the conventional data format. Our measurements are taken from a warmed-up engine and not in a cycle including a cold start as prescribed in the certification procedures. Therefore the data were adjusted to provide an approximate correction for this testing difference. In addition we ran the engine without a catalytic converter which necessitated additional corrections to account for the catalyst's reduction of emissions to the tailpipe level.

C. FUEL ECONOMY EVALUATION

The composite fuel economy as specified in [A-2] is:

$$\text{MPG composite} = \frac{100}{F_1 + F_2} \tag{4.8}$$

where MPG composite denotes the total fuel consumption of both urban and highway cycles; F_1 is the fuel consumed for 55 urban cycle miles (in gallons) and F_2 is the fuel consumed for 45 miles highway driving (in gallons). In our test we measured F_1 and F_2. Therefore the composite fuel economy can be found from (4.8).

The actual urban and highway driving schedules are not 55 and 45 miles respectively but rather 7.46 and 10.25 respectively. Therefore the expression for fuel mass flow is:

$$J = \frac{F_u}{u_d} .55 + \frac{F_H}{H_d} .45 \tag{4.9}$$

where

J = Fuel mass flow (lb/mile)

F_u = Mass of fuel consumed over an urban test (lb)

u_d = 7.46 miles distance of urban driving schedule

F_H = mass of fuel consumed over a highway test (lb)

H_d = 10.25 miles distance of highway driving schedule.

Substituting the values of u_d and H_d in (4.9) yields:

$$J = 0.0738\ F_u + 0.0439\ F_H \tag{4.10}$$

F_u and F_H are found by measuring the fuel flow rate in the hot cycle at the 10 load-speed points (Table 2-8) and adding these values according to their weights C_H^i, C_U^i (also in Table 2-8). Eqn. (4.10), written in terms of fuel rates, is therefore:

$$J_{hot} = 0.0738 \sum_{i=1}^{10} C_U^i \dot{F}_i + 0.0439 \sum_{i=1}^{10} C_H^i \dot{F}_i \tag{4.11}$$

$$= \sum_{i=1}^{10} (0.0738\ C_U^i + 0.0439\ C_H^i) \dot{F}_i$$

The volumetric fuel flow is found by dividing by fuel density yielding:

$$F_{hot} = \frac{J_{hot}}{\rho_F} = \frac{1}{\rho_F} \sum_{i=1}^{10} (0.0738\ C_U^i + 0.0439\ C_H^i)\dot{F}_i \qquad (4.12)$$

where

F_{hot} = the volumetric fuel flow gallon/mile

ρ_F = fuel density = 6.3 lb/gallon

Data was collected from a hot engine. We are actually interested in the "cold/hot"* cycle fuel economy which is related to the hot cycle as follows [D-1,E-1]:

$$\text{cold/hot MPG} = 0.96 \times (\text{hot MPG}) \qquad (4.13)$$

or in inverted form

$$\text{cold/hot GPM} = 1.042 \times (\text{hot GPM}) \qquad (4.14)$$

Substituting in (4.12) yields the final expression

$$F_{cold/hot} = \sum_{i=1}^{10} (0.0122\ C_U^i + 0.00726\ C_H^i)\dot{F}_i \ . \qquad (4.15)$$

---

*The term given to the case of a cold start followed by some warmed-up operation.

D. EMISSION CONSTRAINTS EVALUATION

The emission constraints are imposed only on the urban cycle. We measure the concentration in either PPM or in percentage at the 10 load-speed points (Table 2-8) which represent the EPA cycle. The engine was run through a cycle without any catalytic converter. The transformation from our measurements to the conventional gm/mile format for the "cold/hot" cycle with catalytic converter is given below.

1. Hot Cycle Emissions Without a Catalyst

The conversion from concentration to mass flow rate is given in [M-1]:

$$\dot{E} = C_e \times \dot{V}_{ex} \times \rho_e \qquad (4.16)$$

where

$\dot{E}$ = emission mass flow (gm/sec)

C_e = volumetric fraction of emissions in the exhaust

$\dot{V}_{ex}$ = volume delivery of exhaust (ft^3/sec)

ρ_e = density of emissions (gm/ft^3)

C_e is the data obtained in our measurements, ρ_e can be found by knowing exhaust pressure and temperature. The exhaust volume rate flow is given by:

$$\dot{V}_{ex} = \frac{\dot{G}_{ex}}{\rho_{ex}} = \frac{\dot{G}_a + \dot{G}_f + \dot{G}_p}{\rho_{ex}} \qquad (4.17)$$

where

$\dot{G}_{ex}$ = total exhaust mass flow (lb/sec);

$\dot{G}_a$ = inlet air mass flow to the carburetor (lb/sec);

$\dot{G}_f$ = fuel mass flow (lb/sec);

$\dot{G}_p$ = additional air mass flow to the exhaust by air pump (lb/sec);

ρ_{ex} = exhaust density (lb/ft^3) .

$\dot{G}_p$ was determined from air pump calibrations as discussed in II.C and is:

$$\dot{G}_p = \rho_a \times (0.8 \cdot \text{RPM}/100 - 3.3 - 0.667 p_{ex})/60 \qquad \text{RPM} < 2500, \quad (2.1)$$

$$\dot{G}_p = \rho_a \times (0.773\ \text{RPM}/100 - 3.75 - 0.645 p_{ex})/60 \qquad \text{RPM} > 2500,$$

where ρ_a, RPM and p_{ex} are defined in II.C. The need for an accurate exhaust pressure and temperature for the determination of emission density can be overcome by substituting the relationship:

$$\dot{V}_{ex} = \frac{\dot{G}_{ex}}{\rho_{ex}} \tag{4.18}$$

in (4.16) yielding:

$$\dot{E} = C_e \times \dot{G}_{ex} \times \frac{\rho_e}{\rho_{ex}} \quad . \tag{4.19}$$

Using the laws of an ideal gas the density fraction of emission to exhaust can be replaced by the ratio of their molecular weights yielding the final expression:

$$\dot{E} = C_e \times \dot{G}_{ex} \times \frac{M_e}{M_{ex}} \tag{4.20}$$

where

M_e = emission molecular weight;

M_{ex} = exhaust gas molecular weight = 29.8.

The exhaust gas molecular weight slightly depends on air fuel ratio and can vary by 1% over a wide air fuel ratio. An average value was assumed for simplicity.

The general expression for emission mass rate in (4.20) can be written for each of the three emissions as follows:

HC

$$\dot{HC} = \frac{PPM}{10^6} \times \dot{G}_{ex} \times \frac{M_{HC}}{29.8} \tag{4.21}$$

where

M_{HC} = 86.172 (assuming hexane basis)

$\dot{HC}$ = mass rate of hydrocarbon gm/sec

PPM = concentration of HC from emission instrument in ppm.

$\underline{NOx}$ The NOx mass rate depends also on humidity. Therefore eqn. (4.16) is modified to:

$$\dot{NOx} = \frac{PPM\ NOx}{10^6} \times \dot{G}_{ex} \times \frac{M_{NO}}{29.8} \times K_H \qquad (4.22)$$

where

$\dot{NOx}$ = emission mass rate (gm/sec)

M_{NOx} = 46.002 (assuming NO_2)

K_H = humidity correction factor as specified in the federal register [F-1]

K_H is given by:

$$K_H = \frac{1}{0.6745 - 0.0047\ H} \qquad (4.23)$$

where H = absolute humidity in grains per pound of dry air.

$\underline{CO}$ The carbomonoxide mass rate is given by:

$$\dot{CO} = \frac{\%\ CO}{100} \times \dot{G}_{ex} \times \frac{M_{CO}}{29.8} \qquad (4.24)$$

where

$\dot{CO}$ = mass rate (gm/sec)

M_{CO} = 28.01.

The total hot cycle emissions are found by summing the emission rates measured in the 10 load-speed points according to their weights C_U^i (Table 2-8). The average emission per mile is found by dividing the total emissions by the urban driving schedule (7.46 miles). Therefore the expressions for the various emissions are:

$$HC_{hot} = \frac{1}{7.46} \sum_{i=1}^{10} C_U^i\, \dot{CO}^i \quad \text{(gm/mile)} \qquad (4.25)$$

$$NOx_{hot} = \frac{1}{7.46} \sum_{i=1}^{10} C_U^i\, \dot{NOx}^i \quad \text{(gm/mile)} \qquad (4.26)$$

$$CO_{hot} = \frac{1}{7.46} \sum_{i=1}^{10} C_U^i\, \dot{CO}^i \quad \text{(gm/mile)} \qquad (4.27)$$

2. Hot Cycle Emissions with Catalysts

Introduction of a catalytic converter reduces the emissions level according to its efficiency. We shall examine two types of catalysts:

a) oxidizing catalyst (OC);

b) three-way catalyst (TWC).

The ratio of the output to input levels is given by:

$$E_{out} = (1-\eta)E_{in} \tag{4.28}$$

where

E_{out} = emission level in the catalyst outlet

E_{in} = emission level in the catalyst inlet

η = catalyst efficiency.

OXIDIZING CATALYST (OC)

The approximate efficiencies for the various emissions are given in [E-1]

$$\eta_{HC} = 0.75 \tag{4.29}$$

$$\eta_{NOx} = 0.0 \tag{4.30}$$

$$\eta_{CO} = 0.85 \tag{4.31}$$

Therefore using (4.28) and (4.25)-(4.27) for the inlet emission levels the following expressions are obtained for the emission levels in the hot cycle after passing through the oxidizing catalyst.

$$HC_{out} = (1-0.75)HC_{in} = \frac{0.25}{7.46}\sum_{i=1}^{10} C_U^i \dot{HC}^i \quad \text{(gm/mile)} \tag{4.32}$$

$$NOx_{out} = NOx_{in} = \frac{1}{7.46}\sum_{i=1}^{10} C_U^i \dot{NOx}^i \quad \text{(gm/mile)} \tag{4.33}$$

$$CO_{out} = (1-0.85)CO_{in} = \frac{0.15}{7.46}\sum_{i=1}^{10} C_U^i \dot{CO}^i \quad \text{(gm/mile)} \tag{4.34}$$

THREE WAY CATALYST (TWC)

The approximate efficiencies of the three way catalyst are given in [B-1]

$$\eta_{HC} = 0.83 \qquad (4.35)$$

$$\eta_{NOx} = 0.70 \qquad (4.36)$$

$$\eta_{CO} = 0.90 \qquad (4.37)$$

The TWC efficiency strongly depends on fuel mixture and is valid only around stochiometry. Therefore the expressions for the emissions level in the hot cycle after passing through the TWC are:

$$HC_{out} = (1-0.83)HC_{in} = \frac{0.17}{7.46} \sum_{i=1}^{10} C_U^i \dot{HC}^i \quad \text{(gm/mile)} \qquad (4.38)$$

$$NOx_{out} = (1-0.7)NOx_{in} = \frac{0.3}{7.46} \sum_{i=1}^{10} C_U^i \dot{NOx}^i \quad \text{(gm/mile)} \qquad (4.39)$$

$$CO_{out} = (1-0.9)CO_{in} = \frac{0.1}{7.46} \sum_{i=1}^{10} C_U^i \dot{CO}^i \quad \text{(gm/mile)} \qquad (4.40)$$

3. COLD/HOT CYCLE CONVERSION

The expressions derived so far for the emissions level correspond to the hot cycle. The conversion to cold/hot cycle is given in [E-1]:

$$HC_{cold/hot} = HC_{hot} + 0.2 \quad \text{(gm/mile)} \qquad (4.41)$$

$$NOx_{cold/hot} = 0.95 \text{ NOx hot} \quad \text{(gm/mile)} \qquad (4.42)$$

$$CO_{cold/hot} = CO_{hot} + 4 \quad \text{(gm/mile)} \qquad (4.43)$$

where the hot subscript refers to emission levels after passing through the catalyst. Combining equations (4.41)-(4.43) with either (4.32)-(4.34) or with (4.38)-(4.40) gives the desired expression for the emission level in the cold/hot cycle after catalytic conversion for the two types of catalysts.

All the catalyst efficiency assumptions and the cold start correction are great simplifications to an extremely complicated process. Therefore, these conversions are used to arrive at tailpipe emissions that are a crude approximation to an actual cold start cycle test and are useful for comparison purposes. However, due to the crude approximations, the numbers should not be used as actual predictions of dynamometer certification tests.

a. Oxidizing Catalyst

$$HC_{choc} = 0.0335 \sum_{i=1}^{10} C_U^i \dot{HC}^i + 0.2 \quad \text{(gm/mile)} \quad (4.44)$$

$$NOx_{choc} = .1273 \sum_{i=1}^{10} C_U^i \dot{NOx}^i \quad \text{(gm/mile)} \quad (4.45)$$

$$CO_{choc} = 0.02 \sum_{i=1}^{10} C_U^i \dot{CO}^i + 4 \quad \text{(gm/mile)} \quad (4.46)$$

The subscript choc means cold-hot oxidizing catalyst.

b. TWC

The final expressions are

$$HC_{chtc} = 0.0228 \sum_{i=1}^{10} C_U^i \dot{CO}^i + 0.2 \quad \text{(gm/mile)} \quad (4.47)$$

$$NOx_{chtc} = 0.0382 \sum_{i=1}^{10} C_U^i \dot{NOx}^i \quad \text{(gm/mile)} \quad (4.48)$$

$$CO_{chtc} = 0.0134 \sum_{i=1}^{10} C_U^i \dot{CO}^i + 4 \quad \text{(gm/mile)} \quad (4.49)$$

The subscript chtc means cold/hot three-way catalyst and these expressions are valid only around stochiometric points.

final form:

$$\text{Min}((0.0122C_u^i+0.00726C_H^i)\dot{F}_i+C_u^i(\lambda_{HC}\cdot a_1\cdot \dot{HC}_i+\lambda_{NO}\cdot a_2\cdot \dot{NOx}_i+\lambda_{CO}\cdot a_3\cdot \dot{CO}_i)$$

$$\text{for} \quad i = 1,N \qquad (4.55)$$

subject to (4.51) and (4.52).

A reasonable way of solving the optimization problem is guessing an initial value for λ_{HC}, λ_{NO}, λ_{CO} and solving N minimization problems as given in (4.55) subject to (4.52) having the independent variables confined in the drivability range. Once the values of AF_i, SA_i, EGR_i that correspond to the solution of (4.55) have been obtained, the emission levels can be evaluated from (4.51). If these levels do not differ from the desired emission constraints by more than the convergence criteria, the final solution has been obtained. Otherwise the Lagrangian Multipliers have to be modified and the process must be repeated. One way of changing the Lagrange Multipliers is by perturbing them around the current solution and from the way the emission levels are changed, extrapolating so the desired emission levels are met. A flow chart of this process is given in Fig. 4-1.

This method could be justified if we were interested in solving the minimization problem for a particular set of constraints. As trade-off curves are of interest, solving the optimization problem for quite a few constraint levels is wasteful. Instead, a different approach was taken. Each optimization solution is associated with a set of Lagrangian Multipliers. As we are not interested just in one solution, the optimization problem as defined in (4.55) is solved many times, each time with a different value of the λ_i. No iterations of the Lagrange Multipliers are required. The fuel consumption as well as the emissions level are evaluated for each solution using (4.14) and (4.44)-(4.49). A flow chart of the process is given in Fig. 4-2. A listing of OPT is given in Appendix G-1.

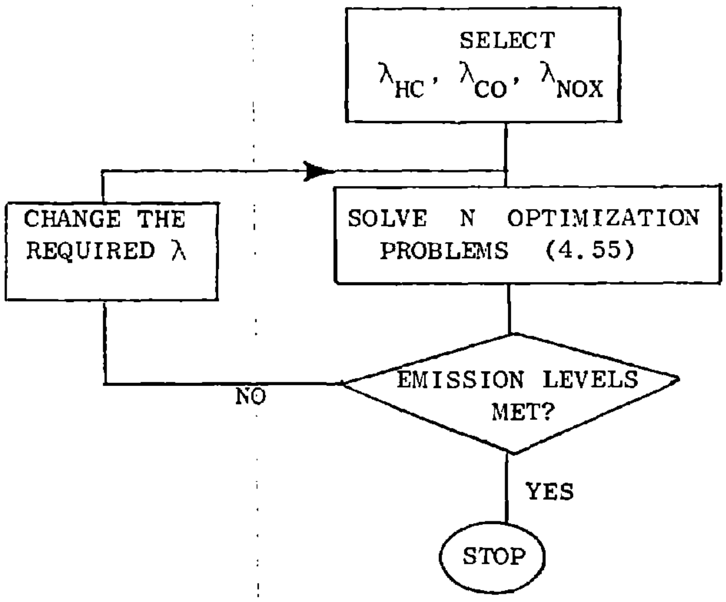

Fig. 4-1 Optimization Algorithm for a Given Emissions Level

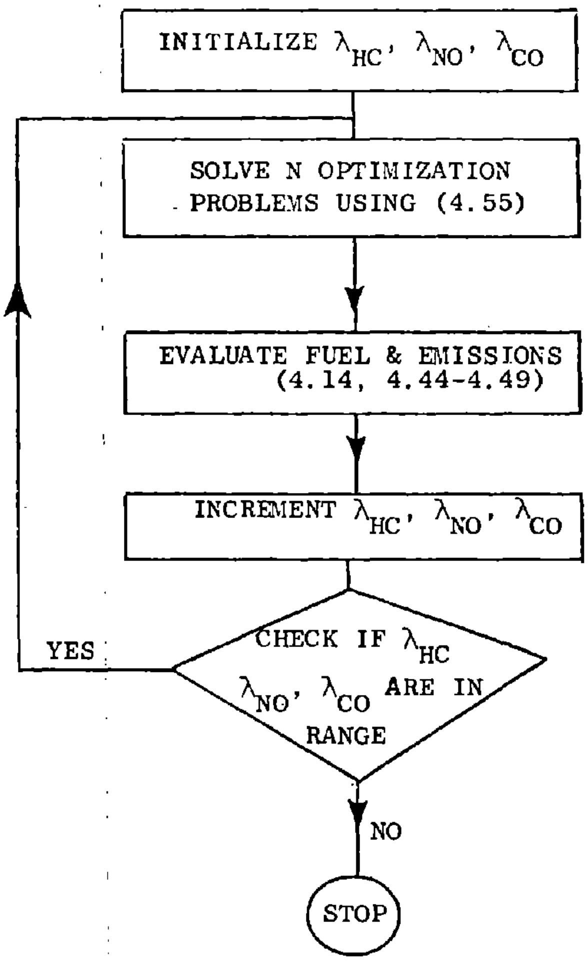

Fig. 4-2 Optimization Algorithm for a Given Range of λ's

E. METHOD OF SOLUTION

Once detailed expressions for both fuel consumption and emission levels have been derived (equations 4.14 and 4.44-4.49) equation (4.1) can be written more explicitly as:

$$\mathrm{Min}\left(\sum_{i=1}^{N} 0.0122\, C_u^i + 0.00726 C_H^i\right)\dot{F}_i \tag{4.50}$$

subject to the emission constraints:

$$\begin{aligned} a_1 \sum_{i=1}^{N} C_u^i \dot{HC}_i + b_1 &\leq HC_0 \\ a_2 \sum_{i=1}^{N} C_u^i \dot{NOx}_i &\leq NO_{x0} \\ a_3 \sum_{i=1}^{N} C_u^i \dot{CO}_i + b_3 &\leq CO_0 \end{aligned} \tag{4.51}$$

and the independent variables constraints:

$$\begin{aligned} AF_i^L \leq\ & AF_i \leq AF_i^H \\ SA_i^L \leq\ & SA_i \leq SA_i^H \qquad \text{for } i = 1,N \\ EGR_i^L \leq\ & EGR_i \leq EGR_i^H \end{aligned} \tag{4.52}$$

where the various a's and b's of (4.51) are given in Table 4-1 for either the oxidizing or the three-way catalyst and the superscripts L and H in (4.52) denote lower and upper bounds respectively on the independent variables as listed in Fig. 4-1. There are 3N unknowns, the values of the three independent variables must be found for all N constant load and speed points.

	a_1	a_2	a_3	b_1	b_2	b_3
Non Catalyst (NC)	0.1340	0.1273	0.1340	0.2	0	4
Oxidizing Catalyst (OC)	0.0335	0.1273	0.02	0.2	0	4
3-Way Catalyst (TWC)	0.0228	0.0382	0.0134	0.2	0	4

TABLE 4-1: Emission Constraints Coefficients for (4.51)

One way of solving this constrained problem is by adjoining the emission constraints (4.51) to the objective function (4.50) and finding the minimum of the following problem (see [BR-1]):

$$\mathrm{Min}\Big(\sum_{i=1}^{N} 0.0122C_u^i+0.00726C_H^i)\dot{F}_i + \lambda_{HC}(a_i \sum_{i=1}^{N} C_u^i\cdot\dot{HC}_i+b_1-HC_0)$$

$$+ \lambda_{NO}(a_2 \sum_{i=1}^{N} C_u^i\dot{NO}x^i-NOx_0)+\lambda_{CO}(a_3 \sum_{i=1}^{N} C_u^i\dot{CO}_i+b_3-CO_0) \tag{4.53}$$

subject to the independent variable constraints given in (4.52). There are three more unknowns - λ_{HC}, λ_{NO}, λ_{CO} yet there are three more equations -- the constraints as given in (4.51). Equation (4.53) can be simplified by collecting the terms in one summation yielding:

$$\mathrm{Min}\Big(\Big(\sum_{i=1}^{N} (0.0122C_u^i+0.00726C_H^i)\dot{F}_i+C_u^i(\lambda_{HC}\cdot a_1\cdot\dot{HC}_i+\lambda_{NO}\cdot a_2\cdot\dot{NO}x_i+\lambda_{CO}\cdot a_3\cdot\dot{CO}_i)\Big)$$

$$+ (\lambda_{HC}(b_1-HC_0)-\lambda_{NO}NOx_0 + \lambda_{CO}(b_3-CO_0)\Big) \quad , \tag{4.54}$$

subject to (4.52). λ_{HC}, λ_{NO}, λ_{CO} are also known as the Lagrangian Multipliers associated with the corresponding constraints.

Equation (4.54) can be decomposed to N separate optimization problems because the independent variables of one set point do not affect fuel or emissions at any other set point. The expression external to the summation operation does not affect the value of the independent variables and can be ignored while looking for the minimum of the adjoint expression of any set point. The optimization problem therefore reduces to the

F. LCMNA PROGRAM

The solution of the optimization problem is based on solving the reduced problem of one set point (4.55) which is a minimization of a nonlinear function in a bounded region. The value of any of the independent variables AF_i, SA_i, EGR_i that corresponds to the minimal point must be within the drivability region. Therefore the suboptimization problem is of the form

$$\text{Min}(f(AF_i, SA_i, EGR_i)) \tag{4.56}$$

subject to

$$\begin{aligned} AF_i^L &< AF_i < AF_i^H \\ SA_i^L &< SA_i < SA_i^H \qquad \text{for} \quad i=1,N \\ EGR_i^L &< EGR_i < EGR_i^H \quad . \end{aligned} \tag{4.52}$$

The package most suitable for solving this problem was LCMNA (Linearly Constrained Modified Newton Algorithm) by P.E. Gill and W. Murray [G-1]. The method basically involves finding the minimum of the function projected into the subspace defined by the currently active constraints. Adding active constraints as necessary and then determining whether any constraint can be deleted from the active set after the minimum is found.

As it is not known beforehand which of the constraints are active, the program arbitrarily selects some of the constraints to be active and transforms the problem to an unconstrained minimization by redefining the problem in a new base. The components of this base describe the linear manifold created by the active constraints. Once the solution is obtained, the Lagrangian Multipliers associated with the constraints assumed to be active are evaluated. A negative value implies that the constraint is not active and is removed from the active constraints. In addition the inactive constraints are also checked and those that violate the solution are introduced. After the active constraint vector has been updated, a new vector base that describes the manifold created by the currently active constraints is generated. If the gradient at the current point is close to zero, and none of the constraints are violated, the final solution has been obtained. Otherwise, a minimization search along a new direction takes place, and the whole sequence is repeated. The Hessian matrix is checked to be positive definite at the zero gradient point. A failure in obtaining a positive definite matrix means that a saddle point has been reached and a new search direction has been established.

G. RESULTS

The optimization problem was solved as suggested in equation (4.55); i.e., the values of the independent variables. AF, SA and EGR at the optimal points as well as the fuel consumption and the emission levels were evaluated for various values of λ_{HC}, λ_{NO}, λ_{CO}. The Lagrangian Multiplier associated with CO can be set to zero because solving the optimization problem subject to the HC and NO constraints drives the engine into the lean side thus satisfying the CO level automatically. The existence of only two Lagrangian Multipliers, λ_{HC} and λ_{NO} makes a graphical display of the results quite easy. The results can be plotted with NO level as abscissa, fuel as ordinate, and HC, CO and the independent variables as parameters. Each solution of (4.55) for certain values of λ_{HC} and λ_{NO} yields optimal values of fuel, HC, NO and CO as well as the value of the independent variables, AF, SA, EGR, for the 10 set points. A point that corresponds to fuel and NO can be marked now on the diagram. Each point is associated with certain values of HC, CO and the independent variables. Points having the same parameter value (e.g., HC) are connected, thus yielding lines of constant HC, CO, etc. Drawing diagrams for any of the 30 independent variables could be quite exhaustive and confusing. Therefore a single average was evaluated based on the following formula:

$$\widehat{AF} = \frac{\sum_{i=1}^{N} (C_u^i + C_H^i) AF_i}{\sum_{i=1}^{N} C_u^i + C_H^i} \qquad (4.57)$$

with similar expressions for $\widehat{SA}$ and $\widehat{EGR}$.

Actually equation (4.55) has to be solved only 9 times because the fourth point 2250/50 does not affect the urban cycle due to C_u^4 being 0. As emissions are considered only in the urban cycle, all that is required is finding the minimum fuel consumption at the point with constraints imposed only on the independent variables. Once the solution has been obtained, the fuel consumption of this point can be added to the general expression (4.11) which is evaluated for any λ_{HC}, λ_{NO}.

As a solution for two types of converters is desired, as well as the solution without any converter, the above procedure has to be repeated twice. Solving (4.55) subject to the independent variable constraints as given in Table 2-9 and evaluating the emissions using the coefficients of the first two rows of Fig. 4-1 yields the solution for either the NC (Non-Catalyst) case or for the OC (Oxidizing Converter) case. If a solution for the TWC (Three Way Catalyst) is desired, the bounds on AF as given in Table 2-9 must be modified as the converter efficiency strongly depends on fuel mixture. In this case the following relationship is used

$$14.5 \le AF_i \le 14.7 \qquad i = 1,N \tag{4.58}$$

and the coefficients of the third row in Fig. 4-1 are used to evaluate emissions.

The optimization problem as defined in (4.55) was solved 86 times for the NC and OC case and 96 times for the TWC cases. A typical computer output for either the NC or the OC cases for $\lambda_{HC} = 0.01$ and $\lambda_{NO} = 0.001$ is given in Table 4-2.

The trade-off curves for the NC and OC case as well as CO level and the value of the independent variables at the various optimal points are given in Figs. 4-3 to 4-5. HC and CO differ only by the catalyst efficiency while the mapping of the independent variables is the same. The corresponding diagrams for the TWC are given in Figs. 4-6 to 4-7. The extremes of the regions appearing in Figs. 4-3 to 4-7 are found by letting λ_{HC} and/or λ_{NO} be zero.

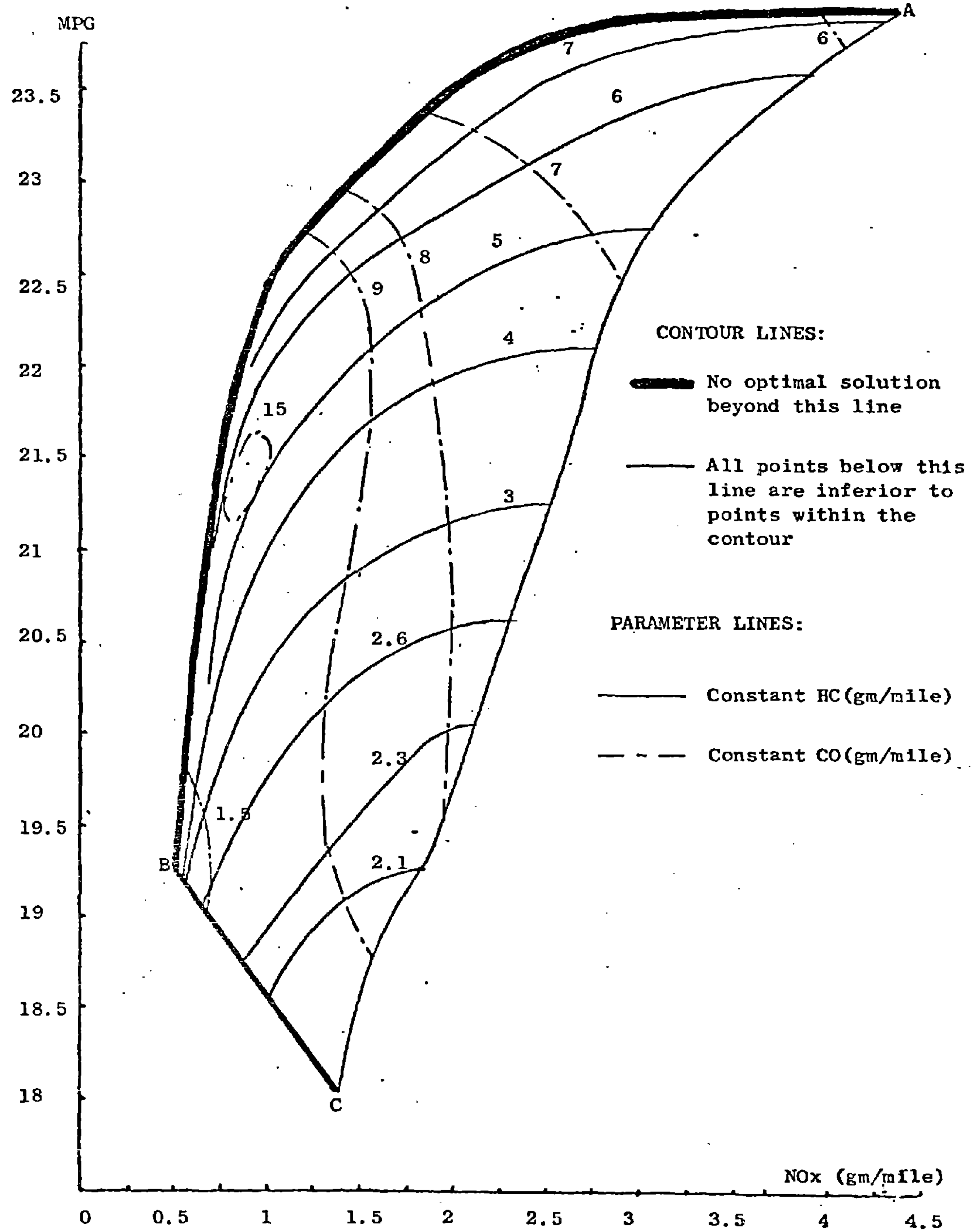

Fig. 4-3 HC AND CO TRADE-OFF CURVES THE NON-CATALYST CASE

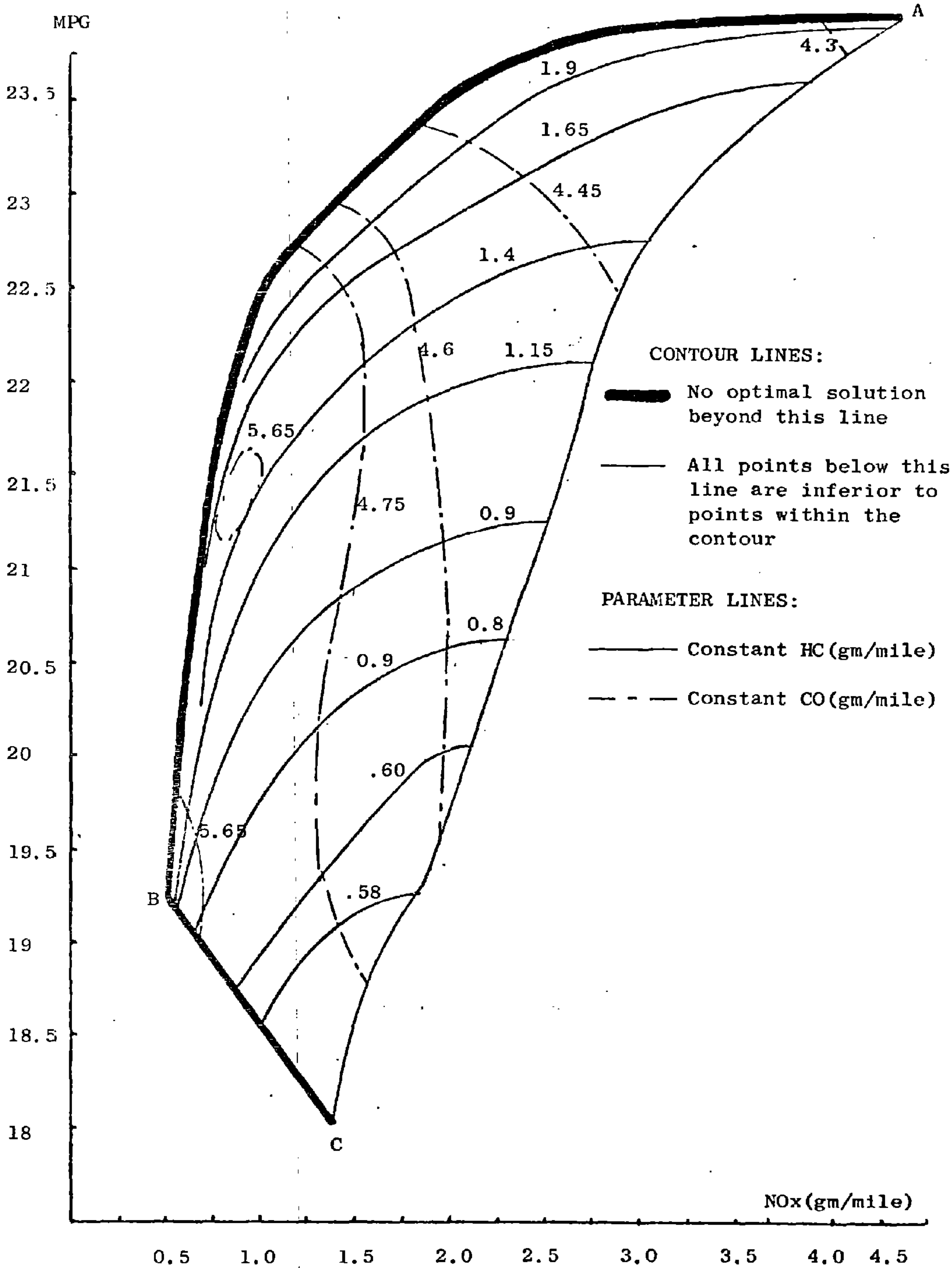

Fig. 4-4 HC AND CO TRADE-OFF CURVES THE OXIDIZING CATALYST CASE

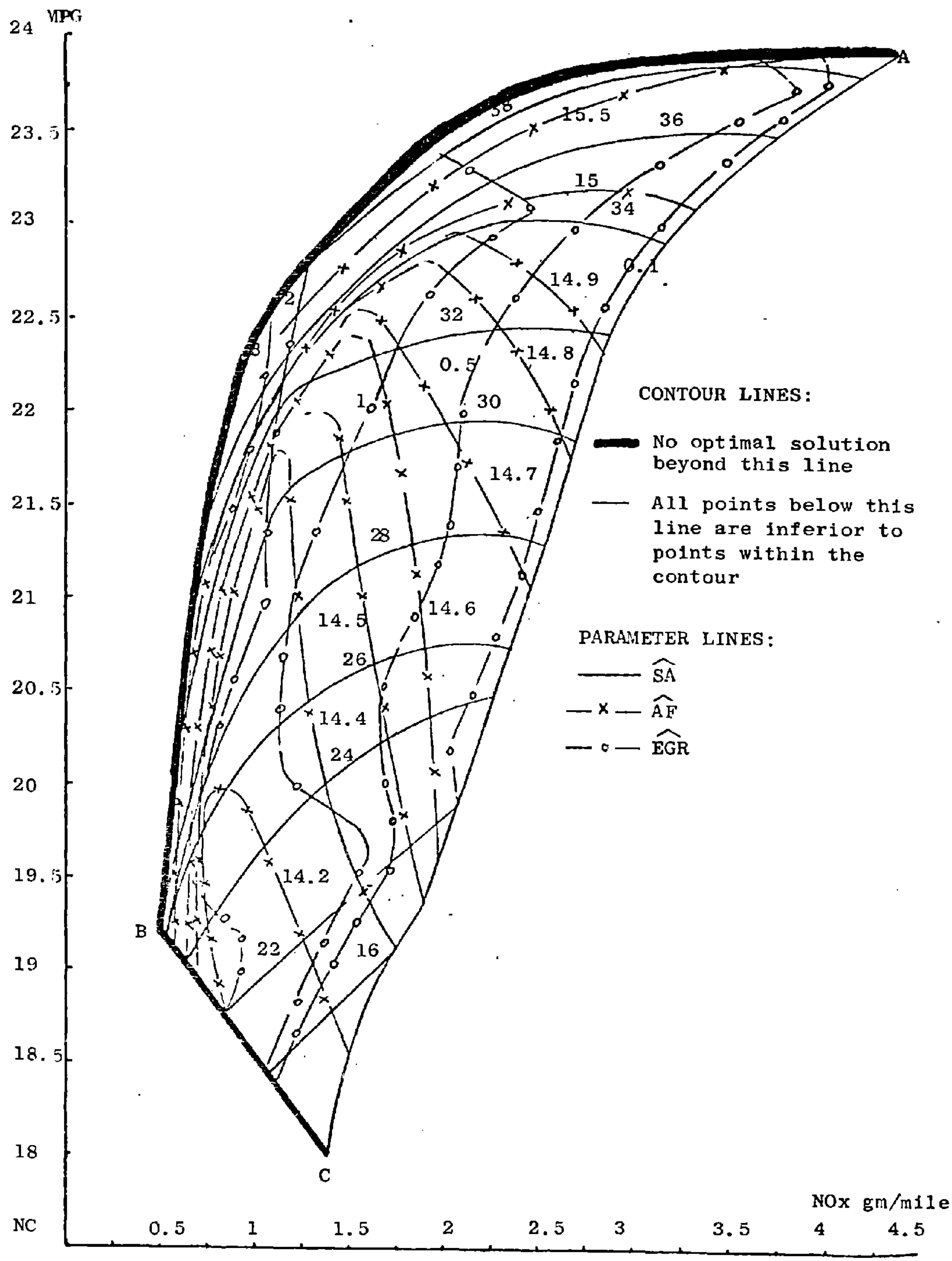

Fig. 4-5 AVERAGE AF, SA & EGR FOR THE NON-CATALYST (NC) AND THE OXIDIZING CATALYST (OC)

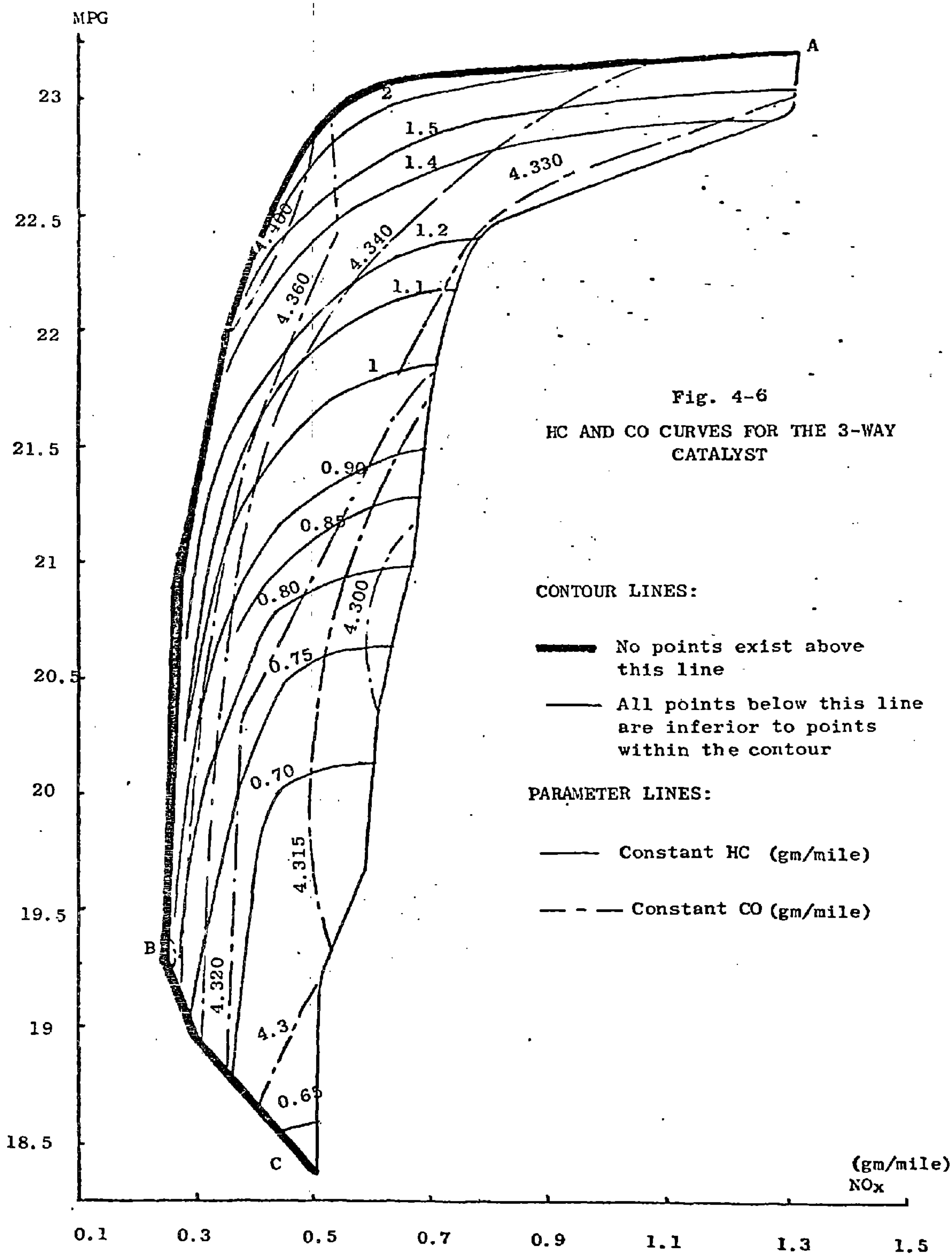

Fig. 4-6

HC AND CO CURVES FOR THE 3-WAY CATALYST

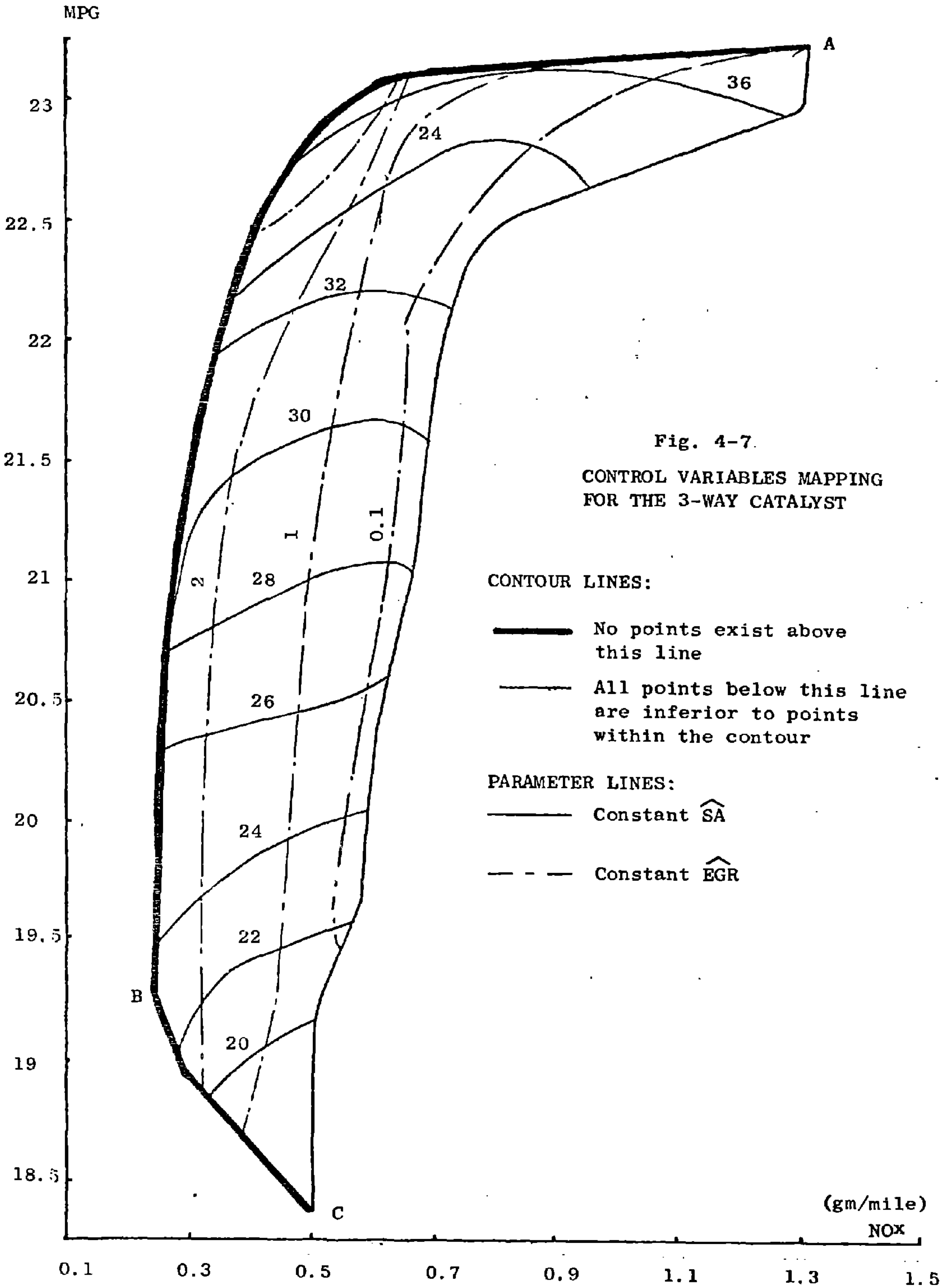

Fig. 4-7

CONTROL VARIABLES MAPPING FOR THE 3-WAY CATALYST

FUEL(MPG)= 21.0762

	HC(G/M)	CO(G/M)	NO(G/M)
ENGINE EMMISIONS	2.6800	7.8768	2.3287
TAIL PIPE WITH OC	0.8700	4.5815	1.6630

LAG HC	LAG CO	LAG NO
0.0100	0.0000	0.0010

THE INDEPENDENT VARIABLES ARE,

TORQUE	RPM	A/F	SPKADV	EGR	FUEL(LB/HR)	HC(G/SEC)	CO(G/SEC)	NO(G/SEC)
50	1700	15.610	10.000	0.000	11.338	16.575	16.652	16.448
25	1800	12.800	20.136	0.000	7.445	16.169	90.744	2.418
75	2100	15.501	15.772	3.340	16.498	15.999	43.495	36.252
50	2250	16.609	41.745	0.000	10.994	0.000	0.000	0.000
38	2600	15.513	39.766	0.000	11.257	23.610	31.061	31.936
20	1400	13.000	27.891	0.000	4.549	15.843	29.400	1.620
85	2500	16.763	24.035	6.200	19.611	13.210	73.737	63.792
72	2900	14.691	35.760	0.000	19.791	33.079	78.815	102.943
-14	1800	12.500	11.332	0.000	3.805	14.294	4.681	0.104
15	750	14.950	30.000	0.000	2.245	9.830	0.487	0.077

TABLE 4-2: AN OPTIMIZATION SOLUTION FOR $\lambda_{HC} = 0.01$, $\lambda_{NO} = 0.001$

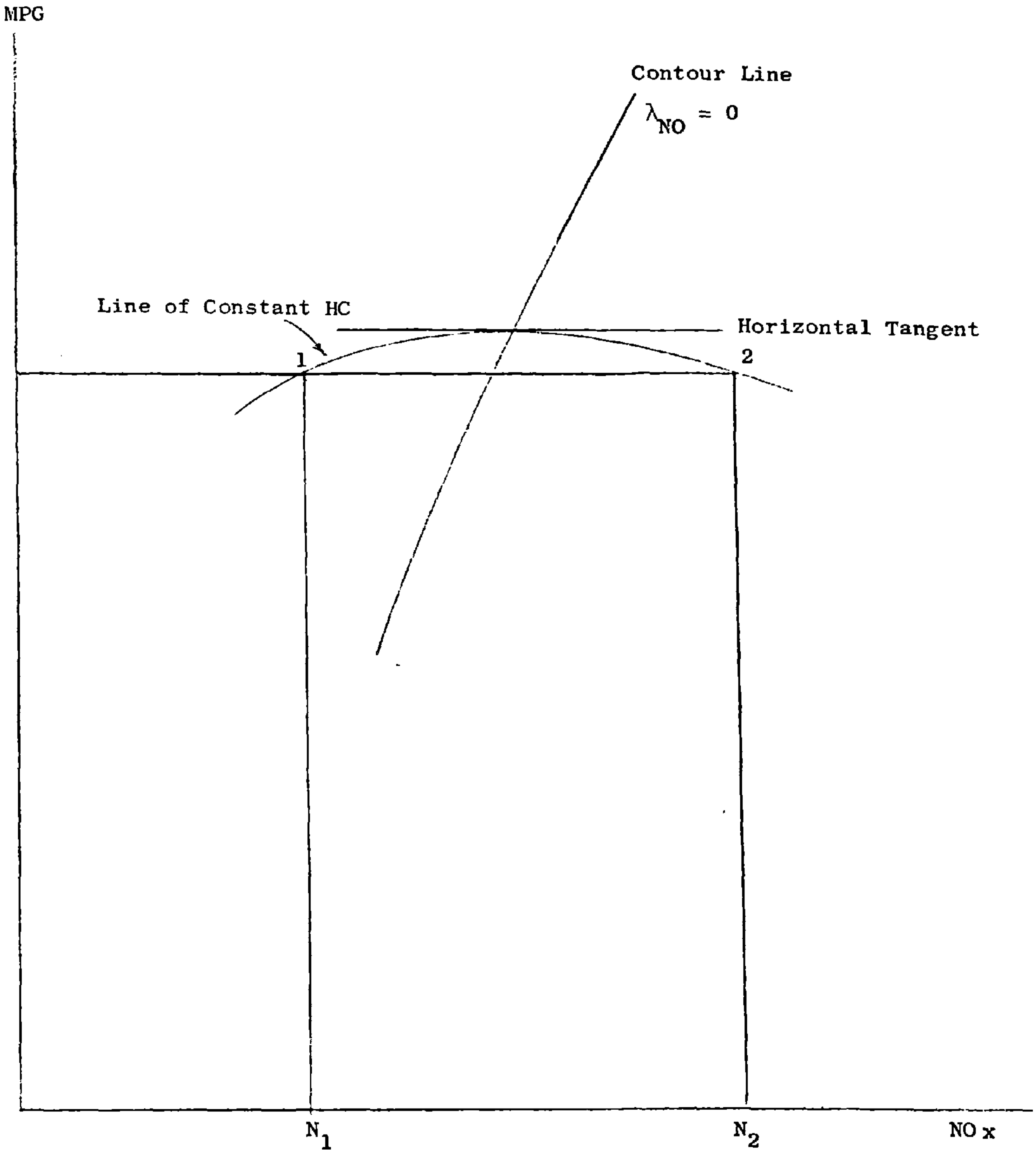

Fig. 4-8 Two feasible solutions having the same fuel and HC levels. 1 is optimal, 2 is not.

The uppermost point (A) corresponds to the unconstrained fuel consumption, that is, $\lambda_{HC} = \lambda_{NO} = 0$. The leftmost point B corresponds to the point of minimum NO . The lowest point (C) corresponds to the minimum of HC. The line connecting the point of minimum fuel with that of minimum NO is found by holding $\lambda_{HC} = \lambda_{CO} = 0$ and gradually increasing λ_{NO}. Similarly, the line connecting the point of minimum fuel with that of minimum HC is found by letting $\lambda_{CO} = \lambda_{NO} = 0$ and gradually increasing λ_{HC}.

The confined area represents therefore the loci of all feasible optimal solutions. There are no solutions left of line AB (which is equivalent to saying that there are no points having lower NO for the same fuel consumption) because line AB is the optimal solution. Quite in contrast, there are solutions to the right of line AC which are not optimal. Line AC is composed of all points of minimum fuel consumption for a given HC level. Therefore, the tangent to lines of constant HC is horizontal at the points of intersection with the contour line AC. Had it not been so we could keep moving along a line of constant HC upwards thus improving fuel economy for the same amount of HC. Some combination of the control variables can generate solutions right to line AC. These are non-optimal solutions because there exists another point with less NOx for the same amount of fuel and HC (see Fig. 4-8).

The zero slope of lines of constant HC at the intersection with line AC could also be explained by using the relationship:

$$\lambda = -\frac{\partial J_0}{\partial C} \qquad (4.58)$$

where J_0 is the performance index at the optimal point which is:

$$J = F_{\text{composite at optimum}} \; . \qquad (4.59)$$

Note that $F_{composite}$ is the inverse of the fuel economy in Fig. 4-6 . C is the constraint level. From the way line AC was constructed

$$\lambda_{NO} = 0 \Big|_{\text{along AC}} \; . \qquad (4.60)$$

Therefore substituting in (4.58) yields

$$\left.\frac{\partial F}{\partial NOx}\right|_{\text{along AC}} = 0 \quad . \tag{4.61}$$

The ordinate in Fig. 4-5 is actually 1/F but

$$\partial(1/F) = -\frac{\partial F}{F^2} \quad ,$$

therefore

$$\frac{\partial F}{\partial NOx} = -\frac{F^2 . \partial(1/F)}{\partial NOx_0} \quad , \tag{4.62}$$

from which

$$\frac{\partial(1/F)}{\partial NOx} = 0 \quad . \tag{4.63}$$

The 4.35 gm/mile NOx and the 5.69 gm/mile CO that correspond to the unconstrained optimal fuel with no catalyst are quite close to the figures quoted in other sources whereas the HC level of 7.95 gm/mile that corresponds to this point seems somewhat higher. It was suggested that this high figure is attributed to the shape of the sample line and the way it is connected to the exhaust tube. The sample line is connected to the exhaust tube approximately 20 inches downstream from the exhaust manifold. This short distance and the heated line avoid any condensation or any further oxidation that could take place had we tapped much downstream.

The HC-NOx tradeoff curves for the NC case are given in Fig. 4-3 from which it is seen that the higher the HC level, the more efficient the engine is running. It is possible to maintain the same fuel economy and reduce NOx levels if the HC level can go up. Yet driving the NOx level down while keeping the same HC value results in worse fuel economy following the law of diminishing returns, while we move along a line of constant HC in the right side of the diagram. NOx could be reduced substantially with only a moderate loss of fuel economy, whereas near the left boundary any attempt to further reduce NOx results in substantial loss in fuel economy. Similarly moving along a vertical line (constant NOx) while trying to reduce HC yields the same behavior. Reducing the HC level while holding the NO level constant results in lowering fuel economy. Yet the lower the HC level is, a smaller additional improvement is obtained for the same reduction in fuel economy.

The CO level is meeting the desired specifications in most of the cases. Only in a small portion (see the shaded area in Fig. 4-3) does the CO level exceed 15 gm/mile.

The change in the independent variables can be analyzed from Fig. 4-5. Unconstrained fuel consumption is obtained for AF = 15.4, SA = 39.0 and no EGR. Minimizing NO requires leaning the fuel mixture to 17.1, retarding the spark to 29.8 and increasing EGR to 3.95. Minimizing HC requires enriching the mixture to 14.1, one might expect a lean mixture at the minimum. Yet in some of the set points, minimization of the HC occurred for lean mixtures, while in some other cases the solution was obtained for a rich mixture. The weighted average yields a rich mixture. The SA must be retarded further to 19, and only slight level of EGR is required (0.29). Therefore reducing the HC for a given amount of NO results in enriching the mixture retarding the spark and decreasing EGR.

The solution of the optimization problem by Auiler, et al., [A-1] yielded similar results. The dynamic programming method was used to evaluate fuel economy for the 2.3 liter engine in various emission constraints.

A 1.8/2.3 gm/mile of HC/NOx resulted in fuel economy of 24.7 mpg and average AF of 15.70.

Reducing NOx levels to 0.64 resulted in fuel economy of 19.5 and average AF value of 15.28. A similar distribution of solution of the suboptimal problems of points of constant speed and load with respect to AF ratio was observed.

A similar analysis was performed for the three way catalyst (TWC) case (see Figs. 4-6 and 4-7). The confined region is smaller than that of the NonCatalyst case because tightening the constraint on air fuel ratio decreases the region of possible solution. Only in a very small region did the CO level exceed 3.4 gm/mile which justifies disregarding the CO constraint (Fig. 4-6). The HC trade-off curves are quite similar in shape to those of the previous case and the same analysis follows here. The control variables behave similarly (Fig. 4-7). Reducing NOx results in an increasing EGR, and reducing any of the constraints results in retarding the spark.

A detailed listing of the optimal fuel and emission levels as well as the average of the control variables AF, SA, EGR for various values of λ_{HC}, λ_{NO} for both the NO, OC and the TWC cases is given in Appendix Figs. G-2 to G-4.

V. CLOSED LOOP OPTIMAL CONTROL

A. INTRODUCTION

Internal combustion engine fuel consumption and emission levels are known to be sensitive to mechanical degradation and environmental changes. A survey done by NHTSA [B-4] revealed that fuel consumption can decrease as much as 11% after tun-up, while HC and CO can decrease by 22% and 12% respectively. Another survey made by Champion Spark Plug Co. [W-1] revealed a high percentage improvement of emission levels after tune-up; for example, CO could decrease 45% in idle and 25% at 55 MPH and HC could decrease 60%. Fuel economy increased 11.4% after tune-up.

The traditional open loop systems controlling spark advance, air/fuel ratio and exhaust gas recirculation cannot compensate for mechanical deterioration or for external disturbances. A closed loop system which continuously monitors engine performance and changes the control variables as needed is likely to reduce these effects.

Direct emissions measurements as the feedback signal are most desirable. However, this idea is impractical due to a lack of inexpensive reliable sensors. As a result, another measurement which reflects engine performance has to be used. The pressure trace is a good candidate for such a measurement. It was found in [H-3] that maintaining the angle that corresponds to peak pressure at 15^{o}ATDC, by changing the spark timing as required, keeps the engine operating at best fuel economy regardless of external disturbances. No attempt has been made so far to use this signal in the closed loop control of an engine over a speed-load range to minimize fuel consumption subject to emission constraints.

This chapter presents a design of a closed loop scheme, using the angle that corresponds to peak pressure as a feedback signal, to keep the engine operating optimally regardless of external disturbances. This closed loop scheme holds over a wide torque-speed range and will minimize fuel consumption for given emission constraints.

The peak pressure angle (θ_{pp}) is more directly related to pressure history than spark timing. Therefore this angle can be used as a feedback signal for spark control.

The measured angle is sensitive to changes in spark timing over a wide spark timing range. Usually, θ_{pp} changes roughly the same as spark timing. This relationship holds for wide spark timing regions except for very retarded spark timing for which θ_{pp} decreases as spark timing is retarded. This phenomenon imposes a limitation on the closed loop control, using θ_{pp} as a feedback signal, for tight emissions which require retarded spark timing.

Reasons for using the pressure trace, as well as the control logic and the hardware to measure the feedback signal, are given below. The limitations imposed on the closed loop scheme are also discussed.

The uneven air and fuel distribution among the cylinders can cause different optimal solutions for the various cylinders. A variation in the peak pressure angle of the individual cylinders might prove the existence of an uneven mixture distribution and the need for individual cylinder spark control. Some peak pressure angle measurements of the individual cylinders and a discussion of the possible individual cylinder controls are given below.

The chapter concludes with an analysis of the sensitivity of both the open and the closed loop systems to a humidity increase which can be regarded as a representative disturbance applied to the engine.

B. THEORETICAL BACKGROUND

Most of the current internal combustion engines are equipped with open loop systems. A definition of an open loop and closed loop system and the benefits of a closed loop system are given below. A pressure trace history is known to reflect engine performance as will be shown later.

1. Open Loop vs. Closed Loop Systems

In open loop control systems the output has no effect on the control action. The input/output relationship is shown in Fig. 5.1.

Fig. 5.1 Open Loop Control System

The input/output relationship depends on the controller calibration. Any error in the calibration or any disturbance will change the output. The output is not compared with the input. Therefore there is no way to compensate for the errors.

In a closed loop control system (Fig. 5.2), the controller is directly affected by the output signal. The output or its derivatives

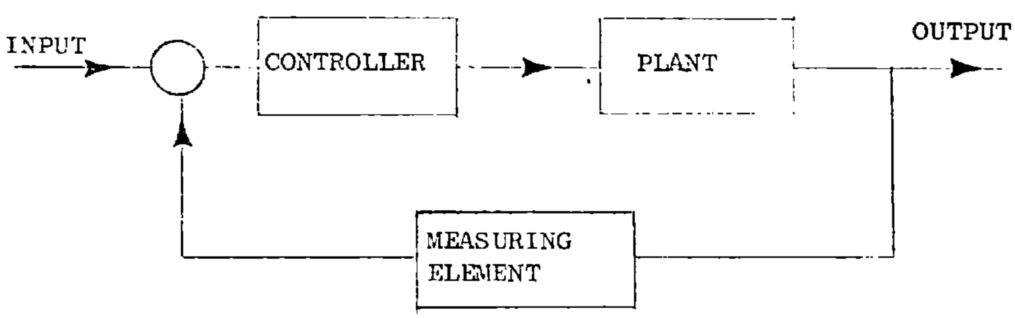

Fig. 5.2 Closed Loop Control System

are compared with the input, and it is the error which is the difference between the desired and actual values that drives the controller to reduce the error.

The great advantages of the closed loop system are the elimination of the precise calibration of the controller and the reduction of the system sensitivity to disturbances and to variations in system parameters.

The traditional spark timing system, for example, is an open loop control system in which spark timing is determined by engine speed and load. Centrifugal weights provide the desired spark advance as engine speed goes up by advancing the distributor base. The required retard in spark timing as load goes up, is provided by the inlet manifold pressure which acts on the distributor base. This is an open loop system because no attempt is made to measure engine performance and to correct for any deviation.

2. Cylinder Pressure Signal

The fundamental control being accomplished by spark advance is the positioning of the pressure time history with respect to crank angle. The location of the peak pressure (θ_{pp}) in the engine cycle is more directly related to this pressure time history than spark timing as was shown previously [H-3].

Furthermore, the value of θ_{pp} that corresponds to an optimal engine setting is less sensitive to external disturbances or to variations in engine operating conditions than the actual spark timing. These features of θ_{pp} make it superior for spark timing control than other known schemes.

Figure 5.3 a-c show typical pressure traces for spark timings of 30°, 20° and 10°BTDC. The marks on the top represent the timing marks of 60°BTDC and 120°ATDC. As seen in Fig. 5.3, the pressure trace has a flat part that corresponds to the intake stroke where the piston moves down and a fresh charge is admitted. Pressure builds up as the piston goes up and both the intake and exhaust valves are closed. The slope of the trace becomes steeper when the spark is ignited and the

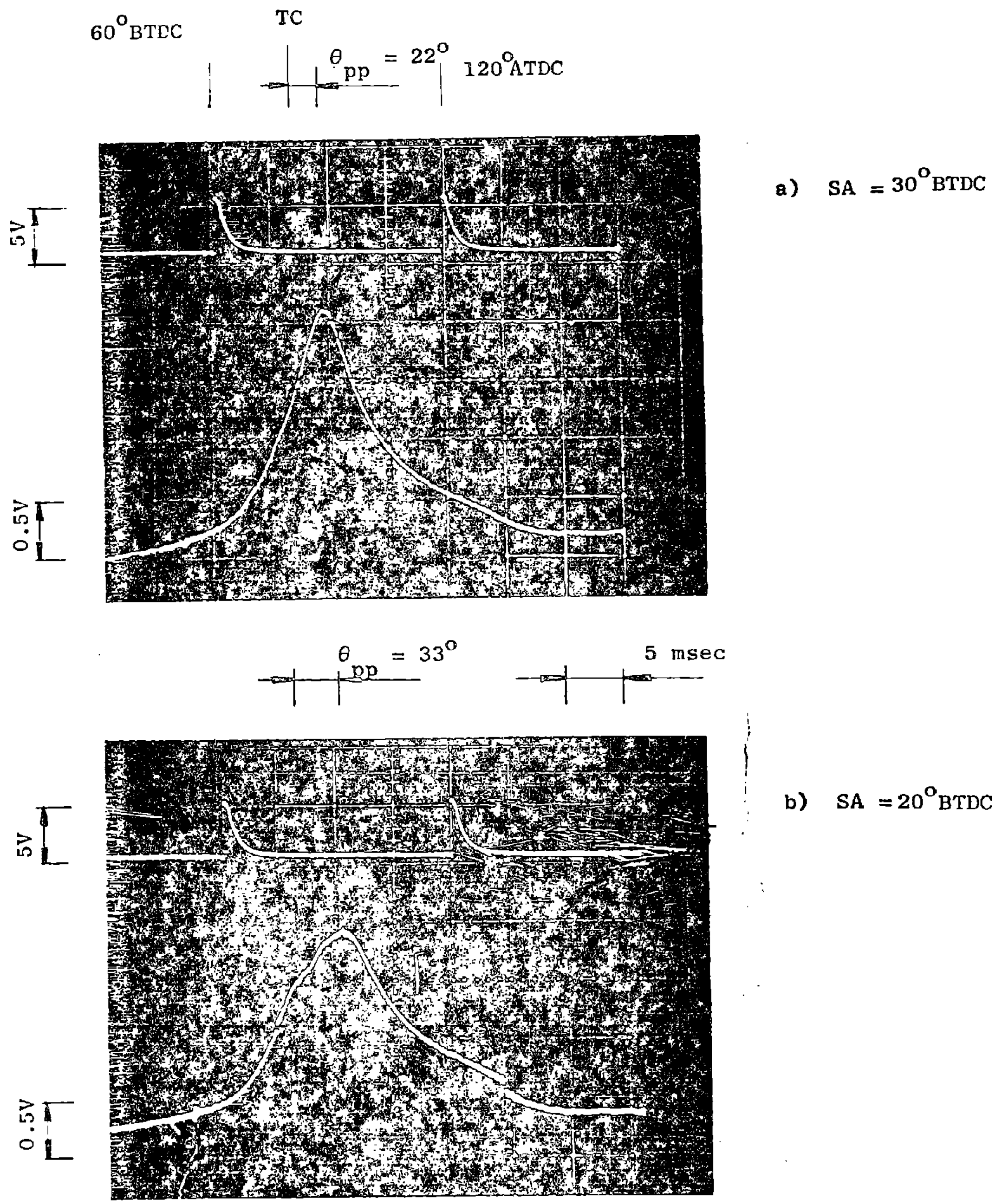

Fig. 5.3 Cylinder pressure traces for various spark settings (40/1500 lb ft/rpm, AF/EGR = 12.5/0)

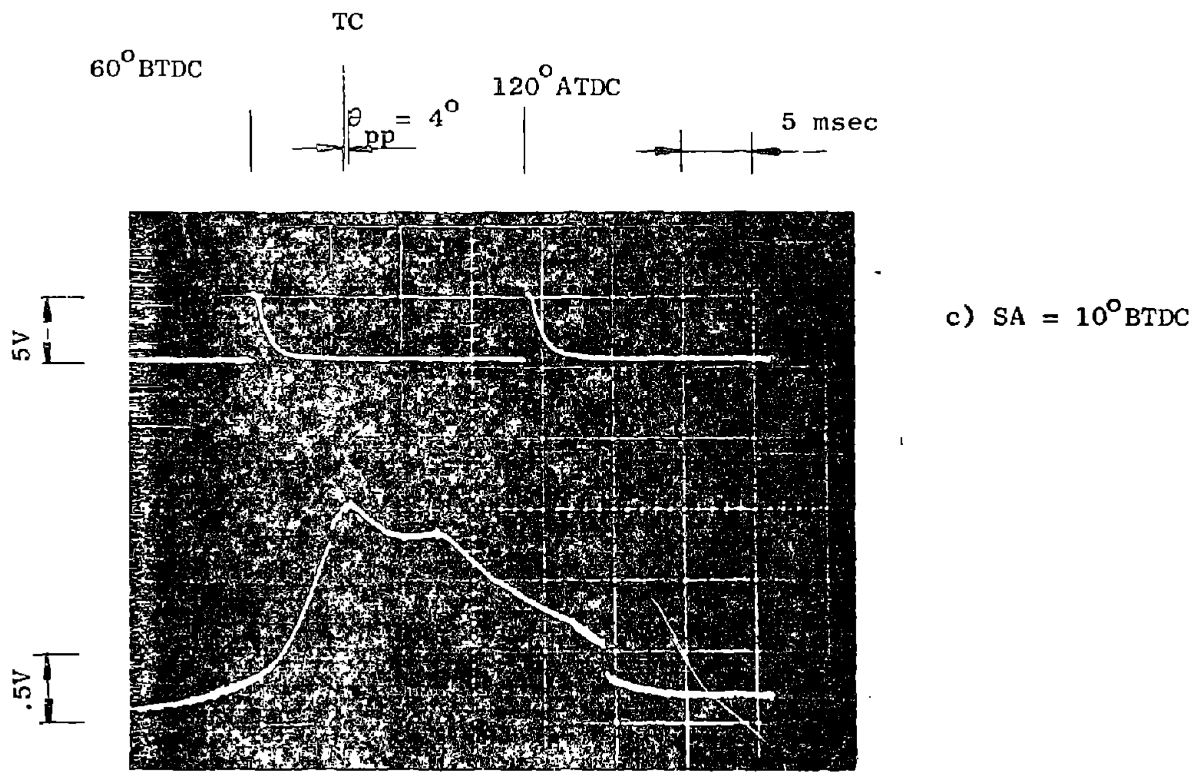

Fig. 5.3 (cont.) Cylinder pressure traces for various spark settings (40/1500 lb ft/rpm, AF/EGR = 12.5/0)

θ_{pp} increases as spark timing is retarded up to a point beyond which θ_{pp} starts to decrease.

trace reaches its peak a few degrees ATDC. Pressure declines thereafter due to the expansion stroke and to the opening of the exhaust valve (see Fig. 5.3 a).

Figure 5.3b follows this pattern. When the spark is retarded to 20^{o}BTDC, peak pressure timing moves roughly the same amount. The shape of the pressure trace changes when spark timing retards, peak pressure decreases and the gradient goes down, since the pressure build-up due to the combustion process is counteracted by the downward movement of the piston in the expansion stroke. When spark timing is retarded greatly, the distinct sharp peak disappears (Fig. 5.3c) and the relationship between θ_{pp} and spark timing is different than that for advanced spark timing.

Engine performance can be detected from various features of the pressure trace. The angle that corresponds to peak pressure can be measured more conveniently as opposed to peak pressure amplitude which requires sensor calibration. Any change in engine performance which is reflected by a change in the pressure trace can be detected by measuring θ_{pp}. External disturbances and mechanical deterioration can contribute to such changes. Typical examples of external disturbances are changes in humidity, ambient pressure and temperature; whereas examples of mechanical degradation are changes in air/fuel ratio, deposit build-up, etc. An increase in θ_{pp} implies an increase in fuel consumption since it indicates a slower flame which causes fuel consumption to go up. A decrease in θ_{pp} implies an increase in emissions since it indicates a faster flame. The faster flame brings up combustion temperature which is essential to the formation of NOx. Therefore maintaining θ_{pp} in its nominal value is likely to reduce the external disturbances and mechanical deterioration effects both on fuel and emissions.

C. CONTROL LAW

An optimal closed loop scheme for a wide torque and speed range is desired. A control law maintaining the engine in MBT in a constant load/speed point was presented in [H-3]; the angle that corresponds to peak pressure is held roughly at 15° ATDC by changing the spark as needed. The angle can also be used as a feedback signal over a wide torque/speed range while accounting also for emission constraints. The control law will be derived over the EPA cycle since it is convenient to base the derivation of the closed loop on the results obtained from the optimization solution.

The control law will be derived for a particular level of emissions, yet the method of solution is quite general and can be adopted very easily to other levels of emissions. Each optimization solution is the minimization of fuel consumption over the EPA cycle subject to emission constraints and is associated with optimal values of the control variables and the feedback signals. The optimal control variables are AF, SA and EGR at the 10 load/speed points, and the feedback signals are the values of θ_{pp} that were measured with the controls tuned to their optimal values under nominal conditions.

A local control strategy controls the engine at one of the 10 torque/speed points (see Fig. 5.4). A local control strategy is as

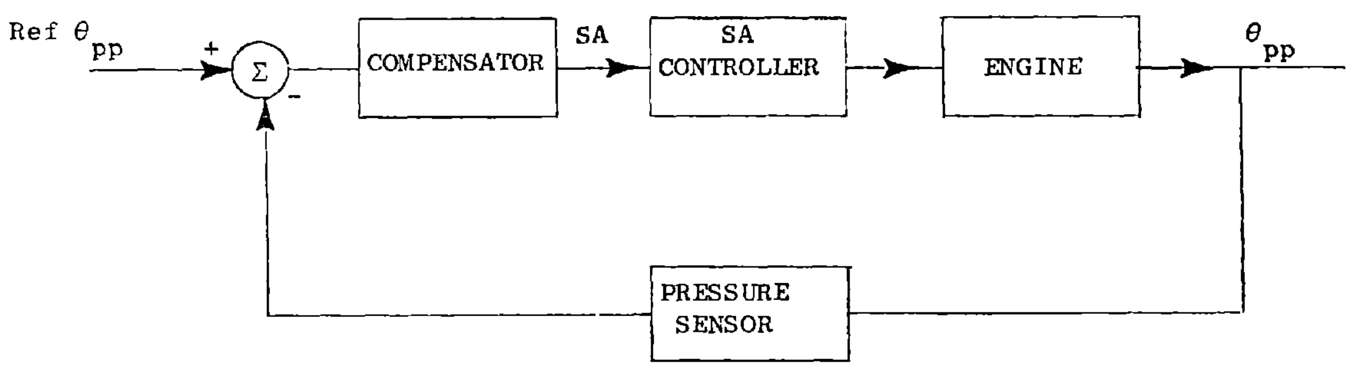

Fig. 5.4 A local peak pressure controller for constant torque and speed

follows: air/fuel ratio and exhaust gas recirculation will be set to the nominal values found in the optimization solution and spark advance will be adjusted to keep θ_{pp} in its optimal value. As discussed earlier, this optimal value corresponds to a particular emission level.

Applying this local control strategy to all the torque/speed points, where θ_{pp}^{opt} at each point is determined by the optimal solution will provide optimal closed loop control in these discrete points but not at any intermediate torque/speed values. A control law over the engine operating range can be determined by finding a general relationship between the feedback signal θ_{pp}^{opt} and some engine parameters such as torque, rpm, inlet manifold pressure, power, etc., that includes the optimal solutions at all points. This can be done by fitting some function to the measured values of the feedback signal. The accuracy of this function depends on the number of measurements. The EPA cycle is approximated by running the engine at 10 torque/speed points. An increase in this number will improve the accuracy of this expression. When an expression relating the optimal feedback signal to some measured engine parameters is found, the local control law can be expanded by continuously updating the reference value of θ_{pp}.

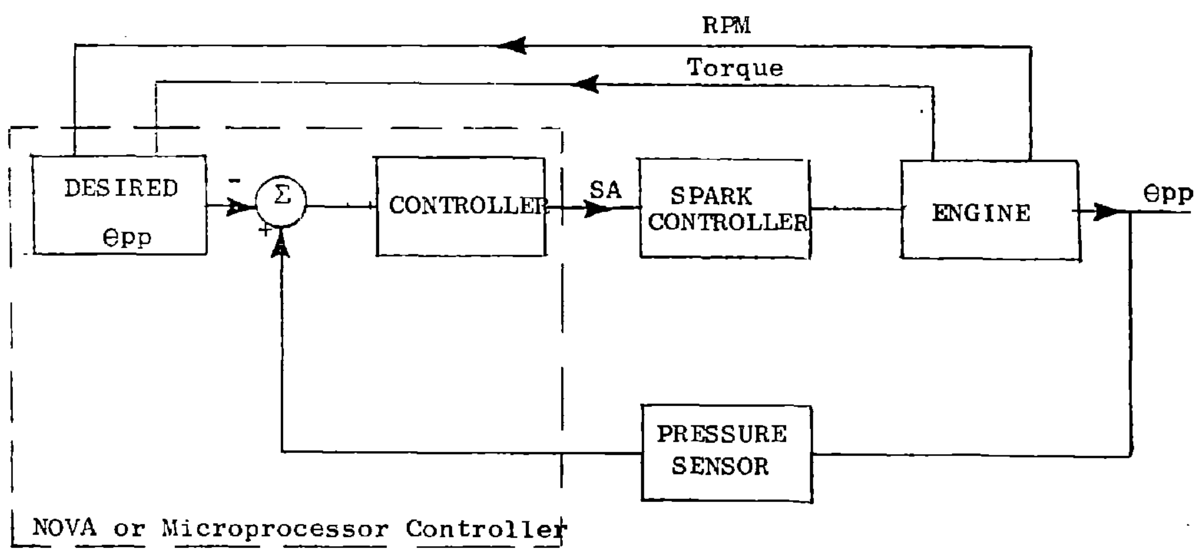

Fig. 5.5 An optimal closed loop peak pressure controller. Spark advance controller changes spark timing when θ_{pp} deviates from the desired reference value.

This updating process follows the relationship obtained in the function fitting discussed above (see Fig. 5.5).

D. PEAK PRESSURE TIMING DETECTION CIRCUITRY

The angle that corresponds to peak pressure was detected by an electronic circuit, the schematic of which is shown in Fig. 5.6.

The cylinder pressure is converted into a voltage by a piezoelectric transducer which is installed between the spark plug and the engine head. This signal is amplified and fed into the first card which generates a pulse that corresponds to peak pressure. The second card generates a voltage which is proportional to the time between a reference mark on the crankshaft - 60^{o}BTDC and peak pressure. This analog signal is directed to the NOVA which converts it to degrees by considering the engine speed as well.

The piezoelectric transducer was built according to K.W. Randall's recommendations [R-4]. The sensor is composed of a piezoelectric ring held between two electrodes which are embedded in an insulating material (see Figs. 5.7-5.8). The PZT-5A piezoelectric ceramic composed of lead, zirconium and titanium was selected because of its high sensitivity (voltage to strain ratio), high time stability and resistivity at elevated temperatures with Curie point of 365^{o}C. The electrodes were made of copper for good conductivity. Ground is provided by the electrode which is in contact with the engine head. The other electrode is positive in the sense that pressure build-up in the cylinder that relieves the pretorqued load on the sensor generates positive voltage with respect to engine ground.

The insulating mold material selected is Kinel 5514 which is a fiberglass reinforced polyimide plastic able to withstand high temperatures and corrosive environments having a heat distortion temperature of 350^{o}C. The various parts of the sensor are held together by a high temperature epoxy.

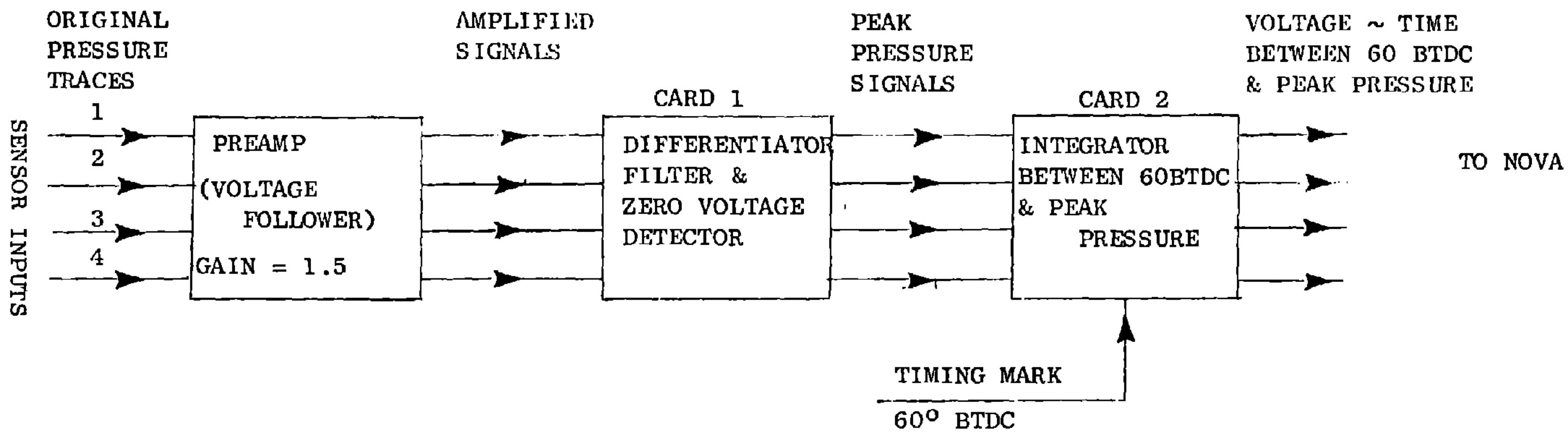

PEAK PRESSURE TIMING DETECTION CIRCUIT

Figure 5.6

The sensor inputs are amplified by the preamp. Card 1 differentiates and filters for high frequency noise. It outputs a signal when peak pressure occurs. Card 2 outputs a voltage proportional to the time between 60°BTDC and peak pressure event.

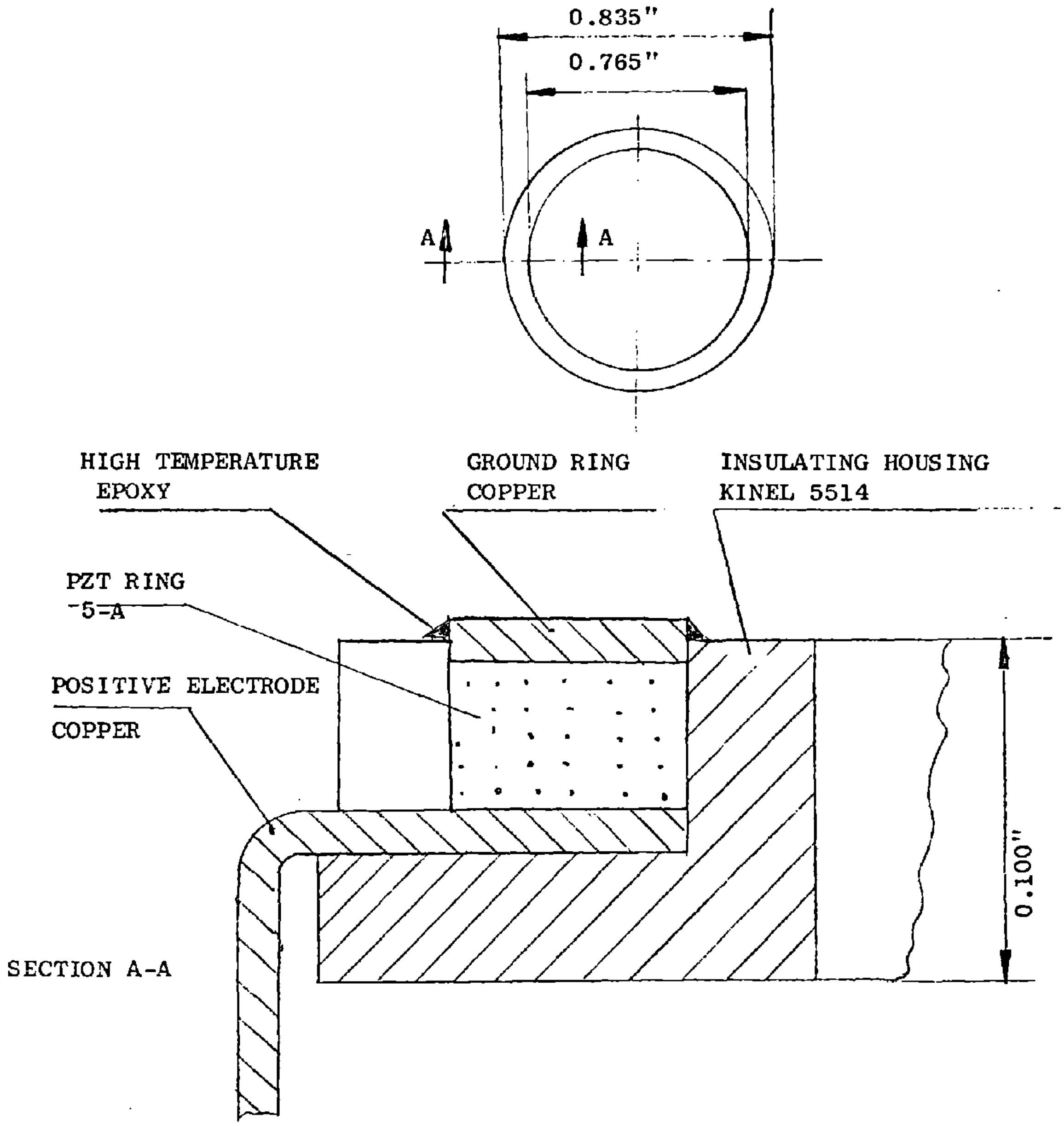

PZT PRESSURE TRANSDUCER

Figure 5.7

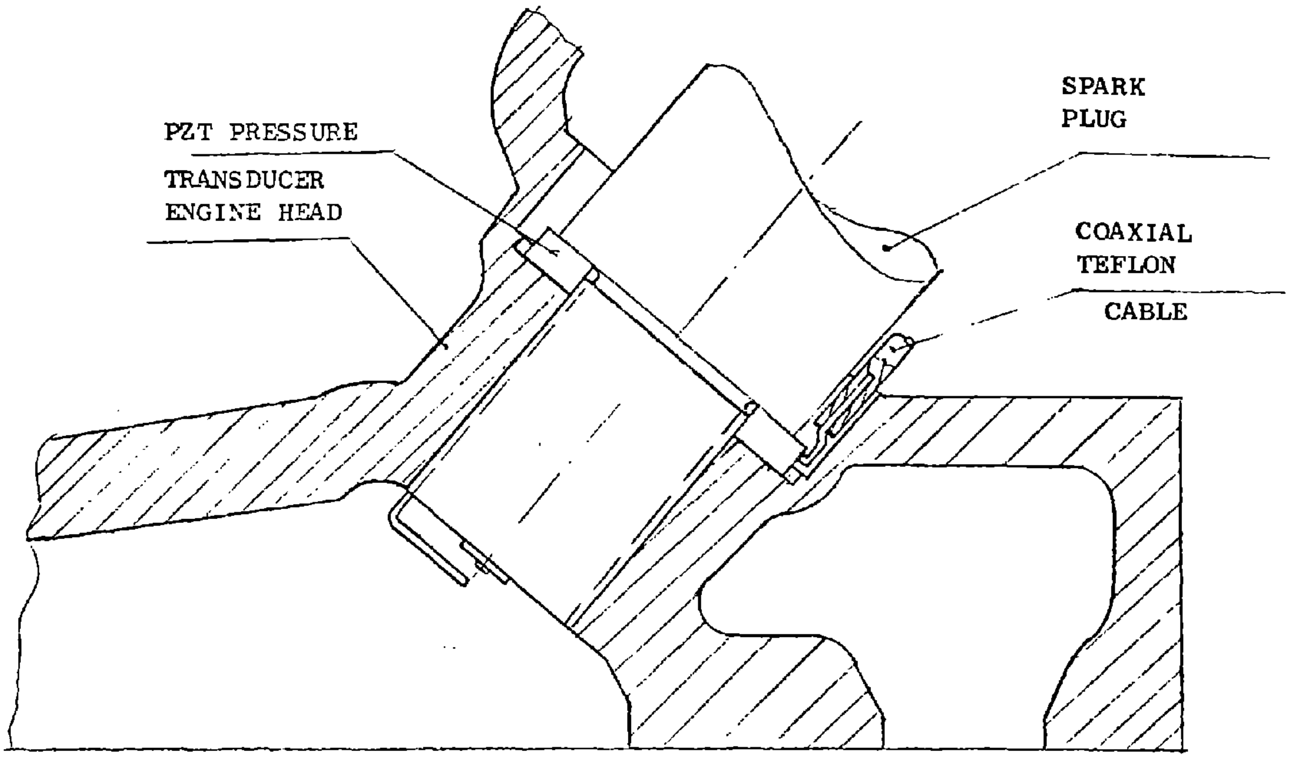

PRESSURE TRANSDUCER MOUNTING ON ENGINE HEAD

Figure 5.8

The signal is conducted in a teflon coaxial cable selected for its high temperature resistance. The shield was grounded to reduce interference from the spark plug high voltage. As this shielding was not sufficient, the spark plug wires were also placed in grounded copper braids. Discontinuities in the pressure trace could be detected at points corresponding to spark plug firings.

1. Preamplifier:

The preamplifier is built of a RCA 741 operational amplifier with 2 FET amplifiers on the input side both on the signal line and the ground line to reject the common mode. The PZT element is a voltage generator with essentially no current; therefore, a voltage follower circuit providing the right current is required. The preamp circuit has a voltage gain of 1.5 (seee Appendix H1).

The high resistance of 110MΩ on the input side between the signal line and the ground is required to avoid any signal distortion.

The PZT element can be regarded as a voltage source V_{CO} (see Fig. 5.9) with capacitance C. This capacitance together with the capacitance of the coaxial cables C_L and the high impedance resistor R form a high pass filter having a transfer function of:

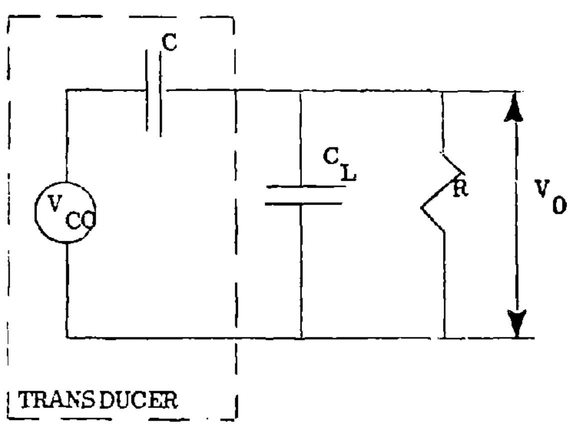

$$\frac{V_0}{V_{CO}} = \frac{SCR}{1 + SR(C+C_L)}$$

Fig. 5.9 PZT Sensor Electric Schematic

$$\frac{V_0}{V_{CO}} = \frac{S \cdot CR}{1+SR(C+C_L)} = \frac{C}{C+C_L} \quad \frac{S/\omega_0}{1 + S/\omega_0} \tag{5.1}$$

where

$\omega_0 = \frac{1}{R(C+C_L)}$;

V_{CO} = sensor output voltage;

V_0 = circuit output voltage.

This circuit acts as a high pass filter which behaves like a differentiator for frequencies less than ω_0, and as a pass through filter for frequencies higher than ω_0. It would have been preferable to set $\omega_0 = 0$ to avoid any signal distortion. However, the break frequency is inherent in the circuit design; therefore, it is desired to drive ω_0 as low as possible to reduce the signal distortion effects.

Typical values of the sensor and coaxial cable capacitance are:

$$C = 440 \text{ PF}$$
$$C_L = 90 \text{ PF} \tag{5.2}$$
$$R = 110 \quad .$$

Therefore substituting in (5.1) yields

$$\omega_0 = 16.95 \text{ rad/sec}$$

or

$$f_0 = \frac{\omega_0}{2\pi} = 2.7 \text{ Hz} \quad .$$

Equation (5.1) will be:

$$\frac{V_0}{V_{CO}} = 0.85 \quad \frac{S/16.95}{1+ S/16.95} \quad . \tag{5.3}$$

This frequency is 5-10 times smaller than the engine speed, therefore no signal distortion is expected.

The high frequency gain is found by letting ω go to infinity in (5.1) which yields

$$\left.\frac{V_0}{V_{C0}}\right|_{\omega\to\infty} = \frac{C}{C+C_L} = \frac{1}{1+C_L/C} \quad . \tag{5.4}$$

From this it is concluded that the pass through gain may vary when sensor capacitance changes. The breakpoint ω_0 evaluated in (5.3) was found for typical C values. The smallest values of C did not differ considerably from 440 PF assumed in (5.2); therefore, no significant distortion of the sensor voltage is expected.

The level of the output signal can be controlled by an attenuator which is installed on the output line. This was done to match the signal-to-noise ratio in various signal levels, as will be discussed below.

2. Peak Detector:

This device outputs pulses that occur at peak pressure (see Appendix H2). The pressure signal is differentiated and filtered to attenuate the noise by a low pass filter having a breakpoint of 482 Hz and a slope of -40 db/decade for higher frequencies.

The differentiator and filter transfer function is given by

$$\frac{V_1}{V_0} = 10.4\,\frac{S/\omega_1}{(1+S/\omega_1)^3} \tag{5.5}$$

where

- V_1 is the output voltage;
- V_0 is the input voltage;
- ω_1 is the breakpoint.

The total transfer function from the sensor to the differentiated signal is the product of (5.3) and (5.5) which is

$$\frac{V_1}{V_{C0}} = \frac{V_0}{V_{C0}} \times \frac{V_1}{V_0} = 8.71 \frac{(S/\omega_0)(S/\omega_1)}{(1+S/\omega_0)(1+S/\omega_1)^3} . \qquad (5.6)$$

The bode plot of this transfer function is given in Fig. 5.10. ω_1 was selected to meet the requirement that the first few harmonics of the pressure trace would not be filtered out. The pressure trace frequency roughly matches engine frequency. Therefore, at 3000 RPM, which corresponds to 50 Hz, this requirement will be met. The lowest speed, 750 RPM or 12.5 Hz, will still be above the sensor breakpoint.

The noise frequency is assumed to be at least 50 times higher than the engine speed, which means that it will be around 600 Hz for the lowest engine speed. This guarantees the noise attenuation.

The differentiated signal is detected for a zero voltage crossover. Both the signal and the reference voltages are fed into an amplifier which goes into saturation when these two values are not equal. The sign of the saturated voltage depends on relative magnitudes of the signal voltage to the reference voltage which was set to be zero. A Zenyr diode arrangement on the output side keeps the output voltage from going into saturation, but rather sends it to -0.6v when the signal is less than 0.16v and to +4.7v when the signal becomes positive again. This hysterysis was introduced intentionally to eliminate system response to noise. The threshold voltage of 0.16v guarantees that no false triggering will occur when the differentiated noise signal is equal to zero, due to the fact that the noise level is small compared to that value. The signal noise can be adjusted by the preamp attenuators so the noise level will be maintained below the threshold level (see Appendix H1).

A typical pressure trace, its derivative and the associated peak pressure pulses are shown in Fig. 5.11. The pressure trace, the peak pressure pulse and the timing mark corresponding to 60^{o}BTDC are shown in Fig. 5.12. T_1 denotesthe time corresponding to peak pressure measured

Fig. 5.10 BODE DIAGRAM OF PRESSURE SIGNAL FILTERING

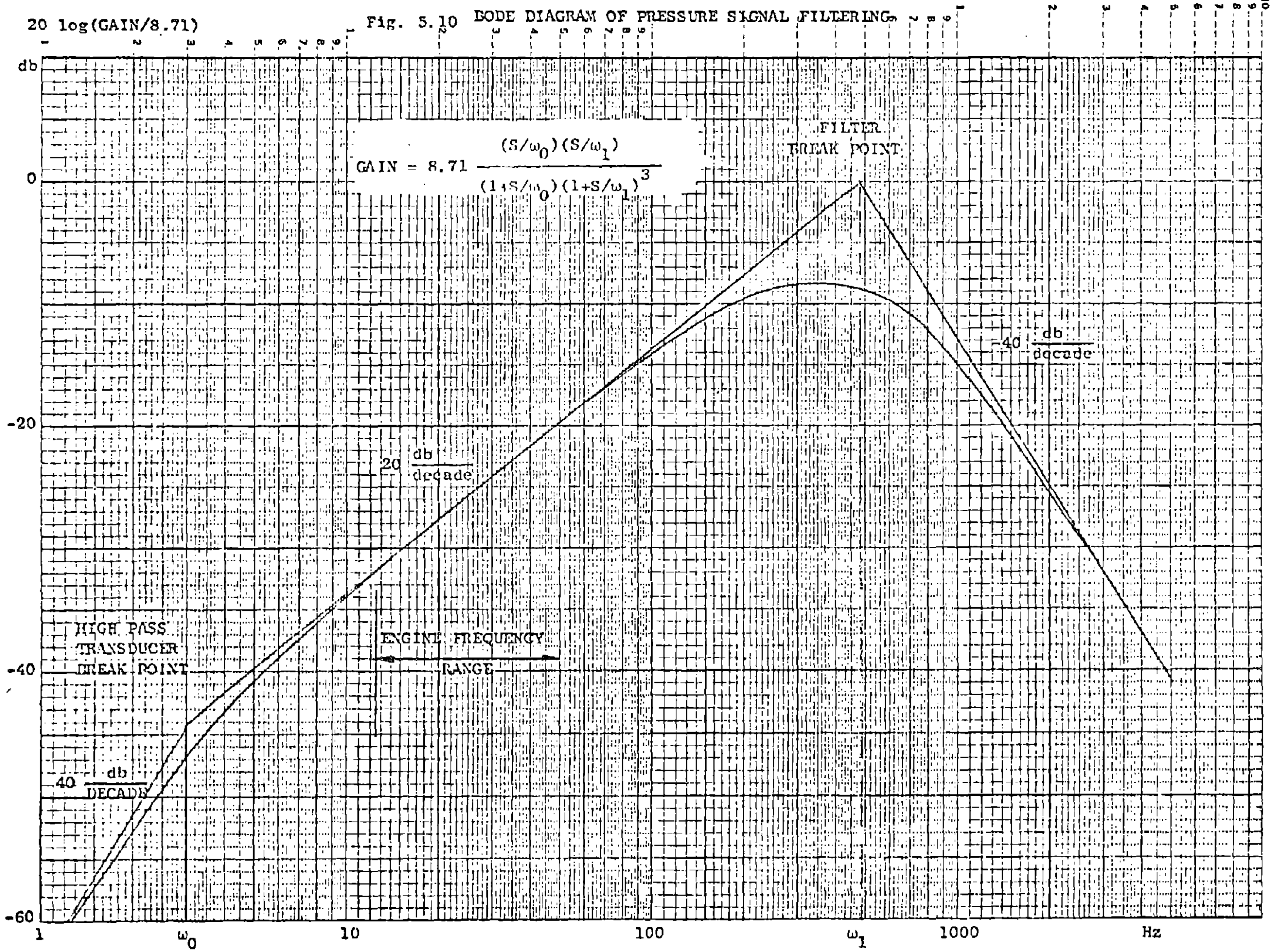

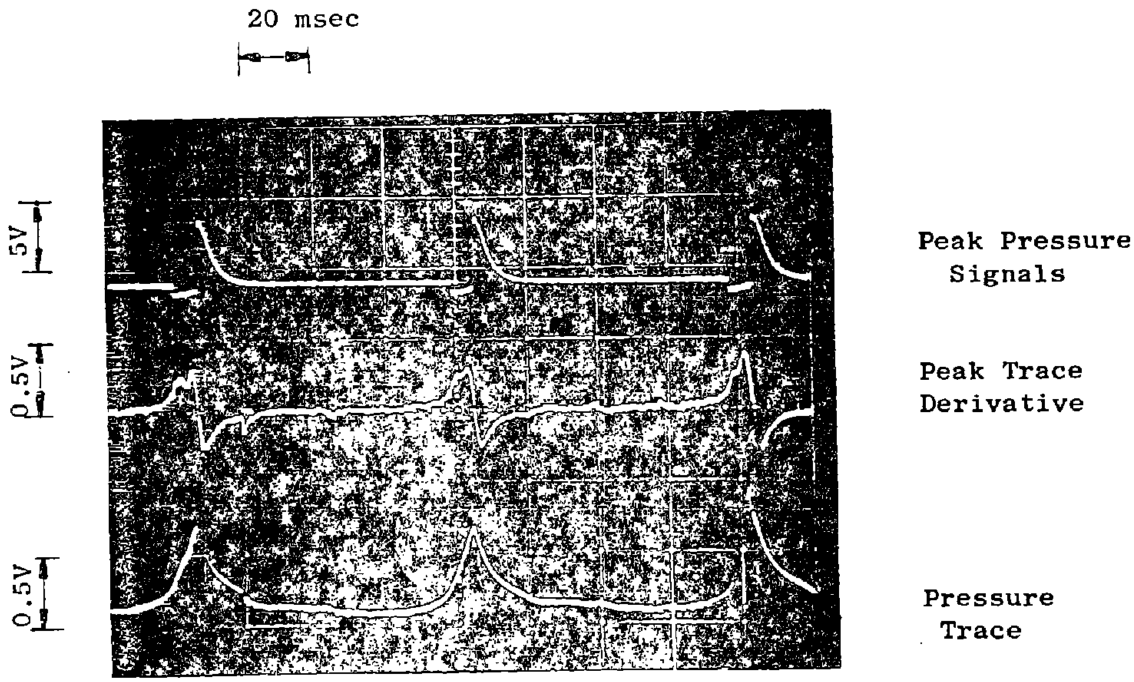

Fig. 5.11 Typical pressure pulses and the associated peak pressure signals (38/1500 lb ft/rpm), AF/SA/EGR = 12.5/30/0)

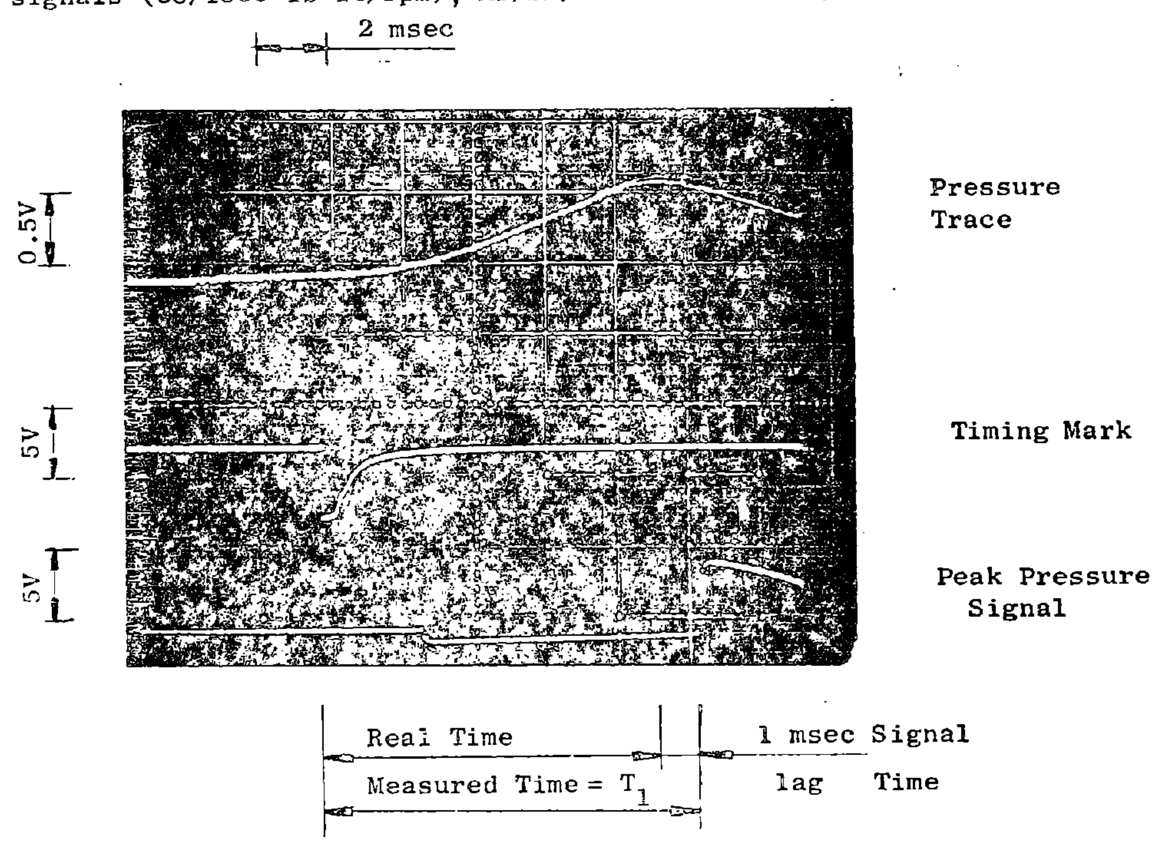

Fig. 5.12 Peak pressure timing (38/1500 lb ft/rpm, AF/SA/EGR = 12.5/20/0)

from the reference signal. It can be seen that the upgoing edge of the peak pressure signal lags beyond the peak pressure by 1 msec. This time lag is introduced into the signal by the noise attenuation filter. The 1 msec value was found to be almost the same over a wide range of torque and speed and was accounted for in the conversion from time to degrees as will be discussed below.

3. Peak Angle Measurement:

This circuit outputs a voltage which is proportional to the time between the timing mark of 60^{o}BTDC and the upgoing edge of the peak pressure signal. The relationship between this circuit and the other circuits is shown in Fig. 5.6. The circuit schematic is shown in Appendix H3. The output signals are directed to the NOVA minicomputer. The input signals are the peak pressure pulses and the timing marks.

As can be seen from Fig. 5.13 there are 4 timing marks between any two peak pressure signals, since two engine cycles are required for each thermodynamic cycle with each cycle delivering 2 timing marks at

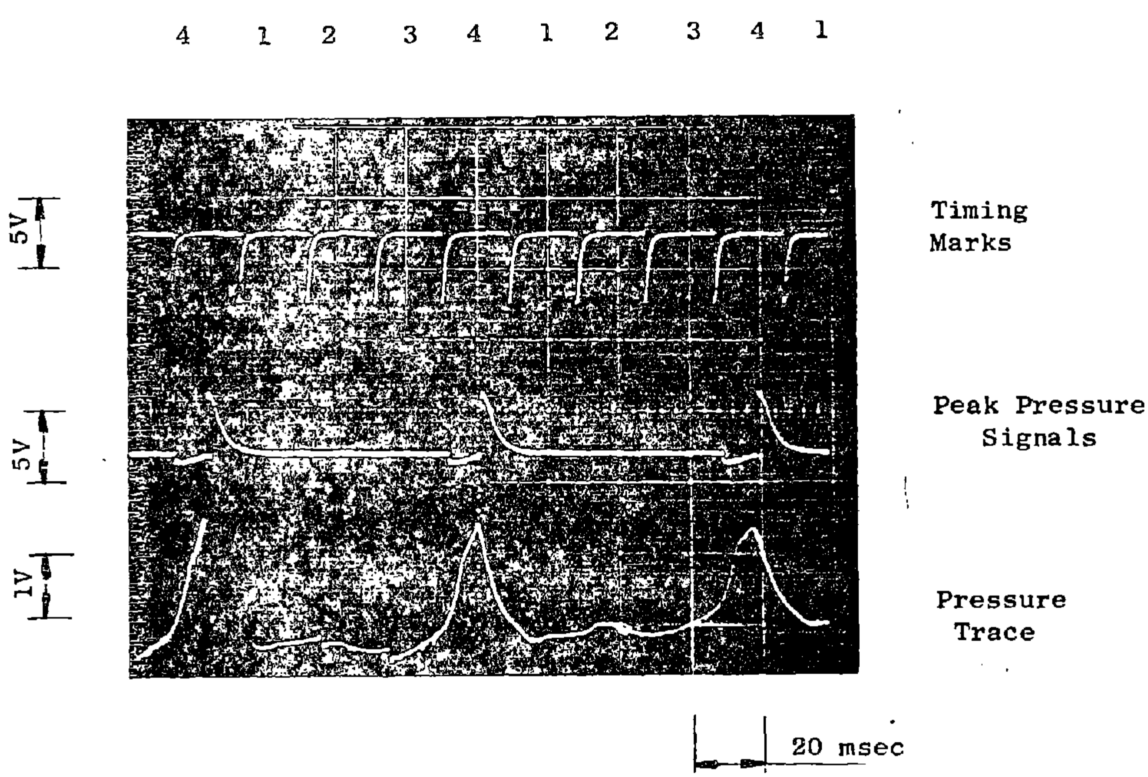

Fig. 5.13 Timing marks and peak pressure signals

60^{o}BTDC and 120^{o}ATDC. Therefore a circuit capable of distinguishing the appropriate timing mark is required. A negative constant voltage is integrated starting at 60^{o}BTDC and terminated when peak pressure occurs, resulting in an output which is proportional to the time between these two events.

A digital counter is used to select the appropriate timing mark. The counter is reset by the peak pressure signal. The timing marks are counted from this event. Therefore count number 4 triggers the integration which will be terminated by the peak pressure signal. Count number 2 latches the integrator ourput to the hold circuit and count number 3 resets the integrator making it ready for the next round. Therefore the output voltage is latched only one quarter of the time.

A filter and an amplifier serve as a hold circuit to smooth the integrator output. The filter time constant was chosen to be 0.5 sec so it would be able to absorb the integrator output discontinuities, yet be compatible with the NOVA 10 Hz sampling rate.

The circuit gain is 3 msec/v which means that each volt measured by the NOVA corresponds to 3 msecs.

4. Peak Pressure Angle Calculation

The crankshaft angle that corresponds to peak pressure can be found by combining the time-to-peak pressure measurement with the engine speed. The time in msec of one engine cycle is:

$$\tau = \frac{60000}{RPM} \quad . \tag{5.7}$$

The time τ_1 in msec between 60^{o}BTDC and peak pressure signal is determined by the gain of the circuit and is given by

$$\tau_1 = 3V \tag{5.8}$$

where V is the output sampled by the NOVA. The actual time-to-peak pressure must be corrected for the peak pressure signal lag effect (see Fig. 5.12) yielding:

$$\tau_1 = 3V-1 \quad . \tag{5.9}$$

Therefore the angle α in degrees between 60^oBTDC and peak pressure is

$$\alpha = \frac{\tau_1}{\tau} \cdot 360 \quad . \tag{5.10}$$

The final expression for α can be found by substituting for τ and τ_1 from (5.7) and (5.9) yielding:

$$\alpha = 0.006 \text{ RPM } (3V-1) \ . \tag{5.10}$$

The NOVA A/D converter has 11 bits. Therefore 10V corresponds to 2048 or:

$$1V \rightarrow 204.8$$

combining that with (5.10) and subtracting 60 yields the angle corresponding to peak pressure measured from TDC:

$$\theta_{pp} = 0.006 \left(\frac{I}{204.8} - 1\right) \times \text{RPM} - 60 \tag{5.11}$$

where I is the integer read by the NOVA. The resolution can be found by letting I = 1 in (5.11) yielding:

$$\Delta\theta_{pp} = 0.006/204.8 \times \text{RPM} = 0.03 \text{ deg/1000 rpm}$$

which is quite satisfactory.

E. RESULTS

1. Optimal Peak Pressure Angle Analysis

An optimal closed loop scheme was derived for a desired emission level of HC/CO/NO = 2/15/2 gm/mile without any catalytic converter. As discussed in Chapter IV, any optimal solution is associated with some values of Lagrange multipliers λ_{HC}, and λ_{NO}. The desired emissions level is quite close to that of $\lambda_{HC} = 0.03$ and $\lambda_{NO} = 0$ as given in Table 5-1 yielding HC/CO/NO of 2.174/8/2.03 gm/mile and fuel consumption of 19.52 mpg. A detailed solution of the 10 individual torque and speed points is given in Table 5-1. The angle that corresponds to peak pressure was measured at these 10 points while tuning AF, SA and EGR to the optimal settings outlined in Table 5-1.

The angles measured at these various points are given in Table 5-1. The measurements vary between a few degrees ATDC to 30°ATDC. The optimal setting of point number 4 (50/2250 lb ft/rpm) is at the point of best fuel economy because $C_U^4 = 0$. θ_{pp}^4 was found to be 20°ATDC which is close to the value stated in [H-3] for best fuel economy. θ_{pp} that corresponds to high power points varies between 20° to 30° because the spark timing θ_{pp} of the low power points was usually below 20°ATDC. This does not indicate spark timing advanced from MBT but rather spark timing retarded to the region where the relationship between spark timing and peak pressure angle reverses and a double peak in the pressure trace can be noticed (see Fig. 5.3 c). θ_{pp} is measured at the first peak, therefore yielding values of only a few degrees.

The relationship between θ_{pp} and spark timing for two levels of torque of 20 and 40 lb ft at 1500 rpm is given in Fig. 5.14. Retarding the spark timing from an advanced setting increases θ_{pp}, as discussed above, with a slope $\left(\frac{\partial \theta_{pp}}{\partial SA}\right)$ of 0.67 for 40 lb ft and a slope of 0.4 for 20 lb ft. As spark timing is retarded beyond a certain point, the slope becomes negative meaning that θ_{pp} goes down as spark timing is retarded. The transition point depends on torque and occurs at more advanced timing as torque goes down since the pressure trace loses its

Lagrange Multipliers:

$\lambda_{HC} = 0.03$

$\lambda_{CO} = 0.0$

$\lambda_{NO} = 0.0$

CASE	1	2	3	4	5	6	7	8	9	10
INDEPENDENT VARIABLES										
Torque (ft lb)	50	25	75	50	38	20	85	72	-14	15
RPM (rpm)	1700	1800	2100	2250	2600	1400	2500	2900	1800	750
Power (HP)	16.39	8.68	30.36	21.69	19.05	5.40	40.97	40.25		2.89
AF	15.784	12.800	15.259	16.609	14.776	13.000	17.333	13.863	12.500	15.500
Spark Timing	10.000	10.000	15.000	41.745	35.606	10.038	22.027	32.943	10.000	10.000
EGR	0.000	0.000	2.106	0.000	0.000	0.000	6.210	0.000	0.000	0.000
OUTPUT VARIABLES										
Fuel (lb/hr)	11.342	8.498	16.713	10.944	11.713	6.159	20.323	20.730	3.912	2.760
HC (mg/sec)	16.531	6.995	13.797	0.000	16.321	7.706	7.859	13.612	13.158	8.470
CO (mg/sec)	15.941	47.327	46.052	0.000	38.698	38.623	86.962	123.943	4.718	0.634
NOx (mg/sec)	16.697	2.268	34.849	0.000	23.398	1.460	53.230	73.190	0.112	0.058
SENSOR VARIABLE										
θ_{pp}^{opt} (ATDC)	8.7	3.2	31.4	20.3	21.7	1.9	1.9	22.4	1.2	9.0

Cycle results (based on weighted average of the 10 points)

	FUEL (Mpg)	HC (gm/mile)	CO (gm/mile)	NOx (gm/mile)
Engine	19.5204	2.1739	7.9968	2.0347
Tailpipe with oxidizing catalyst	19.5204	0.6935	4.5995	2.0347

TABLE 5-1 Independent variables, engine and sensor outputs at the 10 load/speed points for the optimization problem of HC/CO/NOx of 2.17/18/2 gm/mile

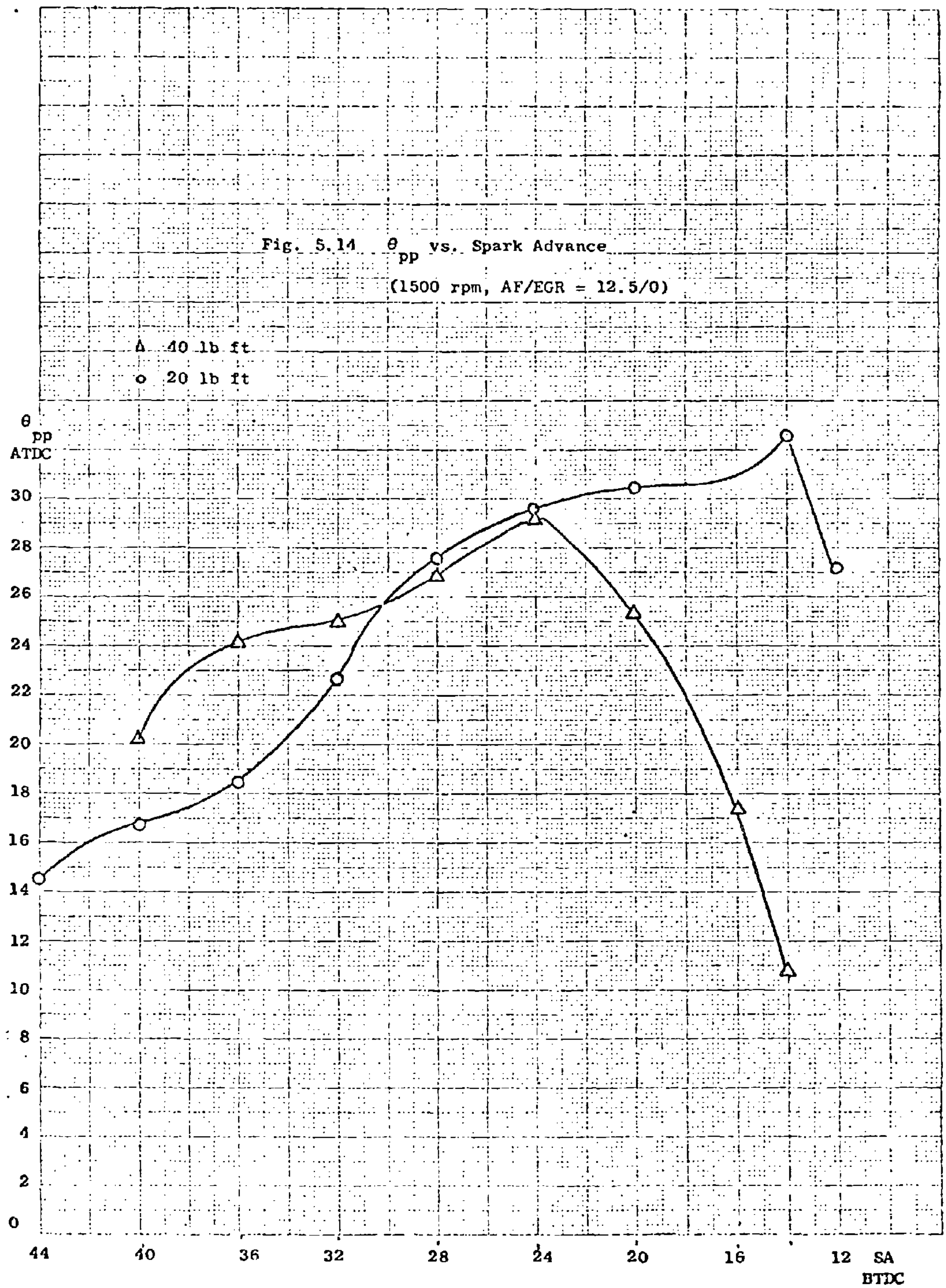
Fig. 5.14 θ pp vs. Spark Advance
(1500 rpm, AF/EGR = 12.5/0)
Δ 40 lb ft
o 20 lb ft
θ pp ATDC
30
28
26
24
22
20
18
16
14
12
10
8
6
4
2
0
44
40
36
32
28
24
20
16
12
SA BTDC

distinct sharp peak in more advanced spark setting as torque goes down. The substitution of the sharp peak by a flat trace or a series of several peaks decreases θ_{pp} as discussed above.

The spark timing that corresponds to the change in slope of θ_{pp} vs SA is not affected very much by engine speed.

The angles of peak pressure that correspond to the optimal solution serve as the reference values in the closed loop scheme as discussed in Chapter 5.3. A closed loop scheme over the entire operating range is desired at more than the 10 discrete torque and speed points. Therefore a function relating θ_{pp}^{opt} to some measured engine quantities is required. Engine speed, torque, power and inlet manifold pressure are good candidates for such measurements. After trying this condition it was found that θ_{pp}^{opt} can be expressed best as a function of the engine power. A function relating θ_{pp}^{opt} to engine power was fit to the data, from which the expression for θ_{pp}^{opt} is

$$\theta_{pp} = 0.3 + 0.435\,\frac{HP}{40} + 76.5\left(\frac{HP}{40}\right)^2 + 38.79\left(\frac{HP}{40}\right)^3 - 89.25\left(\frac{HP}{40}\right)^4 \quad (5.12)$$

This function is compared with the data in Fig. 5.15. The closed loop scheme will be as follows: the reference peak pressure is determined by the controller according to (5.12) whereas the engine power is determined from torque and speed measurements. This angle will be kept constant, as long as the engine power remains the same, by changing the spark timing as necessary. When a change in engine power is detected the reference value of θ_{pp} will be updated according to (5.12) and the spark timing will be changed until θ_{pp} assumes the reference value. The control scheme is given in Fig. 5.5.

The expression of θ_{pp}^{opt} was derived for a particular emission level, whereas the optimal solution corresponding to the selected emission level depends on the range of the independent variables. The optimal spark timing of some of the low power points is 10^{o}BTDC which is the limit imposed on SA (see Table 2-9). Had this boundary not been

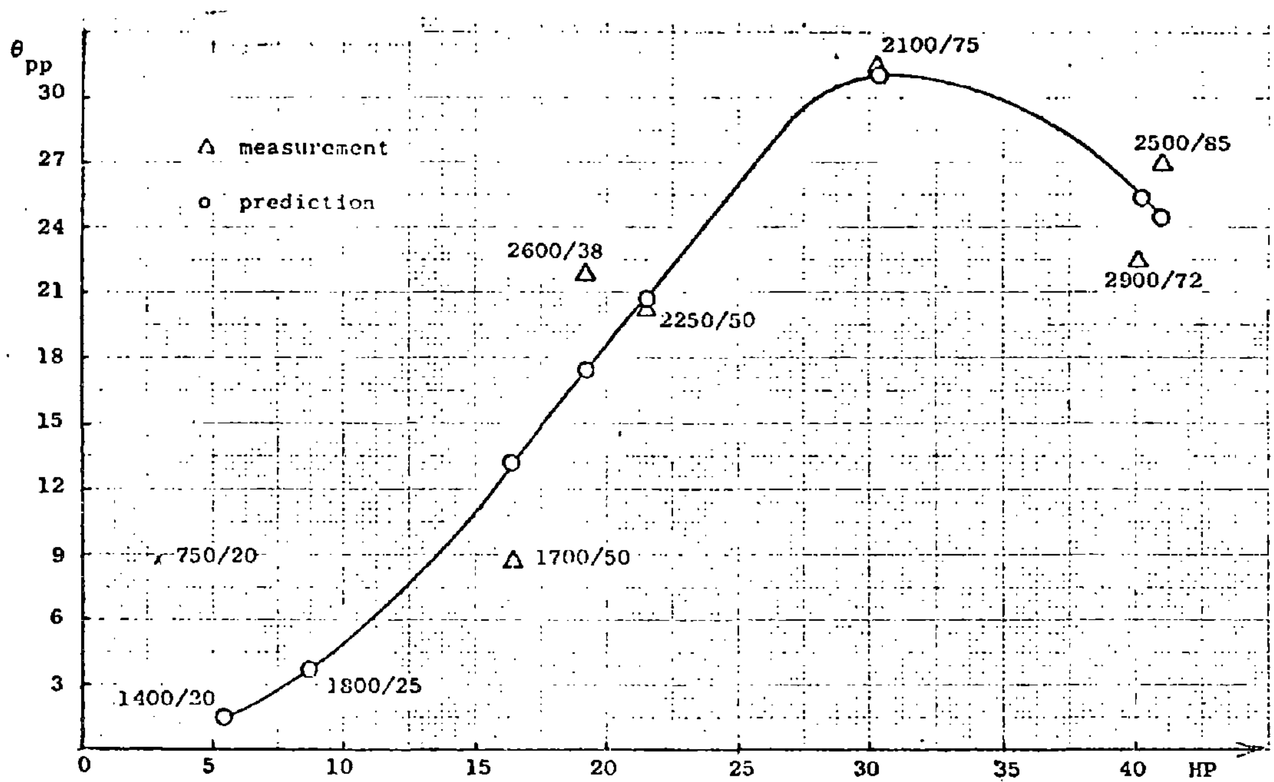

Fig. 5.15 θ_{pp}^{opt} vs. Engine Power for HC/CO/NO of 2.12/8/2 gm/mile. Measurements were taken at various operating points with the controls tuned optimally. The parameters are speed/torque (rpm/lb ft).

set so close to TDC, the phenomenon of θ_{pp} reduction as spark retards would have been eliminated, and the lower portion of the graph in Fig. 5.15 would have been lifted. The desired emission level affects the optimal solution, which in turn affects θ_{pp}^{opt}. Very tight emission constraints will require spark timing retarded into the double peak region where the control law cannot be implemented. A detailed discussion of the control limitations is given at the end of this section. The shape of the function relating θ_{pp}^{opt} to engine power changes with emission level. Only θ_{pp} that corresponds to 50/2250 lb ft/rpm remains the same because this point does not represent any part of the urban cycle and the spark timing is always at MBT with θ_{pp}^{opt} equal to 20^{o}ATDC.

The relationship between θ_{pp}^{opt} and engine power varies with the emission constraints. The range of variation is between the unconstrained case and the tightest level of emissions. The values of θ_{pp}^{opt} and the control variables for the unconstrained optimization problem ($\lambda_{HC} = \lambda_{NO} = \lambda_{CO} = 0$), which is the best fuel economy without any emission constraints, are given in Table 5-2. The engine was run at the 10 load/speed points with the controls tuned as listed in Table 5-4. Figure 5.16 depicts θ_{pp}^{opt} vs engine power from which θ_{pp}^{opt} is confined to a narrow region around 20^{o}ATDC. The only exceptions are the lowest and highest power points for which θ_{pp}^{opt} are 30^{o} and 27^{o}ATDC respectively. The peak pressure angle at the lowest power point is not used as a feedback signal, since the pressure trace is very low and the peak pressure angle hardly depends on spark timing.

The deviation of θ_{pp}^{opt} at the highest power point from the average value of 21^{o} over all points is due to the poor quality of fit of the fuel function at 85/2500 lb ft/rpm. The spark timing for best fuel economy, based on the predicted function is 26^{o}BTDC (see Table 5-2). The actual spark timing for best fuel economy with AF and EGR tuned as listed in Table 5-2 is 32^{o}BTDC. As changes in spark timing shift the peak pressure angle roughly the same amount, the peak pressure angle of the predicted spark timing of best fuel economy will be retarded from the peak pressure angle of the actual spark timing of minimum fuel

Lagrange Multipliers

$\lambda_{HC} = 0.000$

$\lambda_{CO} = 0.000$

$\lambda_{NO} = 0.000$

CASE	1	2	3	4	5	6	7	8	9	10
INDEPENDENT VARIABLES										
Torque (ft lb)	50	25	75	50	38	20	85	72	-14	15
RPM (rpm)	1700	1800	2100	2250	2600	1400	2500	2900	1800	750
Power (HP)	16.39	8.68	30.36	21.69	19.05	5.40	40.97	40.25		2.89
AF	16.895	15.253	16.877	16.609	16.458	14.089	15.910	16.370	12.500	14.570
Spark Timing	42.000	39.177	35.615	41.745	45.000	44.085	25.942	39.908	40.430	30.000
EGR	0.000	0.000	0.000	0.000	0.000	0.000	0.000	0.000	0.000	0.000
OUTPUT VARIABLES										
Fuel (lb/hr)	8.143	6.095	13.667	10.994	10.956	4.124	19.192	19.027	2.656	2.239
HC (mg/sec)	74.829	50.632	68.233	0.000	41.537	24.968	27.907	78.912	114.425	9.938
CO (mg/sec)	10.469	19.198	16.234	0.000	24.719	11.009	70.464	30.475	6.082	0.633
NOx (mg/sec)	34.044	9.444	91.617	0.000	43.096	3.192	103.532	151.081	0.034	0.095
SENSOR OUTPUT										
θ_{pp}^{opt} (ATDC)	21.8	22.1	24.0	20.3	18.8	19.6	27.1	20.6	18.1	30

Cycle results (based on the weighted average of the 10 points)

	FUEL(Mpg)	HC(gm/mile)	CO(gm/mile)	NOx (gm/mile)
Engine	23.9253	7.9048	5.6908	4.3517
Tailpipe with oxidizing catalyst	23.9253	2.1262	4.2536	4.3517

TABLE 5-2 Independent variables, engine and sensor outputs at the 10 load/speed points of the unconstrained optimization problem (best fuel economy

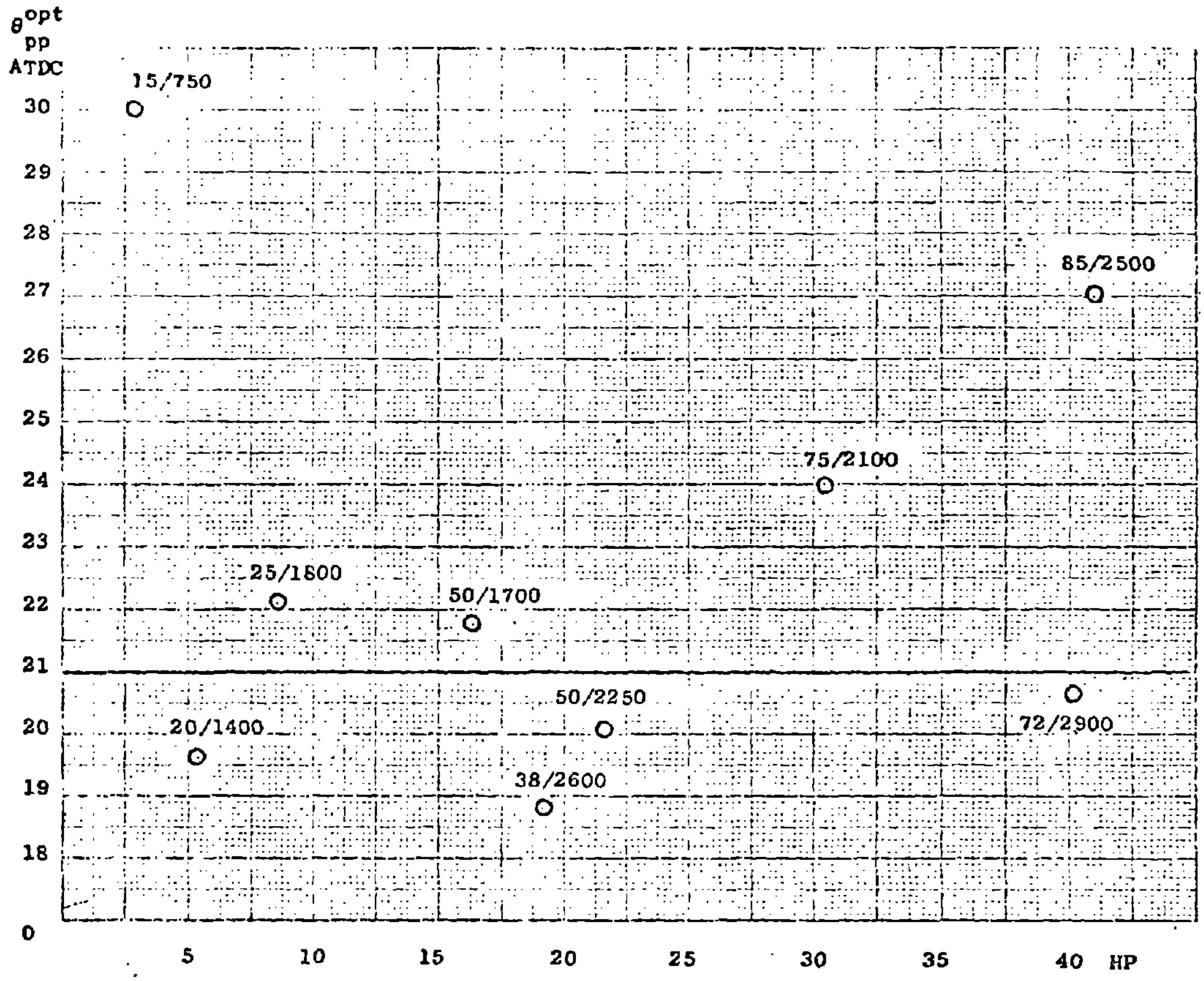

Fig. 5.16 θ_{pp}^{opt} vs Engine Power for the Unconstrained Solution in Various torque/speed points (lb ft/rpm).

consumption. The 27°ATDC peak pressure angle was measured for spark timing of 26°BTDC. Therefore the peak pressure angle that could be measured for spark timing of 32°BTDC is around 21°ATDC.

Figure 5.17 depicts the superposition of both θ_{pp}^{opt} vs engine power curves; the curve that corresponds to the unconstrained optimization and the curve that corresponds to HC/CO/NO of 2.17/8/2 gm/mile. The area between these two curves indicates the range of variation of the θ_{pp} function as emissions change.

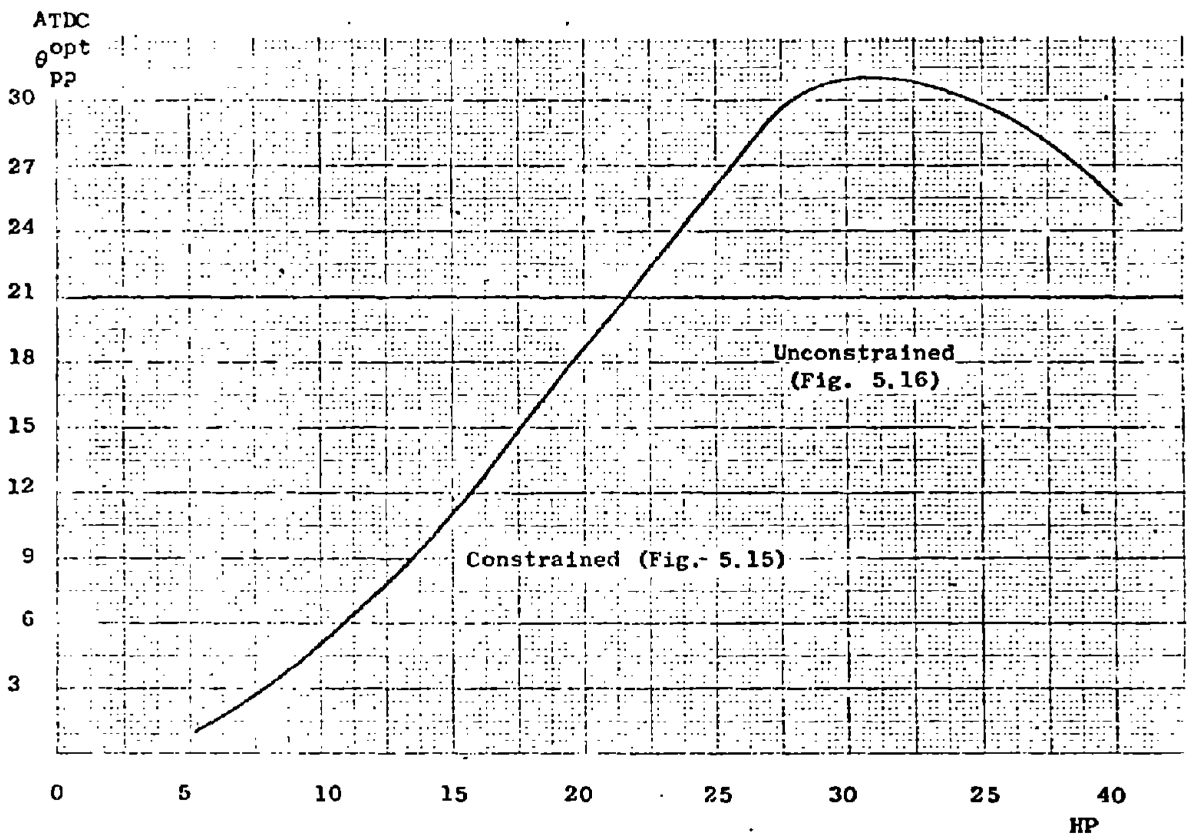

Fig. 5.17 θ_{pp}^{opt} vs Engine Power for the unconstrained and the constrained solutions of HC/CO/NO of 2.17/8/2 GM/Mile.

The change in engine controls also depends on the level of constraints. The amount that spark has to be retarded from MBT as a function of engine power for the particular level of emissions discussed above (HC/CO/NO = 2.17/8/2 gm/mile) is given in Fig. 5.18. Spark timing is retarded considerably in the low power region and is retarded only a few degrees for the high power points. The composite fuel consumption as defined in the optimization procedure (Chap. IV) is evaluated both over the urban and the highway cycle, whereas emissions are evaluated only over the urban cycle. Usually the ratio between the urban and the highway coefficients (see Table 2-8) is large for the low power points and is low for the high power points. High ratio means tighter emission constraints requiring more retarded spark to meet the emission constraints, whereas low ratio means loose emission constraints requiring small spark retard from MBT.

Fig. 5.18 Spark Retard from MBT vs Engine Power for HC/CO/NO of 2.17/8/2 gm/mile for various points of torque/speed (lb ft/rpm).

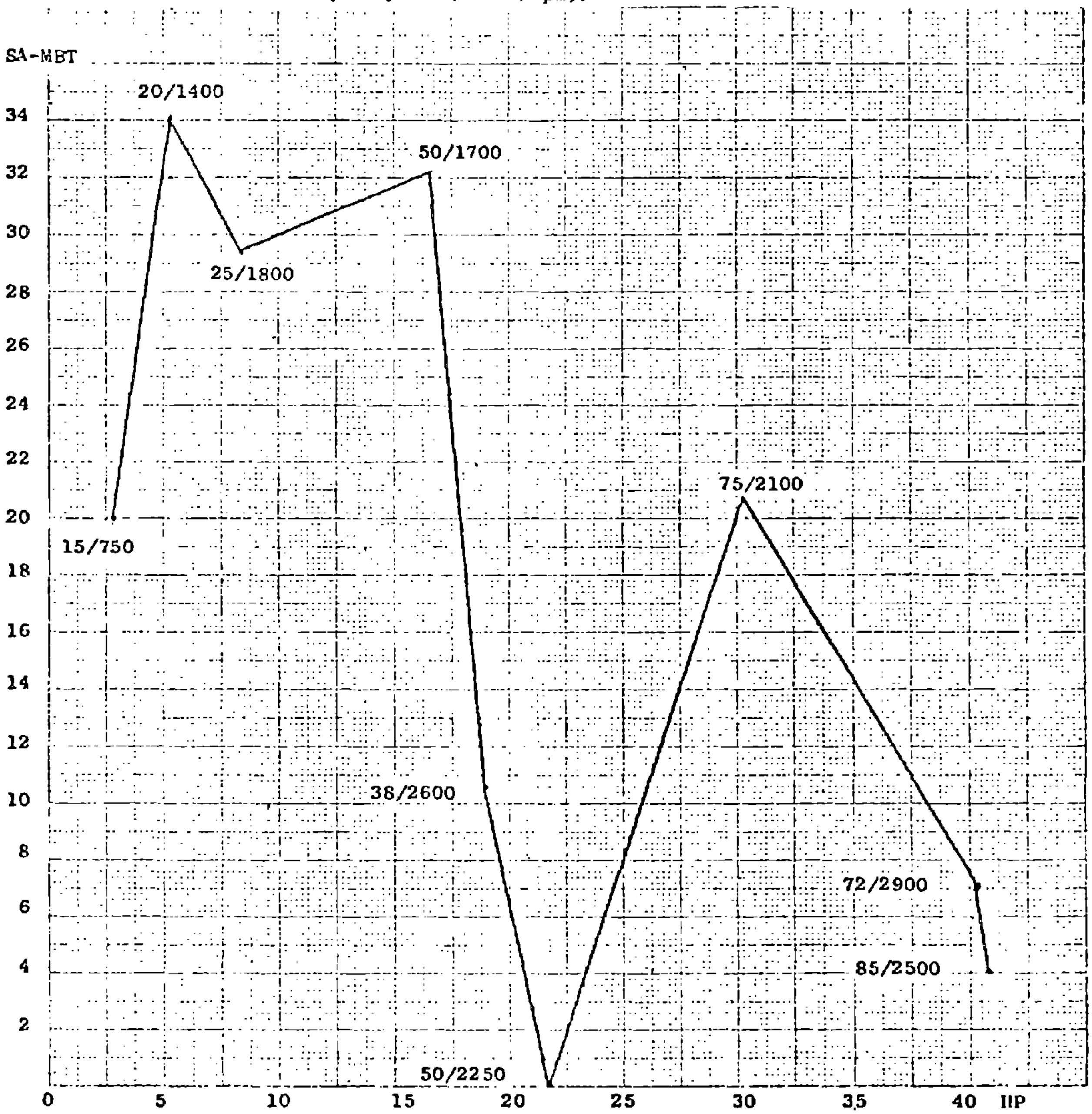

2. Feasibility Analysis of the Closed Loop System

The closed-loop controller that minimizes fuel for given emission constraints over a wide torque/speed range cannot be implemented for any desired level of emissions. As discussed earlier, tight emission constraints require retarded spark timing which drives the engine into the region where the relationship between spark timing and peak pressure angle reverses. Naturally, the engine cannot be controlled under such conditions.

The closed-loop control scheme over a wide torque/speed range was derived for the EPA cycle approximated by running the engine at 10 points of constant torque/speed. Spark timing is not retarded equally at all the discrete load/speed points as emissions are tightened. Usually it is retarded more at points having larger urban coefficients. Therefore the number of constant load/speed points for which spark is retarded into the uncontrollable region grows gradually as emissions are tightening.

The total feasible solution range of the optimization problem, both for the Non-Catalyst and the Three-Way Catalyst, as given in Figs. 4.3-4.7 can be divided into 3 regions which are as follows (Figs. 5.19-5.20):

REGION 1: this includes emission levels for which the optimal closed loop scheme using peak pressure angle can be implemented over the engine operating range that approximates the EPA cycle. Spark timing never gets into the uncontrolled region.

REGION 2: this includes optimal solutions for which spark timing is retarded into the uncontrollable region for a low number of points of constant load/speed approximating the EPA cycle. The control law can still be implemented for this emission level provided that spark timing would not be retarded into the uncontrolled region. This restriction will result in an inferior solution to the optimal one since not retarding the spark timing all the way to the optimal value at a few load/speed points results in increased emission levels and decreased fuel consumption. Region 2 includes all the solutions for which

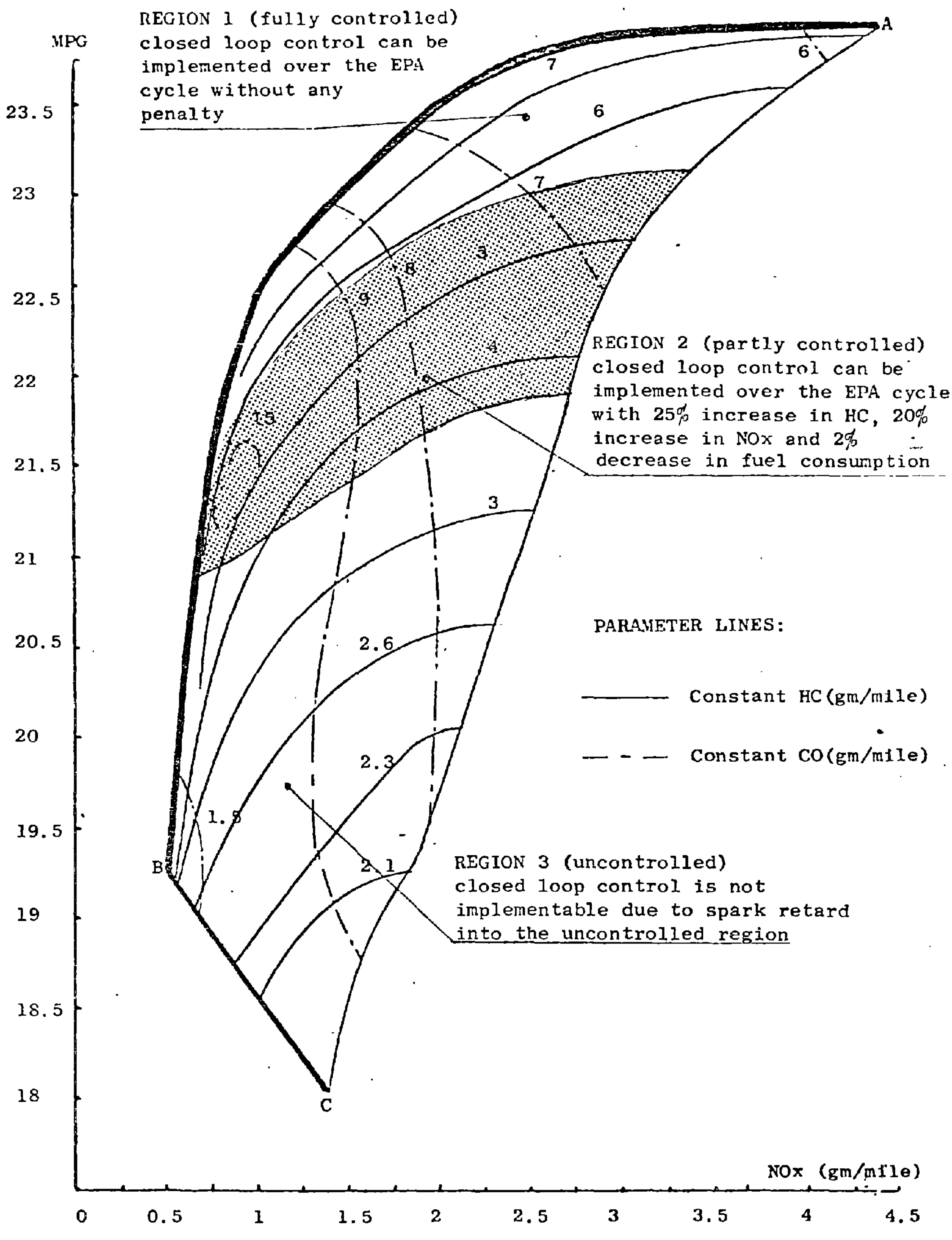

Fig. 5-19 Fully controlled, partly controlled and non-controlled regions of the NonCatalyst optimal solution

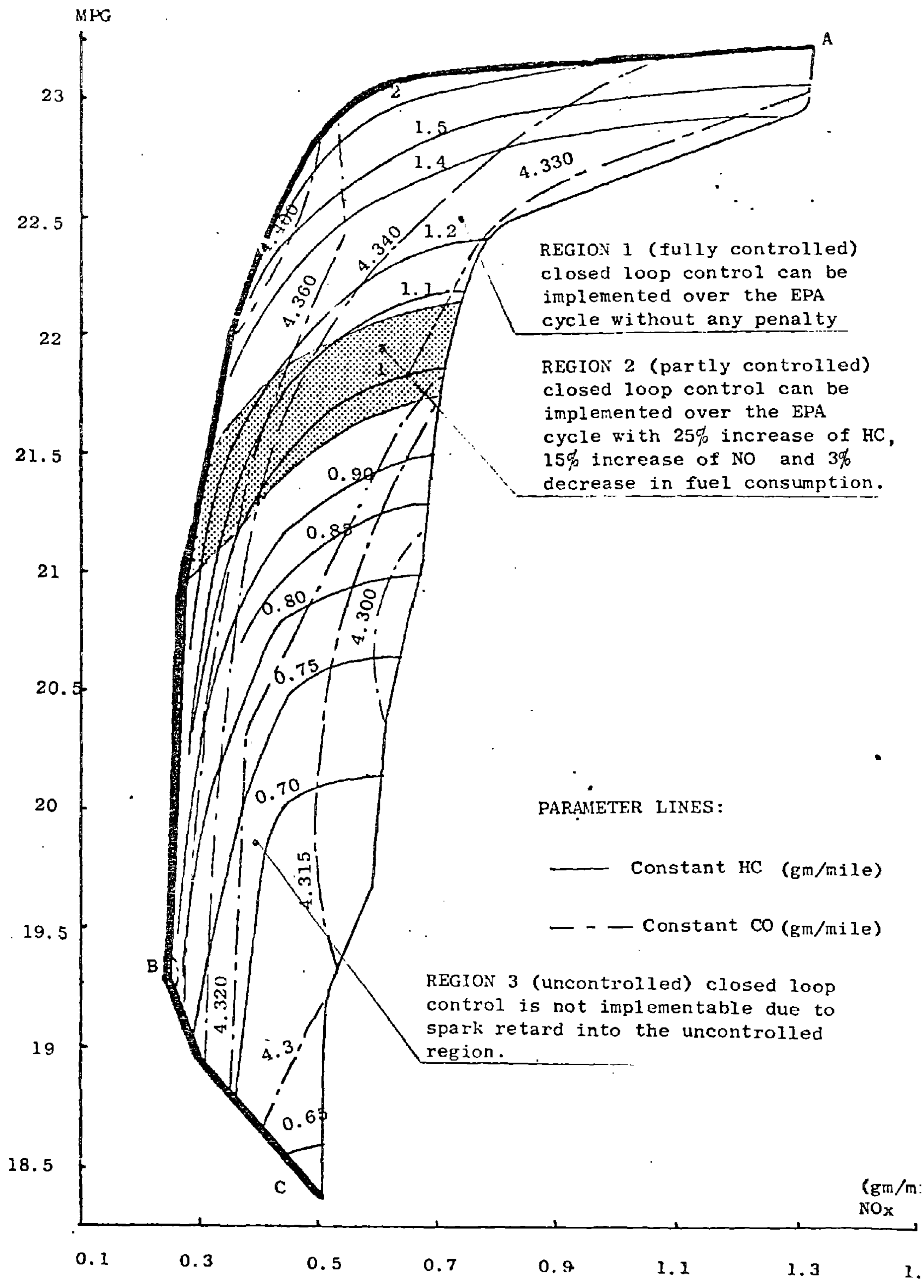

Fig. 5-20 Fully controlled, partly controlled and non-controlled regions of the Three Way Catalyst optimal solution

the restriction on spark timing will increase the composite HC by not more than 25%, the composite NOx by not more than 20% and will decrease composite fuel consumption by 2% for the NonCatalyst system. The Three-Way Catalyst system will yield similar results. HC and NOx will increase by 25% and 15% respectively, whereas fuel consumption will decrease 3%.

REGION 3: this region includes the optimal solutions for the tight emission levels for which the optimal spark timing is in the uncontrollable region for a substantial portion of the EPA cycle. Therefore restricting the spark timing from being retarded, as suggested in Region 2, will result in a high penalty on emissions. This means that the engine cannot be controlled in this region efficiently.

The boundaries between the regions were found as follows. From Fig. 5.14 the reverse in the slope of θ_{pp} with respect to spark timing occurs at 20^{o}BTDC for a torque of 20 lb ft and at 24^{o}BTDC for a torque of 40 lb ft. Each optimal solution given in Appendix G2 for the Non-Catalyst and in Appendix G4 for the Three-Way Catalyst is associated with optimal tuning of the engine at 10 load/speed points. As emissions are tightened the points of constant load/speed to be retarded first into the uncontrolled region are 50/1700 and 75/2100.

Therefore, Region 1 includes all the optimal solutions for which the optimal spark timing at any portion of the EPA cycle is not retarded beyond 24^{o}BTDC. Region 2 includes all optimal solutions for which restricting the spark timing for being retarded more than 24^{o}BTDC does not increase HC by more than 25% relative to the original optimal solution. The increase in emissions was evaluated by letting air/fuel ratio and EGR be equal to their optimal values and by evaluating the increase in emissions as spark is advanced from the optimal solution to the constraint of 24^{o}BTDC. Region 3 includes the rest of the optimal solutions not included in the other two regions.

The boundary lines between the various regions, as appearing in Figs. 5-19 to 5-20 are very close to lines of constant HC. Therefore the optimal region can be divided to fully controlled, partly controlled and uncontrolled regions according to the HC level. The constant HC line of 5.5 gm/mile separates Regions 1 and 2, whereas HC line of 3.8 gm/mile for NOx values down to 1.25 gm/mile and gradually increasing HC values up to 6 gm/mile for smaller NOx values separates Regions 2 and 3 of the Non Catalyst system.

The boundary lines for the Three-Way Catalyst system are as follows: the boundary line between Regions 1 and 2 increases from 1.1 gm/mile of HC to 1.4 gm/mile as NOx decreases. The boundary line between Regions 2 and 3 increases from 0.98 gm/mile of HC to 1.2 gm/mile as NOx levels decrease.

The above analysis of the division of the total accessible emission region to controlled, partly controlled, and non-controlled regions corresponds to a particular Ford engine with a particular emission devices configuration. The boundary lines between the various controlled regions also depend on the catalyst efficiency assumed in Chapter IV. Therefore the way the accessible emission region is divided into controlled, partly controlled and non-controlled areas might be entirely different for other configurations of engines and emission devices.

3. Control Implementation

No attempt was made to implement the closed-loop control law in a variable torque and speed regime, because the current engine-dynamometer configuration is not capable of tracking arbitrary transient cycles. Instead, the closed-loop scheme was implemented for a constant torque and speed. The loop was closed through the NOVA minicomputer which sampled the angle that corresponds to peak pressure and changed the spark setting to the microprocessor spark controller as required.

Even though the closed-loop system was implemented with constant torque and speed, the extension to the variable torque and speed range will not cause any difficulty. As was stated earlier, the engine responds essentially instantaneously to spark timing change, and there is no significant transient response involved between the spark timing change and the peak pressure angle change.

The knock detection control scheme that was developed in [H-4] can also be incorporated into the controller. Some spark timings of the optimal solution are either at MBT or retarded only by a few degrees. Therefore knock can be expected due to ambient changes, variation in fuel or mechanical degradation. The knock control system is based on a PZT sensor similar to the one used in this research, which means that only a software change is required to include it in the current control scheme.

4. Sensitivity Analysis

The closed-loop control system is supposed to keep the engine operating optimally regardless of mechanical deterioration and external disturbances. Anything causing changes in the flame speed and hence in the pressure trace history will be detected by measuring θ_{pp}^{opt}. Any such deviation indicates a drift in the engine performance from the optimal point.

A convenient way of checking how well the closed-loop system can respond to external disturbances is to introduce humidity to the air stream. Engine performance deteriorates as humidity goes up since flame speed goes down. Boiling water provides the required vapor. A variable temperature hot plate provides the desired amount. Humidity is measured by dry and wet bulb thermometers installed above the carburetor (Fig. 5.21).

The combined effect of humidity on the EPA cycle was found by running the engine at the torque/speed points with AF, SA and EGR adjusted as listed in (5.15). A typical impact of humidity on fuel consumption and emission levels is shown in Figs. 5.22-5.24 for 25/1800 lb ft/rpm. Fuel consumption goes up proportionally to the increase in humidity. Fuel consumption goes up 5% as humidity increased from an ambient condition of 10 gm water/kg dry air* to 23 gm water/kg dry air‡. Under these conditions, NOx level declined to 64% of its original level, since increase in humidity decreases θ_{pp}^{opt} increased due to slower flame. The closed-loop system provided the required spark advance to restore θ_{pp}^{opt}. This change was 1-2° which agrees with the numbers quoted in [PO-3].

The advanced spark brought fuel consumption down almost to the original value. NOx and HC increased as spark timing was advanced, yet NOx remained below the original value (64%) and HC increased by 27% from the nominal value.

---

*55% relative humidity at 75F.

‡70% relative humidity at 92F.

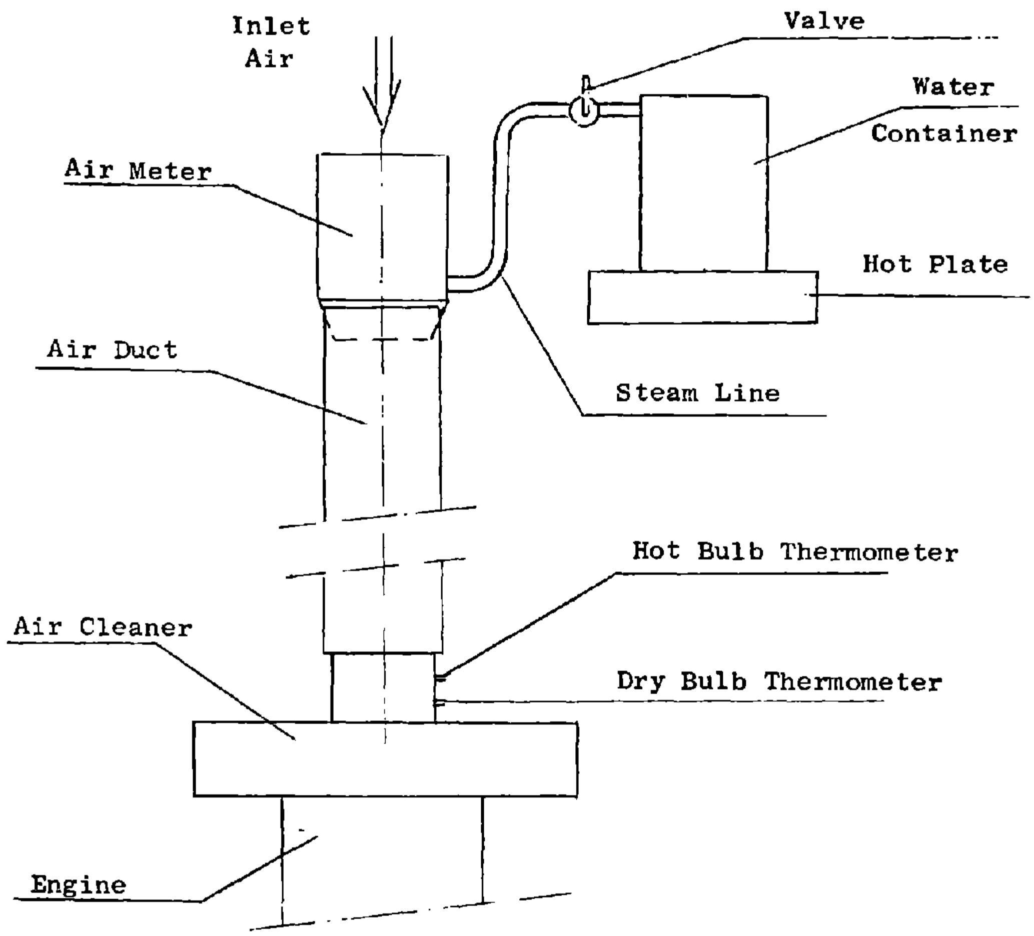

Fig. 5.21 Vapor Generation System

Fig. 5.22 Fuel vs Humidity with open and closed loop controls (25/1800 lb ft/rpm)

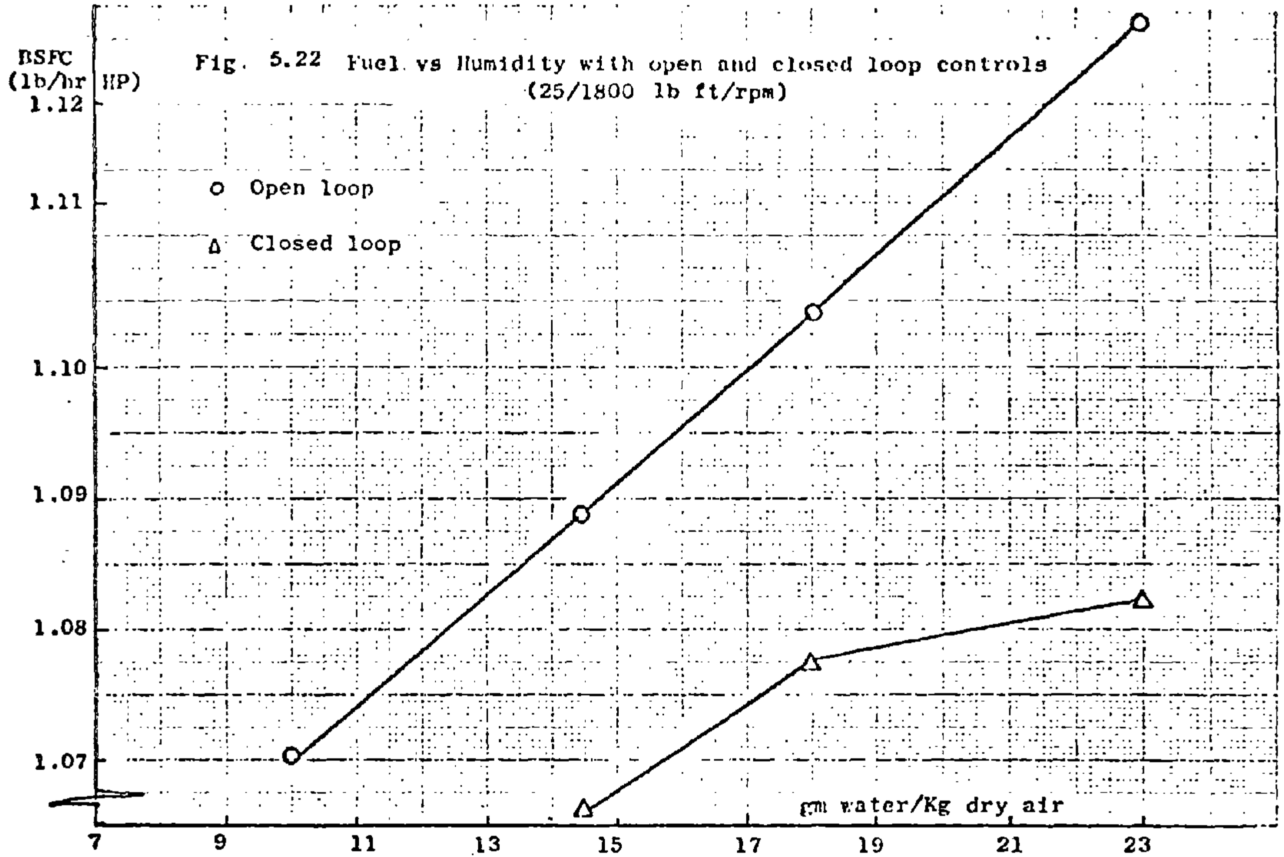

Fig. 5.23 NO vs Humidity with open and closed-loop controls (25/1800 lb ft/rpm)

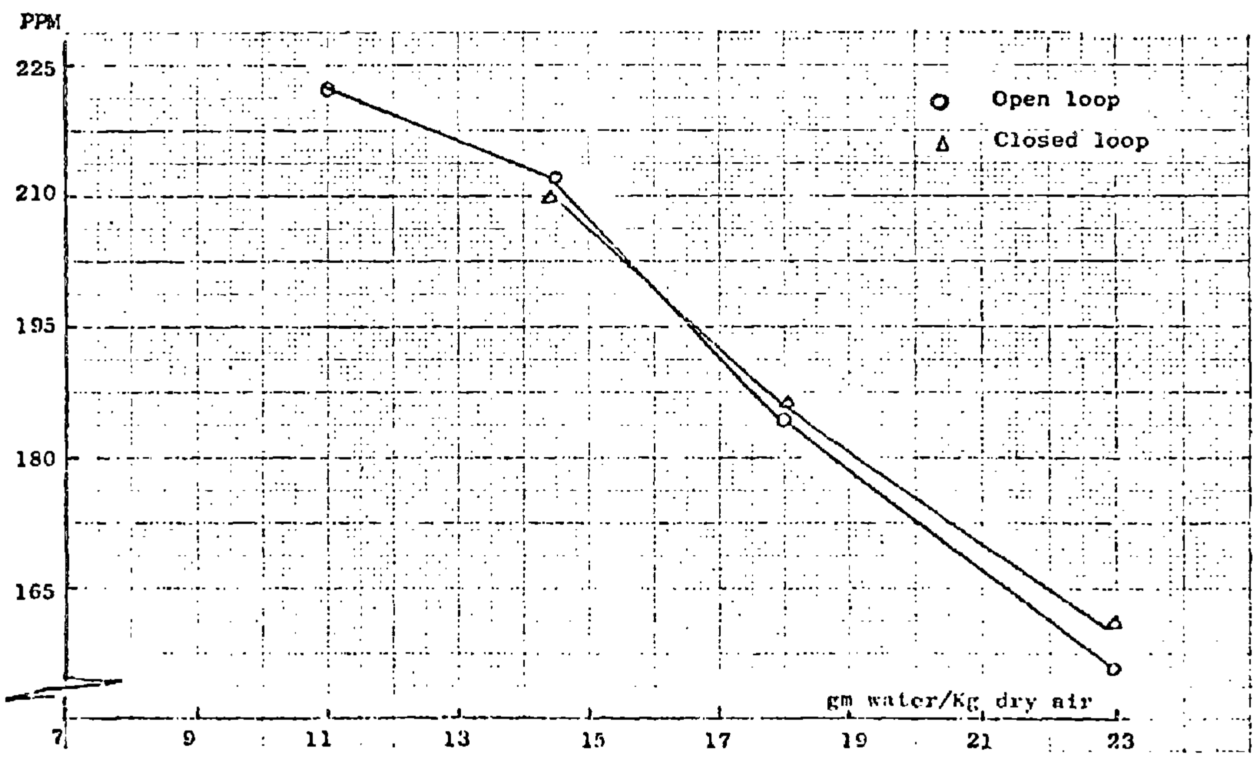

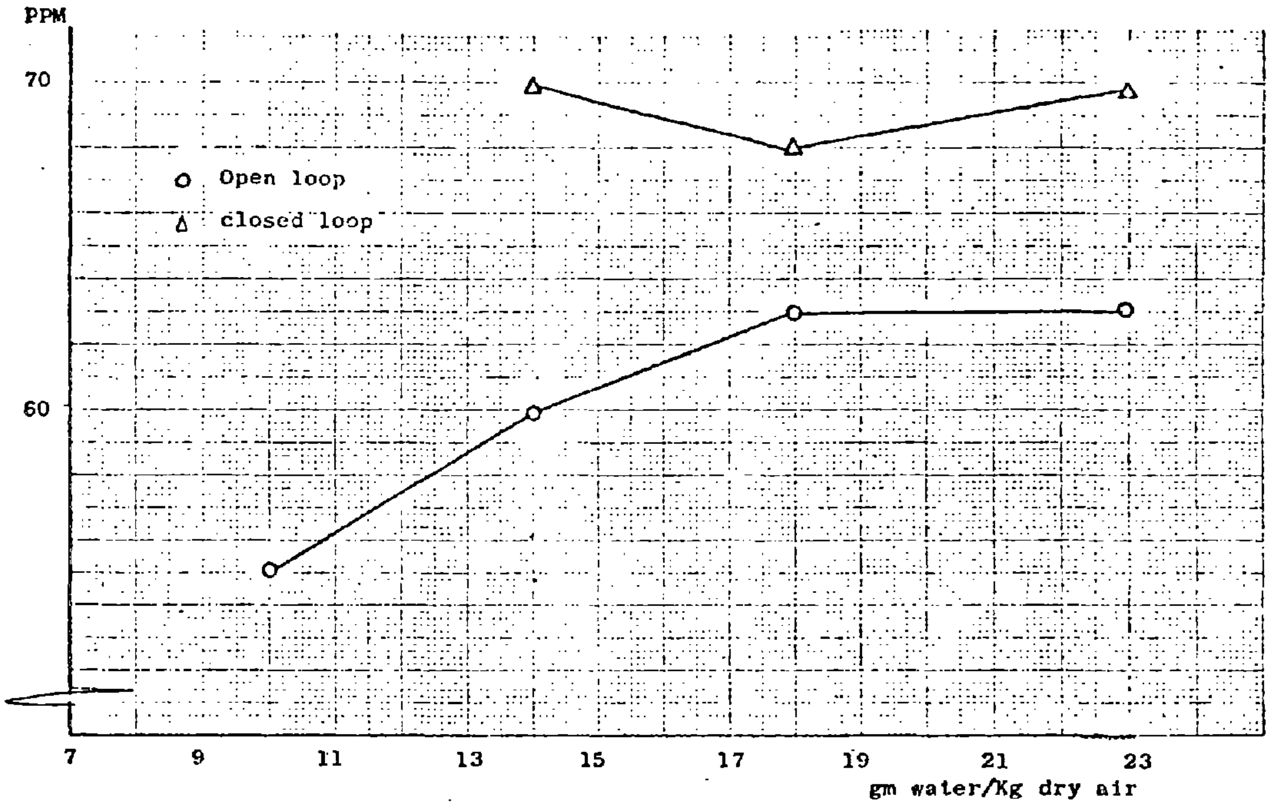

Fig. 5-24 HC vs Humidity with open and closed-loop systems (25/1800 lb ft/rpm).

This procedure was repeated for a few other points of constant speed and load. Table 5-3 depicts the relative changes in fuel consumption and emission levels as humidity increased from 10 to 27 gm water/kg dry air. Three constant load-speed points were excluded; the idle point (15/750 ft lb/rpm) and the negative load point (-14/1800 ft lb/rpm) were excluded since the closed-loop scheme cannot be implemented in these points. This is due to the fact that the maximum cylinder pressure is quite low and θ_{pp} is around TDC and hardly depends on the spark timing. The highest power point (85/2500 ft lb/rpm) was also excluded since the air flow in this point is considerably high and the humidity generating equipment was not capable of increasing the humidity to the desired level.

Only fuel consumption sensitivity to humidity variation was checked at the 50/2250 lb ft/rpm point since this point does not contribute to emissions as C_U^4 is zero.

A sensitivity estimate of the closed loop system over the EPA cycle can now be evaluated by combining the results of the various load-speed points according to their weights (Table 5-4). The highest power point (85/2500 ft lb/rpm) was considered to have the same sensitivity as the average of the measured points. The assumption does not introduce large error since the contribution of this point to the composite fuel consumption and emissions level is quite small. The idle point and the negative torque point, on the other hand, were assumed to operate only in the open loop mode which means that fuel consumption will increase with humidity at these two points and that there will be no mechanism to keep the engine operating optimally at idle and negative torque points. The composite fuel consumption of the open loop system went up by 4% while NOx went down to 70% of its original value and HC to 95% of its original value. The composite fuel consumption of the closed-loop system went up by 2% while NO decreased to 80% of its original value and HC increased to 105%.

	F(lb/hr)			HC			NO		
Pt.	Nom*	o.l.‡	c.l.‡‡	Nom	o.l.	c.l.	Nom	o.l.	c.l.
1700/50	1.00	1.056	1.026				1.00	0.608	0.770
1800/25	1.00	1.037	1.00	1.00	1.11	1.13	1.00	0.64	0.64
2100/75	1.00	1.013	1.013	1.00	0.87	1.02	1.00	0.775	0.860
2250/50	1.00	1.017	1.006						
2600/38	1.00	1.014	1.004	1.00	0.945	1.00	1.00	0.772	0.85
1400/20	1.00	1.06	1.005				1.00	0.58	0.71
2500/85	-------- HIMIDITY GENERATING EQUIPMENT INADEQUATE ------------								
2900/72	1.00	1.008	1.002	1.00	0.86	0.86	1.00	0.88	0.89
1800/-14	-------- NO CL DUE TO LOW PRESSURE --------------------------								
750/15									

TABLE 5-3 Relative changes in fuel consumption and emissions (NOx and HC). Mass flow rates at various TORQUE/RPM points (lb ft/rpm) as humidity changes from ambient (10 gm water/kg dry air) to 27 gm water/kg dry air.

* Nom - engine performance at nominal setting at ambient condition;

‡ o.l.- engine performance at the higher humidity level at the open loop mode;

‡‡ c.l.- engine performance at the higher humidity level at the closed loop mode.

ENGINE PARAMETER	NOMINAL VALUE		HUMIDITY EFFECT			
			OPEN LOOP		CLOSED LOOP	
	Abs.	Rel.	Abs. Value	Rel. Value	Abs. Value	Rel. Value
FUEL(mpg)	19.52	1.00	18.75	.961	19.14	.980
HC(gm/mile)	2.174	1.00	2.087	0.96	2.283	1.05
NO(gm/mile)	2.034	1.00	1.444	0.71	1.648	0.81

TABLE 5-4 Changes in absolute and relative composite engine performance over an approximated EPA cycle as humidity increases from 10 to 27 gm water/kg dry air.

Humidity increases always decreased NO level, whereas the effect on HC was variable. At 25/1800 lb-ft/rpm HC level increased with humidity whereas at the other points it went down. Nevertheless, the changes in HC were much smaller than those of NO. The above analysis is only an example of how engine open and closed-loop systems respond to external disturbance. Humidity effect seems to be quite small, yet the combined effect of other external disturbances such as changes in ambient temperature and pressure, fuel variation and mechanical degradation can accumulate considerably.

The effect of the closed-loop system is likely to be the same in the event of other external disturbances or mechanical degradation as it was shown in the case of humidity. The closed loop system will be able to provide the additional spark advance when necessary to keep the engine running optimally regardless of the external disturbances and the mechanical degradation.

5. Individual Peak Pressure Cylinder Control

Air/fuel ratio varies among the engine cylinders. The carburetor and the intake manifold are major contributors to the mixture nonuniformity. As fuel atomization improves with increased air flow and hence with increased power, the mixture variation among the cylinders often decreases as engine power increases.

The optimal spark timing depends on air/fuel ratio. Therefore an air/fuel ratio variation among the cylinders might cause different optimal spark timings for the various cylinders. Peak pressure angles we were measured at all 4 cylinders. For a given spark timing peak pressure angle depends on air/fuel ratio. Therefore the spread of the individual peak pressure angles can indicate how uneven the air/fuel distribution among the cylinders is. The development of an individual cylinder peak pressure controller can be justified only in the presence of large mixture variations among the cylinders.

The peak pressure angles of the 4 cylinders were measured at points of constant speed and load that correspond to the optimal solution of HC/CO/NOx of 2.17/8/2 gm/mile (see Table 5-5). The points with retarded spark timing are not listed since the peak pressure angles were in the reverse polarity region as discussed in Section 2 of this chapter.

No.	Torque/ Speed (ft lb/rpm)	AF	SA	EGR	θ_{pp}^{opt} of Cylinder NO(degrees ATDC)			
					1	2	3	4
1	50/2250	16.61	41.74	0	20.01	20.24	19.25	21.76
2	38/2600	14.78	35.61	0	22.06	21.94	20.11	22.66
3	85/2500	17.33	22.03	6.21	27.05	28.31	26.77	28.15
4	72/2900	13.86	32.95	0	22.30	22.37	21.44	23.49

TABLE 5-5 Peak pressure angles of the individual cylinders at various torque/speed points.

The variation among the individual peak pressure angles is 1-2^{o}. The standard deviation of the measurements is around 0.5^{o}. This small variation indicates that no gain is expected from individual cylinder peak pressure angle control. Yet, all the measurements listed in Table 5-5 correspond to high engine power for which no large mixture nonuniformity was expected.

Further experimentation might provide a better understanding of the individual cylinder control. It is advised to measure the individual peak pressure angles at low power points with spark timing in the range where no reverse in relationship between spark timing and peak pressure angle occurs. The optimal individual cylinder spark timing can be found by an on-line search which requires a microprocessor based individual cylinder spark controller. Each cylinder spark timing can be perturbed around the optimal solution obtained for the entire engine. A superior solution is obtained only if both fuel and emissions levels go down as spark timing of the individual cylinder is changed from the nominal optimal tuning.

F. DISCUSSION

A closed-loop scheme using the angle that corresponds to peak pressure as a feedback signal can keep the engine operating optimally over an EPA cycle. The closed-loop controller reduces engine sensitivity to variations in the operating conditions. Humidity increase was a representative disturbance. The engine in the open loop mode exhibited increase in fuel consumption and a decrease in NOx level when humidity increased. However, the closed-loop system provided the required additional spark advance which restored peak pressure angle to its original value thus bringing down fuel consumption to almost the nominal value.
The effect of the closed-loop system is likely to be the same in the event of mechanical degradation or other external disturbances. Any such change that affects flame speed and hence peak pressure angle will be detected by the closed loop system that will provide the required optimum spark timing.

The closed-loop control however, cannot be implemented for every desired emission level. As emission constraints tighten, spark timing is retarded into the double peak region where the simple relationship between spark timing and peak pressure angle ceases to exist.

For the particular engine configuration that was investigated, only 25% of the total emission range can be fully controlled for the Non-Catalyst and the Oxidizing Catalyst cases. Another 20% of the total emission range can be partly controlled with 25% increase in HC, 20% increase in NOx and 2% decrease in fuel consumption since spark timing is kept from being retarded all the way to the optimal setting. The remainder of the emission range (55%) is uncontrollable.

Similarly, the total emission range of the Three-Way Catalyst is divided into 35%, 15% and 50% of fully controlled, partly controlled and noncontrolled segments. The penalty in the partly controlled region is 25% in HC, 15% in NOx and a gain of 3% in fuel consumption.

No apparent gain is expected from an individual cylinder control in the medium power range that was investigated for this particular engine. Yet, the low power range must be investigated before any conclusion can be made about the individual cylinder control of the engine over a wide operating range.

VI. CONCLUSIONS

1. A closed-loop scheme using the angle that corresponds to peak pressure as a feedback signal can keep the engine operating optimally over an EPA cycle. The cycle was approximated by running the engine at 10 load/speed points.

2. Increase in humidity from 10 to 27 gm water/kg dry air increased fuel consumption by 4% in the open loop and by 2% in the closed-loop. NO dropped to 70% and 80% of the nominal value with the open and closed-loops respectively and HC varied from 95% to 105% respectively.

3. The various trade-off curves follow the law of diminishing returns. Sacrifice in fuel economy increases for a given decrease in emission level as the level of constraints goes down.

4. Optimum spark setting is retarded as HC and NO constraints tighten. Optimal EGR level goes up as the desired level of NO decreases. The optimal air/fuel ratio becomes rich as HC constraint tightens, and leans as NOx constraint tightens.

5. Global and individual fits were investigated. A global fit is attractive because one expression is valid over the torque/rpm range whereas the local fits are valid only at discrete load/speed points. The global expressions can predict engine outputs for intermediate load/speed values; however, the local fits were found to have smaller residuals. The ranges of R-square of the various local functions are: fuel 0.929-0.989, HC 0.735-0.900, CO 0.835-0.943, NO 0.765-0.937. Typical values of the ratio of rms to average measurements are: 2% for fuel, 35% for HC, 37% for CO and 27% for NO.

6. Closed-loop peak pressure control cannot be implemented for every desired emissions level since tight emissions drive the spark timing into an uncontrollable region. For the particular engine and emission devices configuration investigated, only 25% of the total emission range is fully controlled for the Non-Catalyst and the Oxidizing Catalyst. Another 20% of the emission range are partly controlled since spark timing is kept from retarding into the optimal tuning that is in the uncontrolled region. This results in 25% and 20% increase in HC and NOx, and a 2% decrease in fuel consumption. The rest of the emission range is uncontrollable. The total emission range of the Three-Way Catalyst is divided into 35%, 15% and 50% of fully controlled, partly controlled and non-controlled regions, with a penalty of 25% in HC, 15% in NOx and a 3% decrease in fuel consumption in the partly controlled region.

Appendix A

AIR FUEL EVALUATION BASED ON EMISSIONS

Few methods of evaluating mixture ratio exist. A simple method suggested by Spindt [S-1] is based on carbon balance of the pre and post combustion products. This method was not used here because it is quite inaccurate on the lean side. Instead a method based on oxygen balance which was suggested by D.L. Stivender [S-2] is used. The amounts of the various gases are given in Fig. A-1.

The five unknowns are:

X - the molar ratio of the recirculated exhaust flow;

(H_2O) - the water concentration in the exhaust gas;

a - the number of moles of dry air per mole of gasoline;

(N_2) - the N_2 concentration in the exhaust;

(H_2) - the hydrogen concentration in the exhaust.

The five equations are the atom balance of O, H, C, N and the gas equilibrium equation which are:

<u>O Balance:</u>

$$\frac{\alpha+a}{ED} = \frac{1}{2}\,(1-X)\,(2(O_2)+2(CO_2)+(H_2O)+(CO)+(NO)) \quad ; \qquad (A-1)$$

<u>C Balance:</u>

$$\frac{1}{ED} = (1-X)((CO_2)+(CO)+\ell\,(HC)_D) \quad ; \qquad (A-2)$$

<u>H Balance:</u>

$$(O_2) = (1-X)\,(2\,(H_2)+m\,(HC)_D+2\,(H_2O)) \quad ; \qquad (A-3)$$

<u>N Balance:</u>

$$\frac{\alpha+a}{ED} = \frac{1-X}{2\cdot 3.76}\,(2\,(N_2)+(NO)) \quad ; \qquad (A-4)$$

<u>Gas Equilibrium:</u>

$$K = \frac{(H_2O)(CO)}{(CO_2)(H_2)} \quad . \qquad (A-5)$$

A value of 3.5 is assumed for K. Eliminating (H_2) from equations (A-3), (A-5), solving for (H_2O) and then eliminating (1-X) by using (A-1) and (A-2) yields the water concentration in the exhaust:

$$(H_2O) = \frac{n/2\,((CO_2)+(CO))+0.5(n\ell-m)(HC)_D}{1+(CO)/(K(CO_2))} \quad . \qquad \text{(A-6)}$$

CO, CO_2, O_2 and NO were measured on a dry basis. Only HC was measured on a wet basis. As the hydrocarbon concentration in equations (A-2) and (A-3) was measured on a wet basis, the following conversion is used:

$$(HC)_D = (HC)_W(1+(H_2O)) \qquad \text{(A-7)}$$

where the subscripts D and W denote dry and wet measurements respectively.

A H_mC_ℓ structure was assumed for the measured hydrocarbons. Substituting (H_2O) from (A-6) and solving for $(HC)_D$ yields:

$$(HC)_D = (HC)_W \frac{1+(CO)/(K(CO_2))+0.5n((CO_2)+(CO))}{1+(CO)/(K(CO_2))-0.5(n\ell-m)(HC)_W} \quad . \qquad \text{(A-8)}$$

The desired air fuel ratio a is found by dividing equations (A-1) (A-2):

$$A/F = \alpha + a - \alpha = \frac{0.5(2(O_2)+2(CO_2)+H_2O)+(CO)+(NO))}{(CO_2)+(CO)+\ell(HC)_D} - \alpha \quad . \qquad \text{(A-9)}$$

A typical output of the DSP (Data Sorting Program) that includes air fuel ratio based on emission is given in Table A-1.

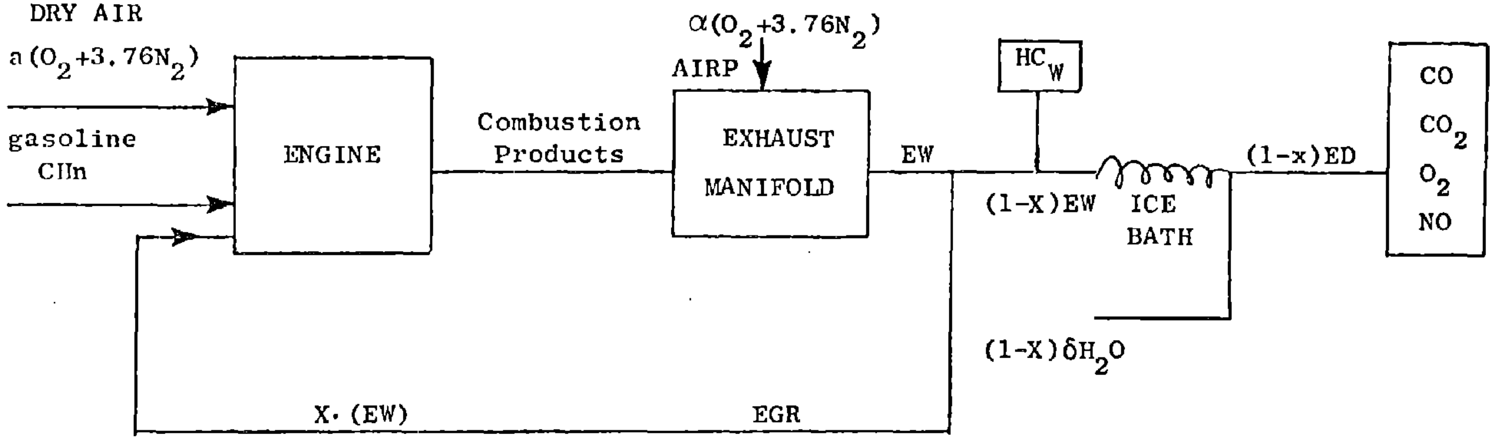

Fig. A-1 Engine Mass Flow Diagram

where:

a = moles of air per mole of gasoline;

n = hydrogen to carbon ratio in fuel;

α = moles of air injected per mole of gasoline;

X = mole fraction of recirculated gas;

EW = moles of wet exhaust before EGR per mole of gasoline;

ED = moles of dry exhaust.

TABLE A-1

DATA SORTING PROGRAM OUTPUT

TORQUE= 72.00RPM= 2900.00 # CASES= 73

A/F	SPKADV	EGR	AIR(L/H)	AIPP(L/H)	MEX(L/H)	AFE
12.5111	42.0000	0.0000	287.3511	50.0573	360.3726	13.0094
12.4879	36.0000	0.0000	283.3291	50.3209	356.3384	13.1328
12.4568	31.0000	0.0000	287.7815	50.0578	356.6164	13.4323
12.5669	26.0000	0.0000	290.1431	49.7867	363.0176	13.6468
12.6613	20.0000	0.0000	305.0217	49.7184	377.8308	13.7200
12.5535	42.0000	7.0000	277.7346	51.3992	351.2478	13.3556
12.6915	36.0000	7.0000	280.4148	51.1221	353.6316	13.6121
12.6519	31.0000	7.0000	284.6560	50.5980	357.7429	13.8526
12.7695	26.0000	7.0000	294.4087	49.7867	367.2510	14.0970
13.1002	20.0000	7.0000	318.2671	48.4513	391.0134	14.1213
12.5543	42.0000	4.5000	277.7256	51.3892	351.2368	12.7708
12.5412	36.0000	4.5000	279.0300	51.1221	352.4011	13.1316
12.6144	31.0000	4.5000	283.6623	50.5990	356.7375	13.5774
12.7774	26.0000	4.5000	294.9239	49.7867	367.7976	13.7892
13.0041	20.0000	4.5000	315.8318	48.4513	388.5703	13.8357
12.5762	42.0000	2.0000	279.9912	50.5880	352.8428	13.3014
12.5922	36.0000	2.0000	279.5481	50.8550	352.6033	13.2646
12.5950	31.0000	2.0000	283.1665	50.5880	356.2368	13.4935
12.6806	26.0000	2.0000	293.0289	49.7867	365.9238	13.6781
12.9658	20.0000	2.0000	315.0801	48.4513	387.8323	13.7682
17.0595	40.0000	0.0000	327.2922	49.2251	395.7026	17.9370
17.2436	35.0000	0.0000	340.7593	48.6998	409.2205	18.0803
17.8786	30.0000	0.0000	372.1526	47.1238	445.4275	18.1925
17.6855	25.0000	0.0000	393.9670	46.3358	462.5791	17.6578
17.8442	40.0000	2.0000	350.5190	48.9624	419.1248	18.0440
18.0244	36.0000	2.0000	364.6370	48.4371	433.3042	18.0343
18.3246	36.0000	2.0000	370.8357	48.4371	439.5098	18.0981
18.1070	32.0000	2.0000	377.1301	48.1744	446.1326	17.7993
17.7246	40.0000	4.5000	349.8621	48.9624	417.5068	18.0872
18.3468	36.0000	4.5000	371.2134	48.4371	439.6835	18.1040
17.8847	40.0000	7.0000	351.6992	49.2251	420.5891	18.3075
18.1975	36.0000	7.0000	369.8108	48.6998	438.8325	18.1945
17.9563	32.0000	7.0000	370.6084	47.9118	439.1597	18.2670
14.4088	40.0000	0.0000	285.6111	51.6955	357.1287	15.6268
14.4376	35.0000	0.0000	286.4360	51.6955	357.9712	15.8311
14.4944	30.0000	0.0000	293.2827	51.1581	364.6750	16.0632
14.5659	25.0000	0.0000	306.0376	50.3521	377.4001	16.2571
14.8714	20.0000	0.0000	330.6560	48.7401	401.6304	16.5616
14.3936	40.0000	2.0000	282.7234	52.2328	354.5986	15.7690
14.5010	35.0000	2.0000	288.1758	51.6955	359.7441	15.9774
14.5839	30.0000	2.0000	298.9236	50.8895	370.3098	16.1316
14.7902	25.0000	2.0000	315.6179	50.0835	387.0410	16.3490
15.5388	20.0000	2.0000	353.6523	47.9341	429.6675	16.5923
14.4469	40.0000	4.5000	281.4280	52.2328	353.1411	16.0155
14.4899	35.0000	4.5000	288.2646	51.6955	359.8545	16.1210
14.6564	30.0000	4.5000	299.5222	50.8895	370.8479	16.1810
14.8469	25.0000	4.5000	319.5972	49.8149	390.9380	16.3014
15.4790	20.0000	4.5000	356.7531	48.2027	428.0085	16.3201
14.3979	40.0000	7.0000	281.4160	52.2328	353.1946	16.3364
14.5447	35.0000	7.0000	288.3494	51.9642	360.1374	16.3772
14.6610	30.0000	7.0000	300.0608	51.1581	371.6855	16.4761
14.9410	25.0000	7.0000	320.4250	50.0835	391.9546	16.4214
15.5560	20.0000	7.0000	358.0159	48.2027	429.2331	16.2991
15.6963	40.0000	0.0000	301.1531	51.6955	372.0349	16.9917
15.7524	35.0000	0.0000	305.0596	51.4268	375.8523	17.1617
15.8537	30.0000	0.0000	317.1785	50.6203	387.8059	17.2046
16.1813	25.0000	0.0000	340.7668	49.2774	411.1035	17.4103
16.5927	23.0000	0.0000	363.0895	47.9341	432.9119	17.6148
15.8133	40.0000	2.0000	303.9704	51.6955	374.8884	16.9997
15.9978	36.0000	2.0000	312.5464	51.1581	383.2415	17.0635
16.1313	32.0000	2.0000	324.6067	50.3521	395.0915	17.1446
16.6387	29.0000	2.0000	351.2615	49.2774	421.6499	17.3279
17.2151	24.0000	2.0000	384.6479	47.9341	454.9258	17.2666
15.9244	40.0000	4.5000	305.4336	51.6955	376.3625	16.9938
16.0673	36.0000	4.5000	314.8467	51.1581	385.6003	17.1432
16.2176	32.0000	4.5000	328.6540	50.3521	399.2734	17.1649
16.8020	28.0000	4.5000	356.3816	49.0088	426.6011	17.2015
17.2329	25.0000	4.5000	381.4431	48.2027	451.7805	17.1471
15.7096	40.0000	7.0000	305.5349	51.4268	376.4106	16.3745
15.8274	36.0000	7.0000	313.9469	50.8895	394.6719	16.4966
16.1058	32.0000	7.0000	330.6521	50.0835	401.2656	16.7196
16.4830	28.0000	7.0000	351.8691	49.0088	422.2253	16.7943
17.0336	25.0000	7.0000	379.2143	48.2027	449.6797	16.9160

The values of n-hydrogen to carbon ratio in fuel, m and ℓ - the number of carbon and hydrogen atom respectively in the measured hydrocarbon are assumed to be:

n - 1.86

m - 6

n - 14 .

The legend of Table A-1 is:

A/F = the air/fuel ratio from direct measurements;

AFE = air/fuel ratio based on emissions;

AIR = mass of inlet air to the engine in (lb/hr);

AIRP = the amount of additional air injected by the air pump in (lb/hr);

MEX = total exhaust mass flow which is:

$$MEX = AIR + AIRP + FUEL \quad . \qquad (A\text{-}10)$$

Appendix B

ENGINE TEST STAND MONITOR SOFTWARE (ETSMS)

```
FILE DDMAIN.FR  6-23-77
MAIN PROGRAM INITIATES THE SUPERVISOR THEN KILLS ITSELF.
  EXTERNAL SUPER
  COMMON/TTSEM/TTOEX/MESS/MESS
TTOEX: EXCLUSION SEMAPHORE TO PREVENT MIXING OF MESSAGES ON CONSOLE
MESS: TRANSMISSION MESSAGE
  INTEGER TTOEX
  DATA TTOEX/0/MESS/1/
  CALL ITASK(SUPER,5,5,IER)
  IF (IER.NE.1) TYPE "SUPER IER=",IER
  CALL XMT(TTOEX,MESS,$20)
20 CALL KILL
  END
```

```
FILE DDSUPER.FR  6-30-77
TASK TO PROVIDE COMMUNICATIONS LINK BETWEEN OPERATOR'S CONSOLE AND
      OTHER TASKS AND SUBROUTINES.
  TASK SUPER
TASKS AND THE USER CLOCK SUBROUTINE MUST BE DECLARED EXTERNAL
      FOR USE IN SUBROUTINE CALLS.
  EXTERNAL DACOL,TTOUT,CLOCK,CONTR,COUNT
  COMMON /TTSET/DATSEL,NREPS/TTSEM/TTOEX/LABELS/LABEL
 2 /OUTCO/DDUMP,LDUMP/CONGO/CONGO
 4 /NDUMP/NFILE
TTSET: CONSOLE OUTPUT SELECTION ARRAY (DATSEL) AND NUMBER OF SAMPLES
      TO BE AVERAGED BEFORE OUTPUT TO THE CONSOLE (NREPS).
TTSEM: EXCLUSION SEMAPHORE (TTOEX) TO PREVENT MORE THAN ONE TASK
      FROM USING CRT AT ANY TIME.
LABELS: MEASURED VARIABLE LABELS.
OUTCO: LOGICAL VARIABLES TO TRANSFER OPERATOR REQUESTS FOR DISK
      DUMPS (DDUMPS) AND LINE PRINTER DUMPS (LDUMPS).
CONGO: LOGICAL VARIABLE TO TRANSFER OPERATOR REQUEST FOR DATA
      OUTPUT TO CONSOLE.
NDUMP: DISK DUMP NUMBER (NFILE) IS INITIALIZED TO 1 BY SUPER.
  DIMENSION ICOMND(2)
  INTEGER CLKCT1,CLKCT2,COMND,DATSEL(10),LABEL(4,50),TTOEX
  LOGICAL DDUMP,LDUMP,CONGO
  MESS=1
  DATA NFILE/1/
  DATA DDUMP,LDUMP,CONGO/3*.FALSE /
THIS SECTION OF CODE WILL NOT START EXECUTION UNTIL THE EXCLUSION
      SEMAPHORE (TTOEX) IS SET TO 1 INDICATING THAT NO TASK IS
      OUTPUTTING TO THE CONSOLE.
  CALL REC(TTOEX,MESSR)
INITIALIZE DATA DISK, DEFINE A USER CLOCK, AND START OTHER TASKS.
  CALL INIT("DP1",0,IER)
  IF (IER.NE.1) TYPE "DP1 INIT IER=",IER
  CALL ITASK(CONTR,1,1,IER)
  IF (IER.NE.1) TYPE "START CONTR IER=",IER
  CALL ITASK(DACOL,2,2,IER)
  IF (IER.NE.1) TYPE "START DACOU IER=",IER
  CALL ITASK(COUNT,31,31,IER)
  IF (IER.NE.1) TYPE "START COUNT IER=",IER
  CALL DUCLK(1,CLOCK,IER)
  IF (IER.NE.1) TYPE "USER CLOCK IER=",IER
  CALL ITASK(TTOUT,21,21,IER)
  IF (IER.NE.1) TYPE "TTOUT IER=",IER
JUMP DIRECTLY TO INPUT TASK INITIALIZATION.
  GO TO 301
109 TYPE "HUH?"   ;OPERATOR INPUT WAS NOT RECOGNIZED.
110 TYPE "="    ; SUPERVISOR IS READY FOR NEW INPUT.
  CALL XMT(TTOEX,MESS,$115)   ; RELEASE CRT FOR OUTPUT BY OTHER TASKS.
115 READ(11,120) ICOMND(1)   ; READ OPERATOR INPUT.
120 FORMAT(S2)
  COMND=ICOMND(1)
  CALL REC(TTOEX,MESSR)   ; EXCLUDE OTHER TASKS FROM CONSOLE USE.
BEGIN COMPARING OPERATOR INPUT TO DEFINED MNEMONICS.
  IF (COMND.NE."T") GO TO 200   ; SELECT CONSOLE OUTPUT.
  TYPE "DEFAULT CONSOLE OUTPUT"
125 DO 130 I=1,10
  N=DATSEL(I)
130 WRITE(10,140) LABEL(1,N)
140 FORMAT(1X,S8,Z)
  WRITE(10,140)
  ACCEPT "CHANGES? ",NCHNG
  IF(NCHNG)160,170,145
145 DO 150 I=1,NCHNG
  ACCEPT "COLUMN,VARIABLE? ",M,N
150 DATSEL(M)=N
  GO TO 125
```

```
160 WRITE(10,161)(I,LABEL(1,I),I=1,50)
161 FORMAT(1X,5(I4,S8))
    GO TO 125
170 ACCEPT "SAMPLES/AVERAGE? ",NREPS
    CONGO=.TRUE.
    GO TO 110
200 IF (COMND.NE."E") GO TO 300   ; TERMINATE PROGRAM.
    CALL EXIT
300 IF (COMND.NE."I") GO TO 500   ; SET UP DATA COLLECTION TASK.
301 CALL SETDACOL
    GO TO 110
500 IF (COMND.NE."L") GO TO 600   ; LINE PRINTER DUMP
    TYPE "LDUMP"
    LDUMP=.TRUE.
    GO TO 110
600 IF (COMND.NE."D") GO TO 700   ; DISK DUMP
    TYPE "DDUMP"
    GO TO 110
700 IF (COMND.EQ."DL") GO TO 710   ; LINE PRINTER AND DISK DUMP.
    IF (COMND.NE."LD") GO TO 800
710 DDUMP=.TRUE.
    LDUMP=.TRUE.
    TYPE "LDDUMP"
    GO TO 110
800 IF (COMND.NE."C") GO TO 900   ; INPUT ENGINE SETPOINTS.
    TYPE "CONTROL SUB"
    CALL COMMAND(1)
    GO TO 110
900 IF (COMND.NE."S") GO TO 109   ; INCREMENT SPARK ADVANCE.
    TYPE "INC SPARK"
    CALL COMMAND(2)
    GO TO 110
    END
```

```
 FILE SETDAC.FR   6/23/77
 SUBROUTINE TO ACCEPT OPERATOR INPUT OF PARAMETERS SUCH AS
       EMISSION INSTRUMENT SCALES, SAMPLE INTERVAL, AND AMBIENT
       CONDITIONS USED IN THE DATA COLLECTION TASK.
    SUBROUTINE SETDACOL
    COMMON/CLKCT/CLKCT1,CLKCT2/DAVAL/DAVAL(9)/A/A/A1/A1/A2/A2/B/B
   1 /SMULT/SMULT(50)/FSOUT/FSOUT(5)/INDATA/INDATA(50)
 CLKCT: COUNTERS USED BY USER CLOCK SUBROUTINE TO TIME DATA COLLECTION
 DAVAL: ARRAY CONTAINING THE PARAMETERS INPUT BY OPERATOR.
 SMULT: MULTIPLIER USED IN DATRANS.
 FSOUT: FULL SCALE OUTPUTS OF EMISSIONS INSTRUMENTS IN VOLTS. USED
      IN THIS SUBROUTINE TO CALCULATE MULTIPLIERS TO CONVERT
       EMISSION INSTRUMENT INPUTS TO ENGINEERING UNITS IN DATRANS.
    INTEGER CLKCT1,CLKCT2
    EQUIVALENCE (SMPINT,DAVAL(6))
    DATA CLKCT1/2*100/
    DATA DAVAL/0.,0.,0.,0.,0.,0.1,0.,0.,0./
    DATA FSOUT/10.,5.,0.1,0.1,5./
 START OPERATOR INPUT OF PARAMETERS
 90 WRITE(10,100)(N,N=1,9)
100 FORMAT(1X,I5,9I8)
110 WRITE(10,200)
200 FORMAT("  NOX SCL   EGR     PEX     DPOR  PAIR   SMP INT",
  1 "  TEMP    PRESS    HUMID")
    WRITE(10,300)(DAVAL(N),N=1,9)
300 FORMAT(1X,10F8.2)
    ACCEPT "CHANGES?",NCHNG
    IF (NCHNG)90,600,305
305 DO 400 ICHNG=1,NCHNG
    ACCEPT "#,VAL ",M,VAR
    IF (M) 90,110,310
310 IF (M-9) 320,320,110
320 DAVAL(M)=VAR
400 CONTINUE
    GO TO 110
 FINISH PARAMETER INPUT AND BEGIN CALCULATION OF EMISSION
       INSTRUMENT MULTIPLIERS.
600 IF (SMPINT.GE.0.1) GO TO 610
    TYPE "SAMPLE INTERVAL MUST BE AT LEAST 0.1 SEC"
    SMPINT=0.1
    GO TO 110
610 CLKCT2=IFIX(SMPINT/0.01666)
    SMULT(9)=DAVAL(1)*A/2048.0
    RETURN
    END
```

```
C    FILE COMMAND.FR  6/23/77
C    SUBROUTINE TO ACCEPT OPERATOR INPUT OF CONTROL SETPOINT.
C          COMPUTED GO TO ON INTRY WILL ALLOW VARIOUS OPTIONS
C          SUCH AS AUTOMATIC INCREMENTING OF SPARK ADVANCE (INTRY=2).
      SUBROUTINE COMMAND(INTRY)
      COMMON /CPRAM/TORQUE,RPM,SPKADV,DSPK,AFRAT,DAF,EGR,TH
     1 /CONSET/NCOM,DESRPM,CHRPM/ICHNG/ICHNG/THROTTLE/THROTTLE
     2 /AUTSET/NAUTO,NAUTSV,MANCON,NSTEP,NSTPS/CNSA/CNSA
C    CPRAM: CONTROL SETPOINT PARAMETERS INPUT BY OPERATOR.
C    CONSET: DESIRED RPM (DESRPM) AND LOGICAL VARIABLE (CHRPM) FOR
C          PROGRAM CONTROL SENT TO CONTROLLER TASK.
C    AUTSET: LOGICAL VARIABLE (MANCON) USED FOR PROGRAM CONTROL IN
C          CONTROLLER TASK.
      LOGICAL CHRPM,CNSA
      INTEGER DESRPM,THROTTLE
      DIMENSION CPRAM(8)
      EQUIVALENCE (CPRAM(1),TORQUE)
      DATA TORQUE/15.,1800.,0.,0.5,0.,90.,0.5,4.5/
      GO TO (1000,2000) INTRY
C    OPERATOR MAY CHANGE ANY SETPOINT PARAMETER.
 1000 WRITE(10,1100)(N,N=1,8)
 1100 FORMAT (1X,I5,9I8)
 1110 WRITE(10,1200)
 1200 FORMAT (1X," TORQUE     RPM    SPK ADV  PP-OA     A/F     P-PRE ",
     1 "    EGR     THROT ")
      WRITE(10,1300)(CPRAM(N),N=1,8)
 1300 FORMAT(1X,10F8.2)
      ACCEPT "CHANGES?",NCHNG
      IF (NCHNG) 900,1600,1305
  900 ICHNG=NCHNG
      IF(NCHNG NE (-5)) GOTO 1000
      CPRAM(2)=1000.
      CPRAM(8)=5.5
      GOTO 1500
 1305 DO 1400 LCHNG=1,NCHNG
      ACCEPT "#,VAL ",M,VAR
      IF (M) 1000,1110,1310
 1310 IF (M-8) 1320,1320,1110
 1320 CPRAM(M)=VAR
 1400 CONTINUE
 1500 IF(TH LT 0 ) GOTO 1000
      IF (TH GT 92 ) GOTO 1000
      T=TH/.045
      IT=IFIX(T)
      IF((T-IT).GT.0.5) IT=IT+1
      THROTTLE=IT
      IF(TORQUE LT 0.0) GOTO 1000
      IF(TORQUE GT 100) GOTO 1000
      GO TO 1110
C    TRANSMIT DESIRED RPM CHANGE TO CONTROLLER TASK.
C          MANCON IS SET TRUE TO ALLOW INTERRUPTION OF AUTOMATIC RPM MAP.
 1600 CNSA=.FALSE.
      MANCON=.TRUE
      DESRPM=IFIX(RPM)
      CHRPM=.FALSE.
      RETURN
C    AUTOMATIC SPARK ADVANCE INCREMENT.
 2000 SPKADV=SPKADV+DSPK
      GO TO 1110
      END
```

```
C    FILE BLOKDAT.FR  6-23-77
      BLOCK DATA
A     .TITL BLOKD
      COMMON /LABELS/LABEL/INSTS/INST
     1 /CONSTS/CONST/TISET/DATSEL,NREPS
     2 /LDSEL/LDSEL(48)
C    LABELS: STRING MATRIX OF MEASURED VARIABLE LABELS USED FOR DISK,
C          LINEPRINTER, AND CONSOLE OUTPUT.
C    INSTS: SIMULATED COMPUTER MACHINE LANGUAGE INSTRUCTIONS FOR USER
C          DEFINED VARIABLES.
C    CONSTS: CONSTANTS FOR USER DEFINED VARIABLES.
C    TISET: VARIABLE OUTPUT SELECTION ARRAY(DATSEL) AND NUMBER OF
C          SAMPLES/OUTPUT (NREPS) FOR CONSOLE OUTPUT
C    LDSEL: MATRIX TO MAP CONSTANT MEASURED VARIABLE ARRAY (LABELS)
C          TO LINEPRINTER AND DISK DUMP FORMATS
      INTEGER DATSEL(10)
      DIMENSION LABEL(4,50),INST(100),CONST(15)
```

Appendix B

```
      DATA LABEL/
     1 "                                            "
     2."                                NOX     HC  "
     3."   CO       CO2      O2       FUEL     IAT  "
     4."   OT       EGT      WT        IMP   TORQUE "
     5."   ZOS      PP1      PP2       PP3     PP4  "
     6."   AF       PAIR     AFE       AFS    EGRDP "
     7."  PEX       EGR      RPM   THROTTLE SPK ADV"
     8."   ES       HCS      AIR   USE FAC  DESRPM "
     9." COMRPM    CNRPM    TEMP     PRESS     HUM  "
     A."  USER1    USER2    USER3    USER4   USER5 "/
      DATA LDSEL/33,20,34,14,38,35,9,10,11,12,13,15
     1,19,21,22,23,24,25,16,17,18,39,43,44,45,30
     2,31,27,28,29,42,36,37,1,2,3,4
     3,5,6,7,8,26,46,47,32,40,41,48/
      DATA CONST/2 0.3 0.4 0.5 0.6 0.7 0.8 0.9 0.10 0.100.0
     1 ..1, 01.3.14/
      DATA INST/1.1.1.2,5.1.5.4.7.2.3.1.10,4.1.13.6.7/
      DATA DATSEL/33.20.35,14.28.32.9.10.11.18/
      END

C     FILE CONTROL.FR    6/27/77
C     TASK TO CONTROL THE ENGINE TEST STAND   RUNS AT HIGHEST PRIORITY.
C           RECEIVES SETPOINTS FROM THE SUPERVISOR VIA THE SUBROUTINE
C           COMMAND.  THIS TASK IS CLOCKED AT 10 HZ BY THE USER CLOCK
C           SUBROUTINE
      TASK CONTROLLER
      COMMON /CONSET/COMRPM.DESRPM.CNRPM/CONKY/CONKY/DPKEY/DPKEY.NTRY
     1 /CONCT/NWAIT.NCNTW/MSKBD/MASK/IDVIO/IDEVIO/INDATA/INDATA(50)
     2 /AUTSET/NAUTO.NAUTSV.MANCON.NSTEP.NSTPS/MPRPM/MPRPM(10)
     3 /OUTCO/DDUMP.LDUMP/CPRAM/CPRAM(8)/ERROR/ERROR
     4/THROTTLE/THROTTLE/ICH0/ICH0/ICH1/ICH1/ICH2/ICH2/NCH/NCH(2)
     5/ICHNG/ICHNG/CNSA/CNSA
C     CONSET: COMMANDED RPM TO THE DYNO SPEED CONTROLLER (COMRPM).
C           DESIRED RPM FROM SUPERVISOR (DESRPM). AND LOGICAL VARIABLE
C           FOR PROGRAM CONTROL (CNRPM)
C     CONKY: MESSAGE CHANNEL FROM CLOCK TO CONTROLLER TASK.
C     DPKEY: MESSAGE CHANNEL FROM CONTROLLER TASK TO CONSOLE OUTPUT TASK
C     CONCT: 0 1 SEC COUNTS BETWEEN 1 RPM STEPS
C     AUTSET:  COUNTS BETWEEN RPM MAP STEPS(NAUTSV). LOGICAL VARIABLE FOR PROGRAM
C           CONTROL (MANCON). NUMBER OF STEPS IN MAP (NSTPS)
C     MPRPM: RPM MAP ARRAY
C     OUTCO. LOGICAL VARIABLES FOR LINEPRINTER DUMP AND DISK DUMP
C     CPRAM: CONTROL PARAMETERS
      LOGICAL CNRPM.MANCON.DDUMP.LDUMP.CNSA
      INTEGER COMRPM.DESRPM.DIFRPM.CONKY.DPKEY.THROTTLE.RPMD
      EQUIVALENCE(CPRAM(1).DTORQUE)
      DATA COMRPM/1800.1000. FALSE /NWAIT/1.1/CNSA/ FALSE /
      DATA MASK/-1/IDEVIO/4RDS/ DDUMP/0/THROTTLE/100/LDUMP/0 /
      DATA NCH/4352.19/ICH0/-8192/ICH1/-8191/ICH2/-8190/ICHNG/-1/
      SANEW=20
      IFO=0
      PIFF=0
      DTORQUE=15.
      CTORQUE=15
      IPOIN=1
      PGAIN=2 2
      RGAIN=7.
      EK3=0
      EK2=0
      EK1=0
      FTORQUE=15
      FDTORQUE=15.
   10 CALL REC(CONKY.MESSR)
C     CONSOLE OUTPUT TASK (TTOUT) WILL OUTPUT AN ERROR MESSAGE
      IF (MESSR EQ 1) GO TO 100
      NTRY=2
      CALL XMT(DPKEY.MESSR.$100)
  100 IF(IPOIN NE.1) GOTO 450
      IF (CNRPM) GO TO 450
      DIFRPM=IABS(DESRPM-COMRPM)
      IF (DIFRPM.GT. 10) GO TO 200
C     COMMANDED RPM IS NOW EQUAL TO DESIRED RPM.
      COMRPM=DESRPM
      CPRAM(2)=FLOAT(COMRPM)
      CNRPM=.TRUE.
      GO TO 300
C     KEEP CHANGING RPM 1 RPM AT A TIME UNTIL COMMANDED RPM IS EQUAL
C           TO DESIRED RPM
  200 COMRPM=COMRPM+10*((DESRPM-COMRPM)/DIFRPM)
C     THIS ROUTINE CONVERTS A BINARY INTEGER TO BCD FOR OUTPUT TO SPEED
C           CONTROLLER
```

```
      CALL DOLW(1,IDEVDO,-8192,MASK,MSTAT)
      IF(MSTAT.NE.1) TYPE "DOLW CHAN SEL MSTAT=",MSTAT
  300 NCOM=0
      IRPM=COMRPM
      NPLAC=1000
      DO 400 I=1,3
      NCOM=16*NCOM+IRPM/NPLAC
      IRPM=MOD(IRPM,NPLAC)
  400 NPLAC=NPLAC/10
      NCOM=NCOM.OR.(-4096)
C   OUTPUT COMMANDED RPM TO SPEED CONTROLLER.
      CALL DOLW(1,IDEVDO,NCOM,MASK,MSTAT)
      IF (MSTAT.NE.1) TYPE "DOLW MSTAT=",MSTAT
  450 IPOIN=IPOIN+1
C  THROTTLE AND TORQUE CONTROL
      IF(ICHNG.EQ.(-2)) GOTO 500
      IF(ICHNG.EQ.(-4)) GOTO 500
C  OPEN LOOP THROTTLE CONTROL
      CALL DOLW(1,IDEVDO,ICH1,MASK,MSTAT)
      NTHR=THROTTLE-4096
      CALL DOLW(1,IDEVDO,NTHR,MASK,MSTAT)
      CONT=CPRAM(8)
      CONT1K=CONT
      CONT2K=CONT
      GOTO 1000
C  TORQUE CONTROL
  500 DT=ABS(DTORQUE-CTORQUE)
      IF(DT.GT.10.) GOTO 600
      CTORQUE=DTORQUE
      GOTO 700
  600 CTORQUE=CTORQUE+DT/(DTORQUE-CTORQUE)*10.
  700 EK4=EK3
      EK3=EK2
      EK2=EK1
      EK1=ERROR
      CONT3K=CONT2K
      CONT2K=CONT1K
      CONT1K=CONT
      CALL AIRDW(1,NCH,I,MSTAT)
      TORQUE=-6.1+0.075486*I
      FTORQUE=.3*TORQUE+.7*FTORQUE        ;MEASURED TORQUE FILTER
      FDTORQUE=.2*CTORQUE+.8*FDTORQUE     ;COMMANDED VALUE FILTER
      ERROR=FDTORQUE-FTORQUE
      CONT=1.9*CONT1K-1.1025*CONT2K+.2025*CONT3K+(PGAIN/RGAIN)*
     *(ERROR-2.6*EK1+2.2525*EK2-.65025*EK3)
      IF(CONT.GT.80) CONT=80
      IF(CONT.LT.1) CONT=1
      FTHROTTLE=CONT/0.045
      THROTTLE=IFIX(FTHROTTLE)
      IF(FTHROTTLE-THROTTLE.GT.0.5) THROTTLE=THROTTLE+1
      NTHR=THROTTLE-4096
      CALL DOLW(1,IDEVDO,ICH1,MASK,MSTAT)
      CALL DOLW(1,IDEVDO,NTHR,MASK,MSTAT)
  900 IF(IPOIN.EQ.5) CALL GAIN1(INDATA(33),TORQUE,GAIN,RGAIN,RPM8)
 1000 IF(ICHNG.EQ.(-3)) GOTO 1050
      IF(ICHNG.EQ.(-4)) GOTO 1050
      GOTO 1100
 1050 CALL DATRANS(23,RETVAL)
      PP=RETVAL
      PPF=(1.-CPRAM(7))*PPF+CPRAM(7)*PP
      SANEW=SANEW-CPRAM(4)*DPO
      DPO=PPF-CPRAM(6)
      IF(SANEW.LT.20 ) SANEW=20.
      IF(SANEW.GT.45 ) SANEW=45.
      GOTO 1200
C    SPARK ADVANCE CONTROL
C   OUTPUT 2 BCD DIGITS
 1100 IF(CHSA) GOTO 1500
      SANEW=CPRAM(3)
 1200 IS=IFIX(SANEW)
      NOSA=0
      NPLAC=10
      DO 1600 I=1,2
      NOSA=NOSA*16+IS/NPLAC
      IS=MOD(IS,NPLAC)
 1600 NPLAC=NPLAC/10
      NOSA=NOSA.OR.(-4096)
      CALL DOLW(1,IDEVDO,ICH2,MASK,MSTAT)
      CALL DOLW(1,IDEVDO,NOSA,MASK,MSTAT)
      CHSA=.TRUE.
 1500 IF(IPOIN.GT.10) IPOIN=1
      GO TO 10
      END
```

```
C     FILE GAIN1.FR   7-2-78
C     SUBROUTINE TO LOOK-UP CLOSED-LOOP GAIN   TABLE INDICES ARE
C     FUNCTIONS OF TORQUE AND RPM.  RPM IS ASSUMED TO BE FOUR (4) BCD DIGITS.
      SUBROUTINE GAIN1(IR1,TORQUE,GAIN,RGAIN,RPMB)
      INTEGER RPMB
      COMMON/TK/TK(4,6)/TK1/TK1(4,6)
      DATA TK/
     1 0.0413,0.0388,0.0272,0.0155
     2,0.0596,0.0456,0.0310,0.0235
     3,0.0456,0.0337,0.0408,0.0250
     4,0.0304,0.0456,0.0470,0.0258
     5,0.0304,0.0517,0.0517,0.0554
     6,0.0304,0.0775,0.0775,0.0775/
      DATA TK1/
     1 30.0,8.0,5.7,5.0
     2,5.2,5.1.5,0.3.3
     3,5.1,4.6,3.8,3.1
     4,5.1,3.4,3.3,3.0
     5,5.1,1.9,1.9,1.8
     6,5.1,1.5,1.5,1.5/
      J=(TORQUE+30)/20
      IF(TORQUE.LT.20)J=1
      IF(TORQUE.GT.100)J=6
C     CONVERT TWO MOST SIGNIFICANT BCD DIGITS TO BINARY TIMES 100
      RPMB=0
      IBCD=4096
      IRPM=IR1
      DO 100 I=1,4
      RPMB=RPMB*10+IRPM/IBCD
      IRPM=MOD(IRPM,IBCD)
  100 IBCD=IBCD/16
      I=RPMB/500
      IF(RPMB.LT.1000)I=1
      IF(RPMB.GT.2000)I=4
      GAIN=TK(I,J)
      RGAIN=TK1(I,J)
      RETURN
      END

C     FILE DACO1.FR 6/30/77
C     TASK TO INPUT DATA,STORE DATA, REDUCE AND OUTPUT DATA.
      TASK DACOL
      COMMON /OUTCO/DDUMP,LDUMP/CONGO/CONGO/DPKEY/DPKEY1,NTRY
     1 /TTSET/DATSEL,NREPS/TTVAL/OUTVAL(10)/KEYS/CLKEY1
     2 /IDEV/IDEV(3)/IDVDI/IDEVDI/NDEV/NDEV/IDVDO/IDEVDO/MSKDO/MASK
     3 /INDATA/INDATA(50)/LDSEL/LDSEL(48)/SMULT/SMULT(50)/FSOUT/FSOUT(5)
     4 /USECO/IUSECTR,ISAVUSE/A2/A2/A/A/B/B/A1/A1/M1/M1(2)/IDB/IDB(2)
     2 /INSAVE/INSAVE(18,50)
C     OUTCO: LOGICAL VARIABLES FOR DUMP REQUESTS.
C     TTVAL: ARRAY OF VARIABLES (OUTVAL) TO BE OUTPUT TO THE CONSOLE.
C     TTSET: ARRAY OF VARIABLES SELECTED FOR OUTPUT TO CONSOLE (DATSEL),
C            AND NUMBER OF INPUTS TO BE AVERAGED BEFORE OUTPUT (NREPS).
C     KEYS: MESSAGE CHANNEL FROM USER CLOCK SUBROUTINE TO THIS TASK.
C     DPKEY: MESSAGE CHANNEL FROM THIS TASK TO CONSOLE OUTPUT TASK FOR
C            SIGNALING WHEN AVERAGES ARE READY FOR OUTPUT.
      EQUIVALENCE (IVALDI(0),INDATA(33))
      INTEGER DPKEY1,DATSEL(10),CLKEY1
      LOGICAL DDUMP,LDUMP,CONGO
      DIMENSION SAVAL(10),IVALDI(0:5),ID(2)
      DATA IDEV/4352,0,31/NDEV/32/
      DATA IDEVDI/4609/M1/-1,-1/IDB/4609,4608/
      NDPREP=1
      MESS=1
C    BEGIN DATA INPUT
 1000 IPOIN=1
 1100 CONTINUE
C    WAIT HERE UNTIL THE USER CLOCK SUBROUTINE SENDS THE MESSAGE INDICATING
C           TIME TO SAMPLE DATA.
      CALL REC(CLKEY1,MESSR)
      ISAVUSE=IUSECTR
      IUSECTR=0
      IF (MESSR.EQ.1) GO TO 1150
      NTRY=1       ; TELL CONSOLE OUTPUT TASK TO OUTPUT AN ERROR MESSAGE.
      CALL XMT(DPKEY1,MESSR,$1150)
 1150 CALL DOLW(1,IDEVDO,-8192,MASK,MSTAT)
      CALL DIW(1,IDEVDI,IVALDI(0),MSTAT)   ;DIGITAL INPUT CALL
      IF(MSTAT.NE.1) TYPE "DIW MSTAT=",MSTAT
      CALL DOLW(1,IDEVDO,-8191,MASK,MSTAT)
      CALL DIW(1,IDEVDI,IVALDI(1),MSTAT)
      IF(MSTAT.NE.1) TYPE"MSTAT1=",MSTAT
      CALL DOLW(1,IDEVDO,-8190,MASK,MSTAT)
      CALL DIW(1,IDEVDI,IVALDI(2),MSTAT)
      IF(MSTAT.NE.1) TYPE"MSTAT2=",MSTAT
```

```
      CALL DOLW(1,IDEVDO,-A189,MASK,MSTAT)
      CALL DIW(1,IDEVDI,IVALDI(3),MSTAT)
      IF(MSTAT NE 1) TYPE"MSTAT3=",MSTAT
      CALL DOLW(1,IDEVDO,-A186,MASK,MSTAT)
      CALL DIW(1,IDEVDI,IVALDI(4),MSTAT)
      IF(MSTAT.NE.1) TYPE"MSTAT4=",MSTAT
      CALL DOLW(1,IDEVDO,-A187,MASK,MSTAT)
      CALL DIW(1,IDEVDI,IVALDI(5),MSTAT)
      IF(MSTAT.NE.1) TYPE"MSTAT5=",MSTAT
      CALL DOLW(1,IDEVDO,-8177,MASK,MSTAT)
      IF(MSTAT NE 1) TYPE"MSTAT15=",MSTAT
      CALL AISQW(NDEV,IDEV,INDATA,MSTAT)   ;ANALOG INPUT CALL
      IF (MSTAT.NE 1) TYPE "AISQW MSTAT=",MSTAT
      ID(1)=INDATA(14)
      ID(2)=INDATA(38)+4096
      CALL DOL(2,ID8,ID,M1,MSTAT)
C  NOX RANGE
      A=500.0
      MAN=(IVALDI(3).AND.15)
      IF(MAN.EQ.36) GOTO 100
      IF(MAN.EQ.1) A=1.0
      IF(MAN.EQ.2) A=10.0
      IF(MAN.EQ.4) A=100 0
      IF(MAN.EQ.8) A=1000.0
      MAN=(IVALDI(3).AND.112)
      IF(MAN.EQ.16) B=10.0
      IF(MAN.EQ.32) B=5.0
      IF(MAN.EQ.64) B=2.0
      A=A*B
C CHECK CO RANGE
  100 MA=(IVALDI(3).AND.4096)
      A1=5.0
      IF(MA.EQ.4096) A1=2.0
C CHECK CO2 RANGE
      MAN=(IVALDI(3).AND.8192)
      B=16.0
      IF(MAN.EQ.8192) B=5.0
C CHECK HC RANGE
      A2=50.0
      MAN=(IVALDI(4).AND.63)
      IF(MAN.EQ.8) GOTO 150
      IF(MAN.EQ.1) A2=1.0
      IF(MAN.EQ.2) A2=5.0
      IF(MAN.EQ.4) A2=10.0
      IF(MAN.EQ.16) A2=100.0
      IF(MAN.EQ.32) A2=500.0
  150 SMULT(10)=A2*.046613962
C    END DATA INPUT AND BEGIN SELECTED DATA STORAGE
      DO 2000 I=1,18
      INDAT=LDSEL(I)
 2000 INSAVE(I,IPOIN)=INDATA(INDAT)
C    END DATA STORAGE AND BEGIN CONSOLE OUTPUT
      IF (.NOT.CONGO) GO TO 3000
      IF (NDPREP.NE.1) GO TO 2200
      DO 2100 I=1,10
 2100 SAVAL(I)=0
 2200 DO 2300 I=1,5
      INDAT=DATSEL(I)
      CALL DATRANS(INDAT,DATAVAL)      ; CONVERT INPUTS TO ENGINEERING UNITS.
 2300 SAVAL(I)=SAVAL(I)+DATAVAL       ; SUM THE DATA UNTIL TIME FOR AVERAGE.
      IF (NDPREP.LT.NREPS) GO TO 2600
      DO 2400 I=1,5
 2400 OUTVAL(I)=SAVAL(I)/NREPS       ; GET AVERAGE BY DIVIDING SUM BY NREPS.
      DO 2450 N=6,10
      INDAT=DATSEL(N)
      CALL DATRANS(INDAT,DATAVAL)
 2450 OUTVAL(N)=DATAVAL
C    TELL CONSOLE OUTPUT TASK THAT THE OUTPUT BUFFER IS FULL.
      CALL XMT(DPKEY1,MESS,$2500)
 2500 NDPREP=0
 2600 NDPREP=NDPREP+1
C    END CONSOLE OUTPUT AND TEST FOR DUMP REQUESTS
 3000 IF (DDUMP.OR.LDUMP) CALL DUMPS
 4000 IPOIN=IPOIN+1
      IF (IPOIN.GT.50) GO TO 1000
      GO TO 1100
      END
```

```
C    FILE SUBDUMPS.FR   6-23-77
C    SUBROUTINE TO CONDENSE ENGINE TEST DATA AND DUMP RESULTS TO DISK
C    AND/OR LINEPRINTER
       SUBROUTINE DUMPS
       COMMON/NDUMP/NFILE/LDSEL/LDSEL(48)/OUTCO/DDUMP,LDUMP/LABELS/LABEL
      1 /CPRAM/TORQUE,RPM,SPKADV,DSPK,AFRAT,DAF,EGR,DEGR
      2 /INDATA/INDATA(50)/INSAVE/INSAVE(18,50)
C    NDUMP: DISK FILE NUMBER (NFILE)
C    LDSEL: MATRIX FOR STATISTICAL CALCULATION AND OUTPUT FORMAT
C           SELECTION.
C    OUTCO: SWITCHES SET BY OPERATOR IN SUPERVISOR FOR LPT DUMP (LDUMP)
C           OR DISK DUMP (DDUMP).
C    LABELS. STRING MATRIX OF OUTPUT VARIABLE NAMES.
C    CPRAM. NOMINAL CONTROLLER SETPOINTS INPUT IN SUBROUTINE COMMAND.
C    INDATA: CURRENT INPUT DATA FROZEN WHEN DUMP IS REQUESTED.
       DIMENSION LABEL(4,50),DSAVE(50),DVALS(48),SIGMAS(18),DEVMAX(18)
      1 ,IDATE(3),ITIME(3)
       LOGICAL DDUMP,LDUMP
       REAL MAXVAL
C    BEGIN CALCULATIONS TO CONDENSE DATA
       DO 2990 J=1,18
       SAVAL=0
       DO 2000 K=1,50
       NDX=LDSEL(J)
       INDATA(NDX)=INSAVE(J,K)
       CALL DATRANS(NDX,RETVAL)
       SAVAL=SAVAL+RETVAL
 2000  DSAVE(K)=RETVAL
       AVEVAL=SAVAL/50              ;AVERAGE
       DVALS(J)=AVEVAL
       SAVAL=0
       MAXVAL=0
       SQRVAL=0
       DO 2100 K=1,50
       SQUARE=(DSAVE(K)-AVEVAL)**2
       SAVAL=SAVAL+SQUARE
       IF(SQUARE.LT.SQRVAL) GOTO 2050
       SQRVAL=SQUARE
       MAXVAL=DSAVE(K)
 2050  CONTINUE
 2100  CONTINUE
       SIGMAS(J)=SQRT(SAVAL/50)          ;STD DEV
       DEVMAX(J)=MAXVAL             ;GREATEST DEVIATION
 2990  CONTINUE
C  END STATISTICAL CALCS AND FINISH FILLING OUTPUT BUFFER
       DO 3100 J=19,48
       INSEL=LDSEL(J)
       CALL DATRANS(INSEL,RETVAL)
 3100  DVALS(J)=RETVAL
C  END CALCS AND OUTPUT TO LINEPRINTER AND DISK
       CALL DATE(IDATE,IER)
       CALL TIME(ITIME,IER)
       WRITE(12,100)(IDATE(I),I=1,3),(ITIME(I),I=1,3)
  100  FORMAT("0ENGINE TEST DATA",10X,I2,1H/,I2,1H/,I2,10X,I2,1H:,I2
      1 ,1H:,I2)
       IF (.NOT.DDUMP) GO TO 1000
C   DISK DUMP
       DDUMP=.FALSE.
       WRITE(12,200) NFILE
  200  FORMAT(" DISK DUMP",10X,"FILE #",I3)
       CALL APPEND(5,"DP1:ENGDATA",IERR)
       IF (IERR.NE.1) TYPE "APPEND IERR=",IERR
       WRITE BINARY(5) ITYPE,NFILE,(IDATE(I),I=1,3),(ITIME(I),I=1,3)
      1 ,TORQUE,RPM,SPKADV,AFRAT,EGR,(LDSEL(I),I=1,48)
       WRITE BINARY(5)(DVALS(I),I=1,43),(SIGMAS(I),I=1,18)
      1 ,(DEVMAX(I),I=1,18)
       NFILE=NFILE+1
       CALL CLOSE(5,IERR)
       IF (IERR.NE.1) TYPE "CLOSE IERR=",IERR
 1000  WRITE(12,1100)
 1100  FORMAT("0NOMINAL",11X,"TORQUE",2X,"RPM",3X,"SPKADV",5X,
      1"A/F",4X,"EGR")
       WRITE(12,1200) TORQUE,RPM,SPKADV,AFRAT,EGR
 1200  FORMAT(16X,5F8.2)
       IF (.NOT.LDUMP) GO TO 9999
C  LINE PRINTER DUMP
       LDUMP=.FALSE.
       DO 5300 I=1,2
       JEND=9*I
       JSTART=JEND-8
       WRITE(12,5050)
 5050  FORMAT(1H0,8X,Z)
```

```
      DO 5150 J=JSTART,JEND
      INSEL=LDSEL(J)
      WRITE(12,5100)LABEL(1,INSEL)
 5100 FORMAT(1X,S8.2)
 5150 CONTINUE
      WRITE(12,5700)
      WRITE(12,5200) (DVALS(J),J=JSTART,JEND)
 5200 FORMAT(" AVE",5X,9F8.2)
      WRITE(12,5300)(SIGMAS(J),J=JSTART,JEND)
 5300 FORMAT(" VAR",5X,9F8.2)
      WRITE(12,5400)(DEVMAX(J),J=JSTART,JEND)
 5400 FORMAT(" WORST   ",9F8.2)
 5500 CONTINUE
      DO 5800 L=19,19,1
      M=L+9
      WRITE(12,5700)
      DO 5650 I=L,M
      INSEL=LDSEL(I)
      WRITE(12,5100) LABEL(1,INSEL)
 5650 CONTINUE
      WRITE(12,5700)
      WRITE(12,5700)(DVALS(I),I=L,M)
 5700 FORMAT(1X,10(1X,F7.2))
 5800 CONTINUE
 9999 RETURN
      END


C     FILE DATRANS.FR  6-23-77
C     SUBROUTINE TO CONVERT INPUTS TO ENGINEERING UNITS.  INPUT IS
C           VECTORED TO AN APPROPRIATE CONVERSION ROUTINE BY A
C           COMPUTED GO TO STATEMENT ON THE ROUTING MATRIX (NROUT).
      SUBROUTINE DATRANS(IDNUM,RETVAL)
      COMMON /ROUTN/NROUT/CONSTS/CONST
     1 /DAVAL/DAVAL(9)/SMULT/SMULT(50)/INDATA/INDATA(50)
     2 /CONSET/COMRPM,DESRPM,CHRPM/AFE/AFE/AFS/AFS/A1/A1/B/B
     3 /OFFSET/OFFSET(50)
     4 /USECO/IUSECTR,ISAVUSE
C     ROUTN: MATRIX (NROUT) TO VECTOR INPUTS TO CONVERSION ROUTINES
C     IDENTS: INTEGER MATRIX (IDENT) USED IN SOME CONVERSIONS.
C     SMULT,OFFSET: REAL MATRICES USED IN SOME CONVERSIONS.
C     INSTS: SIMULATED COMPUTER PROGRAM FOR USER DEFINED VARIABLES.
C     CONSTS: CONSTANTS FOR USER DEFINED VARIABLES.
C     DAVAL: ARRAY CONTAINING TEMP. PRESS AND HUM FROM
C           SETDACOL SUBROUTINE
C     INDATA: ARRAY CONTAINING CURRENT INPUT DATA
C     CONSET  CONTROL VARIABLES.
      EQUIVALENCE (TEMP,DAVAL(7)),(PRESS,DAVAL(8)),(HUM,DAVAL(9))
     1 ,(SMPINT,DAVAL(6)),(EGR,DAVAL(2)),(PFX,DAVAL(3)),(DPOR,DAVAL(4))
     2,(PAIR,DAVAL(5))
      DIMENSION NROUT(50),CONST(15),STACK(15)
      INTEGER COMRPM,DESRPM
      LOGICAL CHRPM
      DATA NROUT/10*6,23,24,2*6,12,13,14,15,3*6,4*26,27,25,21,22
     1,16,17,18,7,20,19,2*6,7,11,10,8,9,3,4,5,5*2/
      DATA SMULT/12*0.,-.043323,.04383,4*0.,-.00444960,0.075426,1.0,
     ,4*1.,8*0.,4*1.,13*0./
      DATA OFFSET/18*0.,7.35,-6.1,30*0.0/
C     VECTOR INPUT TO CONVERSION ROUTINE.
      N=NROUT(IDNUM)
      GO TO (100,1000,3000,3100,3200,4000,5000,6000,7000,8000,9000
     1,4100,4200,4300,4400,4500,4600,4700,4800,4900,3300,3400
     2,3500,3600,3700,3800,3900),N
C     DIRECT READING OF INTEGER INPUT.
  100 RETVAL=INDATA(IDNUM)
      RETURN
 1000 RETURN
 3000 RETVAL=TEMP
      RETURN
 3100 RETVAL=PRESS
      RETURN
 3200 RETVAL=HUM
      RETURN
C  AFE-A/F BASED ON EMISSION,AFS-A/F BASED ON DIRECT MEASUREMENT
 3300 RETVAL=AFE
      RETURN
 3400 RETVAL=AFS
      RETURN
C  EVALUATE CO READING
 3500 A=INDATA(IDNUM)/2048.
      IF(A1.EQ.5.) GOTO 3550
```

```
C     0-2% RANGE
      RETVAL=.0084+1.3383*A+.6349*A**2
      RETURN
C     0-5%  RANGE
 3550 IF(A.GT..59) GOTO 3570
      RETVAL=.0026+2.3422*A+2.4337*A**2
      RETURN
 3570 RETVAL=.6642+4.4127*A**2
      RETURN
C   CO2 VALUE
 3600 A=INDATA(IDNUM)/2048.
      IF(B.EQ.16.) GOTO 3650
C     0-5%  RANGE
      RETVAL=.1245+2.08*A+2.8774*A**2
      RETURN
C  0-16% RANGE
C   CHECK FOR PORTION OF SCALE
 3650 IF(A.GT..71) GOTO 3670
C   LOW PORTION OF SCALE
      RETVAL=.0955+4.0676*A+9.3106*A**2
      RETURN
C   HIGH PORTION OF SCALE
 3670 RETVAL=3.4915+11.7391*A**3
      RETURN
 3700 RETVAL=PAIR
      RETURN
 3800 CALL DATRANS(33,RPM)
      RETVAL=(INDATA(IDNUM)*8.7890625+1.0E-5-0.006)*RPM
      RETURN
C     AIR FUEL RATIO
 3900 CALL DATRANS(14,FUEL)
      CALL DATRANS(33,AIR)
      RETVAL=AIR/FUEL
      RETURN
C   ROUTINE TO MULTIPLY INPUT BY A CONSTANT AND ADD CONSTANT OFFSET.
 4000 RETVAL=SMULT(IDNUM)*INDATA(IDNUM)+OFFSET(IDNUM)
      RETURN
C AIR TEMPERATURE CENTIGRADES
 4100 A=INDATA(IDNUM)/500.
      RETVAL=71.566+12.5838*A+.34164*A**2+.1206*A**3
      RETURN
C OIL TEMPERATURE CENTIGRADES
 4200 A=INDATA(IDNUM)/250.
      RETVAL=198.139+7.335*A+.09072*A**2+.01026*A**3
      RETURN
CEXAHAUST TEMPERATURE CENTIGRADES
 4300 A=INDATA(IDNUM)/100.
      RETVAL=1167.42+18.3132*A+.12726*A**2+.0009*A**3
      RETURN
C WATER TENERATURE CENTIGRADES
 4400 A=INDATA(IDNUM)/500
      RETVAL=109.6+15.4665*A+.40068*A**2+.03982*A**3
      RETURN
 4500 RETVAL=DPOR
      RETURN
 4600 RETVAL=PEX
      RETURN
 4700 RETVAL=EGR
      RETURN
C  SPARK ADVANCE READING- INVERTED BCD
 4800 INREVS=.NOT.INDATA(IDNUM)
      GOTO 5100
C  THROTTLE READING INVERTED 4 DIGIT BCD
 4900 I=.NOT.INDATA(IDNUM)
      INREVS=I.AND.32767
      NT=0
      IF(I.LT.0) NT=8
      GOTO 5100
C   ROUTINE TO CONVERT FROM BCD DIGITAL INPUT.
 5000 INREVS=INDATA(IDNUM)
 5100 D1=INREVS.AND.-4096
      D2=INREVS.AND.3840
      D3=INREVS.AND.240
      D4=INREVS.AND.15
      RETVAL=D1/4.096+D2/2.56+D3/1.6+D4
      IF(IDNUM.EQ.38) RETVAL=RETVAL*.272727
      IF(IDNUM.EQ.35) RETVAL=RETVAL*.1
      IF(IDNUM.EQ.34) RETVAL=.01*(RETVAL+NT*1000)
      RETURN
 6000 RETVAL=COMRPM
      RETURN
 7000 RETVAL=0
```

```
      IF (CNRPM) RETVAL=1
      RETURN
 8000 RETVAL=DESRPM
      RETURN
 9000 RETVAL=1.0-ISAVUSE/(SMPINT*1561)
      RETURN
      END
```

```
C    FILE DDTTOUT.FR  6-30-77
C    TASK TO OUTPUT DATA AND ERROR MESSAGES TO THE OPERATORS CONSOLE.
      TASK TTOUT
      COMMON/TTSET/DATSEL,NREPS/LABELS/LABEL/DPKEY/DPKEY1,NTRY
     1 /TTVAL/OUTVAL/TTSEM/TTOEX
C    TTSET: OUTPUT SELECTION ARRAY USED TO GET LABELS.
C    LABELS: OUTPUT VARIABLE LABEL ARRAY.
C    DPKEY: MESSAGE CHANNEL TO COMMUNICATE THAT OUTPUT TO CONSOLE SHOULD START.
C    TTVAL: OUTPUT BUFFER FILLED BY DACOL.
C    TTSEM: CRT EXCLUSION SEMAPHORE.
      DIMENSION LABEL(4,50),OUTVAL(10)
      INTEGER DATSEL(10),DATAVAL,DPKEY1,TTOEX
      MESS=1
  100 DO 200 I=1,10
      CALL REC(DPKEY1,MESSR)      ; WAIT HERE UNTIL OUTPUT BUFFER IS FULL.
      CALL REC(TTOEX,MESSR2)      ; WAIT UNTIL CRT IS FREE.
      IF (MESSR.NE.1) GO TO 300      ; JUMP TO THE ERROR MESSAGES.
      IF (I.NE.1) GO TO 190
C    PRINT A HEADER EVERY TENTH TIME.
      DO 150 J=1,10
      N=DATSEL(J)
  150 WRITE(10,160) LABEL(1,N)
  160 FORMAT(1X,S8,Z)
      WRITE(10,210)
      GO TO 195
C    OUTPUT A LINE OF DATA.
  190 WRITE(10,210)(OUTVAL(N),N=1,10)
  195 CALL XMT(TTOEX,MESS,$100)   ; RELEASE CRT TO OTHER TASKS.
  210 FORMAT(1X,10F8.2)
  200 CONTINUE
      GO TO 100
C    COMPUTED GO TO VECTORS PROGRAM TO ERROR MESSAGE.
  300 GO TO (400,500) NTRY
  400 TYPE "DACOL CLOCK XMT ERROR ",MESSR
      GO TO 195
  500 TYPE "CONTR CLOCK XMT ERROR",MESSR
      GO TO 195
      END
```

```
;  FILE CLOCK.SR 6-30-77
; USER CLOCK ROUTINE: DECREMENTS CLCTR, AN INTEGER SET BY SUPER, TO 0
; THEN SENDS A MESSAGE TO DACOL TO SAMPLE INPUT DATA.  ALSO DECREMENTS
;  CNCTR, A LOCAL INTEGER, TO 0 THEN SENDS A MESSAGE TO CONTROLLER TO PERFORM
;  CONTROL FUNCTIONS.
        .TITL CLOCK
        .COMM CLKCT 2    ;TIMING COUNTERS SET BY SUPER FOR DACOL
        .COMM KEYS  1    ;MESSAGE CHANNEL TO DACOL
        .COMM CONKY 1   ;MESSAGE CHANNEL TO CONTROLLER
        .ENT  CLOCK
        .EXTN .UCEX
        .EXTN .IXMT
        .NREL
CLOCK:  STA 3 SAC3     ;SAVE RETURN ADDRESS
        LDA 1 P1
        DSZ   @CLCTR  ;START DATA SAMPLING COUNT LOOP
        JMP   CNCLK
        LDA 0 CLKY1
        .IXMT          ;SEND MASSAGE TO DACOL TO SAMPLE DATA
        STA 2 @CLKY1  ;RETURN ERROR MESSAGE IN CLKY1
        LDA 3 @CLCT1  ;RESTORE COUNTS FOR NEXT LOOP
        STA 3 @CLCTR
CNCLK:  DSZ   CNCTR   ;DECREMENT CONTROLLER TIMER AND TEST FOR ZERO
        JMP   CLOUT
        LDA 0 CHKEY
        .IXMT           ;TRANSMIT MESSAGE TO START CONTROLLER
        STA 2 @CNKEY    ;SEND ERROR MESSAGE IN CNKEY
        LDA 3 CONCT     ;RESTORE CONTROLLER TIMER
        STA 3 CNCTR
CLOUT:  LDA 3 SAC3     ;RESTORE RETURN ADDRESS
        .UCEX
```

```
CLCTR:   .GADD   CLKCT 0
CLCT1:   .GADD   CLKCT 1
CNCTR:   6
CONCT:   6
CNKEY:   .GADD CONKY 0
CLKY1:   .GADD   KEYS 0
SAC3:    0
P1:      1
         END
```

```
C   FILE USECTR.FR  8/1/77
      TASK COUNT
      COMMON /USECO/IUSECTR,ISAVUSE
    5 X=1.5*2
A     ISZ @.+3
A     JMP .+3
A     JMP .+2
A     .GADD USECO,0
      GO TO 5
      END
```

Appendix C

REGRESSOR VARIABLES OF THE GLOBAL FUNCTIONS

A global function of either fuel or log (emissions) depends on AF, SA, EGR, RPM and TORQUE and can be evaluated by the formula:

$$F = \sum_{i=1}^{56} b_i x_i \tag{C-1}$$

where b_i are the regression coefficients listed in Appendix D for the various functions both for second and third order polynomials. x_i are the regressor variables which are products of the independent variables and F is the function value.

The various x_i are as follows:

$$x_1 = 1 \tag{C-2}$$

$$x_2 = \frac{AF}{15} = \overline{AF} \tag{C-3}$$

$$x_3 = \frac{SA}{40} = \overline{SA} \tag{C-4}$$

$$x_4 = \frac{EGR}{7} = \overline{EGR} \tag{C-5}$$

$$x_5 = \frac{RPM}{1500} = \overline{RPM} \tag{C-6}$$

$$x_6 = \frac{TORQUE}{15} = \overline{TORQUE} \tag{C-7}$$

$$x_7 = \overline{AF}^2 \tag{C-8}$$

$$x_8 = \overline{SA}^2 \tag{C-9}$$

$$x_9 = \overline{EGR}^2 \tag{C-10}$$

$$x_{10} = \overline{RPM}^2 \quad (C-11)$$

$$x_{11} = \overline{TORQUE}^2 \quad (C-12)$$

$$x_{12} = \overline{AF} \cdot \overline{SA} \quad (C-13)$$

$$x_{13} = \overline{AF} \cdot \overline{EGR} \quad (C-14)$$

$$x_{14} = \overline{AF} \cdot \overline{RPM} \quad (C-15)$$

$$x_{15} = \overline{AF} \cdot \overline{TORQUE} \quad (C-16)$$

$$x_{16} = \overline{SA} \cdot \overline{EGR} \quad (C-17)$$

$$x_{17} = \overline{SA} \cdot \overline{RPM} \quad (C-18)$$

$$x_{18} = \overline{SA} \cdot \overline{TORQUE} \quad (C-19)$$

$$x_{19} = \overline{EGR} \cdot \overline{RPM} \quad (C-20)$$

$$x_{20} = \overline{EGR} \cdot \overline{TORQUE} \quad (C-21)$$

$$x_{21} = \overline{RPM} \cdot \overline{TORQUE} \quad (C-22)$$

$$x_{22} = \overline{AF}^3 \quad (C-23)$$

$$x_{23} = \overline{SA}^3 \quad (C-24)$$

$$x_{24} = \overline{EGR}^3 \quad (C-25)$$

$$x_{25} = \overline{RPM}^3 \quad (C-26)$$

$$x_{26} = \overline{TORQUE}^3 \quad (C-27)$$

$$x_{27} = \overline{AF}^2 \cdot \overline{SA} \quad (C-28)$$

$$x_{28} = \overline{AF}^2 \cdot \overline{EGR} \quad (C\text{-}29)$$

$$x_{29} = \overline{AF}^2 \cdot \overline{RPM} \quad (C\text{-}30)$$

$$x_{30} = \overline{AF}^2 \cdot \overline{TORQUE} \quad (C\text{-}31)$$

$$x_{31} = \overline{SA}^2 \cdot \overline{AF} \quad (C\text{-}32)$$

$$x_{32} = \overline{SA}^2 \cdot \overline{EGR} \quad (C\text{-}33)$$

$$x_{33} = \overline{SA}^2 \cdot \overline{RPM} \quad (C\text{-}34)$$

$$x_{34} = \overline{SA}^2 \cdot \overline{TORQUE} \quad (C\text{-}35)$$

$$x_{35} = \overline{EGR}^2 \cdot \overline{AF} \quad (C\text{-}36)$$

$$x_{36} = \overline{EGR}^2 \cdot \overline{SA} \quad (C\text{-}37)$$

$$x_{37} = \overline{EGR}^2 \cdot \overline{RPM} \quad (C\text{-}38)$$

$$x_{38} = \overline{EGR}^2 \cdot \overline{TORQUE} \quad (C\text{-}39)$$

$$x_{39} = \overline{RPM}^2 \cdot \overline{AF} \quad (C\text{-}40)$$

$$x_{40} = \overline{RPM}^2 \cdot \overline{SA} \quad (C\text{-}41)$$

$$x_{41} = \overline{RPM}^2 \cdot \overline{EGR} \quad (C\text{-}42)$$

$$x_{42} = \overline{RPM}^2 \cdot \overline{TORQUE} \quad (C\text{-}43)$$

$$x_{43} = \overline{TORQUE}^2 \cdot \overline{AF} \quad (C\text{-}44)$$

$$x_{44} = \overline{TORQUE}^2 \cdot \overline{SA} \quad (C\text{-}45)$$

$$x_{45} = \overline{TORQUE}^2 \cdot \overline{EGR} \quad (C-46)$$

$$x_{46} = \overline{TORQUE}^2 \cdot \overline{RPM} \quad (C-47)$$

$$x_{47} = \overline{AF} \cdot \overline{SA} \cdot \overline{EGR} \quad (C-48)$$

$$x_{48} = \overline{AF} \cdot \overline{SA} \cdot \overline{RPM} \quad (C-49)$$

$$x_{49} = \overline{AF} \cdot \overline{SA} \cdot \overline{TORQUE} \quad (C-50)$$

$$x_{50} = \overline{AF} \cdot \overline{EGR} \cdot \overline{RPM} \quad (C-51)$$

$$x_{51} = \overline{AF} \cdot \overline{EGR} \cdot \overline{TORQUE} \quad (C-52)$$

$$x_{52} = \overline{AF} \cdot \overline{RPM} \cdot \overline{TORQUE} \quad (C-53)$$

$$x_{53} = \overline{SA} \cdot \overline{EGR} \cdot \overline{RPM} \quad (C-54)$$

$$x_{54} = \overline{SA} \cdot \overline{EGR} \cdot \overline{TORQUE} \quad (C-55)$$

$$x_{55} = \overline{SA} \cdot \overline{RPM} \cdot \overline{TORQUE} \quad (C-56)$$

$$x_{56} = \overline{EGR} \cdot \overline{RPM} \cdot \overline{TORQUE} \quad (C-57)$$

$\overline{AF}$, $\overline{SA}$, $\overline{EGR}$, $\overline{RPM}$ and $\overline{TORQUE}$ are given in (C-3) - (C-7).

Appendix D

REGRESSION COEFFICIENTS OF GLOBAL FITS

SUMMARY TABLE OF REGRESSION COEFFICIENTS

GLOBAL FUNCTIONS-SECOND ORDER

	1	2	3	4	5	6	7	8	9	10
FUEL	-2.0345	0.0000	0.0000	0.0000	5.8715	4.8574	1.6963	0.0000	0.0000	0.0000
HC	-1.1503	0.0000	8.1070	3.3900	-0.4902	0.0000	3.2061	-2.3007	-0.7346	0.0000
CO	-2.2745	0.0000	6.6601	0.0000	1.9572	8.8889	2.3209	0.0000	-0.4071	0.0000
NO	-5.0571	0.0000	-1.5417	-1.7372	5.5432	2.7157	-2.2885	2.1845	1.1499	-2.1439

	11	12	13	14	15	16	17	18	19	20
FUEL	0.0000	0.0000	1.2583	0.0000	-5.2842	-0.8039	-1.9825	-1.5002	0.0000	-0.2713
HC	1.1744	-5.1711	-0.4929	1.4469	-1.4192	0.2306	0.4254	2.8048	-0.9358	-0.4696
CO	0.0000	-7.5128	1.1197	0.0000	-4.8525	-0.4288	0.6716	0.0000	-0.0951	-0.0365
NO	-1.3235	-0.3751	0.3489	2.9528	1.4565	-0.5038	-1.0132	1.4575	-0.0342	-0.0314

	21	22	23	24	25	26	27	28	29	30
FUEL	5.5903	0.0000	0.0000	0.0000	0.0000	0.0000	0.0000	0.0000	0.0000	0.0000
HC	-2.1131	0.0000	0.0000	0.0000	0.0000	0.0000	0.0000	0.0000	0.0000	0.0000
CO	-1.9741	0.0000	0.0000	0.0000	0.0000	0.0000	0.0000	0.0000	0.0000	0.0000
NO	0.0000	0.0000	0.0000	0.0000	0.0000	0.0000	0.0000	0.0000	0.0000	0.0000

	31	32	33	34	35	36	37	38	39	40
FUEL	0.0000	0.0000	0.0000	0.0000	0.0000	0.0000	0.0000	0.0000	0.0000	0.0000
HC	0.0000	0.0000	0.0000	0.0000	0.0000	0.0000	0.0000	0.0000	0.0000	0.0000
CO	0.0000	0.0000	0.0000	0.0000	0.0000	0.0000	0.0000	0.0000	0.0000	0.0000
NO	0.0000	0.0000	0.0000	0.0000	0.0000	0.0000	0.0000	0.0000	0.0000	0.0000

	41	42	43	44	45	46	47	48	49	50
FUEL	0.0000	0.0000	0.0000	0.0000	0.0000	0.0000	0.0000	0.0000	0.0000	0.0000
HC	0.0000	0.0000	0.0000	0.0000	0.0000	0.0000	0.0000	0.0000	0.0000	0.0000
CO	0.0000	0.0000	0.0000	0.0000	0.0000	0.0000	0.0000	0.0000	0.0000	0.0000
NO	0.0000	0.0000	0.0000	0.0000	0.0000	0.0000	0.0000	0.0000	0.0000	0.0000

	51	52	53	54	55	56
FUEL	0.0000	0.0000	0.0000	0.0000	0.0000	0.0000
HC	0.0000	0.0000	0.0000	0.0000	0.0000	0.0000
CO	0.0000	0.0000	0.0000	0.0000	0.0000	0.0000
NO	0.0000	0.0000	0.0000	0.0000	0.0000	0.0000

GLOBAL FUNCTIONS-THIRD ORDER

	1	2	3	4	5	6	7	8	9	10
FUEL	12.4891	-20.7755	-1.8918	0.8116	6.8725	0.0000	0.0000	2.9631	0.0000	0.0000
HC	0.9153	0.0000	4.3457	4.5355	0.0000	0.0000	0.0000	0.0000	-2.2800	0.0000
CO	16.3767	-25.5409	0.0000	0.0000	1.8559	7.4948	0.0000	0.0000	0.0000	0.0000
NO	-15.5141	15.3468	0.0000	0.0000	3.2438	3.5267	0.0000	0.0000	0.0000	0.0000

	11	12	13	14	15	16	17	18	19	20
FUEL	0.0000	0.0000	0.0000	0.0000	0.0000	0.0000	-4.2074	0.0000	0.0000	0.0000
HC	3.2049	0.0000	0.0000	-3.8073	0.0000	0.0000	0.0000	0.0000	0.0000	-3.4943
CO	0.0000	5.1010	0.0000	0.0000	-5.6111	0.0000	0.0000	0.0000	0.0000	0.0000
NO	0.0000	0.0000	0.0000	1.2728	0.0000	-1.5805	0.0000	0.0000	-0.8886	0.0000

	21	22	23	24	25	26	27	28	29	30
FUEL	6.8122	7.5757	0.0000	0.0000	0.0000	0.0000	0.0000	0.1508	0.0000	0.0000
HC	0.0000	0.0000	0.0000	0.0000	0.0000	0.0000	-1.0616	0.0000	5.3398	0.0000
CO	0.0000	6.3802	0.0000	0.0000	0.0000	0.0000	-4.9844	0.2858	4.5345	0.0000
NO	0.0000	-4.9833	0.0000	0.0000	-0.2945	-0.5195	-1.2245	0.0000	0.0000	0.0000

	31	32	33	34	35	36	37	38	39	40
FUEL	0.0000	0.0000	0.0000	3.3932	-1.0310	0.4043	0.0000	0.0000	0.0000	0.0000
HC	-1.8753	0.0000	0.0000	0.0000	0.0000	0.0000	0.0000	1.6431	0.0000	0.0000
CO	0.0000	0.0000	0.0000	0.0000	0.0000	0.0000	0.0000	0.0000	-2.0056	0.0000
NO	0.0000	0.0000	1.5421	0.0000	0.0000	1.6617	0.0000	0.0000	0.0000	-0.9809

	41	42	43	44	45	46	47	48	49	50
FUEL	0.0000	-0.1622	-0.6887	0.8444	0.0000	0.0000	0.0000	0.0000	-6.1911	0.4730
HC	0.0000	-0.9777	-3.2009	1.5979	0.0000	0.0000	0.0000	0.0000	0.0000	-0.9242
CO	0.0000	0.0000	0.0000	-0.3132	0.0000	-0.0989	0.0000	0.0000	0.0000	0.0000
NO	0.3017	0.0000	0.0000	-0.4507	0.1881	0.0000	0.0000	0.0000	2.0415	0.0000

	51	52	53	54	55	56
FUEL	0.8554	0.0000	0.0000	-1.8326	0.0000	0.0000
HC	0.0000	0.0000	0.0000	0.8412	0.0000	0.5207
CO	0.0000	0.0000	0.0000	0.0000	0.0000	-0.0168
NO	0.0000	0.0000	0.0000	-0.4735	0.0000	0.0000

Appendix E

REGRESSOR VARIABLES OF THE 40 INDIVIDUAL FUNCTIONS

Any of the functions of fuel or log (emissions) in the various torque/rpm points depends on AF, SA and EGR and can be evaluated by the formula:

$$F = \sum_{i=1}^{35} b_i x_i \qquad \text{(E-1)}$$

where b_i are the regression coefficients given in Appendix F for the various fourth order polynomials, x_i are the regressor variables which are either regular or Legendre polynomials of the independent variables as given below:

$$x_1 = P_0 = 1 \qquad \text{(E-2)}$$

$$x_2 = P_0(\overline{AF}) \qquad \text{(E-3)}$$

$$x_3 = P_1(\overline{SA}) \qquad \text{(E-4)}$$

$$x_4 = P_1(\overline{EGR}) \qquad \text{(E-5)}$$

$$x_5 = P_1(\overline{AF}) \cdot P_1(\overline{SA}) \qquad \text{(E-6)}$$

$$x_6 = P_1(\overline{AF}) \cdot P_1(\overline{EGR}) \qquad \text{(E-7)}$$

$$x_7 = P_1(\overline{SA}) \cdot P_1(\overline{EGR}) \qquad \text{(E-8)}$$

$$x_8 = P_2(\overline{AF}) \qquad \text{(E-9)}$$

$$x_9 = P_2(\overline{SA}) \qquad \text{(E-10)}$$

$$x_{10} = P_2(\overline{EGR}) \qquad \text{(E-11)}$$

$$x_{11} = P_3(\overline{AF}) \qquad \text{(E-12)}$$

$$x_{12} = P_3(\overline{SA}) \tag{E-13}$$

$$x_{13} = P_3(\overline{EGR}) \tag{E-14}$$

$$x_{14} = P_2(\overline{AF}) \cdot P_1(\overline{SA}) \tag{E-15}$$

$$x_{15} = P_2(\overline{AF}) \cdot P_1(\overline{EGR}) \tag{E-16}$$

$$x_{16} = P_2(\overline{SA}) \cdot P_1(\overline{AF}) \tag{E-17}$$

$$x_{17} = P_2(\overline{SA}) \cdot P_1(\overline{EGR}) \tag{E-18}$$

$$x_{18} = P_2(\overline{EGR}) \cdot P_1(\overline{AF}) \tag{E-19}$$

$$x_{19} = P_2(\overline{EGR}) \cdot P_1(\overline{SA}) \tag{E-20}$$

$$x_{20} = P_1(\overline{AF}) \cdot P_1(\overline{SA}) \cdot P_1(\overline{EGR}) \tag{E-21}$$

$$x_{21} = P_4(\overline{AF}) \tag{E-22}$$

$$x_{22} = P_4(\overline{SA}) \tag{E-23}$$

$$x_{23} = P_4(\overline{EGR}) \tag{E-24}$$

$$x_{24} = P_3(AF) \cdot P_1(\overline{SA}) \tag{E-25}$$

$$x_{25} = P_3(\overline{AF}) \cdot P_1(\overline{EGR}) \tag{E-26}$$

$$x_{26} = P_3(SA) \cdot P_1(\overline{AF}) \tag{E-27}$$

$$x_{27} = P_3(SA) \cdot P_1(\overline{EGR}) \tag{E-28}$$

$$x_{28} = P_3(\overline{EGR}) \cdot P_1(\overline{AF}) \tag{E-29}$$

$$x_{29} = P_3(\overline{EGR}) \cdot P_1(\overline{SA}) \tag{E-30}$$

$$x_{30} = P_2(\overline{AF}) \cdot P_2(\overline{SA}) \tag{E-31}$$

$$x_{31} = P_2(\overline{AF}) \cdot P_2(\overline{EGR}) \quad \text{(E-32)}$$

$$x_{32} = P_2(\overline{AF}) \cdot P_1(\overline{SA}) \cdot P_1(EGR) \quad \text{(E-33)}$$

$$x_{33} = P_2(\overline{SA}) \cdot P_2(\overline{EGR}) \quad \text{(E-34)}$$

$$x_{34} = P_2(\overline{SA}) \cdot P_1(\overline{AF}) \cdot P_1(\overline{EGR}) \quad \text{(E-35)}$$

$$x_{35} = P_2(\overline{EGR}) \cdot P_1(\overline{AF}) \cdot P_1(\overline{SA}) \quad \text{(E-36)}$$

where

$$\overline{AF} = AF/15 \quad \text{E-37)}$$

$$\overline{SA} = SA/40 \quad \text{(E-38)}$$

$$\overline{EGR} = EGR/7 \quad \text{(E-39)}$$

and

$$P_1(x) = x \quad \text{(E-40)}$$

$$P_2(x) = x^2 \quad \text{(E-41)}$$

$$P_3(x) = x^3 \quad \text{(E-42)}$$

$$P_4(x) = x^4 \quad \text{(E-43)}$$

for: NO at 1800/250 RPM/lb ft, HC at 2250/50 rpm/ft lb, NO at 2900/72 rpm/lb ft and HC at 750/15 rpm/ft lb.

For the rest of the 35 functions P_1-P_4 are the Legendre Polynomials which are:

$$P_1(x) = x \quad \text{(E-44)}$$

$$P_2(x) = 1.5x^2 - 0.5 \quad \text{(E-45)}$$

$$P_3(x) = 2.5x^3 - 1.5x \quad \text{(E-46)}$$

$$P_4(x) = 4.375x^2 + .375 \quad . \quad \text{(E-47)}$$

Appendix F

REGRESSION COEFFICIENTS OF THE INDIVIDUAL FUNCTIONS

SUMMARY TABLE OF REGRESSION COEFFICIENTS.

TORQUE/RPM		1	2	3	4	5	6	7	8	9	10	11	12
50 1700	F	22.7576	-9.8003	-7.0155	0.4794	0.0000	0.0000	0.0000	0.0000	0.0000	0.0000	0.0000	2.9693
50 1700	HC	9.3397	-9.6367	0.0000	0.0000	5.6573	0.0000	0.0000	0.0000	0.0000	0.0000	0.0000	0.0000
50 1700	CO	37.3947	-40.8967	2.6924	0.0000	0.0000	0.0000	0.0000	0.0000	0.0000	0.0000	5.5417	0.0000
50 1700	NO	-11.7952	18.8727	0.0000	-2.7054	0.0000	0.0000	-1.8597	0.0000	0.0000	1.9511	-2.4657	1.7731
25 1800	F	8.2119	0.0000	1.3948	5.1342	-4.8030	0.0000	-3.2540	0.0000	0.0000	-2.1249	0.0000	0.0000
25 1800	HC	2.9465	-1.9957	0.0000	0.0000	0.0000	0.0000	7.7517	0.0000	0.0000	0.0000	0.0000	0.0000
25 1800	CO	27.8468	-31.3532	3.9037	0.0000	0.0000	0.0000	0.0000	0.0000	0.0000	0.0000	4.5541	0.0000
25 1800	NO	-7.2621	11.0149	0.0000	0.0000	0.0000	0.0000	0.0000	0.0000	0.0000	0.0000	0.0000	0.0000
75 2100	F	33.3898	-14.1013	0.0000	0.0000	-8.3633	0.0000	0.0000	0.0000	0.0000	0.0000	0.0000	1.9760
75 2100	HC	-2.3601	0.0000	12.4241	0.0000	-1.4251	-0.4383	-0.1174	0.0000	0.0000	0.0000	0.0000	0.0000
75 2100	CO	32.5914	-32.4646	0.0000	0.0000	0.0000	0.0000	0.0000	0.0000	0.0000	0.0000	5.5354	0.0000
75 2100	NO	-11.8013	17.0327	1.4481	-0.4389	0.0000	0.0000	0.0000	0.0000	0.0000	0.0000	-1.9934	0.0000
50 2250	F	26.6252	-14.7111	0.0000	0.0000	0.0000	0.0000	0.0000	0.0000	0.0000	0.0000	0.0000	0.0000
50 2250	HC	3.4778	0.0000	0.0000	0.0000	9.1329	0.0000	0.0000	-7.8612	0.0000	0.0000	0.0000	0.0000
50 2250	CO	29.2160	-32.5131	4.6103	0.0000	0.0000	0.0000	0.0000	0.0000	0.0000	0.0000	4.4036	0.0000
50 2250	NO	-11.6101	16.8322	0.0000	-3.0905	0.0000	0.0000	0.0000	0.0000	0.0000	1.6591	-1.5487	0.0000
38 2600	F	33.3408	-12.6247	-14.6044	0.0000	0.0000	1.5886	0.0000	0.0000	4.6311	0.0000	0.0000	0.0000
38 2600	HC	2.1339	0.0000	0.0000	0.0000	0.0000	0.0000	0.0000	0.0000	0.0000	0.0000	0.0000	0.0000
38 2600	CO	22.3169	-24.8241	3.0973	0.0000	0.0000	0.0000	2.0397	0.0000	0.0000	-0.7545	3.8096	0.0000
38 2600	NO	-10.1776	15.7697	0.0000	-1.4026	0.0000	0.0000	0.0000	0.0000	0.0000	0.2726	-2.2591	1.9002
20 1400	F	7.9705	0.0000	-6.5198	3.3401	0.0000	0.0000	0.0000	0.0000	2.8667	-1.5037	0.0000	0.0000
20 1400	HC	0.9724	0.0000	0.0000	0.0000	0.0000	0.0000	10.1921	0.0000	0.0000	0.0000	0.0000	0.0000
20 1400	CO	19.6061	-19.5869	0.0000	0.5805	0.0000	0.6767	0.0000	0.0000	0.0000	-0.5983	2.6796	0.0000
20 1400	NO	1.7545	0.0000	0.0000	-7.2395	0.0000	0.0000	0.0000	0.0000	0.0000	3.5579	0.0000	0.0000
85 2500	F	47.5703	0.0000	0.0000	0.0000	-46.0703	0.0000	0.0000	0.0000	0.0000	3.5076	0.0000	12.1546
85 2500	HC	-2.0538	0.0000	7.4700	0.0000	0.0000	0.0000	0.0000	0.0000	0.0000	0.0000	0.0000	0.9722
85 2500	CO	21.5680	-18.8487	0.0000	0.0000	0.0000	6.9125	0.0000	0.0000	0.0000	0.0000	2.0252	0.0000
85 2500	NO	-8.0632	12.2784	0.0000	0.0000	4.0973	-2.2714	0.0000	0.0000	0.0000	0.0000	0.0000	0.0000
72 2900	F	46.5121	-21.9220	0.0000	0.0000	-7.5864	0.0000	0.0000	0.0000	0.0000	0.0000	0.0000	0.0000
72 2900	HC	-24.3820	29.0921	0.0000	0.0000	0.0000	0.0000	2.2472	0.0000	8.2745	0.0000	0.0000	0.0000
72 2900	CO	17.9426	-19.2061	4.6830	0.8354	0.0000	0.0000	0.0000	0.0000	0.0000	-0.1944	2.4497	0.0000
72 2900	NO	-9.3670	18.9162	0.0000	-1.8490	0.0000	0.0000	0.8320	0.0000	0.0000	0.8564	-5.8728	0.0000
-14 1800	F	5.4284	0.0000	-5.1133	2.3113	0.0000	0.0000	0.0000	0.0000	1.4478	0.0000	0.0000	0.0000
-14 1800	HC	-4.6609	7.3382	2.4602	2.3462	0.0000	0.0000	0.0000	0.0000	0.0000	0.0000	0.0000	0.0000
-14 1800	CO	-2.2001	4.9281	-0.5925	0.1667	0.0000	0.0000	0.0000	0.0000	0.0000	0.0000	0.0000	0.0000
-14 1800	NO	2.2205	-3.6673	-3.0784	-2.0676	0.0000	0.0000	0.0000	0.0000	0.7341	0.9485	0.0000	0.0000
15 750	F	3.7375	0.0000	0.0000	0.0000	0.0000	0.0000	0.0000	0.0000	0.0000	0.0000	0.0000	0.0000
15 750	HC	1.9316	0.0000	1.0032	0.0000	0.0000	0.0000	0.0000	0.0000	0.0000	0.0000	0.0000	0.0000
15 750	CO	19.0531	-20.8827	0.0000	0.0000	0.0000	0.0000	0.0000	0.0000	0.0000	0.0000	0.0000	1.3280
15 750	NO	-14.1088	14.3519	0.0000	0.0000	0.0000	0.0000	0.0000	0.0000	0.0000	0.0000	0.0000	-3.7642

TORQUE/RPM		13	14	15	16	17	18	19	20	21	22	23	24
50 1700	F	0.0000	0.0000	0.0000	0.0000	0.0000	0.0000	0.0000	0.0000	0.7737	0.0000	0.0778	0.0000
50 1700	HC	0.0000	0.0000	0.0000	0.0000	0.0000	-0.3139	0.0000	0.0000	0.1949	0.0000	0.0000	1.3082
50 1700	CO	0.0000	0.0000	0.0000	-1.3125	0.0000	0.0000	0.0000	0.0000	0.0000	0.0000	-0.1441	-0.4110
50 1700	NO	0.0000	0.0000	0.0000	0.0000	0.0000	0.0000	0.0000	0.0000	0.0000	-0.7432	-0.2392	-0.6069
25 1800	F	0.0000	0.0000	0.0000	0.0000	0.0000	0.0000	0.0000	0.0000	0.5030	0.4652	0.0000	0.0000
25 1800	HC	0.7016	0.0000	0.0000	0.0000	0.0000	0.0000	-6.1141	0.0000	0.7497	-0.2087	-0.4538	-1.1593
25 1800	CO	0.0000	0.0000	0.0000	-1.5472	0.0000	0.0000	-0.5684	0.0000	0.0000	0.0000	0.0000	-0.6230
25 1800	NO	0.0000	0.0000	0.9120	0.0000	0.0000	0.0000	0.0000	-5.5132	-2.4941	1.0579	0.0000	0.0000
75 2100	F	0.0000	0.0000	0.0000	0.0000	0.0000	0.0000	0.0000	0.0000	1.0938	0.0000	0.0000	0.4375
75 2100	HC	1.0002	0.0000	0.0000	-3.8964	0.0000	0.0000	0.0000	0.0000	0.0000	0.0000	-0.4665	0.0000
75 2100	CO	0.0000	0.0000	-0.7343	2.0861	-0.2804	0.0000	0.0000	0.0000	0.0000	-0.5362	-0.2487	-3.0513
75 2100	NO	0.0000	0.0000	0.0000	0.0000	0.0000	-0.2565	0.0000	0.0000	0.0000	0.1010	0.0000	-0.3359
50 2250	F	0.0000	-0.7111	1.8384	-2.1560	-0.8363	0.0000	0.0000	0.0000	1.1716	0.7059	0.0000	0.0000
50 2250	HC	0.0000	0.0000	0.0000	0.0000	0.0000	0.0000	0.0000	0.0000	4.9763	0.0000	0.0000	-3.2946
50 2250	CO	0.0000	0.0000	0.0000	-1.6392	0.0000	0.0000	0.0000	0.0000	0.0000	0.0000	0.0000	-0.2611
50 2250	NO	0.0000	0.0000	0.0000	0.0000	0.0000	0.0000	0.0000	0.0000	0.0000	-0.6311	-0.3359	-1.7115
38 2600	F	0.0000	0.0000	0.0000	0.0000	0.0000	0.0000	-0.9000	0.0000	1.7353	0.0000	0.0000	-1.5591
38 2600	HC	-1.1473	0.0000	0.0000	0.0000	5.7168	0.0000	0.0000	0.0000	1.0944	0.0000	0.7534	-1.4839
38 2600	CO	0.0000	0.0000	0.0000	-0.7760	0.0000	0.0000	0.0000	0.0000	0.0000	0.0000	0.2843	-0.5568
38 2600	NO	0.0000	0.0000	0.0000	0.0000	0.0000	0.0000	0.0000	0.0000	0.0000	0.0000	0.0000	0.0000
20 1400	F	0.0000	0.0000	-0.6956	-1.0313	0.0000	0.0000	0.0000	0.0000	0.2451	0.0000	0.0000	0.0000
20 1400	HC	0.0000	0.0000	0.0000	0.0000	-3.7258	0.0000	-5.5703	0.0000	0.8131	0.0000	0.6702	-1.3443
20 1400	CO	0.0000	-0.9755	0.0000	0.0000	-1.1784	0.0000	0.0000	0.0000	0.0000	0.0000	0.0000	0.0000
20 1400	NO	0.0000	0.0000	4.1800	0.0000	0.0000	0.0000	0.0000	0.0000	-0.5464	-0.0720	0.0000	0.0000
85 2500	F	-1.4402	0.0000	0.0000	0.0000	-3.7683	0.0000	0.0000	0.0000	1.8477	-3.4014	0.7077	0.0000
85 2500	HC	0.0000	0.0000	0.0000	0.0000	0.0000	0.0000	0.0000	0.0000	0.0000	0.0000	0.0000	0.0000
85 2500	CO	0.0000	0.0000	0.0000	0.0000	0.0000	0.0000	0.0000	-8.6143	0.0000	0.0514	0.0000	0.0000
85 2500	NO	0.0000	-2.1394	0.0000	0.0000	0.7772	0.0000	0.0000	0.0000	-0.6184	-0.3072	-0.1982	0.0000
72 2900	F	0.0000	0.0000	1.5378	0.0000	0.0000	0.0000	0.0000	0.0000	2.3609	0.9614	0.0000	-0.6320
72 2900	HC	0.0000	0.5157	0.0000	0.0000	0.0000	0.0000	0.0000	0.0000	-4.1874	0.0000	-0.3638	0.0000
72 2900	CO	0.0000	0.0000	0.0000	0.0000	0.0000	0.0000	0.0000	0.0000	0.0000	0.0000	-0.1633	0.0000
72 2900	NO	0.0000	1.1566	0.0000	0.0000	0.0000	0.0000	0.0000	0.0000	0.0000	0.0000	0.0000	0.0000
-14 1800	F	-1.1328	0.0000	0.0000	0.0000	0.0000	0.0000	0.0000	0.0000	0.3906	0.0000	0.5768	-0.5047
-14 1800	HC	-13.8349	0.0000	0.0000	-0.7360	0.0000	0.0000	0.0000	0.0000	0.0000	0.0000	0.0000	-1.1866
-14 1800	CO	-4.2147	0.0000	0.0000	0.0000	0.0000	0.0000	0.0000	0.0000	-0.1563	0.0000	0.0000	-0.3325
-14 1800	NO	0.0000	0.0000	1.1313	0.0000	0.0000	0.0000	0.0000	0.0000	0.0000	0.0000	0.0000	0.4970
15 750	F	0.0000	-4.8187	0.0000	1.2224	0.0000	0.0000	0.0000	0.0000	0.0000	0.0000	0.0000	2.4178
15 750	HC	0.0000	0.0000	0.0000	-0.7095	0.0000	0.0000	0.0000	0.0000	0.0000	0.0000	0.0000	0.0000
15 750	CO	0.0000	0.0000	0.0000	0.0000	0.0000	0.0000	0.0000	0.0000	0.5869	0.0000	0.0000	1.3104
15 750	NO	0.0000	0.0000	0.0000	0.0000	0.0000	0.0000	0.0000	0.0000	-1.5959	-0.3529	0.0000	-1.5744

TORQUE/RPM		25	26	27	28	29	30	31	32	33	34	35
50 1700	F	0.1533	-2.2828	0.0977	-1.2035	1.7636	0.0000	0.0000	0.0000	-2.0447	1.6060	0.0000
50 1700	HC	0.0000	0.0000	0.0000	0.0000	0.0000	-2.5590	0.0000	0.7692	0.0000	0.0000	0.0000
50 1700	CO	0.0751	0.0000	0.0000	0.0000	0.3372	0.0000	0.0000	0.0000	-0.3104	0.4143	-0.2511
50 1700	NO	0.1617	0.0000	0.0000	0.0000	0.0000	0.0000	0.0000	0.0000	0.2944	0.0000	0.0000
25 1800	F	-0.2727	0.0000	0.0000	0.0000	0.0000	0.0000	0.0000	0.0000	0.0000	0.0000	1.4600
25 1800	HC	0.7965	0.0000	0.0000	0.0000	2.4801	0.0000	-1.0686	0.4252	-0.3433	0.0000	0.0000
25 1800	CO	0.2008	0.0000	0.0000	0.0000	0.1779	0.0000	0.0000	0.5072	-0.0766	0.0000	0.0000
25 1800	NO	0.0000	0.0000	0.0000	0.0000	0.0000	0.0000	-0.5162	0.0000	0.0000	0.0000	3.7607
75 2100	F	0.3157	0.0000	0.0719	0.0000	0.0000	0.0000	-0.3287	0.0000	0.0000	-0.7279	0.3453
75 2100	HC	0.0000	0.0000	0.0000	0.0000	-0.6737	0.0000	-0.2068	0.9375	0.0000	0.0000	0.0000
75 2100	CO	0.7756	0.0000	0.0000	0.0000	0.3237	0.0000	0.0000	0.0000	0.0000	0.0000	0.0000
75 2100	NO	0.0000	0.0000	0.0106	0.2653	0.1768	0.0000	0.0000	0.0000	0.0000	0.0000	0.0000
50 2250	F	0.0000	0.0000	0.0000	0.0000	0.2295	0.0000	-0.9623	0.0000	0.0000	0.0000	0.1499
50 2250	HC	0.0000	0.0000	0.0000	0.0000	0.0000	-2.1910	0.0000	0.0000	-0.3270	0.6343	0.0000
50 2250	CO	0.2931	0.0000	0.0000	0.0000	0.0000	0.0000	0.0000	-0.5774	-0.1043	0.2772	0.0000
50 2250	NO	0.0000	1.7954	0.0000	0.0000	0.0000	0.0000	0.0000	0.0000	0.1174	-0.2339	0.0000
38 2600	F	-0.3109	0.0000	0.0000	0.0000	0.0000	0.0000	0.0000	0.5717	0.0000	0.0000	0.0000
38 2600	HC	0.0000	0.2936	-1.6732	0.0000	0.6668	0.0000	0.0000	0.0000	-1.5064	-0.6087	0.0000
38 2600	CO	0.0000	0.0000	0.0000	0.0000	0.0000	0.0000	0.0000	0.2077	0.0000	-0.7654	-0.1255
38 2600	NO	0.0000	-1.1813	0.0000	0.0000	0.0000	0.0000	0.1281	0.0000	0.7589	-1.2321	0.0000
20 1400	F	0.0000	0.0000	0.0000	0.0000	0.0000	0.0000	0.3294	0.0000	-0.1477	0.0540	0.0000
20 1400	HC	0.0000	0.0000	0.0000	0.0000	0.0000	0.7744	0.0000	0.0000	1.9975	0.0000	0.0000
20 1400	CO	0.0000	0.0000	0.0000	0.0000	0.0000	0.0000	0.0000	0.0000	0.0000	1.1321	0.0000
20 1400	NO	0.0000	0.5287	0.0000	0.0000	0.0000	0.0000	-1.8597	-0.7529	0.0000	0.0000	0.0000
85 2500	F	0.0000	0.0000	1.6201	0.0000	0.0000	11.9048	0.0000	0.0000	0.9558	0.0000	-3.1923
85 2500	HC	-1.0886	-2.8210	1.9406	-0.2638	0.4253	0.0000	0.0000	2.1451	-1.8737	0.0000	0.5005
85 2500	CO	0.0000	1.3416	1.6539	0.0000	0.0000	0.0000	-0.8126	0.0000	0.0000	0.0000	0.5431
85 2500	NO	0.1476	0.0000	-0.8579	0.0000	0.0000	0.0000	0.0000	0.0000	-0.2465	0.0000	1.5036
72 2900	F	0.0000	0.0000	0.0000	0.0000	0.0000	0.0000	0.0000	-1.3623	0.0000	0.0000	-0.2033
72 2900	HC	0.0000	-5.4513	4.0413	0.0000	0.0000	0.0000	0.0000	0.0000	0.2923	-5.5417	0.0000
72 2900	CO	0.0000	0.0000	0.5679	0.0000	0.0000	-1.7406	0.0000	-0.2740	0.0000	-0.6539	0.0000
72 2900	NO	0.0000	0.0000	0.0000	0.0000	0.0000	0.0000	0.0000	0.0000	0.0000	0.0000	-0.2186
-14 1800	F	0.0913	0.0000	0.0000	0.0000	1.9067	0.0000	0.0000	0.0000	0.0000	1.0963	-1.9740
-14 1800	HC	0.0000	0.0000	0.0000	10.1786	5.7330	0.0000	-2.5767	3.7435	-1.8785	0.0000	0.0000
-14 1800	CO	0.0000	0.0000	0.0000	2.0084	3.0447	-0.3471	0.0000	0.0000	-1.4248	1.4480	0.0000
-14 1800	NO	0.0000	0.0000	0.0000	0.0000	0.0000	0.0023	-0.6193	0.3864	0.0000	0.0000	0.0000
15 750	F	0.0000	0.0000	0.0000	0.0000	0.0000	0.0000	0.0000	0.0000	0.6510	0.0000	0.0000
15 750	HC	0.0000	0.0000	0.0000	0.0000	0.0000	0.0000	0.0000	0.0000	0.0000	0.0000	0.0000
15 750	CO	0.0000	-2.0281	0.0000	0.0000	0.0000	0.0000	0.0000	0.0000	3.0292	0.0000	0.0000
15 750	NO	0.0000	6.1585	0.0000	0.0000	0.0000	0.0000	0.0000	0.0000	0.0000	0.0000	0.0000

Appendix G

OPTIMIZATION PROGRAM

Figures G.1 - G.4

Fig. G-1

```
      IMPLICIT REAL*8(A-H,O-Z)
C   THE OPT PROGRAM EVALUATES OPTIMAL FUEL CONSUMPTION SUBJECT TO
C   EMMISION CONSTRAINTS(HC,CO,NO) AND CHECKS THAT THE INDEPENDENT
C   VARIABLES-AIR FUEL RATIO(AF),SPARK ADVANCE(SA) AND EXHAUST GAS
C   RECIRCULATION(EGR) ARE IN THE DRIVEABILITY RANGE.
C   TWO METHODS OF SOLUTION ARE AVAILABLE:
C   1. IG=0   OPTIMAL FUEL AND EMISSIONS ARE EVALUATED FOR GIVEN
C      VALUES OF LAGRANGE MULTIPLIERS(LAG MULT).
C   2. IG=1   OPTIMAL FUEL IS EVALUATED FOR A GIVEN EMISSION CONSTRAINTS.
C      THE LAG MULTS ARE ITERATED UNTIL A CONVERGENCE CRITERIA HAS BEEN
C      MET.
C
      DOUBLE PRECISION X(3),EL(3),D(3),Y(10,3),G(3),G1(3),G2(3),
     1DG(6),XX(10,3),B(4,35),X1(3),CU(10),CH(10),
     2C(3),A(70),A1(4),B1(4),C1(4),C2(3),DE(10,4),YY(10,6),RO,A3(6),
     3D1(3),CL(3),S(3),AL(6,3),BL(6),Q(3,3),R(6),U(3),GO(3),
     4GG(3),ELL(3),DD(3),YL(3),YS(10,3),FO(4,4),BB(40,35)
      COMMON/OPT/G,B,A1,C1,NV,NC,I,NC1
      COMMON/PAR/IP
      COMMON/YM/YY,S,CU,CH,FO,IOC
      DIMENSION ISTATE(6),INDEX(6),IOC(4),ITOR(10),IRPM(10)
      LOGICAL CONV,NACTVE
      EXTERNAL FUNGRD,HESS
C
C    THE MEANING OF THE VARIABLES APPEARING IN THE PROGRAM:
C     LL- # OF TERMS IN REGRESSION EQUATION.
C    NP- # OF POINTS OF CONSTANT RPM AND TORQUE.
C    NC1-# OF ACTIVE FUNCTIONS
C    IC- IF 0 THE ENGINE EMISSIONS AND THE OXIDIZING CATALYST(OC)
C         EMISSIONS ARE EVALUATED. OTHERWISE THE THREE WAY CATALYST
C         (TWC) EMISSIONS ARE EVALUATED.
C    NV1- # OF INDEPENDENT VARIABLES.
C    IP-  A FLAG DETERMINING THE AMOUNT OF THE PROGRAM PRINTOUT.
C    IG- AN INDEX SELECTING THE TYPE OF OPTIMIZATION PROGRAM.
C    IPRINT- A PRINTOUT FLAG FOR THE LCMNA SUBROUTINE.
C    NG- # OF TIMES THE LAG MULT IS CHANGED WHILE IN THE IG=0 MODE.
C    IOC- A 4 ELEMENT VECTOR. 1 ACTIVATES THE CORRESPONDING FUNCTION.
C    I.E. IF IOC(1)=1 THE FUEL FUNCTION IS CONSIDERED.
C    SUBSCRIPT 2-HC, 3-CO, 4-NO.
C    XX IS THE INITIAL POINTS MATRIX.
C    D1- THE DESIRED CHANGE IN THE LAG MULT.
C    C- THE VECTOR OF DESIRED EMISSIONS FOR IG=1
C    A3,B1- INCLUDE COEFICIENTS FOR THE CATALYST TYPE.
C    G- THE INITIAL LAG MULT VECTOR.
C    RO- FUEL DENSITY(LB/GALLON)
C    G- VECTOR OF LAG MULT: HC, CO, NO
C
      DATA A3/1.3405D-1,1.3405D-1,1.9530D-1,3.35D-2,2.0D-2,1.567D-1/
      DATA B1/0.0D0,2.0D-1,4.0D0,0.0D0/
      DATA ITOR/50,25,75,50,38,20,85,72,-14,15/,IRPM/1700,1000
     ,,2100,2250,2600,1400,2500,2900,1800,750/
      NNG=0
      DO 10 K=1,3
      DG(K)=0.0D0
      X1(K)=0.0D0
   10 X(K)=0.0D0
      RO=6.3D0
      IC=0
C    INITIALIZE LCMNA PARAMETERS
      ML=6
      NADIM=6
      NGDIM=3
      NACTVE=.FALSE.
      ZTOTOL=1.0D-2
      STEPMX=1.5D0
C  READ LAG MULTS,LCMNA CONVERGENCE CRITEIA,AND SYSTEM INFORMATION.
      READ(5,1010)(G(K),K=1,3),ACZTOL,EPSMCH,ETA
      EPS=DSQRT(EPSMCH)
      READ(5,1020)LL,NP,NC1,IC,NV1,IP,IG,IPRINT,NG,(IOC(L),L=1,4)
      NV=NV1
C READ INITIAL POINT ARRAY AND INITIAL VALUE OF FUNCTION
      READ(5,1030)((XX(I,J),J=1,NV),I=1,NP)
C READ INCREMENT IN LAGRANGE MULTIPLIER AND EMMISION LEVEL
      READ(5,1010) (D1(K),K=1,3),(C(K),K=1,3)
C    NC2- # OF CONSTRAINTS
C     A1 TERMS ARE:
C            1- A MULTIPLIER OF THE FUEL FUNCTION WHICH IS A
C               FUNCTION OF CU AND CH(EPA URBAN AND EPA CYCLE)
C            2:4 -MULTIPLIERS OF EMISSION FUNCTIONS(A3 TERMS)
C                 WHICH REFLECT CATALYST TYPE TO BE USED.
C     C1 TERMS ARE:
C            1- 1.
C            2:4 -LAG MULT. OF HC, CO, NO
```

```
      NC2-NC1-1
      N-NV
      C1(1)-1.0D0
      DO 20 K-2,NC1
      L-K-1
      A1(K)-A3(L)
      C1(K)-O(L)
   20 CONTINUE
      J1-1
      IJ-0
C     READ POLYNOMIAL  COEFFICIENTS
      DO 30 L -1,40
      READ(5,1040)(DD(L,K),K-1,35)
   30 CONTINUE
   40 KK-0
   50 DO 70 K-1,6
      IF(K.GT.3) GOTO 60
      O1(K)-O(K)
      DC(K)-0.0D0
      GOTO 70
   60 DO(K)-DC(K-3)
C   PRINT THE INITIAL VALUES'
   70 CONTINUE
      IF(IP.LT.2) GOTO 80
      WRITE(6,1030)(G(K),K-1,3)
      WRITE(6,1020)LL2,NP,NC1,NC,IC,NV,IP,IO
      WRITE(6,1030)((XX(I,J),J-1,NV),I-1,NP)
      WRITE(6,1030) CU(1),A1(1),A1(2),(C1(I),I-1,4)
      WRITE(6,1030) D1(1),C(1)
C
C     START THE MAIN ITERATIVE LOOP:
C EVALUATE THE MINIMUM OF THE N SEPARATE ADJOINT FUNCTIONS
C     THE EXPRESSION TO BE MINIMIZED IS:
C     SUM(A1(k)*C1(k)*F(k))  k=1,4
C     k=1    FUEL
C     k=2    HC
C     k=3    CO
C     k=4    NO
C     THE TERMS TO BE CNSIDERED ARE THOSE WITH IOC(K)=1.
C
   80 F2=0.0D0
      DO 240 I=1,NP
C     INITIALIZE CONSTRAINT EQUATION
      DO 90 K=1,6
      DO 90 M=1,3
   90 AL(K,M)=0.0D0
      DO 100 K=1,6
      J=K
      IF(K.GT.3) J-K-3
      AL(K,J)=1.0D0
      ISTATE(K)=1
      IF(K.GT.3) ISTATE(K)=-1
  100 CONTINUE
      BL(1)=YY(I,1)/S(1)
      BL(2)=YY(I,3)/S(2)
      BL(3)=YY(I,5)/S(3)
      BL(4)=YY(I,2)/S(1)
      BL(5)=YY(I,4)/S(2)
      BL(6)=YY(I,6)/S(3)
      IF(I.NE.10) GOTO 110
      N=2
      NV=2
  110 CUI=CU(I)
      IF(CU(I).EQ.0.0D0) CUI=1.0D0
      A1(1)=(7.68D-2*CU(I)+4.573D-2*CH(I))/(RO*CUI)
C  FILL THE POLYNOMIAL COEFFICIENTS INTO THE B MATRIX WHICH IS 4*35
C ELEMENTS. EACH LINE CONTAINS COEFICIENTS OF ANOTHER FUNCTION
C IN THE FOLLOWING ORDER:FUEL,HC,CO,NO.
      DO 130 L=1,NC1
      DO 120 K=1,LL
      IK=4*(I-1)+L
      B(L,K)=DB(IK,K)
  120 CONTINUE
  130 CONTINUE
      IF(IP.LT.2) GOTO 140
      WRITE(6,1050)((B(M1,N1),N1=1,LL),M1=1,NC1)
C     LOAD THE INITIAL GUESS OF POINT I INTO X.
  140 DO 150 K=1,NV
  150 X(K)=XX(I,K)
C  BYPASS LCMNA FOR 2250/50.
      IF(I.EQ.4) GOTO 160
C EVALUATE THE MINIMUM OF THE UNCONSTRAINT ADJOINT FUNCTION
      CALL LCMNA(N,ML,NADIM,AL,BL,ISTATE,NACTVE,FUNGRD,M-59,ZTOTOL,
```

```
     1ACZTOL,EPSMCH,EPS,STEPMX,ETA,IPRINT,NODIM,X,FMIN,G,INDEX,
     2R,U,EL,D,CO,CGD,ELL,DD,Q,YL,NUMF,NUMG,ITNUM,CONV)
      GOTO 170
C LOAD OPTIMAL VALUES OF 2250/50.
  160 X(1)=1.1072422600
      X(2)=1.0436180D0
      X(3)=0.0D0
  170 L=1
      DO 180 K=1,NV
  180 X1(K)=X(K)
      IF(I.EQ.10) X1(3)=0.0D0
      IF(I.EQ.4) GOTO 200
C EVALUATE THE EMMISION LEVEL
      DO 190 K=2,NC1
      CALL FUN(B,X1,IO,I,K,F1)
      DE(I,K)=DEXP(F1)
      DO(KK+K-1)=DO(KK+K-1)+DE(I,K)*CU(I)
      WRITE(6,1060) I,K,DE(I,K)
  190 CONTINUE
C EVALUATE THE FUEL CONSUMPTION
  200 IF(I.NE.4) GOTO 210
      F1=1.09937D1
      GOTO 220
  210 CALL FUN(B,X1,IO,I,1,F1)
  220 WRITE(6,1070) I,F1
      DE(I,1)=F1
      F2=F2+F1*A1(1)*CUI
      DO 230 K=1,NV
  230 Y(I,K)=X1(K)
  240 CONTINUE
C   ASSIGN ZERO VALUES FOR EMISSIONS AND THE UNCONSTRAINED FUEL
C   SOLUTION FOR 2250/50.
      DE(4,1)=1.09937D1
      DE(4,2)=0.0D0
      DE(4,3)=0.0D0
      DE(4,4)=0.0D0
      NV=NV1
      N=NV1
      IF(NC1.EQ.1) GOTO 260
C EVALUATE DEVIATION OF EMMISIONS FROM CONSTRAINT LEVELS
      DO 250 K=2,NC1
      CL(K-1)=DO(KK+K-1)*A1(K)/1.0D3+B1(K)
  250 CONTINUE
C   CONVERT FUEL TO MPO
  260 F2=3.6D3/F2
C   EVALUATE OC EMISSIONS.
      C11=.25D0*CL(1)+.15D0
      C12=.15D0*CL(2)+3.4D0
      C13=.8D0*CL(3)
      WRITE(6,1080) F2,(CL(KK+K-1),K=2,NC1),C11,C12,C13
      IF(IC.EQ.0) GOTO 270
C   EVALUATE TWC EMISSIONS.
      C11=1.7D-1*CL(1)+1.68D-1
      C12=1.0D-1*CL(2)+3.6D0
      C13=3.0D-1*CL(3)
      WRITE(6,1090) C11,C12,C13
  270 WRITE(6,1100) (C1(L),L=2,4)
      WRITE(22,1110) F2,(CL(K),K=1,3),(C1(K),K=1,4)
      WRITE(6,1120)
C   LOAD THE OPTIMAL SOLUTION OF THE INDEPENDENT VARIABLES INTO Y.
      Y(10,3)=0.0D0
      DO 280 I=1,NP
      DO 280 J=1,3
  280 YS(I,J)=Y(I,J)*S(J)
      DO 290 I=1,NP
      WRITE(6,1130)ITOR(I),IRPM(I),(YS(I,J),J=1,NV),(DE(I,K),K=1,4)
      WRITE(23,1140) (YS(I,J),J=1,NV),(DE(I,K),K=1,4)
  290 CONTINUE
      IF(IO.EQ.0) GOTO 350
C   FOR THE SECOND ALGORITHM EVALUATE DEVIATON OF EMISSIONS FROM
C   THE DESIRED CONSTRAINTS.
      DO 300 K=2,NC2
  300 DO(KK+K-1)=CL(K-1)-C(K-1)
C CHECK DEVIATION OF EMISSION FROM CONSTRAINT
      IF(DABS(DO(1)).LE.1.0D-4.AND.DABS(DO(2)).LE.1.0D-4.AND.
     1DABS(DO(3)).LE.1.0D-4) STOP
      KK=KK+3
      IF(KK.EQ.6) KK=0
      J1=J1+1
      IF(J1.GT.12) STOP
      IJ=IJ+1
      IF(IO.EQ.1) GOTO 320
      IF(IJ.NE.2) GOTO 320
```

```
      IJ=0
C UPDATE LAGRANGE MULTIPLIERS  BY LINEAR INTRPOLATION.
      DO 310 I=1,NC2
      Q(I)=C1(I)-(C2(I)-C1(I))/(DQ(3+I)-DQ(I))*DQ(I)
  310 CONTINUE
      GOTO 50
C  CHANGE LAG MULTS SLIGHTLY TO CHECK EMISSION LEVEL SENSITIVITY
C  AND RETURN TO THE MAIN LOOP.
  320 DO 330 I1=1,NC2
      C2(I1)=C1(I1)+D1(I1)
  330 CONTINUE
      DO 340 K=1,NC2
  340 C(K)=C2(K)
      GOTO 80
  350 DO 360 K=2,4
  360 C1(K)=C1(K)+D1(K-1)
      NNG=NNG+1
      IF(NNG.EQ.NG) STOP
C   THE INITIAL GUESS FOR THE NEXT LAG MULT IS THE CURRENT SOLUTION.
      DO 370 I=1,NP
      DO 370 K=1,NV
      XX(I,K)=Y(I,K)
  370 CONTINUE
      GOTO 40
 1010 FORMAT(6D10.4)
 1020 FORMAT(16I5)
 1030 FORMAT(3D10.4)
 1040 FORMAT(5D10.4)
 1050 FORMAT(1X,10D12.4)
 1060 FORMAT(1H0,'EMISSION MASS FLOW AT POINT #',I3,'OF EMISSION #',I3
     ,,'=',D10.4,'  (MG/SEC)')
 1070 FORMAT(1H0,'FUEL CONSUMPTION OF POINT #',I3,F10.4,'  (LB/HR)')
 1080 FORMAT(//,1X,'FUEL(MPG)=',F15.4,//,23X,'HC(G/M)',7X,'CO(G/M)'
     *,8X,'NO(G/M)',/1X,'ENGINE EMMISIONS',2X,3F15.4,/,
     *1X,'TAIL PIPE WITH OC',1X,3F15.4)
 1090 FORMAT(1X,'TAIL PIPE EMISSIONS WITH THC',3F15.4)
 1100 FORMAT(10X,'LAG HC',10X,'LAG CO',8X,'LAG NO',/,1X,3F15.4)
 1110 FORMAT(8F15.4)
 1120 FORMAT(//,31H THE INDEPENDENT VARIABLES ARE,//,1X,'TORQUE',
     *3X,'RPM',8X,'A/F',10X,6HSPKADV,10X,3HEGR,7X,'FUEL(LB/HR)',
     *6X,'HC(G/SEC)',6X,'CO(G/SEC)',6X,'NO(G/SEC)')
 1130 FORMAT(I4,4X,I4,7F15.3)
 1140 FORMAT(7F15.4)
      END
      SUBROUTINE FUNGRD(N,X,IFLAG,F,GR)
C     THIS SUBROUTINE EVALUATES THE FUNCTION AND GRADIENTS OF THE ADJOINT
C     FUNCTION FOR THE LCMNA SUBROUTINE.
C     N- # OF INDEPENDENT VARIABLES.
C     X- VECTOR OF INDEPENDENT VARIABLES.
C     IFLAG- 1 ONLY THE FUNCTION IS EVALUATED.
C            2 ONLY GRADIENT IS EVALUATED.
C            3 BOTH FUNCTION AND GRADIENT ARE EVALUATED.
C     F- RETURNED VALUE OF FUNCTION.
C     GR- RETURNED VALUE OF GRADIENT.
C     THE ADJOINT FUNCTION HAS THE FOLLOWING FORM:
C     SUM(A1(i)*C1(i)*FUN) WHERE
C     FUN IS EITHER THE FUEL FUNCTION OR EMISSION DEPENDING ON THE
C     APPROPRIATE TERM IN IOC.
C
      DOUBLE PRECISION X(N),GR(N),F,C(3),B(4,35),Z(3),F1,
     ,A1(4),C1(4),YY(10,6),S(3),CU(10),CH(10),F3,GR1,FO(4,4)
      COMMON/OPT/Q,B,A1,C1,NV,NC,I,NC1
      COMMON/PAR/IP
      COMMON/YM/YY,S,CU,CH,FO,IOC
      DIMENSION IOC(4)
      DO 10 K=1,3
   10 Z(K)=0.0D0
      WRITE(6,1010)(X(J),J=1,3)
      WRITE(6,1020) IFLAG,I
      DO 20 K=1,NV
      Z(K)=X(K)
   20 CONTINUE
      IF(IFLAG.EQ.2) GOTO 60
C   EVALUTE FUNCTION.
C   THE FUNCTION IS THE POLYNOMIAL FOR FUEL AND ITS EXPONENTIAL
C   FOR EMISSIONS MULTIPLIED BY A1*C1.
C
      F=0.0D0
      DO 40 K=1,NC1
      IF(IOC(K).EQ.0) GOTO 40
      IF(IP.LT.2) GOTO 30
      WRITE(6,1010)(Z(I1),I1=1,3)
   30 CALL FUN(B,Z,10,I,K,F1)
```

G-1 Continued

```
        CALL EX(F1,K,F3)
        FG(K,1)=F3
        FG(1,1)=1.0D0
        F=F+F3*A1(K)*C1(K)
        IF(IP.LT.2) GOTO 40
        WRITE(6,1030) F,A1(K),C1(K),K
   40 CONTINUE
        F=F*CU(I)
        IF(IP.LT.2) GOTO 50
        WRITE(6,1040) F
   50 IF(IFLAG.EQ.1) RETURN
C     THE GRADIENT OF EMISSIONS WHERE THEIR VALUE IS GIVEN BY
C        F=EXP(P) IS
C      GRAD=F*GRAD(P).
C      DF/DX
   60 J=1
   70 IF(N.EQ.1) RETURN
        GR(J)=0.0D0
        DO 80 K=1,NC1
        IF(IOC(K).EQ.0) GOTO 80
        CALL FUN(B,Z,1,I,K,GR1)
        FG(K,2)=GR1
        F3=FG(K,1)*GR1
        FG(1,2)=0.0D0
        GR(J)=GR(J)+F3*A1(K)*C1(K)
        IF(IP.LT.2) GOTO 80
        WRITE(6,1050) GR1,FG(K,1),A1(K),C1(K)
   80 CONTINUE
        GR(J)=GR(J)*CU(I)
        IF(IP.LT.2) GOTO 90
        WRITE(6,1060) GR(J),J
   90 J=J+1
C      DF/DY
        GR(J)=0.0D0
        DO 100 K=1,NC1
        IF(IOC(K).EQ.0) GOTO 100
        CALL FUN(B,Z,2,I,K,GR1)
        FG(K,3)=GR1
        F3=FG(K,1)*GR1
        FG(1,3)=0.0D0
        GR(J)=GR(J)+F3*A1(K)*C1(K)
        IF(IP.LT.2) GOTO 100
        WRITE(6,1050) GR1,FG(K,1),A1(K),C1(K)
  100 CONTINUE
        GR(J)=GR(J)*CU(I)
        IF(IP.LT.2) GOTO 110
        WRITE(6,1070) GR(J),J
  110 J=J+1
        IF(N.EQ.2) RETURN
C      DF/DZ
        GR(J)=0.0D0
        DO 120 K=1,NC1
        IF(IOC(K).EQ.0) GOTO 120
        CALL FUN(B,Z,3,I,K,GR1)
        FG(K,4)=GR1
        F3=FG(K,1)*GR1
        FG(1,4)=0.0D0
        GR(J)=GR(J)+F3*A1(K)*C1(K)
        IF(IP.LT.2) GOTO 120
        WRITE(6,1050) GR1,FG(K,1),A1(K),C1(K)
  120 CONTINUE
        GR(J)=GR(J)*CU(I)
        IF(IP.LT.2) GOTO 130
        WRITE(6,1080) GR(J),J
  130 RETURN
 1010 FORMAT(1X,10D12.4)
 1020 FORMAT(1X,8I10)
 1030 FORMAT(1X,3H F=,D15.4,6HA1(K)=,D15.4,6HC1(K)=,D15.4,3HK=,I10)
 1040 FORMAT(1X,3H F=,D15.4)
 1050 FORMAT(1X,'GR1=',D15.5,'FG(K,1)=',D15.5,'A1(K)=',D15.5,
     1'C1(K)=',D15.5)
 1060 FORMAT(1X,8H GR1(J)=,D15.4,2HJ=,I10)
 1070 FORMAT(1X,8H GR2(J)=,D15.4,2HJ=,I10)
 1080 FORMAT(1X,8H GR3(J)=,D15.4,2HJ=,I10)
        END
        SUBROUTINE HESS(N,X,EL,D)
C      THIS SUBROUTINE EVALUATES THE HESSIAN MATRIX FOR LC(?)A.
C      EL CONTAINS THE DIAGONAL TERMS: D2F/DX2,D2F/DY2,D2F/DZ2.
C      D CONTAINS THE OFF DIAGONAL TERMS: D2F/DXDY,D2F/DXDZ,D2F/DYDZ.
C      THE SECOND DERIVATIVE OF THE FUNCTION GIVEN BY:
C       F=EXP(P(X1,X2,X3)  IS:
C      D2F/DX1DX2=F*(DF/DX1*DF/DX2+D2F/DX1DX2)
        EXTERNAL FUNGRD
```

G-1 Continued

```
      DOUBLE PRECISION C(3),X(N),D(N),EL(3),B(4,35)
     ..Z(3),A1(4),C1(4),YY(10,6),S(3),CU(10),CH(10),D3,F3,EL1,FC(4,4)
      COMMON/OPT/C,D,A1,C1,NV,NC,I,NC1
      COMMON/PAR/IP
      COMMON/YM/YY,S,CU,CH,FO,IOC
      DIMENSION IOC(4)
      DO 10 K=1,NV
   10 Z(K)=0.0D0
      DO 20 K=1,NV
      Z(K)=X(K)
   20 CONTINUE
      IF(IP.LT.2) GOTO 30
      WRITE(6,1010) (Z(K),K=1,NV)
   30 J=1
C     D2F/DX2
      D(J)=0.0D0
      DO 40 K=1,NC1
      IF(IOC(K).EQ.0) GOTO 40
      CALL FUN(B,Z,4,I,K,D3)
      F3=FC(K,1)*(FC(K,2)**2+D3)
      D(J)=D(J)+F3*A1(K)*C1(K)
      IF(IP.LT.2) GOTO 40
      WRITE(6,1020) D3,F3,D(J),K,J
   40 CONTINUE
      D(J)=D(J)*CU(I)
      J=J+1
      IF(NV.EQ.1) RETURN
C     D2F/DY2
      D(J)=0.0D0
      DO 50 K=1,NC1
      IF(IOC(K).EQ.0) GOTO 50
      CALL FUN(B,Z,5,I,K,D3)
      F3=FO(K,1)*(FO(K,3)**2+D3)
      D(J)=D(J)+F3*A1(K)*C1(K)
      IF(IP.LT.2) GOTO 50
      WRITE(6,1040) D3,F3,D(J),K,J
   50 CONTINUE
      D(J)=D(J)*CU(I)
      IF(IP.LT.2) GOTO 60
      WRITE(6,1030)(D(L),L=1,NV)
   60 J=J+1
      IF(NV.EQ.2) GOTO 80
C     D2F/DZ2
      D(J)=0.0D0
      DO 70 K=1,NC1
      IF(IOC(K).EQ.0) GOTO 70
      CALL FUN(B,Z,6,I,K,D3)
      F3=FO(K,1)*(FC(K,4)**2+D3)
      D(J)=D(J)+F3*A1(K)*C1(K)
      IF(IP.LT.2) GOTO 70
      WRITE(6,1020) D3,F3,D(J),K,J
   70 CONTINUE
      D(J)=D(J)*CU(I)
   80 J=1
      IF(NV.EQ.1) RETURN
C    D2F/DXDY
      EL(J)=0.0D0
      DO 90 K=1,NC1
      IF(IOC(K).EQ.0) GOTO 90
      CALL FUN(B,Z,7,I,K,EL1)
      F3=FO(K,1)*(FC(K,2)*FC(K,3)+EL1)
      EL(J)=EL(J)+F3*A1(K)*C1(K)
      IF(IP.LT.2) GOTO 90
      WRITE(6,1040) EL1,F3,EL(J),K,J
   90 CONTINUE
      EL(J)=EL(J)*CU(I)
      J=J+1
      IF(NV.LT.3) GOTO 120
C    D2F/DXDZ
      EL(J)=0.0D0
      DO 100 K=1,NC1
      IF(IOC(K).EQ.0) GOTO 100
      CALL FUN(B,Z,8,I,K,EL1)
      F3=FO(K,1)*(FC(K,2)*FO(K,4)+EL1)
      EL(J)=EL(J)+F3*A1(K)*C1(K)
      IF(IP.LT.2) GOTO 100
      WRITE(6,1040) EL1,F3,EL(J),K,J
  100 CONTINUE
      EL(J)=EL(J)*CU(I)
      J=J+1
C   D2F/DYDZ
      EL(J)=0.0D0
      DO 110 K=1,NC1
```

```
          IF(IOC(K).EQ.0) GOTO 110
          CALL FUN(B,Z,9,I,K,EL1)
          F3=FC(K,1)*(FO(K,3)*FO(K,4)+EL1)
          EL(J)=EL(J)+F3*A1(K)*C1(K)
          IF(IP.LT.2) GOTO 110
          WRITE(6,1040) EL1,F3,EL(J),K,J
      110 CONTINUE
          EL(J)=EL(J)*CU(I)
          J=J+1
      120 J1=J-1
          IF(IP.LT.2) RETURN
          WRITE(6,1050) J,(EL(K),K=1,J1)
          RETURN
     1010 FORMAT(1X,13HZ OF HESS ARE,3D10.4)
     1020 FORMAT(/,1X,'D3=',F15.4,'  F3=',D15.4,'  D(J)=',F15.4,'  K=',I3
         ,,'  J=',I3)
     1030 FORMAT(1X,6H D(L)=,3D15.4)
     1040 FORMAT(/,1X,'EL1=',F15.4,'  F3=',F15.4,'  EL(J)=',F15.4,'  K=',
         ,I5,'  J=',I5)
     1050 FORMAT(1X,14H EL TERMS ARE=,I5,3D15.4)
          END
          SUBROUTINE FUN(B,Z,IK,I,K,F1)
C        THIS SUBROUTINE RETURNS THE VALUE OF EITHER THE FUNCTION OR THE
C        GRADIENT OR THE HESSIAN TERM FOR A SINGLE FUNCTION- FUEL OR ANY
C        EMISSION.
C        B- INCLUDES POLYNOMIAL COEFFICIENTS FOR SET POINT I.
C        K- INDICATES WHICH TYPE OF FUNCTION IS DESIRED
C           1-FUEL, 2-HC, 3-CO, 4-NO.
C        Z- VECTOR OF THE INDEPENDENT VARIABLES.
C        IK- SELECTS THE DESIRED EXPRESSION:
C             1- DF/DX
C             2- DF/DY
C             3- DF/DZ
C             4- D2F/DX2
C             5- D2F/DY2
C             6- D2F/DZ2
C             7- D2F/DXDY
C             8- D2F/DXDZ
C             9- D2F?DYDZ
C            10- F
C             F1- THE RETURNED VALUE.
          DOUBLE PRECISION B(4,35),Z(3),F1,Z1,Z12,Z13,Z14,Z2,Z22,Z23,Z24,
         ,Z3,Z32,Z33,Z34
          COMMON/PAR/IP
C       SELECT BETWEEN A REGULAR(J=1) AND LAGRANGE(J=2) POLYNOMIAL
        5 J=1
          IF(I.EQ.2.AND.K.EQ.4) J=2
          IF(I.EQ.4.AND.K.EQ.2) J=2
          IF(I.EQ.8.AND.K.EQ.2) J=2
          IF(I.EQ.8.AND.K.EQ.4) J=2
          IF(I.EQ.10.AND.K.EQ.2) J=2
          IF(IK.NE.10) GOTO 30
          Z1=Z(1)
          Z2=Z(2)
          Z3=Z(3)
          IF(J.EQ.2) GOTO 10
          Z12=1.5D0*Z(1)**2-.5D0
          Z13=2.5D0*Z(1)**3-1.5D0*Z(1)
          Z14=4.375*Z(1)**4-3.75D0*Z(1)**2+.375D0
          Z22=1.5D0*Z(2)**2-.5D0
          Z23=2.5D0*Z(2)**3-1.5D0*Z(2)
          Z24=4.375*Z(2)**4-3.75D0*Z(2)**2+.375D0
          Z32=1.5D0*Z(3)**2-.5D0
          Z33=2.5D0*Z(3)**3-1.5D0*Z(3)
          Z34=4.375*Z(3)**4-3.75D0*Z(3)**2+.375D0
          GOTO 20
       10 Z12=Z1**2
          Z13=Z1**3
          Z14=Z1**4
          Z22=Z2**2
          Z23=Z2**3
          Z24=Z2**4
          Z32=Z3**2
          Z33=Z3**3
          Z34=Z3**4
          IF(IP.LT.3) GOTO 4
          WRITE(6,300)(Z(II),II=1,3)
        4 IF(IP.LT.2) GOTO 20
          WRITE(6,320) K
       20 F1=B(K,1)+B(K,2)*Z1+B(K,3)*Z2+B(K,4)*Z3+B(K,5)*Z1*Z2+
         ,B(K,6)*Z1*Z3+B(K,7)*Z2*Z3+B(K,8)*Z12+B(K,9)*Z22+B(K,10)*Z32
         ,+B(K,11)*Z13+B(K,12)*Z23+B(K,13)*Z33+B(K,14)*Z12*Z2+
         ,B(K,15)*Z12*Z3+B(K,16)*Z22*Z1+B(K,17)*Z22*Z3+B(K,18)*Z32*Z1+
```

```
     .B(K,19)*Z32*Z2+B(K,20)*Z1*Z2*Z3+B(K,21)*Z14+B(K,22)*Z24+
     .B(K,23)*Z34+B(K,24)*Z13*Z2+B(K,25)*Z13*Z3+B(K,26)*Z23*Z1+
     .B(K,27)*Z23*Z3+B(K,28)*Z33*Z1+B(K,29)*Z33*Z2+B(K,30)*Z12*Z22+
     .B(K,31)*Z12*Z32+B(K,32)*Z12*Z2*Z3+B(K,33)*Z22*Z32+
     .B(K,34)*Z22*Z1*Z3+B(K,35)*Z32*Z1*Z2
      IF(IP.LT.3) RETURN
      WRITE(6,330) F1
      RETURN
   30 IF(J.EQ.2) GOTO 40
      GOTO(50,60,70,80,90,100,110,120,130) IK
   40 GOTO(140,150,160,170,180,190,200,210,220) IK
C     SELECT THE LAGRANGE EXPRESSION
C     DF/DX
   50 F1=(B(K,2)+3.0D0*Z(1)*(B(K,8)+B(K,14)*Z(2)+B(K,15)*
     AZ(3)+B(K,30)*(1.5D0*Z(2)**2-0.5)+B(K,31)*(1.5D0*Z(3)**2-0.5D0
     B)+B(K,32)*Z(2)*Z(3))+Z(2)*(B(K,5)+B(K,20)*Z(3)+B(K,24)*(7.5D0
     C*Z(1)**2-1.5D0)+B(K,35)*(1.5D0*Z(3)**2-.5D0))+
     DZ(3)*(B(K,6)+B(K,25)*(7.5D0*Z(1)**2-1.5D0)+B(K,34)*(1.5D0*
     EZ(2)**2-.5D0))+B(K,11)*(7.5D0*Z(1)**2-1.5)+B(K,16)*(1.5D0*Z(2)
     F**2-.5D0)+B(K,18)*(1.5*Z(3)**2-.5)+B(K,21)*(1.75D1*Z(1)**3-
     G7.5D0*Z(1))+B(K,26)*(2.5*Z(2)**3-1.5D0*Z(2))+B(K,28)*
     H(2.5D0*Z(3)**3-1.5*Z(3)))
      RETURN
C     DF/DY
   60 F1=(B(K,3)+3.0D0*Z(2)*(B(K,9)+B(K,16)*Z(1)+B(K,17)*Z(3)
     A+B(K,30)*(1.5D0*Z(1)**2-.5D0)+B(K,33)*(1.5D0*Z(3)**2-0.5D0)+
     BB(K,34)*Z(1)*Z(3))+Z(1)*(B(K,5)+B(K,26)*(7.5*Z(2)**2-1.5D0)+
     CB(K,35)*(1.5D0*Z(3)**2-.5D0))+Z(3)*(B(K,7)+B(K,20)*Z(1)+
     DB(K,27)*(7.5D0*Z(2)**2-1.5D0)+(1.5D0*Z(1)**2-.5D0)*B(K,32))+
     EB(K,12)*(7.5D0*Z(2)**2-1.5D0)+B(K,14)*(1.5D0*Z(1)**2-.5D0)+
     FB(K,19)*(1.5*Z(3)**2-.5D0)+B(K,22)*(1.75D1*Z(2)**3-7.5D0*Z(2))+
     GB(K,24)*(2.5D0*Z(1)**3-1.5D0*Z(1))+B(K,29)*(2.5D0*Z(3)**3-1.5D0
     H*Z(3)))
      RETURN
C     DF/DZ
   70 F1=(B(K,4)+3.0D0*Z(3)*(B(K,10)+B(K,18)*Z(1)+B(K,19)*Z(2)
     A+B(K,31)*(1.5D0*Z(1)**2-.5D0)+B(K,33)*(1.5D0*Z(2)**2-.5D0))+
     BZ(1)*(B(K,6)+B(K,20)*Z(2)+B(K,28)*(7.5D0*Z(3)**2-1.5D0)+
     .B(K,34)*(1.5D0*Z(2)**2-.5D0)+3.0D0*B(K,35)*Z(2)*Z(3))
     C+Z(2)*(B(K,7)+B(K,29)*(7.5D0*Z(3)**2-1.5D0)+
     DB(K,32)*(1.5*Z(1)**2-.5D0))+B(K,13)*(7.5*Z(3)**2-1.5)+
     EB(K,15)*(1.5*Z(1)**2-.5)+B(K,17)*(1.5D0*Z(2)**2-.5D0)+
     FB(K,23)*(1.75D1*Z(3)**3-7.5D0*Z(3))+B(K,25)*(2.5D0*Z(1)**3-1.5D0
     G*Z(1))+B(K,27)*(2.5D0*Z(2)**3-1.5D0*Z(2)))
      RETURN
C     D2F/DX2
   80 F1=(15.0D0*Z(1)*(B(K,11)+3.5D0*B(K,21)*Z(1)+B(K,24)
     .*Z(2)+B(K,25)*Z(3))+3.0D0*Z(2)*(B(K,14)+1.5D0*B(K,30)*Z(2)+
     .B(K,32)*Z(3))+3.0D0*Z(3)*(B(K,15)+1.5D0*B(K,31)*Z(3))+
     .1.5D0*(2.0D0*B(K,8)-5.0D0*B(K,21)-B(K,30)-B(K,31)))
      RETURN
C     D2F/DY2
   90 F1=(15.0D0*Z(2)*(B(K,12)+3.5D0*B(K,22)*Z(2)+B(K,26)
     .*Z(1)+B(K,27)*Z(3))+3.0D0*Z(3)*(B(K,17)+1.5D0*B(K,33)*Z(3)+
     .B(K,34)*Z(1))+3.0D0*Z(1)*(B(K,16)+1.5D0*B(K,30)*Z(1))+
     .1.5D0*(2.0D0*B(K,9)-5.0D0*B(K,22)-B(K,30)-B(K,33)))
      RETURN
C     D2F/DZ2
  100 F1=(15.0D0*Z(3)*(B(K,13)+3.5D0*B(K,23)*Z(3)+B(K,28)*
     .Z(1)+B(K,29)*Z(2))+3.0D0*Z(1)*(B(K,18)+1.5D0*B(K,31)*Z(1)+
     .B(K,35)*Z(2))+3.0D0*Z(2)*(B(K,19)+1.5D0*B(K,33)*Z(2))+
     .1.5D0*(2.0D0*B(K,10)-5.0*B(K,23)-B(K,31)-B(K,33)))
      RETURN
C     D2F/DXDY
  110 F1=(3.0D0*Z(1)*(B(K,14)+2.5D0*B(K,24)*Z(1)+
     .3.0D0*B(K,30)*Z(2)+B(K,32)*Z(3))+3.0D0*Z(2)*(B(K,16)+
     .2.5D0*B(K,26)*Z(2)+B(K,34)*Z(3))+Z(3)*(B(K,20)+1.5D0*B(K,35)*Z(3))
     .+(B(K,5)-1.5D0*B(K,24)-1.5D0*B(K,26)-.5D0*B(K,35)))
      RETURN
C     D2F/DXDZ
  120 F1=(3.0D0*Z(1)*(B(K,15)+2.5D0*B(K,25)*Z(1)+3.0D0*
     .B(K,31)*Z(3)+B(K,32)*Z(2))+Z(2)*(B(K,20)+1.5D0*B(K,34)*Z(2)
     .+3.0D0*B(K,35)*Z(3))+3.0D0*Z(3)*(B(K,18)+2.5D0*B(K,28)*Z(3))+
     .(B(K,6)-1.5D0*B(K,25)-1.5D0*B(K,28)-.5*B(K,34)))
      RETURN
C     D2F/DYDZ
  130 F1=(Z(1)*(B(K,20)+1.5D0*B(K,32)*Z(1)+3.0D0*B(K,34)*Z(2)
     .+3.0D0*B(K,35)*Z(3))+3.0D0*Z(2)*(B(K,17)+2.5D0*B(K,27)*Z(2)+3.0D0
     . *B(K,33)*Z(3))+3.0D0*Z(3)*(2.5D0*B(K,29)*Z(3)+B(K,19))+
     .(B(K,7)-1.5D0*B(K,27)-1.5D0*B(K,29)-.5D0*B(K,32)))
      RETURN
C     SELECT THE EXPRESSION BASED ON REGULAR POLYNOMIALS
  140 F1=B(K,2)+2.0D0*Z(1)*(B(K,8)+1.5D0*B(K,11)*Z(1)+B(K,14)*Z(2)+
```

```
     .B(K,15)*Z(3)+2.0D0*B(K,21)*Z(1)**2+1.5D0*B(K,24)*Z(1)*Z(2)+
     .1.5D0*B(K,25)*Z(1)*Z(3)+B(K,30)*Z(2)**2+B(K,31)*Z(3)**2+
     .B(K,32)*Z(2)*Z(3))+Z(2)*(B(K,5)+B(K,16)*Z(2)+B(K,20)*Z(3)+
     .B(K,26)*Z(2)**2+B(K,34)*Z(2)*Z(3)+B(K,35)*Z(3)**2)+
     .Z(3)*(B(K,6)+B(K,18)*Z(3)+B(K,28)*Z(3)**2)
      RETURN
C   DF/DY
  150 F1=B(K,3)+2.0D0*Z(2)*(B(K,9)+1.5D0*B(K,12)*Z(2)+B(K,16)*Z(1)+
     .B(K,17)*Z(3)+2.0D0*B(K,22)*Z(2)**2+1.5D0*B(K,26)*Z(1)*Z(2)+
     .1.5D0*B(K,27)*Z(2)*Z(3)+B(K,30)*Z(1)**2+B(K,33)*Z(3)**2+
     .B(K,34)*Z(1)*Z(3))+Z(3)*(B(K,7)+B(K,19)*Z(3)+B(K,20)*Z(1)+
     .B(K,29)*Z(3)**2+B(K,32)*Z(1)**2+B(K,35)*Z(1)*Z(3))+
     .Z(1)*(B(K,5)+B(K,14)*Z(1)+B(K,24)*Z(1)**2)
      RETURN
C   DF/DZ
  160 F1=B(K,4)+2.0D0*Z(3)*(B(K,10)+1.5D0*B(K,13)*Z(3)+B(K,18)*Z(1)+
     .B(K,19)*Z(2)+2.0D0*B(K,23)*Z(3)**2+1.5D0*B(K,28)*Z(1)*Z(3)+
     .1.5D0*B(K,29)*Z(2)*Z(3)+B(K,31)*Z(1)**2+B(K,33)*Z(2)**2
     .+B(K,35)*Z(1)*Z(2))+Z(1)*(B(K,6)+B(K,15)*Z(1)+
     .B(K,20)*Z(2)+B(K,25)*Z(1)**2+B(K,32)*Z(1)*Z(2)+B(K,34)*Z(2)**2
     .)+Z(2)*(B(K,7)+B(K,17)*Z(2)+B(K,27)*Z(2)**2)
      RETURN
C   D2F/DX2
  170 F1=2.0D0*B(K,8)+6.0D0*Z(1)*(B(K,11)+2.0D0*B(K,21)*Z(1)+
     .B(K,24)*Z(2)+B(K,25)*Z(3))+2.0D0*Z(2)*(B(K,14)+B(K,30)*Z(2)
     .+B(K,32)*Z(3))+2.0D0*Z(3)*(B(K,15)+B(K,31)*Z(3))
      RETURN
C   D2F/DY2
  180 F1=2.0D0*B(K,9)+6.0D0*Z(2)*(B(K,12)+2.0D0*B(K,22)*Z(2)+
     .B(K,26)*Z(1)+B(K,27)*Z(3))+2.0D0*Z(3)*(B(K,17)+B(K,33)*Z(3)
     .+B(K,34)*Z(1))+2.0D0*Z(1)*(B(K,16)+B(K,30)*Z(1))
      RETURN
C   D2F/DZ2
  190 F1=2.0D0*B(K,10)+6.0D0*Z(3)*(B(K,13)+2.0D0*B(K,23)*Z(3)+
     .B(K,28)*Z(1)+B(K,29)*Z(2))+2.0D0*Z(1)*(B(K,18)+B(K,31)*Z(1)
     .+B(K,35)*Z(2))+2.0D0*Z(2)*(B(K,19)+B(K,33)*Z(2))
      RETURN
C   D2F/DXDY
  200 F1=B(K,5)+2.0D0*Z(1)*(B(K,14)+1.5D0*B(K,24)*Z(1)+2.0D0*B(K,30)
     .*Z(2)+B(K,32)*Z(3))+Z(2)*(2.0D0*B(K,16)+3.0D0*B(K,26)*Z(2)+
     .2.0D0*B(K,34)*Z(3))+Z(3)*(B(K,20)+B(K,35)*Z(3))
      RETURN
C   D2F/DXDZ
  210 F1=B(K,6)+2.0D0*Z(1)*(B(K,15)+1.5D0*B(K,25)*Z(1)+2.0D0*B(K,31)
     .*Z(3)+B(K,32)*Z(2))+Z(3)*(2.0D0*B(K,18)+3.0D0*B(K,23)*Z(3)+
     .2.0D0*B(K,35)*Z(2))+Z(2)*(B(K,20)+B(K,34)*Z(2))
      RETURN
C   D2F/DYDZ
  220 F1=B(K,7)+2.0D0*Z(2)*(B(K,17)+1.5D0*B(K,27)*Z(2)+2.0D0*B(K,33)
     .*Z(3)+B(K,34)*Z(1))+Z(3)*(2.0D0*B(K,19)+3.0D0*B(K,29)*Z(3)+
     .2.0D0*B(K,35)*Z(1))+Z(1)*(B(K,20)+B(K,32)*Z(1))
      RETURN
  300 FORMAT(1X,3D14.6)
  320 FORMAT(1X,I5)
  330 FORMAT(1X,10H F OF FUN=,D10.4)
      END
      SUBROUTINE EX(CR,K,F1)
C     THIS SUBROUTINE RETURNS THE SAME VALUE FOR K=1
C     AND THE EXPONENTIAL VALUE FOR ANY OTHER K.
      DOUBLE PRECISION CR,F1
      F1=CR
      IF(K.NE.1) F1=DEXP(CR)
      RETURN
      END
      BLOCK DATA
C     THIS SUBROUTINE INITIALIZES SEVARAL MATRICES:
C     YY- INDEPENDENT VARIABLES RANGE.
C     S- INDEPENDENT VARIBLES NORMALIZING FACTOR.
C     CU , CH- URBAN AND HIGHWAY FACTORS TO SIMULATE THE EPA CYCLE.
      COMMON/YH/YY,S,CU,CH,FC,IOC
      DOUBLE PRECISION YY(10,6),S(3),CU(10),CH(10),FC(4,4)
      DATA YY/1.25D1,1.28D1,1.25D1,2*1.24D1,1.3D1,1.27D1,1.3D1,
     A1.25D1,1.1D1,7*1.85D1,2*1.8D1,1.55D1,2*1.0D1,2*1.5D1,1.8D1,1.0D1
     B,2.1D1,2.4D1,2*1.0D1,2*4.2D1,3.8D1,3*4.5D1,3.8D1,4.2D1,4.5D1,
     C3.0D1,10*0.0D0,8*7.0D0,4.5D0,0.0D0/
      DATA S/1.5D1,4.0D1,7.0D0/
      DATA CU/2.56D2,8.7D1,4.5D1,0.0D0,7.7D1,3.17D2,6.0D0,2.4D1,1.17D2,
     A4.31D2/,CH/2.4D1,6.8D1,2.6D1,1.52D2,2.97D2,0.0D0,6.0D0,1.28D2,
     B4.8D1,1.0D1/
      END
```

Figure G-2

SUMMARY TABLE OF FUEL EMISSIONS AND CNTROL VARIABLES FOR VARIOUS OPTIMAL SOLUTIONS -THE NON CATALYST CASE

N	FUEL(L/M)	HC(G/M)	CO(G/M)	NO(G/M)	A/F	SA	EGR	LAO FUEL	LAO HC	LAO CO	LAO NO
1	23.9233	7.9048	5.6908	4.3517	15.4072	39.2808	0.0000	1.0000	0.0000	0.0000	0.0000
2	18.0517	2.0184	10.2608	1.4097	14.1152	15.1166	0.2894	0.0000	1.0000	0.0000	0.0000
3	19.2601	34.3612	9.2827	0.5520	17.0854	29.8009	3.9320	0.0000	0.0000	0.0000	1.0000
4	20.3437	19.3792	10.5930	0.6090	15.9663	33.5708	2.8060	1.0000	0.0000	0.0000	0.0420
5	20.7695	16.7595	9.8455	0.6676	16.0010	34.9809	2.8481	1.0000	0.0000	0.0000	0.0520
6	21.0946	16.0072	9.5774	0.7239	16.0689	35.4094	2.8403	1.0000	0.0000	0.0000	0.0420
7	21.5961	15.6557	9.2693	0.7700	16.6994	37.4219	2.5072	1.0000	0.0000	0.0000	0.0320
8	21.9881	14.2320	9.8375	0.8917	16.4256	37.6595	2.6331	1.0000	0.0000	0.0000	0.0225
9	22.5491	14.6565	11.3658	1.0392	15.5396	37.6663	3.1068	1.0000	0.0000	0.0000	0.0120
10	23.3654	10.6333	5.9184	2.1381	15.3008	38.9784	2.9831	1.0000	0.0000	0.0000	0.0020
11	22.9711	10.9028	7.6424	1.4438	15.4531	30.2972	1.4674	1.0000	0.0000	0.0000	0.0030
12	23.1189	13.3046	7.4094	1.5785	15.5007	39.4491	1.2931	1.0000	0.0000	0.0000	0.0059
13	23.2750	9.8959	7.2187	1.7436	15.5436	38.6192	1.1414	1.0000	0.0000	0.0050	0.0038
14	23.4589	9.3389	6.9010	1.9762	15.5008	38.7391	0.9994	1.0000	0.0000	0.0000	0.0047
15	23.6713	8.8868	6.6069	2.3085	15.5956	39.8724	0.8660	1.0000	0.0000	0.0000	0.0036
16	23.7656	8.8621	6.0323	2.4942	15.6399	38.8696	0.8561	1.0000	0.0000	0.0000	0.0025
17	23.8720	8.6317	5.8700	2.8575	15.5731	39.1292	0.8635	1.0000	0.0000	0.0000	0.0036
18	18.9832	2.0741	8.7662	1.6297	14.3943	17.5218	0.2893	1.0000	0.0900	0.0000	0.0000
19	19.0956	2.0871	8.5233	1.6991	14.4386	17.7489	0.2873	1.0000	0.0750	0.0000	0.0000
20	19.2134	2.1046	8.3335	1.7852	14.4883	18.0186	0.2774	1.0000	0.0600	0.0000	0.0000
21	19.3519	2.1301	8.1684	1.8911	14.5485	18.3370	0.2657	1.0000	0.0450	0.0000	0.0000
22	19.5204	2.1739	7.9968	2.0347	14.6304	18.8399	0.2596	1.0000	0.0300	0.0000	0.0000
23	20.6836	2.6151	7.7850	2.2830	14.6888	25.6614	0.2494	1.0000	0.0150	0.0000	0.0000
24	20.8409	2.7103	7.7759	2.3721	14.6743	26.2003	0.0592	1.0000	0.0130	0.0000	0.0000
25	21.0233	2.8364	7.7857	2.4442	14.6897	26.9327	0.0563	1.0000	0.0110	0.0000	0.0000
26	21.2647	3.0317	7.6432	2.5436	14.7240	27.9175	0.0534	1.0000	0.0090	0.0000	0.0000
27	21.5715	3.3394	7.3689	2.6648	14.7789	29.1493	0.0497	1.0000	0.0070	0.0000	0.0000
28	22.1657	4.0993	7.1377	2.8319	14.8432	31.0858	0.0359	1.0000	0.0050	0.0000	0.0000
29	23.0168	5.5022	6.9219	3.2618	14.9529	34.1626	0.0000	1.0000	0.0030	0.0000	0.0000
30	19.1590	2.2892	11.3105	0.8317	14.1592	22.7964	2.4854	1.0000	0.0200	0.0000	0.0150
31	19.6644	2.3091	7.9972	1.5367	14.5421	23.1844	1.9789	1.0000	0.0250	0.0000	0.0010
32	19.7521	2.9273	13.2502	0.7340	14.0545	23.3777	2.0091	1.0000	0.0100	0.0000	0.0210
33	20.0330	2.9060	10.9785	0.9181	14.2486	23.7331	1.8627	1.0000	0.0100	0.0000	0.0110
34	20.1921	2.7664	11.3605	1.0477	14.1910	23.6914	1.0378	1.0000	0.0100	0.0000	0.0130
35	20.3209	2.7667	10.6823	1.1436	14.2965	23.8718	0.9939	1.0000	0.0100	0.0000	0.0136
36	20.4723	2.7773	9.6244	1.2724	14.4068	26.1049	0.9186	1.0000	0.0105	0.0000	0.0082
37	20.6504	2.7998	8.8095	1.4595	14.4831	26.3876	0.7733	1.0000	0.0100	0.0000	0.0059
38	20.8566	2.8272	8.2159	1.7846	14.5778	26.7541	0.5443	1.0000	0.0100	0.0000	0.0034
39	21.0762	2.8800	7.8768	2.3287	14.6827	27.2303	0.2671	1.0000	0.0100	0.0000	0.0010
40	19.4707	3.9499	11.5295	0.7499	14.8880	26.1473	2.1586	1.0000	0.0030	0.0000	0.0310
41	19.6272	3.8726	11.1928	0.7911	14.9669	26.4341	2.1139	1.0000	0.0030	0.0000	0.0410
42	20.2479	3.9816	18.3449	0.7273	14.3095	27.4029	2.2251	1.0000	0.0050	0.0000	0.0310
43	20.6525	4.0598	14.1231	0.8486	14.4602	28.2677	2.1726	1.0000	0.0050	0.0000	0.0210
44	21.0609	4.1094	11.2341	1.0495	14.5973	29.2490	2.0625	1.0000	0.0050	0.0000	0.0110
45	21.2494	3.7803	10.9375	1.2021	14.3983	28.8172	1.0515	1.0000	0.0050	0.0000	0.0100
46	21.3757	3.8081	9.9049	1.2967	14.4803	29.0508	1.0197	1.0000	0.0050	0.0000	0.0083
47	21.5185	3.8493	9.1099	1.4141	14.4189	29.3503	0.9425	1.0000	0.0050	0.0000	0.0065
48	21.6748	3.8381	8.3348	1.5910	14.5327	29.6374	0.9120	1.0000	0.0050	0.0000	0.0049
49	21.8572	3.9452	7.7468	1.8664	14.6036	29.9910	0.8913	1.0000	0.0030	0.0000	0.0032
50	19.8445	6.5763	10.9734	0.6707	15.2333	28.8569	2.5255	1.0000	0.0020	0.0000	0.0310
51	21.1515	6.0125	22.0002	0.7691	14.7344	31.0153	2.2752	1.0000	0.0020	0.0000	0.0315
52	21.4651	5.9674	19.3879	0.8706	14.6294	31.4812	2.2733	1.0000	0.0020	0.0000	0.0210
53	21.8801	5.9973	13.0131	1.0039	14.4472	32.4564	2.2226	1.0000	0.0020	0.0000	0.0110
54	22.0729	5.7634	12.0027	1.1989	14.5083	31.9945	1.3509	1.0000	0.0020	0.0000	0.0130
55	22.2943	5.7775	10.3073	1.3747	14.6219	32.2720	1.2335	1.0000	0.0020	0.0000	0.0081
56	22.5259	5.9737	9.0843	1.5690	14.5332	32.7271	1.0831	1.0000	0.0020	0.0000	0.0062
57	22.7799	6.0244	7.9783	1.8560	14.7346	33.2411	1.0293	1.0000	0.0020	0.0000	0.0043
58	23.0932	6.1343	7.1002	2.3431	14.9853	34.4015	0.8665	1.0000	0.0020	0.0000	0.0024
59	23.7965	6.4127	6.2313	3.8244	15.2810	37.3998	0.7126	1.0000	0.0020	0.0000	0.0003
60	20.3558	2.7670	10.3960	1.1728	14.3242	25.9193	0.9799	1.0000	0.0100	0.0000	0.0150
61	20.5733	2.9676	10.4319	1.1748	14.3368	26.6334	0.9999	1.0000	0.0085	0.0000	0.0100
62	20.8313	3.2395	10.6282	1.1819	14.3538	27.4674	1.0181	1.0000	0.0070	0.0000	0.0150
63	21.1328	3.6161	10.9189	1.1947	14.3801	28.4408	1.0414	1.0000	0.0055	0.0000	0.0100
64	21.4965	4.2058	11.0592	1.2064	14.4355	29.6764	1.1009	1.0000	0.0040	0.0000	0.0100
65	21.9175	5.2411	11.6165	1.1996	14.4917	31.3128	1.2618	1.0000	0.0025	0.0000	0.0150
66	21.0062	2.9460	7.9854	2.1829	14.6392	27.0222	0.3133	1.0000	0.0100	0.0000	0.0020
67	21.1787	2.9925	7.8955	2.2062	14.6590	27.7287	0.3364	1.0000	0.0085	0.0000	0.0020
68	21.4745	3.2944	7.7255	2.2183	14.6856	28.7163	0.3560	1.0000	0.0070	0.0000	0.0020
69	21.8493	3.7494	7.5687	2.2455	14.7221	29.9225	0.3838	1.0000	0.0055	0.0000	0.0025
70	22.3243	4.4666	7.4240	2.3182	14.7825	31.4326	0.4359	1.0000	0.0040	0.0000	0.0020
71	22.9738	5.6318	7.0798	2.4718	14.9075	33.8684	0.7011	1.0000	0.0025	0.0000	0.0020
72	23.7676	7.1447	6.1749	2.7933	15.4521	37.5716	0.8110	1.0000	0.0010	0.0000	0.0020
73	21.0762	2.8800	7.8768	2.3287	14.6027	27.2303	0.2671	1.0000	0.0100	0.0000	0.0010
74	21.2605	3.0331	7.7175	2.3977	14.7110	27.9776	0.2636	1.0000	0.0085	0.0000	0.0010
75	21.5336	3.3078	7.5271	2.4510	14.7431	28.9512	0.2636	1.0000	0.0070	0.0000	0.0010
76	21.9266	3.7817	7.3611	2.5096	14.7805	30.2261	0.2604	1.0000	0.0055	0.0000	0.0010
77	22.4942	4.4997	7.0682	2.7480	14.9063	32.3081	0.2091	1.0000	0.0040	0.0000	0.0015
78	23.1095	5.8053	6.9847	2.8937	14.9736	34.3974	0.3298	1.0000	0.0025	0.0000	0.0015
79	23.8529	6.9607	6.0329	3.3276	15.3962	37.7800	0.7793	1.0000	0.0010	0.0000	0.0010
80	21.1079	2.9009	7.8363	2.3912	14.7022	27.3429	0.2353	1.0000	0.0100	0.0000	0.0005
81	21.2959	3.0601	7.6467	2.4674	14.7342	28.1117	0.2335	1.0000	0.0085	0.0000	0.0005
82	21.5543	3.3215	7.4478	2.5379	14.7701	29.0764	0.2308	1.0000	0.0070	0.0000	0.0005
83	21.9589	3.8126	7.2794	2.6038	14.0088	30.3963	0.2462	1.0000	0.0055	0.0000	0.0005
84	22.5206	4.5362	7.0054	2.8752	14.9232	32.5160	0.1894	1.0000	0.0040	0.0000	0.0005
85	23.7194	6.1827	6.3411	4.0167	15.2097	36.8878	0.2052	1.0000	0.0025	0.0000	0.0005
86	23.0579	6.7577	6.0005	3.8767	15.3272	37.9959	0.2541	1.0000	0.0010	0.0000	0.0005

Figure G-3

SUMMARY TABLE OF FUEL EMISSIONS AND CONTROL VARIABLES FOR VARIOUS OPTIMAL SOLUTIONS -THE OXIDIZING CATALYST CASE.

N	FUEL(L/M)	HC(G/M)	CO(G/M)	NO(G/M)	A/F	BA	EGR	LAO FUEL	LAO HC	LAO CO	LAO NO
1	23.9253	2.1262	1.1936	4.3517	15.4072	39.2020	0.0000	1.0000	0.0003	0.0000	0.0000
2	10.0517	0.6546	1.0791	1.4097	14.1152	15.1165	0.2094	0.0000	1.0003	0.0000	0.0000
3	19.2601	8.7403	1.7324	0.5520	17.0054	29.0009	3.9520	0.0000	0.0000	0.0000	1.0000
4	20.3437	4.9940	1.9290	0.6090	15.9665	33.5700	2.8060	1.0000	0.0000	0.0000	0.0620
5	20.7695	4.3399	1.8168	0.6676	16.0018	34.9009	2.8481	1.0000	0.0000	0.0000	0.0520
6	21.0046	4.1710	1.7766	0.7239	16.0609	35.4094	2.8403	1.0000	0.0000	0.0000	0.0420
7	21.5961	4.0509	1.7304	0.7700	16.6994	37.4219	2.5072	1.0000	0.0000	0.0000	0.0320
8	21.9081	3.7050	1.8156	0.8017	16.4256	37.6593	2.6031	1.0000	0.0000	0.0000	0.0220
9	22.5491	3.8091	2.0449	1.0372	15.5396	37.6663	3.1068	1.0000	0.0000	0.0000	0.0120
10	23.5654	2.8076	1.2278	2.1091	15.3038	39.9704	2.9031	1.0000	0.0000	0.0000	0.0020
11	22.5711	2.8757	1.4664	1.4438	15.4531	30.2972	1.4674	1.0000	0.0000	0.0000	0.0080
12	23.1189	2.7452	1.4514	1.5705	15.5007	38.4491	1.2931	1.0000	0.0000	0.0000	0.0069
13	23.2750	2.6240	1.4220	1.7436	15.5436	38.6192	1.1414	1.0000	0.0000	0.0000	0.0058
14	23.4589	2.4547	1.3752	1.9762	15.5808	38.7391	0.9994	1.0000	0.0000	0.0000	0.0047
15	23.6713	2.3717	1.3310	2.3085	15.5956	38.0724	0.8660	1.0000	0.0000	0.0000	0.0036
16	23.7656	2.3655	1.2448	2.4942	15.6399	38.8696	0.8561	1.0000	0.0000	0.0000	0.0025
17	23.8720	2.3379	1.2205	2.8575	15.5731	39.1292	0.8635	1.0000	0.0000	0.0000	0.0014
18	18.9892	0.6685	1.6549	1.6287	14.3743	17.5218	0.2083	1.0000	0.0900	0.0000	0.0000
19	19.0956	0.6718	1.6185	1.6991	14.4386	17.7489	0.2873	1.0000	0.0750	0.0000	0.0000
20	19.2154	0.6762	1.5900	1.7852	14.4083	18.0186	0.2774	1.0000	0.0600	0.0000	0.0000
21	19.3517	0.6825	1.5655	1.8911	14.5405	18.3570	0.2657	1.0000	0.0450	0.0000	0.0000
22	19.5204	0.6935	1.5375	2.0347	14.6304	18.0399	0.2596	1.0000	0.0300	0.0000	0.0000
23	20.6036	0.8030	1.5078	2.2830	14.6608	25.6514	0.2494	1.0000	0.0150	0.0000	0.0000
24	20.8409	0.8276	1.5064	2.3721	14.6743	26.2005	0.0592	1.0000	0.0130	0.0000	0.0000
25	21.0235	0.8591	1.5079	2.4442	14.6897	26.9327	0.0563	1.0000	0.0110	0.0000	0.0000
26	21.2647	0.9079	1.4855	2.5436	14.7240	27.9175	0.0534	1.0000	0.0090	0.0000	0.0000
27	21.5715	0.9846	1.4453	2.5648	14.7789	29.1493	0.0487	1.0000	0.0070	0.0000	0.0000
28	22.1657	1.1748	1.4107	2.8019	14.8432	31.0858	0.0359	1.0000	0.0050	0.0000	0.0000
29	23.0168	1.5256	1.3783	3.2618	14.9529	34.1625	0.0000	1.0000	0.0030	0.0000	0.0000
30	19.1590	0.7720	2.0356	0.8317	14.1592	22.7964	2.4854	1.0000	0.0200	0.0000	0.0160
31	19.6644	0.7273	1.5396	1.5267	14.5421	23.1844	1.9789	1.0000	0.0200	0.0000	0.0010
32	19.7521	0.8818	2.3275	0.7340	14.0545	25.3777	2.0091	1.0000	0.0100	0.0000	0.0210
33	20.0330	0.8765	1.9858	0.9181	14.2486	25.7331	1.8627	1.0000	0.0100	0.0000	0.0110
34	20.1921	0.8416	2.0441	1.0477	14.1910	25.6914	1.0378	1.0000	0.0100	0.0000	0.0130
35	20.3209	0.8417	1.9423	1.1436	14.2965	25.8718	0.9939	1.0000	0.0100	0.0000	0.0106
36	20.4723	0.8443	1.7837	1.2724	14.4068	26.1049	0.9105	1.0000	0.0100	0.0000	0.0082
37	20.6504	0.8500	1.6614	1.4555	14.4081	26.3875	0.7733	1.0000	0.0100	0.0000	0.0058
38	20.8566	0.8568	1.5724	1.7046	14.5778	26.7541	0.5443	1.0000	0.0100	0.0000	0.0034
39	21.0762	0.8700	1.5215	2.3287	14.6827	27.2305	0.2671	1.0000	0.0100	0.0000	0.0010
40	19.4707	1.1375	2.0693	0.7499	14.8980	26.1473	2.1585	1.0000	0.0050	0.0000	0.0510
41	19.6272	1.1181	2.0189	0.7911	14.9669	26.4341	2.1159	1.0000	0.0050	0.0000	0.0410
42	20.2499	1.1454	3.0917	0.7273	14.3095	27.4029	2.2251	1.0000	0.0050	0.0000	0.0310
43	20.6585	1.1650	2.4585	0.8485	14.4602	28.2677	2.1726	1.0000	0.0050	0.0000	0.0210
44	21.0609	1.1771	2.0251	1.0499	14.5973	29.2490	2.0625	1.0000	0.0050	0.0000	0.0110
45	21.2494	1.0951	1.9806	1.2021	14.3983	28.8172	1.0515	1.0000	0.0050	0.0000	0.0100
46	21.3757	1.1020	1.8257	1.2967	14.4803	29.0608	1.0197	1.0000	0.0050	0.0000	0.0083
47	21.5185	1.1121	1.7055	1.4141	14.4189	29.3605	0.9425	1.0000	0.0050	0.0000	0.0066
48	21.6748	1.1220	1.5932	1.5910	14.5327	29.6374	0.9120	1.0000	0.0050	0.0000	0.0049
49	21.8572	1.1363	1.5020	1.8664	14.6836	29.9910	0.8713	1.0000	0.0050	0.0000	0.0032
50	19.0445	1.7941	1.9860	0.6707	15.2333	28.0069	2.5255	1.0000	0.0020	0.0000	0.0510
51	21.1515	1.6531	3.6400	0.7691	14.7344	31.0153	2.2752	1.0000	0.0020	0.0000	0.0310
52	21.4651	1.6419	3.2402	0.8706	14.6294	31.4812	2.2733	1.0000	0.0020	0.0000	0.0210
53	21.8801	1.6493	2.2920	1.0039	14.4472	32.4564	2.2226	1.0000	0.0020	0.0000	0.0110
54	22.0730	1.5909	2.1404	1.1989	14.5083	31.9945	1.3509	1.0000	0.0020	0.0000	0.0100
55	22.2943	1.5944	1.8061	1.3747	14.6219	32.2720	1.2335	1.0000	0.0020	0.0000	0.0081
56	22.5259	1.6184	1.7026	1.5690	14.5932	32.7271	1.0331	1.0000	0.0020	0.0000	0.0062
57	22.7798	1.6561	1.5367	1.8560	14.7346	33.2411	1.0293	1.0000	0.0020	0.0000	0.0043
58	23.0982	1.6836	1.4062	2.3431	14.9853	34.4015	0.8665	1.0000	0.0020	0.0000	0.0024
59	23.7965	1.7532	1.2747	3.6244	15.2810	37.2090	0.7126	1.0000	0.0020	0.0000	0.0005
60	20.3558	0.8417	1.8994	1.1728	14.3242	25.9193	0.9799	1.0000	0.0100	0.0000	0.0100
61	20.5733	0.8919	1.9048	1.1749	14.3358	26.6334	0.9999	1.0000	0.0085	0.0000	0.0100
62	20.8313	0.9599	1.9342	1.1819	14.3539	27.4674	1.0181	1.0000	0.0070	0.0000	0.0100
63	21.1328	1.0540	1.9778	1.1947	14.3801	28.4408	1.0414	1.0000	0.0055	0.0000	0.0100
64	21.4965	1.2017	1.9989	1.2064	14.4365	29.6764	1.1069	1.0000	0.0040	0.0000	0.0100
65	21.9175	1.4603	2.0825	1.1996	14.4917	31.3128	1.2618	1.0000	0.0025	0.0000	0.0100
66	21.0062	0.8615	1.5378	2.1029	14.6372	27.0222	0.3135	1.0000	0.0100	0.0000	0.0020
67	21.1787	0.8981	1.5243	2.2062	14.6590	27.7287	0.3064	1.0000	0.0085	0.0000	0.0020
68	21.4745	0.9736	1.4908	2.2183	14.6856	28.7163	0.3560	1.0000	0.0070	0.0000	0.0020
69	21.8493	1.0873	1.4753	2.2455	14.7221	29.9725	0.3038	1.0000	0.0055	0.0000	0.0020
70	22.3243	1.2667	1.4536	2.3102	14.7625	31.4326	0.4359	1.0000	0.0040	0.0000	0.0020
71	22.9730	1.5580	1.4020	2.4710	14.9875	33.8684	0.7011	1.0000	0.0025	0.0000	0.0020
72	23.7676	1.9362	1.2662	2.7933	15.4521	37.5716	0.8110	1.0000	0.0010	0.0000	0.0020
73	21.0762	0.8700	1.5215	2.3287	14.6827	27.2305	0.2671	1.0000	0.0100	0.0000	0.0010
74	21.2605	0.9083	1.4976	2.3977	14.7110	27.9776	0.2656	1.0000	0.0085	0.0000	0.0010
75	21.5336	0.9769	1.4691	2.4510	14.7431	28.9512	0.2635	1.0000	0.0070	0.0000	0.0010
76	21.9266	1.0954	1.4442	2.5096	14.7005	30.2261	0.2604	1.0000	0.0055	0.0000	0.0010
77	22.4942	1.2749	1.4002	2.7409	14.9063	32.3301	0.2051	1.0000	0.0040	0.0000	0.0010
78	23.1035	1.6013	1.3377	2.8937	14.9736	34.3974	0.3298	1.0000	0.0025	0.0000	0.0010
79	23.0629	1.8922	1.2449	3.3276	15.3962	37.9809	0.7793	1.0000	0.0010	0.0000	0.0010
80	21.1079	0.8752	1.5154	2.3912	14.7022	27.3479	0.2553	1.0000	0.0100	0.0000	0.0005
81	21.2959	0.9150	1.4870	2.4674	14.7342	28.1117	0.2535	1.0000	0.0085	0.0000	0.0005
82	21.5543	0.9804	1.4572	2.5379	14.7701	29.0764	0.2508	1.0000	0.0070	0.0000	0.0005
83	21.9507	1.1031	1.4319	2.6050	14.8080	30.3763	0.2462	1.0000	0.0055	0.0000	0.0005
84	22.5206	1.2841	1.3708	2.0752	14.9252	32.5160	0.1094	1.0000	0.0040	0.0000	0.0005
85	23.7154	1.6957	1.2912	4.0167	15.2097	36.8870	0.2052	1.0000	0.0025	0.0000	0.0005
86	23.8579	1.8394	1.2401	3.0767	15.3272	37.9959	0.2541	1.0000	0.0010	0.0000	0.0005

Figure G-4

SUMMARY TABLE OF FUEL EMISSIONS AND CNTROL VARIABLES FOR VARIOUS OPTIMAL SOLUTIONS -THE THREE WAY CATALYST CASE.

N	FUEL(L/H)	HC(G/M)	CO(G/M)	NO(G/M)	A/F	SA	EGR	LAG FUEL	LAG HC	LAG CO	LAG NO
1	23.1742	1.9243	4.3320	1.3057	14.6297	38.5565	0.0000	1.0000	0.0000	0.0000	0.0000
2	18.3859	0.6460	4.3056	0.5079	14.5794	15.0600	0.1990	0.0000	1.0000	0.0000	0.0000
3	19.2246	0.6634	4.3122	0.5183	14.5855	20.8721	0.1778	1.0000	0.0860	0.0000	0.0000
4	19.2592	0.6641	4.3127	0.5213	14.5855	21.0157	0.1707	1.0000	0.0740	0.0000	0.0000
5	19.3244	0.6657	4.3138	0.5280	14.5855	21.2533	0.1565	1.0000	0.0620	0.0000	0.0000
6	19.4063	0.6601	4.3049	0.5435	14.5921	21.5400	0.1190	1.0000	0.0500	0.0000	0.0000
7	19.5061	0.6718	4.3087	0.5615	14.6064	21.9142	0.0004	1.0000	0.0380	0.0000	0.0000
8	19.7731	0.6961	4.3039	0.5835	14.6268	22.8565	0.0674	1.0000	0.0260	0.0000	0.0000
9	20.5248	0.7452	4.2998	0.6189	14.6268	25.8249	0.0640	1.0000	0.0140	0.0000	0.0000
10	22.9194	1.4233	4.3166	1.3002	14.6458	36.1873	0.0441	1.0000	0.0020	0.0000	0.0000
11	19.2759	1.9185	4.4079	0.2323	14.5534	24.6357	3.0914	0.0000	0.0000	0.0000	1.0000
12	20.8163	2.2038	4.3993	0.2726	14.5677	31.5388	3.2544	1.0000	0.0000	0.0000	0.0600
13	20.9214	2.1174	4.3916	0.2769	14.5677	31.7682	3.0304	1.0000	0.0000	0.0000	0.0520
14	21.0373	2.0380	4.3910	0.2829	14.5677	31.9525	2.9342	1.0000	0.0000	0.0000	0.0440
15	21.2841	1.9633	4.3870	0.2980	14.6025	32.3887	2.8379	1.0000	0.0000	0.0000	0.0360
16	21.6411	1.9173	4.3932	0.3243	14.6025	33.0262	2.7871	1.0000	0.0000	0.0000	0.0280
17	22.0285	1.9541	4.4028	0.3609	14.6319	33.8068	2.7883	1.0000	0.0000	0.0000	0.0200
18	22.4079	2.0632	4.4114	0.4145	14.6003	35.0959	2.7072	1.0000	0.0000	0.0000	0.0120
19	22.9374	2.1795	4.3490	0.5607	14.6229	37.6761	3.0048	1.0000	0.0000	0.0000	0.0040
20	18.9628	0.7101	4.3427	0.3009	14.5534	21.4492	2.4597	1.0000	0.0200	0.0000	0.0600
21	19.1135	0.7060	4.3402	0.3033	14.5534	21.9785	2.1772	1.0000	0.0200	0.0000	0.0520
22	19.1636	0.7075	4.3410	0.3059	14.5534	22.1564	2.1250	1.0000	0.0200	0.0000	0.0280
23	19.2392	0.7097	4.3410	0.3119	14.5534	22.3366	2.1168	1.0000	0.0200	0.0000	0.0200
24	19.3258	0.7112	4.3293	0.3255	14.5745	22.5546	2.0655	1.0000	0.0200	0.0000	0.0120
25	19.5167	0.7157	4.3192	0.3865	14.5855	22.7732	1.7179	1.0000	0.0200	0.0000	0.0040
26	19.4884	0.7599	4.3478	0.3051	14.5534	23.4589	2.4436	1.0000	0.0100	0.0000	0.0600
27	19.8277	0.8063	4.3564	0.2935	14.5534	24.4180	2.2089	1.0000	0.0100	0.0000	0.0520
28	19.8515	0.7996	4.3537	0.2977	14.5534	24.6370	2.1602	1.0000	0.0100	0.0000	0.0360
29	19.9304	0.7972	4.3534	0.3059	14.5534	24.9097	2.1256	1.0000	0.0100	0.0000	0.0280
30	20.0054	0.7945	4.3521	0.3164	14.5534	25.1999	2.0770	1.0000	0.0100	0.0000	0.0200
31	20.0742	0.7928	4.3432	0.3337	14.5832	25.5185	2.0051	1.0000	0.0100	0.0000	0.0120
32	20.2969	0.7974	4.3163	0.3988	14.6202	25.9930	1.6755	1.0000	0.0100	0.0000	0.0040
33	20.7514	1.1827	4.3776	0.2844	14.5828	28.5353	2.6302	1.0000	0.0020	0.0000	0.0500
34	20.8137	1.1933	4.3804	0.2870	14.3662	28.8024	2.6114	1.0000	0.0020	0.0000	0.0420
35	20.9883	1.2123	4.3802	0.2968	14.5881	29.3116	2.5777	1.0000	0.0020	0.0000	0.0340
36	21.2305	1.1513	4.3834	0.3236	14.5831	29.4811	2.2569	1.0000	0.0020	0.0000	0.0260
37	21.5045	1.2016	4.3374	0.3430	14.5831	30.3614	2.2421	1.0000	0.0020	0.0000	0.0180
38	21.7973	1.2761	4.3905	0.3733	14.5881	31.5537	2.2265	1.0000	0.0020	0.0000	0.0100
39	22.3323	1.3794	4.3547	0.5705	14.6398	33.5761	1.9321	1.0000	0.0020	0.0000	0.0020
40	19.7999	0.6787	4.3200	0.4325	14.5855	23.5422	1.2942	1.0000	0.0200	0.0000	0.0050
41	19.9733	0.6917	4.3162	0.4392	14.6202	24.1403	1.3085	1.0000	0.0176	0.0000	0.0050
42	20.1292	0.7055	4.3163	0.4420	14.6202	24.7609	1.3271	1.0000	0.0152	0.0000	0.0050
43	20.2875	0.7218	4.3170	0.4456	14.6202	25.4395	1.3507	1.0000	0.0128	0.0000	0.0050
44	20.4533	0.7421	4.3183	0.4492	14.6202	26.1931	1.3823	1.0000	0.0104	0.0000	0.0050
45	20.7365	0.7891	4.3257	0.4425	14.6202	27.2599	1.4239	1.0000	0.0080	0.0000	0.0050
46	21.1097	0.8672	4.3345	0.4424	14.6247	28.5533	1.4863	1.0000	0.0056	0.0000	0.0050
47	21.7182	1.0522	4.3404	0.4550	14.6282	30.6170	1.6776	1.0000	0.0032	0.0000	0.0050
48	22.6133	2.0786	4.4096	0.4568	14.5940	35.6843	2.6712	1.0000	0.0000	0.0000	0.0090
49	21.6464	1.2885	4.3885	0.3806	14.5932	31.7362	2.2220	1.0000	0.0020	0.0000	0.0090
50	21.1760	1.0233	4.3700	0.3555	14.5881	29.3643	2.0392	1.0000	0.0040	0.0000	0.0090
51	20.7255	0.9032	4.3561	0.3466	14.5881	27.7886	1.9762	1.0000	0.0060	0.0000	0.0090
52	20.4005	0.8366	4.3420	0.3449	14.5881	26.6339	1.9924	1.0000	0.0080	0.0000	0.0090
53	19.9702	0.7702	4.3308	0.3432	14.5935	24.9435	1.9573	1.0000	0.0120	0.0000	0.0090
54	19.8098	0.7514	4.3267	0.3422	14.5794	24.2781	1.9476	1.0000	0.0140	0.0000	0.0090
55	20.2369	0.9171	4.3724	0.2585	14.5534	23.8813	2.3104	1.0000	0.0050	0.0000	0.0600
56	20.2871	0.9062	4.3704	0.2927	14.5534	25.9734	2.2541	1.0000	0.0050	0.0000	0.0520
57	20.3256	0.9037	4.3702	0.2943	14.5534	26.1502	2.2349	1.0000	0.0050	0.0000	0.0440
58	20.3942	0.9122	4.3705	0.2981	14.5534	26.4715	2.2113	1.0000	0.0050	0.0000	0.0360
59	20.5466	0.9203	4.3684	0.3083	14.5310	26.9600	2.1779	1.0000	0.0050	0.0000	0.0280
60	20.6803	0.9286	4.3682	0.3195	14.5881	27.4790	2.1363	1.0000	0.0050	0.0000	0.0200
61	20.8383	0.9423	4.3651	0.3374	14.5831	28.1320	2.0569	1.0000	0.0050	0.0000	0.0120
62	21.1256	0.9521	4.3329	0.4166	14.6343	29.0653	1.8080	1.0000	0.0050	0.0000	0.0040
63	20.3869	0.7318	4.3002	0.6105	14.6268	25.2160	0.0655	1.0000	0.0160	0.0000	0.0000
64	21.9075	1.0255	4.3230	0.7153	14.6409	31.2782	0.0517	1.0000	0.0040	0.0000	0.0000
65	20.9578	0.5073	4.3054	0.6076	14.6409	27.6907	0.2009	1.0000	0.0080	0.0000	0.0020
66	21.1319	0.8377	4.3100	0.6069	14.6409	28.2628	0.2789	1.0000	0.0070	0.0000	0.0020
67	21.3119	0.8753	4.3155	0.6076	14.6409	28.8875	0.3206	1.0000	0.0060	0.0000	0.0020
68	21.5131	0.9237	4.3221	0.6106	14.6409	29.5787	0.3487	1.0000	0.0050	0.0000	0.0020
69	21.7883	1.0025	4.3300	0.6172	14.6409	30.5370	0.3883	1.0000	0.0040	0.0000	0.0020
70	22.1169	1.1189	4.3398	0.6297	14.6409	31.6952	0.4547	1.0000	0.0030	0.0000	0.0020
71	22.5114	1.3069	4.3428	0.6465	14.6398	33.1385	0.8149	1.0000	0.0020	0.0000	0.0020
72	22.8599	1.5984	4.3414	0.6405	14.6416	35.0883	1.0323	1.0000	0.0010	0.0000	0.0020
73	20.9913	0.8070	4.2984	0.6467	14.6409	27.8571	0.0838	1.0000	0.0080	0.0000	0.0010
74	21.1604	0.8390	4.3030	0.6492	14.6409	28.4532	0.0829	1.0000	0.0070	0.0000	0.0010
75	21.3477	0.8767	4.3084	0.6543	14.6409	29.1073	0.0819	1.0000	0.0060	0.0000	0.0010
76	21.5592	0.9271	4.3151	0.6636	14.6409	29.8371	0.0811	1.0000	0.0050	0.0000	0.0010
77	21.8519	1.0101	4.3229	0.6808	14.6409	30.0913	0.0806	1.0000	0.0040	0.0000	0.0010
78	22.2166	1.1372	4.3328	0.7137	14.6409	32.1093	0.0841	1.0000	0.0030	0.0000	0.0010
79	22.6662	1.3394	4.3391	0.7986	14.6477	33.8108	0.1479	1.0000	0.0020	0.0000	0.0010
80	22.9951	1.5474	4.3415	0.9098	14.6397	35.3427	0.3939	1.0000	0.0010	0.0000	0.0010
81	20.9976	0.8075	4.2972	0.6584	14.6409	27.9611	0.0673	1.0000	0.0080	0.0000	0.0005
82	21.1699	0.8390	4.3019	0.6613	14.6409	28.5724	0.0664	1.0000	0.0070	0.0000	0.0005
83	21.3610	0.8787	4.3076	0.6671	14.6409	29.2457	0.0654	1.0000	0.0060	0.0000	0.0005
84	21.5779	0.9308	4.3145	0.6776	14.6409	30.0009	0.0642	1.0000	0.0050	0.0000	0.0005
85	21.8797	1.0172	4.3227	0.6971	14.6409	31.0322	0.0627	1.0000	0.0040	0.0000	0.0005
86	22.2669	1.1345	4.3327	0.7399	14.6420	32.3890	0.0611	1.0000	0.0030	0.0000	0.0005
87	22.8121	1.4015	4.3364	0.9151	14.6468	34.5042	0.0601	1.0000	0.0020	0.0000	0.0005
88	23.0483	1.5469	4.3329	1.0913	14.6307	36.1644	0.0679	1.0000	0.0010	0.0000	0.0005
89	22.7192	2.0755	4.4064	0.4838	14.5908	36.1036	2.6938	1.0000	0.0000	0.0000	0.0074
90	22.8315	2.1376	4.3685	0.5136	14.6137	36.9124	2.9706	1.0000	0.0000	0.0000	0.0038
91	23.0013	2.2100	4.3410	0.6003	14.6346	38.3233	2.9360	1.0000	0.0000	0.0000	0.0026
92	23.0410	2.2379	4.3377	0.6437	14.6316	39.0106	2.9289	1.0000	0.0000	0.0000	0.0010
93	21.5938	0.9350	4.3143	0.6926	14.6409	30.1833	0.0340	1.0000	0.0050	0.0000	0.0000
94	21.8052	0.9739	4.3201	0.7068	14.6409	30.9209	0.0323	1.0000	0.0043	0.0000	0.0000
95	22.0565	1.0752	4.3272	0.7301	14.6407	31.7967	0.0306	1.0000	0.0036	0.0000	0.0000
96	22.3797	1.1997	4.3323	0.7708	14.6491	32.7231	0.0482	1.0000	0.0029	0.0000	0.0000

Appendix H

ELECTRONIC SCHEMATICS OF THE PRESSURE DETECTION CIRCUITS

Fig. H-1 Pressure Trace Preamplifier Circuitry

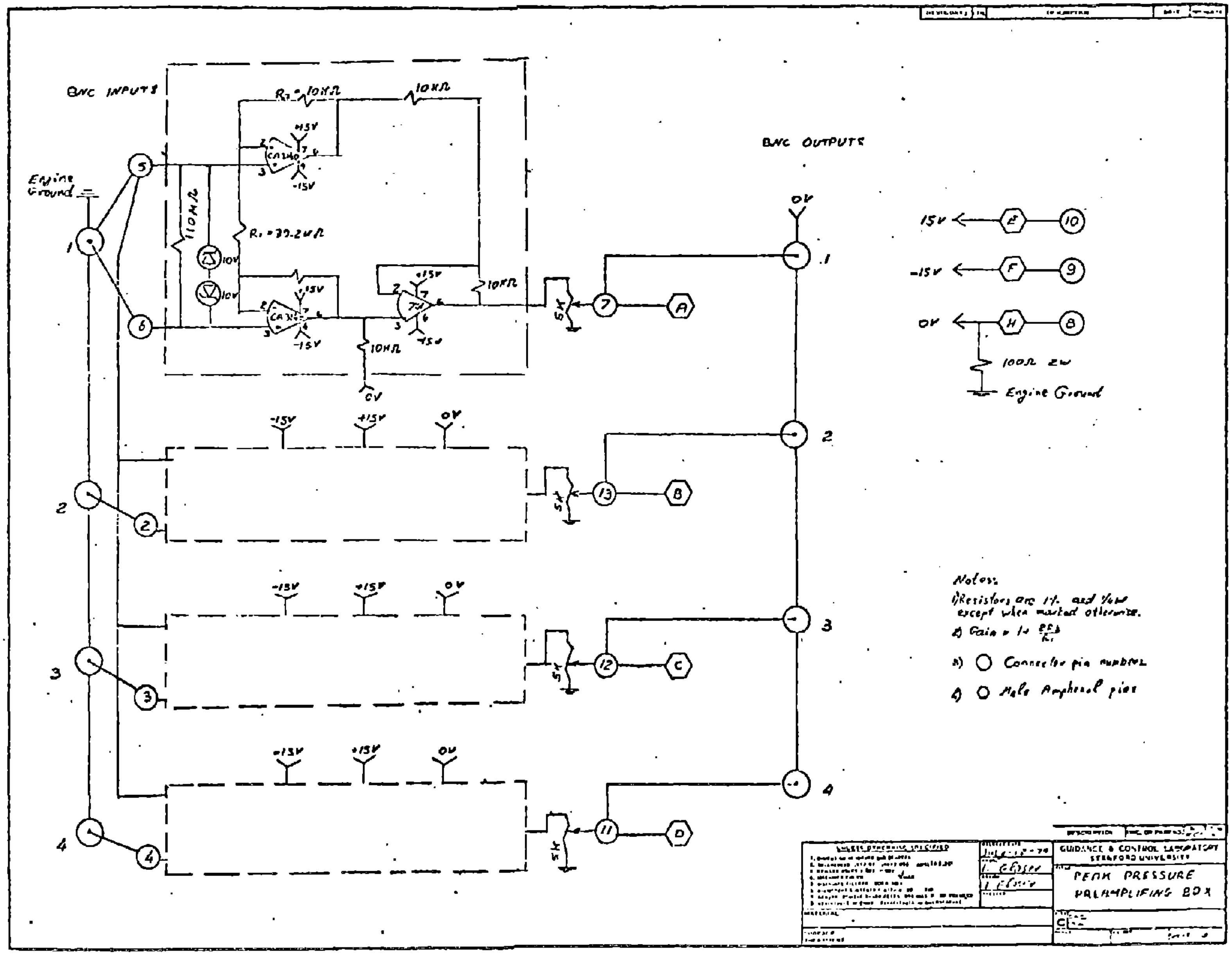

Fig. H-2 Peak Pressure Detection Circuitry

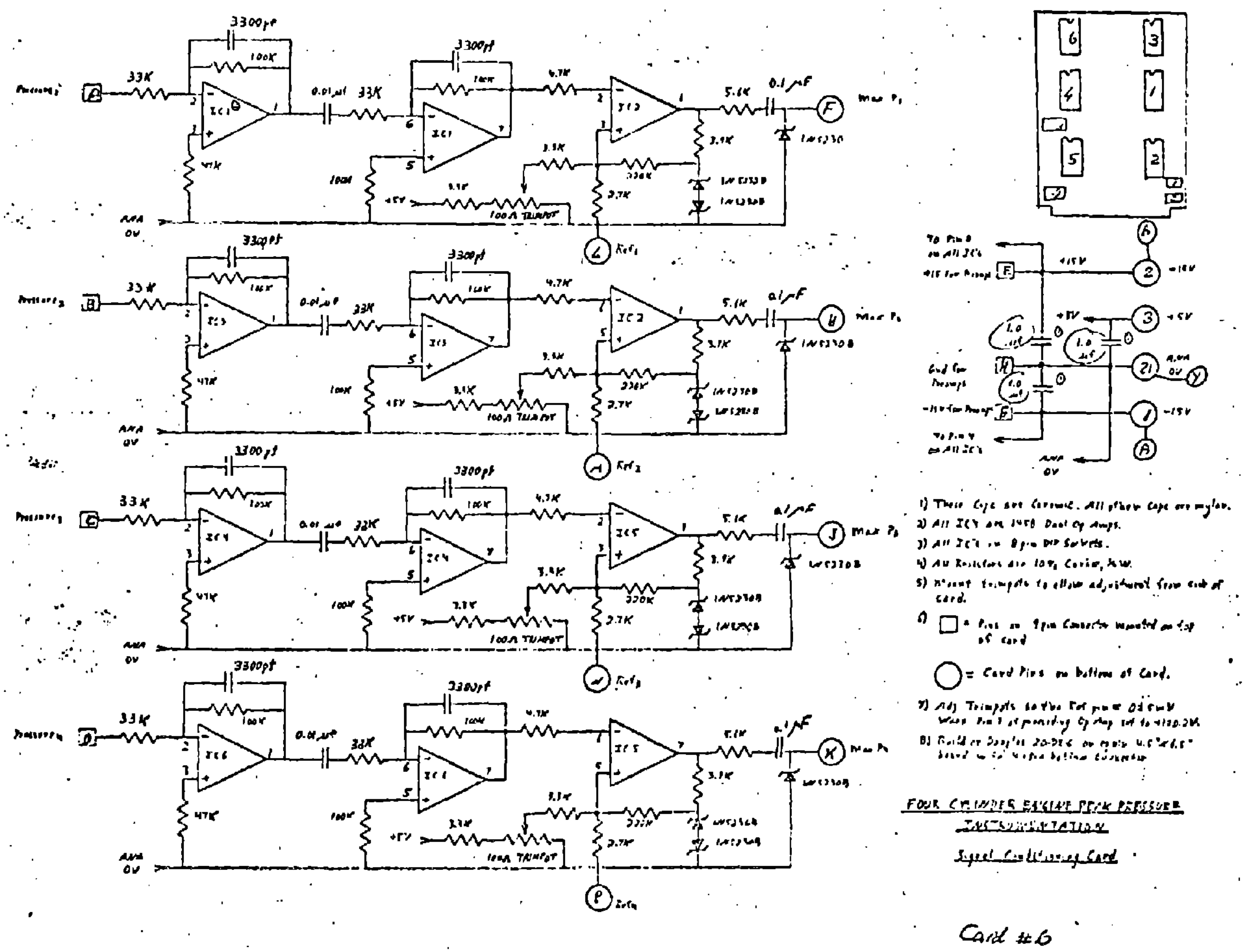

Fig. H-3 Peak Pressure Angle Measurement Circuitry

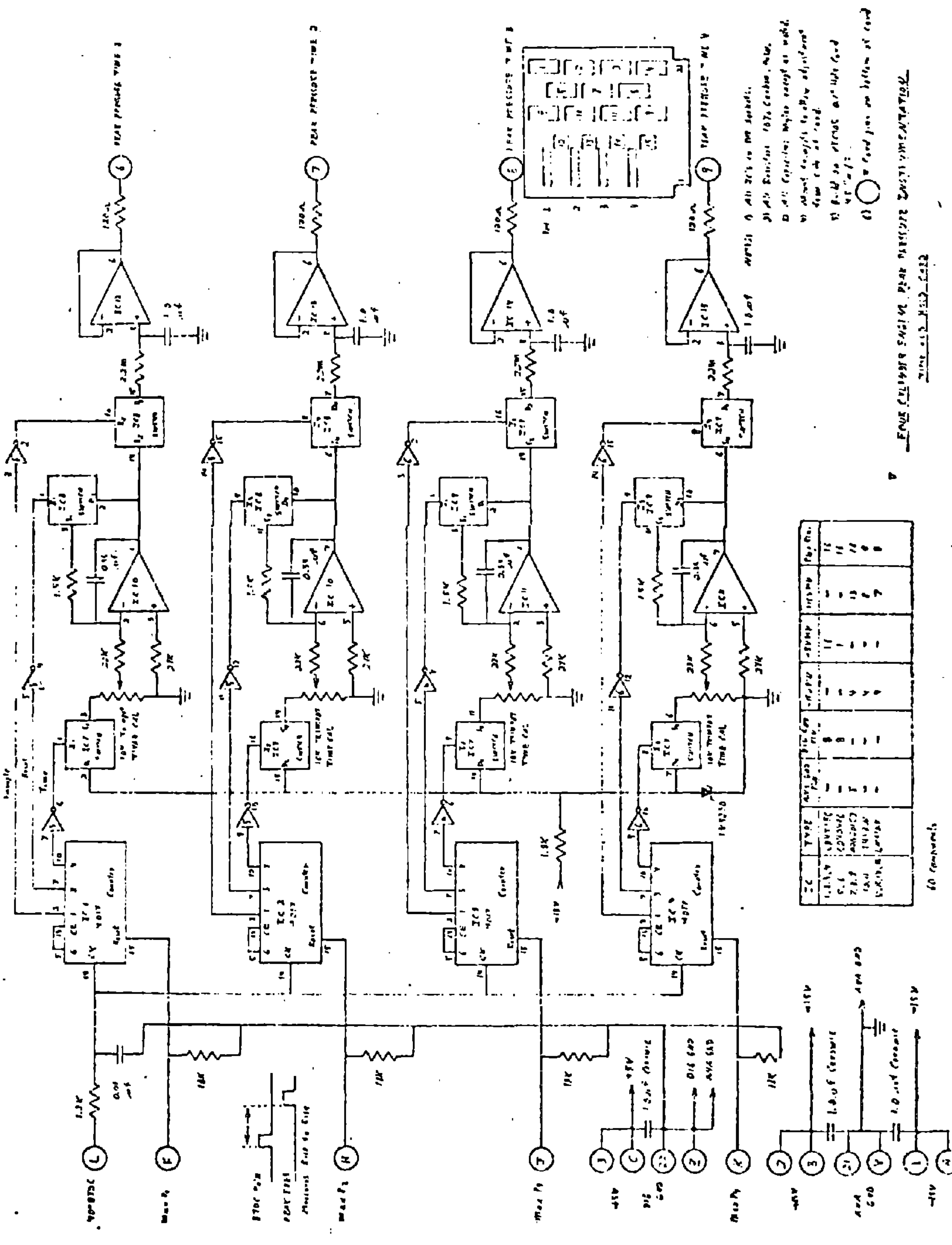

Appendix I

SPARK ADVANCE MEASUREMENT AND CONTROL

1. Introduction

The spark timing computer system is designed to collect spark advance data and to control spark advance on a multicylinder engine. The system may be expanded for collection of peak cylinder pressure timing data and for feedback control of spark advance. Spark advance calculation and data collection is performed by timing from a reference point in the engine cycle to detection of the spark event, and then comparing this time to a reference time which is the time required for half of an engine revolution. The ratio of the two times is used to determine the point in the engine cycle where the spark event occurred. Similarly, spark advance control is implemented by timing half of an engine revolution, calculating the time required to trigger the spark at a desired point in the engine cycle, then timing from an engine reference point until time to trigger the spark. A detailed description of the spark timing algorithms is given in the "Software" section 3. Figure I-1 is an overall schematic of the hardware used to implement the spark timing system. Engine cycle reference is generated by an optical switch which is used to detect the passage of slots machined in the crankshaft pulley at 60^{o} BTDC and 120^{o} ATDC. The signal from the optical switch is amplified and transmitted to the computer. The spark discharge in the #1cylinder is detected by an inductive pickoff and a digital pulse is transmitted to the computer. The spark trigger for the electronic ignition is switch selectable from either the distributer or from the computer. The isolation electronics are used to electrically isolate the engine electrical system from the computer electronics by means of optically coupled isolators. The spark timing computer electronics are on three cards dedicated to engine interface and interrupt generation, CPU and memory functions, and interfacing with a NOVA-3 computer which is used for data collection and engine test stand control. A detailed description of this hardware follows.

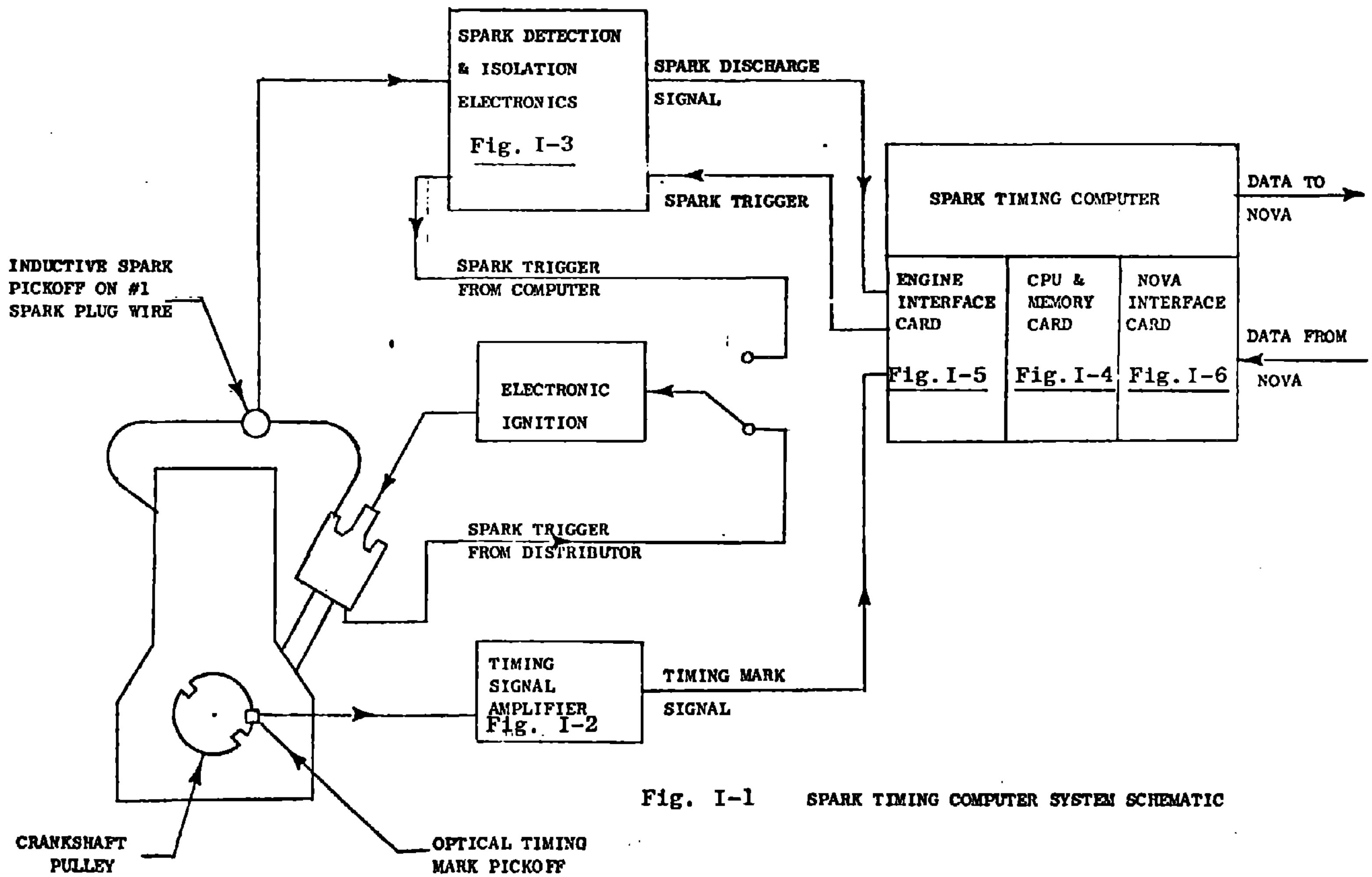

Fig. I-1 SPARK TIMING COMPUTER SYSTEM SCHEMATIC

2. Hardware

The following description deals with design considerations and intended use of the hardward features.

Engine cycle reference is provided by an optical switch which senses the passage of slots machined in the crankshaft pulley at 60^{o}BTDC and 120^{o} ATDC. Figure I-2 is an electrical schematic of the optical switch and buffer. This circuit provides a low logic level pulse to the spark timing computer when a slot on the crankshaft pulley passes through the optical switch.

An inductive spark pickoff is used to detect discharge of the #1 cylinder spark plug. Figure I-3 is an electrical schematic of the spark detection circuitry. This circuit provides a low logic level pulse to the spark timing computer when the #1 cylinder spark plug discharges. A Fairchild 820B optically coupled isolator is used to minimize electrical noise transmission from the spark detection circuit to the computer electronics.

The spark trigger source for the electronic ignition module is switch selectable from either the distributor for conventional spark timing control or from the computer. The spark trigger from the computer is transmitted through an optically coupled isolator for isolation of the computer electronics from the engine electrical system. Figure I-3 contains the electrical schematic of the isolation circuitry for the spark trigger.

The spark timing control computer consists of a Z80 central processing unit with 1K bytes of erasable programmable read-only memory and 256 bytes of static read-write memory. Figure I-4 is an electrical schematic of the computer. The data bus has been split into two buses: an internal, unbuffered data bus provides communications between the CPU and the memory chips, and a buffered, external data bus provides noise immunity and fan-out capability for communication with all input/output devices. Input and output address decoding is provided by BCD decoding chips. The 1K EPROM occupies memory locations $0000\text{-}03FF_{16}$ and

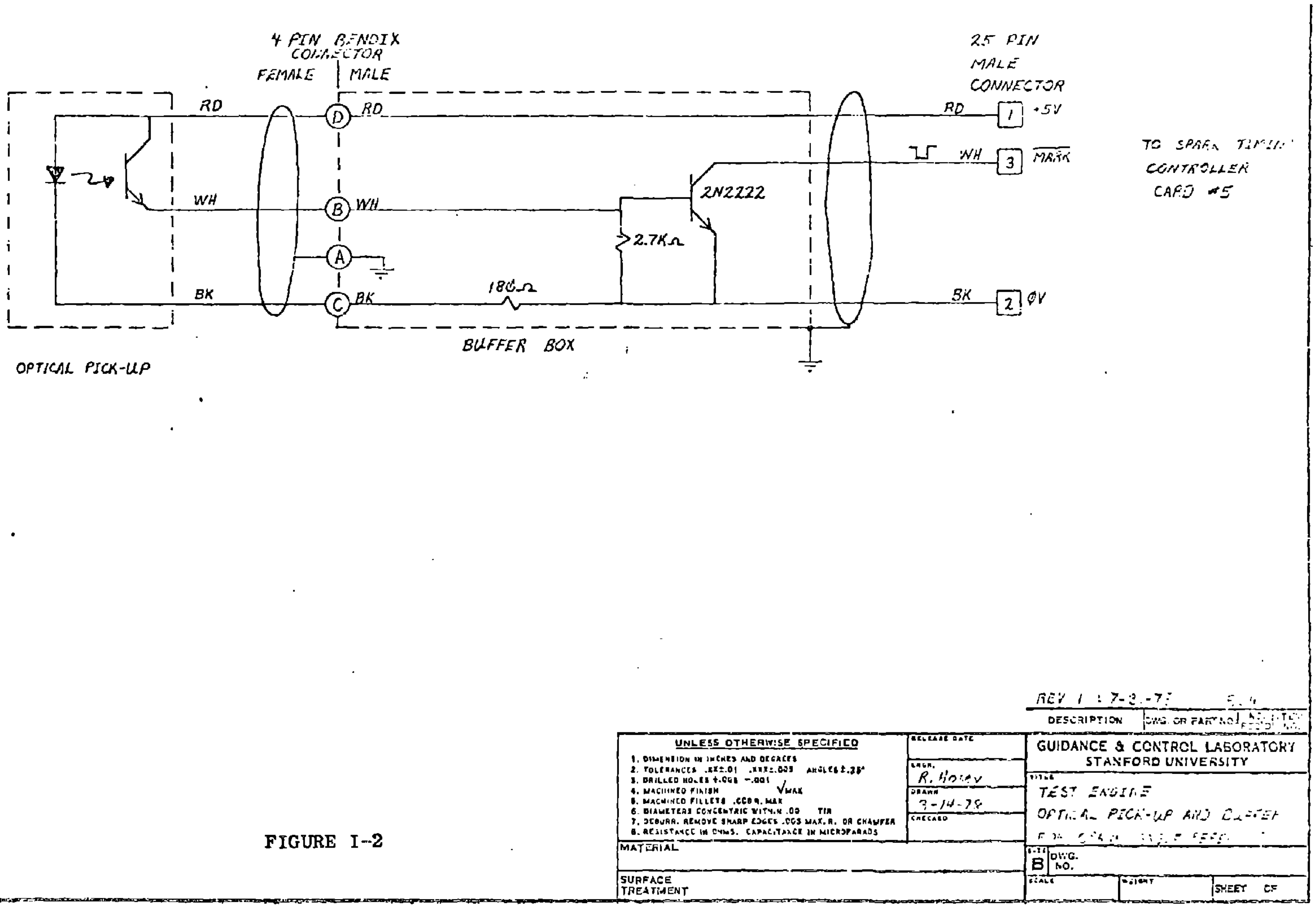
4 PIN BENDIX CONNECTOR
FEMALE
MALE
RD
WH
BK
D
B
A
C
2N2222
2.7KΩ
180Ω
BUFFER BOX
OPTICAL PICK-UP
25 PIN MALE CONNECTOR
1
+5V
3
MARK
2
ØV
TO SPARK TIMING CONTROLLER CARD #5
UNLESS OTHERWISE SPECIFIED
1. DIMENSION IN INCHES AND DEGREES
2. TOLERANCES
3. DRILLED HOLES
4. MACHINED FINISH
5. MACHINED FILLETS
6. DIAMETERS CONCENTRIC WITHIN
7. DEBURR. REMOVE SHARP EDGES
8. RESISTANCE IN OHMS. CAPACITANCE IN MICROFARADS
RELEASE DATE
ENGR.
R. Hovey
DRAWN
3-14-78
CHECKED
MATERIAL
SURFACE TREATMENT
DESCRIPTION
GUIDANCE & CONTROL LABORATORY
STANFORD UNIVERSITY
TITLE
TEST ENGINE
OPTICAL PICK-UP AND BUFFER
B
DWG. NO.
SCALE
WEIGHT
SHEET OF

FIGURE I-2

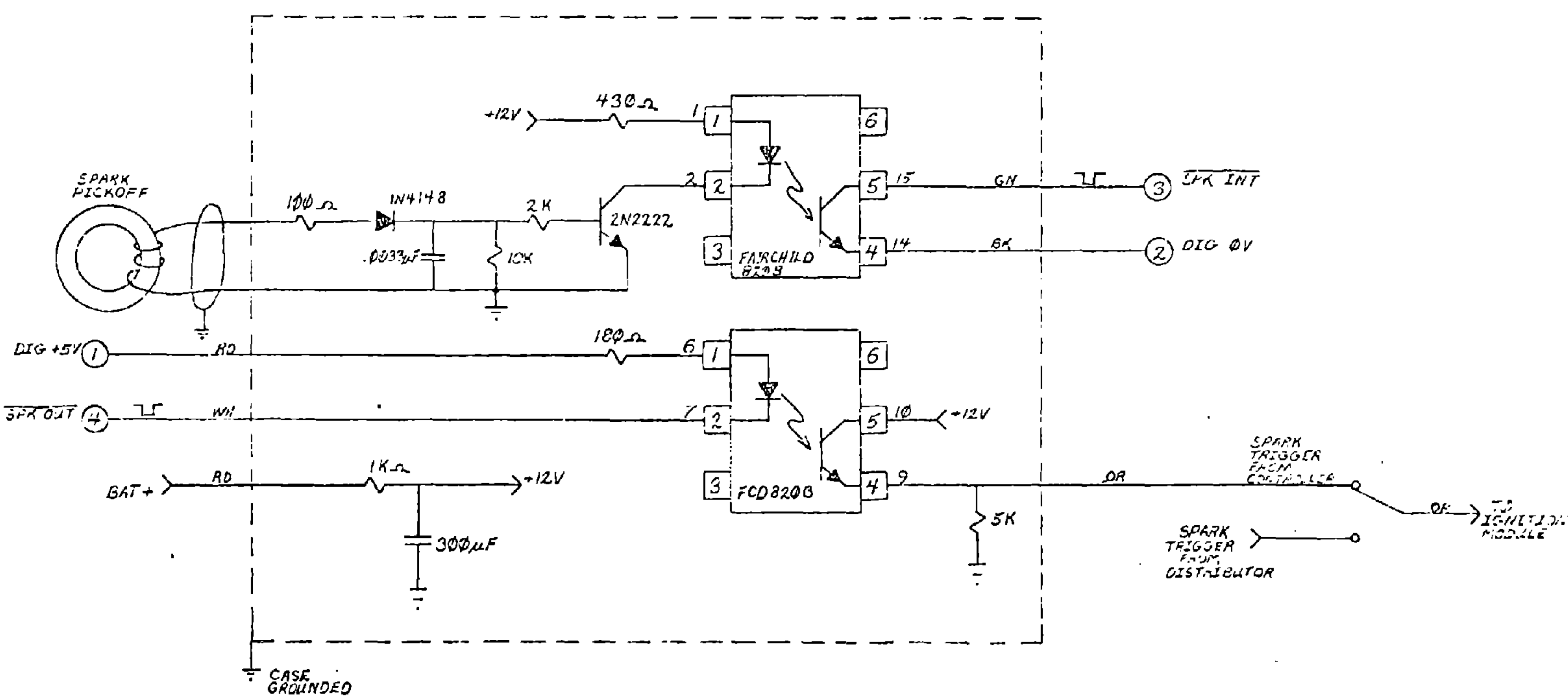

NOTES:

1) ◯ = 15 PIN, FEMALE, AMPHENOL CONNECTOR TO CONSOLE CARD #5

2) ON FCD820B, NUMBERS IN BOXES ARE I.C. PIN NUMBERS AND NUMBERS OUTSIDE OF BOXES ARE 16 DIP SOCKET PIN NUMBERS

FIGURE I-3

UNLESS OTHERWISE SPECIFIED

1. DIMENSION IN INCHES AND DEGREES
2. TOLERANCES .XX±.01 .XXX±.005 ANGLES ±.25°
3. DRILLED HOLES +.003 −.001
4. MACHINED FINISH √MAX
5. MACHINED FILLETS .008 R. MAX
6. DIAMETERS CONCENTRIC WITHIN .00 TIR
7. DEBURR. REMOVE SHARP EDGES .005 MAX. R. OR CHAMFER
8. RESISTANCE IN OHMS. CAPACITANCE IN MICROFARADS

MATERIAL

SURFACE TREATMENT

RELEASE DATE 9-3-78
ENGR. R. HOSEY
DRAWN MJH
CHECKED

DESCRIPTION | DWG. OR PART NO. | REQ. PER ASSY | ITEM NO.

GUIDANCE & CONTROL LABORATORY
STANFORD UNIVERSITY

TITLE TEST ENGINE SPARK TIMING CONTROL IGNITION SYSTEM ISOLATER BOX

SIZE B DWG. NO.

SCALE | WEIGHT | SHEET OF

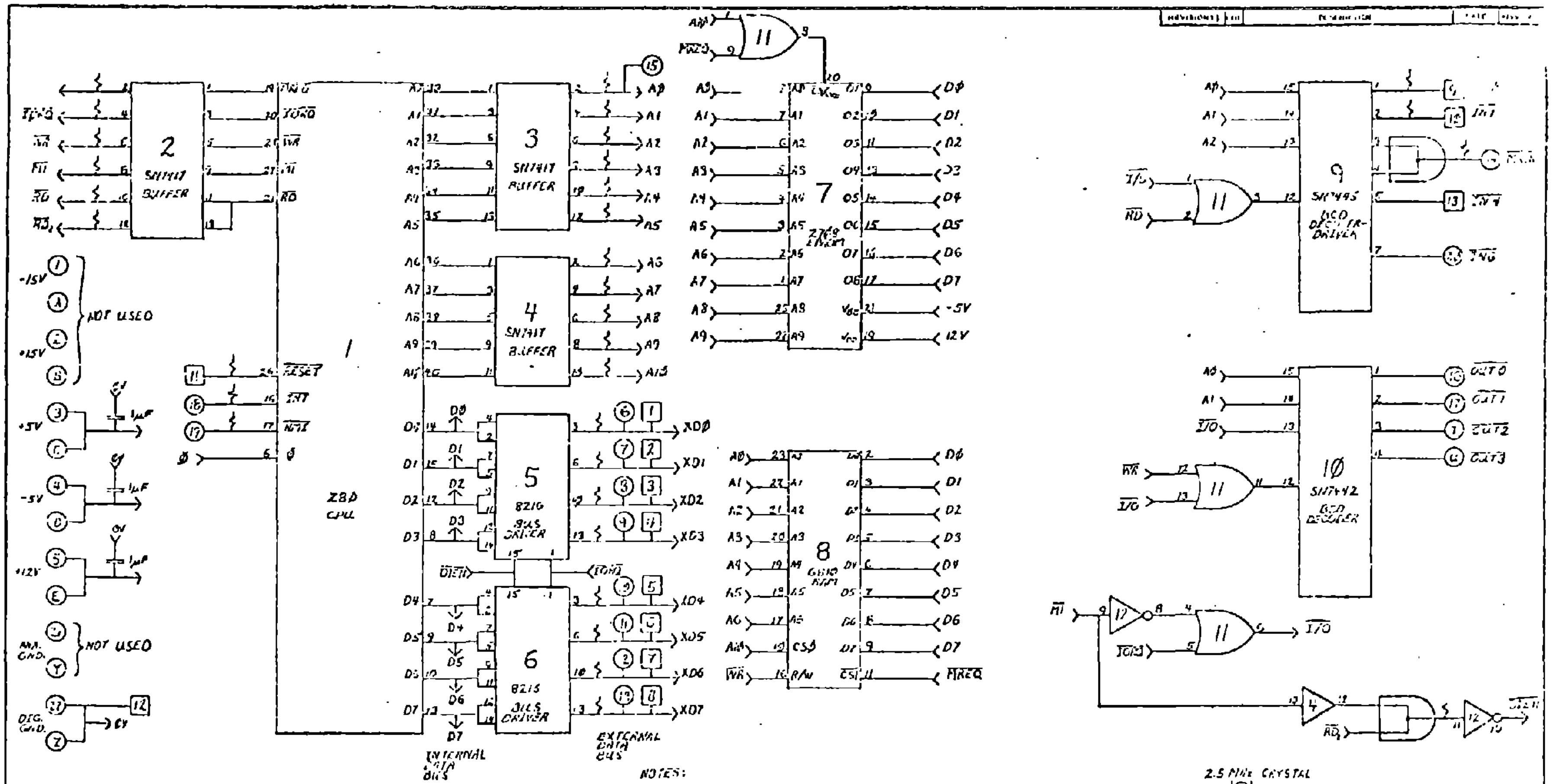

I.C.	TYPE	DESCRIPTION	ØV PINS	5V PINS	CURRENT (mA) TYP.	MAX.	DIP
1	Z80	CPU	29	11,25,24		220	40
2,3,4	SN7417	HEX BUFFER	7	14	29	41	14
5,6	8216	BIDIRECTIONAL BUS DRIVER	8,1	16	95	130	16
7	2708	EPROM	13,12	24	6	10	24
8	6810	RAM	1,12,14,15	24,13			24
9	SN7445	BCD DECODER-DRIVER	8	16	43	70	16
10	SN7442	BCD DECODER	8	16	19	28	16
11	SN7432	QUAD 2-INPUT OR	7	14	23	38	14
12	SN7404	HEX INVERTER	7	14	18	33	14

NOTES:

1) CARD IS DOUGLAS ELECTRONICS, INC. 12-DE-6, 4½"X6"
2) I.C.'s IN SOCKETS
3) RESISTORS ARE 10%, ¼ WATT
4) ◯ = CARD EDGE CONNECTOR PINS
5) ☐ = 15 PIN, MALE, AMPHENOL CONNECTOR
6) resistor symbol = 1KΩ pull-up to +5V
7) POWER SUPPLY CAPACITORS ARE 1µF CERAMIC

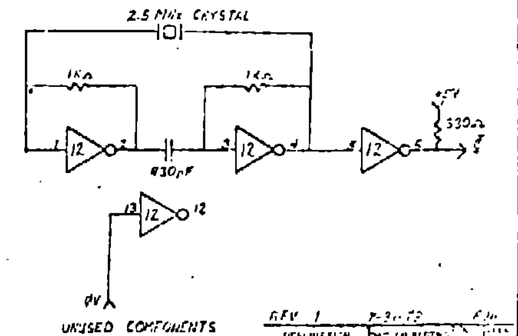

FIGURE I-4

GUIDANCE & CONTROL LABORATORY
STANFORD UNIVERSITY

the 256 byte RAM occupies locations $400\text{-}4FF_{16}$. Circuitry for a 2.5 MHz crystal controlled clock is also provided.

Signal conditioning electronics for noise immunity and for timing compatibility are provided on the engine-computer interface card shown schematically on Fig. I-5. Both timing mark and spark detection pulses are filtered then buffered by a schmidt trigger inverter to minimize effects of noise pickup in the signal lines from the engine. In order to provide timing compatibility with the computer, the negative going edges of these signals are used to clock edge triggered flip-flops. The outputs of the flip-flops are wire-or'ed (negative logic) to the computer interrupt circuitry and they appear as data bits at input port #6: bit 0 is low for a timing mark interrupt and bit 1 is low for a spark detection interrupt. Input port 6 is a quad 2 to 1 multiplexor with tri-state output which will allow eventual expansion to two 4-bit input ports. The flip-flops are reset by the computer strobing output port 3. This circuitry is intended to provide for the following response to detection of either spark or a timing mark:

1) the flip-flop will be set, thus generating an interrupt request;
2) the computer interrupt service routine will read input port 6 to determine which event is generating the interrupt;
3) the computer will strobe output port 6 to reset the flip-flops and remove the interrupt request.

Circuitry is also provided on this card for transmitting a spark ignition trigger. A 5μsec pulse is required to turn on the LED in the optically coupled isolator in the spark triggering circuitry; therefore a one-shot is used to provide a pulse of sufficient duration in response to a computer instruction to output to port 2.

Primary data collection and engine test stand control are provided by a NOVA-3 minicomputer which communicates with the spark timing computer through the interface circuitry shown in Fig. I-6. Twelve bits of data are transmitted from the NOVA to the spark timing computer so two 8 bit input ports are dedicated to reception of commands from the NOVA. Input port 2 receives the 8 least significant bits of data from the NOVA and input port 3 receives the next four significant bits of data in its four

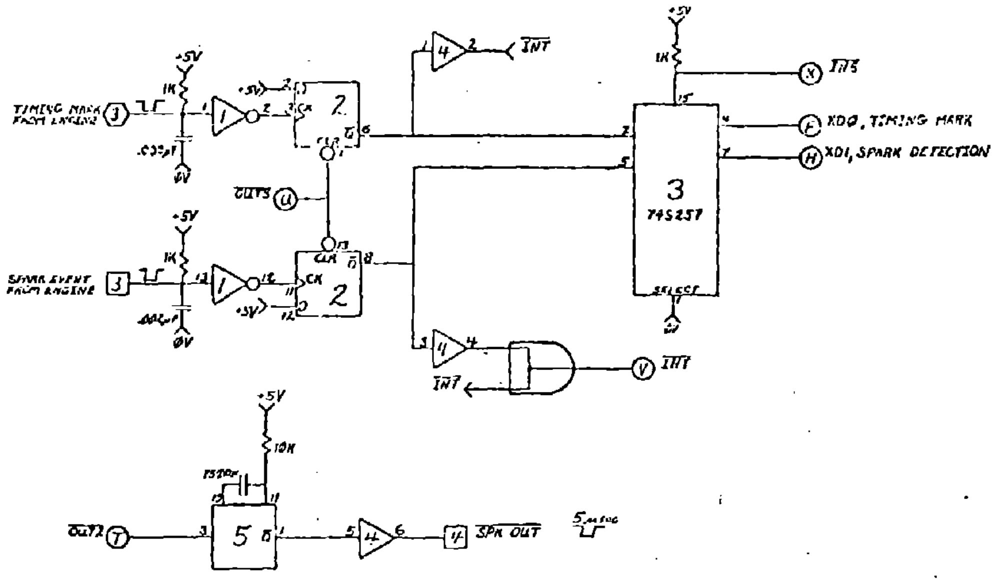

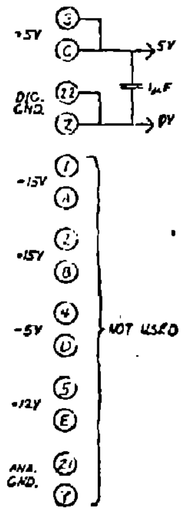

NOTES:

1) CARD IS DOUGLAS ELECTRONICS, INC. 12-DE-6, 4½" X 6"
2) I.C.'s IN SOCKETS
3) RESISTORS ARE 10%, ¼ WATT
4) ◯ = CARD EDGE CONNECTOR PINS
5) □ = 15 PIN, MALE, AMPHENOL CONNECTOR
6) ⬡ = 15 PIN, FEMALE, AMPHENOL CONNECTOR

I.C.	TYPE	DESCRIPTION	0V PINS	5V PINS	CURRENT (mA) TYP	CURRENT (mA) MAX	DIP
1	7414	HEX SCHMIDT TRIGGER INVERTER	7	14	30	48	14
2	7474	DUAL FLIP-FLOP	7	14	17	39	14
3	74S257	QUAD 2-TO-1 MX	8	16	60	93	16
4	7417	HEX BUFFER	7	14	25	56	14
5	74121	ONE SHOT	7	14	13	25	14

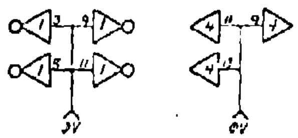

UNUSED COMPONENTS

FIGURE I-5

UNLESS OTHERWISE SPECIFIED

GUIDANCE & CONTROL LABORATORY
STANFORD UNIVERSITY

TEST ENGINE CONTROL
SPARK TIMING CONTROL
ENGINE INTERFACE CARD #5

K. HOLEY

C DWG. NO.

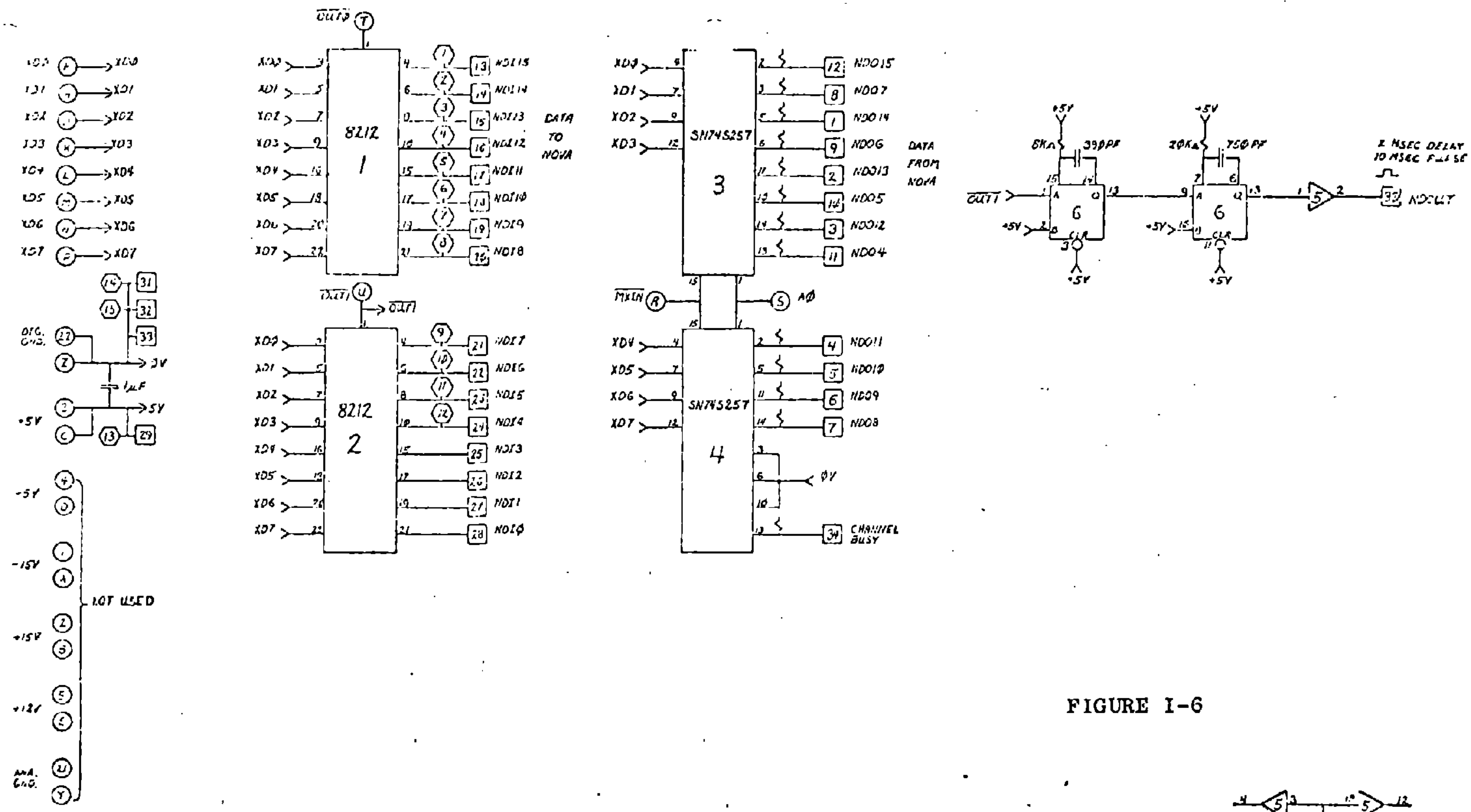

FIGURE I-6

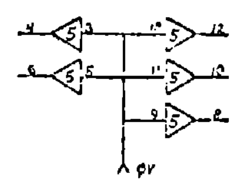

I.C.	TYPE	DESCRIPTION	ØV PINS	5V PINS	CURRENT(MA) TYP.	CURRENT(MA) MAX.	DIP
1,2	8212	TRI-STATE BUFFER	11,12	2,13,14,24	90	13Ø	24
3,4	SN74S257	MULTIPLEXOR	8	16	6Ø	93	16
5	SN7417	HEX BUFFER	7	14	21	30	14
6	SN74221	DUAL ONE SHOT	8	16	18	30	16

NOTES:

1) CARD IS DOUGLAS ELECTRONICS, INC. 12-DE-6, 4½"×6".
2) IC's IN SOCKETS.
3) ○ = CARD EDGE CONNECTOR PINS
4) □ = 37 PIN, FEMALE, AMPHENOL CONNECTOR PINS
5) ⬡ = 15 PIN, FEMALE, AMPHENOL CONNECTOR PINS
6) resistor symbol = +5V, 1KΩ, 10%
7) POWER SUPPLY CAPACITORS ARE 1μF CERAMIC.
8) USE MINIMUM CARD SPACE TO ALLOW FOR SUBSEQUENT EXPANSION.

GUIDANCE & CONTROL LABORATORY, STANFORD UNIVERSITY

TEST ENGINE SPARK TIMING CONTROL I/O

least significant bits. Figure I-7 is a schematic representation of the data transfer between the NOVA and the spark timing computer. The four most significant bits in the NOVA data word are used for control internal to the NOVA; therefore they are not transmitted to the spark timing computer. NOVA data is multiplexed from the NOVA data bus to various digital output ports. When the output port to the spark timing computer is selected, the channel busy signal goes high.

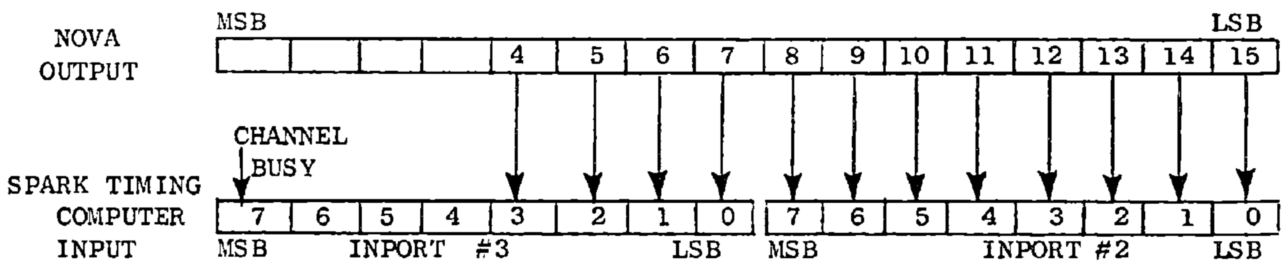

DATA TRANSFER TO SPARK TIMING COMPUTER

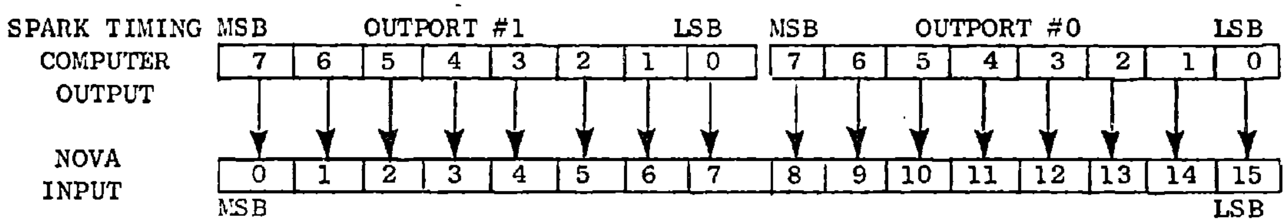

DATA TRANSFER TO NOVA

<u>NOTE</u>: NOVA data bits are numbered from 0 = most significant bit to 15 = least significant bit. Spark timing computer data bits are numbered from 0 = least significant bit to 7 = most significant bit.

Fig. I-7 Data Transfer between NOVA and spark timing computer.

This line is input as data bit 7 of input port #4 of the spark timing computer; therefore it may be used in the spark timing computer software to insure that the NOVA is not outputting new data while the spark timing computer is reading data, a situation which could result in the spark timing computer receiving a split data word.

Input ports 2 and 3 are implemented with two quad 2 to 1 multiplexors with tri-state output. The multiplexor chips are enabled when the $\overline{MXIN}$ line goes low. $\overline{MXIN}$ is a negative logic wire or of $\overline{IN2}$ and $\overline{IN3}$ signals (see Fig. I-4). The multiplexor channel is selected by address line A0 which is low when input port 2 is selected and high when input port 3 is selected.

Sixteen bits of data are transmitted to the NOVA from two spark timing computer output ports. Output port 0 transmits 8 bits of data to the 8 least significant bits of the NOVA 16-bit input port, and output port 1 transmits the eight most significant bits of data to the NOVA (see Fig. I-7). These two output ports are implemented with 8212 tri-state buffers. The output port #1 strobe is also used to activate a time delayed pulse to the NOVA which is used to strobe 16 bits of data into the NOVA data receiving hardware. The transmission of data from the spark timing computer to the NOVA is expected to follow this sequence:

1) the eight least significant bits of data are output to output port 0;
2) the eight most significant bits of data are output to output port 1;
3) a two millisecond delay ensures that the 16 bits of output data will stabilize on the transmission lines from the spark timing computer to the NOVA;
4) the ten millisecond pulse is used by NOVA hardware to latch sixteen bits of stable data.

Also note that the "channel busy" signal is high when the NOVA is reading data from the spark timing computer; so spark timing computer software may monitor this signal to ensure that the NOVA is getting good data; however, the hardware interface between the two computers should ensure that the NOVA never receives a split data word.

The 12 least significant bits of data which are transmitted to the NOVA are also displayed on the front panel of the operator console which houses the spark timing computer. Figure I-8A is an electrical schematic of the wiring for the three BCD, LED displays.

Figure I-8Bis an electrical schematic of the switches mounted on the front panel of the operator console for local control of the spark timing computer. The RUN-RESET switch grounds the $\overline{\text{RESET}}$ line of the Z-80 CPU, thus initializing the computer so that the program may start when the switch is set to the RUN position. The COMPUTER-LOCAL-ENTER switch is monitored by spark timing computer input port 4. When bits 0 and 1 of input port 4 are high, the switch is in the LOCAL position, when bit 1 is low, the switch is in the ENTER position and when bit 0 is low the switch is in the COMPUTER position. Two hexadecimal switch assemblies are mounted on the operator console for local operator input to the spark timing computer. These switches are monitored as input port 0 and input port 1. The diodes prevent the shorting together of the data bus lines through the switch "common." Note that the input from these switches is negative logic; therefore computer software should 1's complement data from input ports 0 and 1.

Figure I-9 summarizes spark timing computer I/O port assignments. Fig. I-10A is an electrical schematic of rack wiring for the TEST ENGINE CONSOLE which houses the spark timing computer in card slots 3,4 and 5. Fig. I-10B shows the physical layout of cards 3,4 and 5 which contain the spark timing computer CPU, NOVA interface and engine interface electronics.

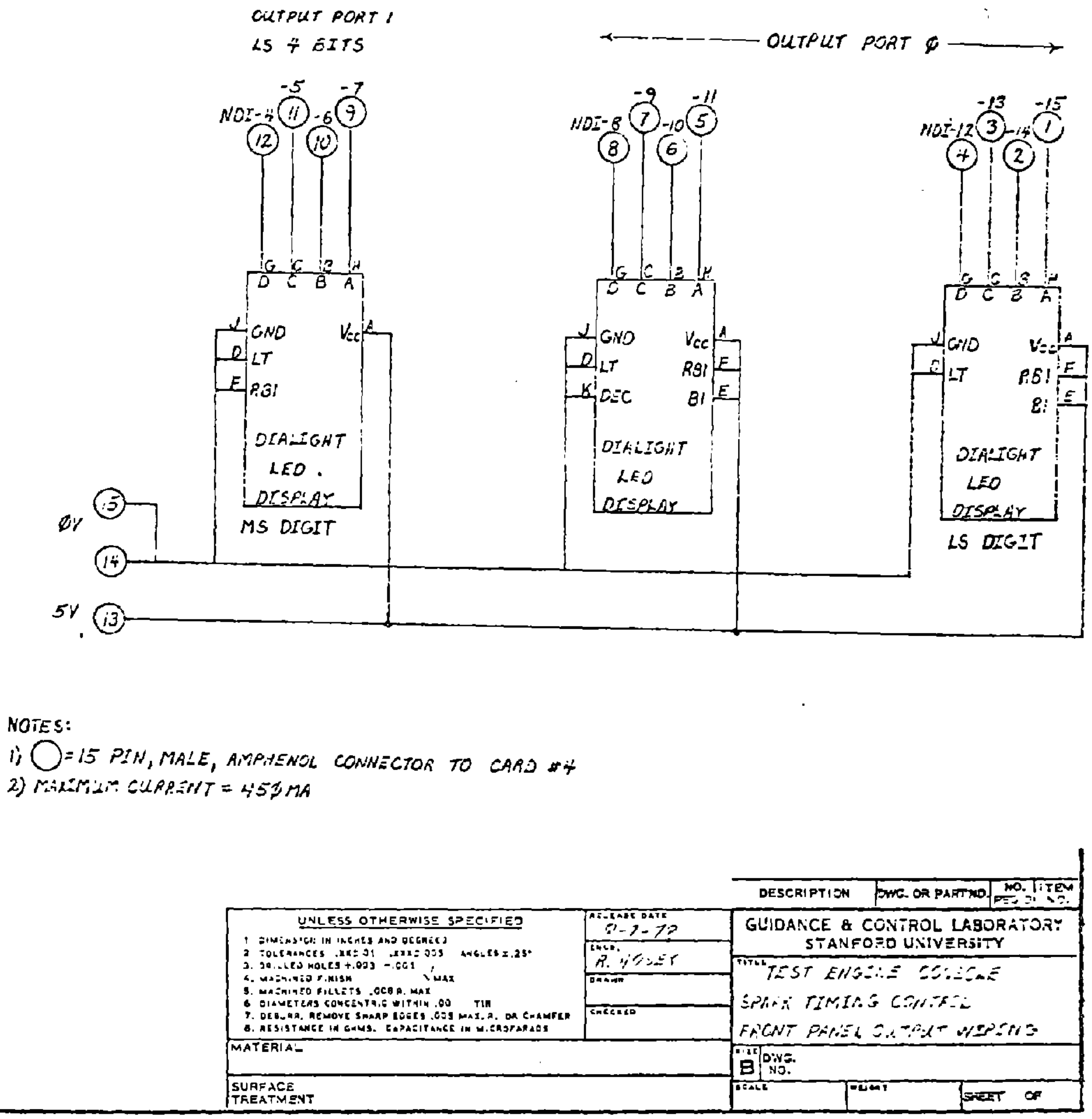

Fig. I-8A FRONT PANEL DISPLAY WIRING

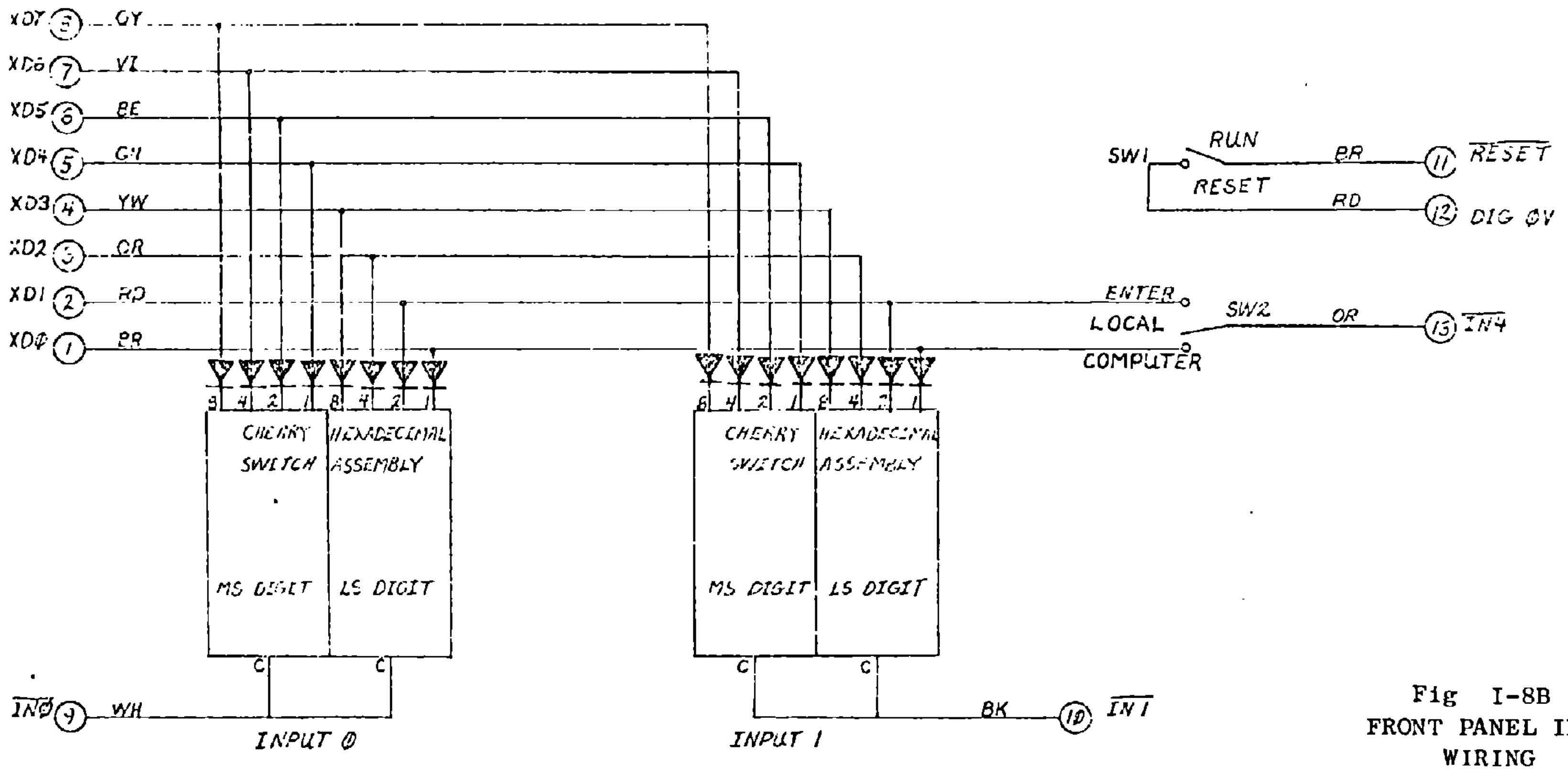

Fig I-8B
FRONT PANEL INPUT WIRING

NOTES:
1) SW1 IS SPST
2) SW2 IS 3 POSITION, MOMENTARY IN THE "ENTER" POSITION
3) DIODES ARE IN4148
4) ◯ = 15 PIN, FEMALE, AMPHENOL CONNECTOR TO CARD #3

DESCRIPTION	DWG. OR PART NO.	NO. REQ'D	ITEM NO.

UNLESS OTHERWISE SPECIFIED
1. DIMENSION IN INCHES AND DEGREES
2. TOLERANCES .XX±.01 .XXX±.005 ANGLES ± .25°
3. DRILLED HOLES +.003 −.001
4. MACHINED FINISH √MAX
5. MACHINED FILLETS .005 R. MAX
6. DIAMETERS CONCENTRIC WITHIN .00 TIR
7. DEBURR, REMOVE SHARP EDGES .005 MAX. R. OR CHAMFER
8. RESISTANCE IN OHMS. CAPACITANCE IN MICROFARADS

RELEASE DATE: 8-3-72
ENGR.: HOSEY
DRAWN:
CHECKED:

GUIDANCE & CONTROL LABORATORY
STANFORD UNIVERSITY

TITLE: TEST ENGINE CONSOLE
SPARK TIMING CONTROL
FRONT PANEL INPUT WIRING

MATERIAL
SURFACE TREATMENT

SIZE B DWG. NO.
SCALE WEIGHT SHEET OF

INPUT	PORTS
0	"INPUT 0" hex switch
1	"INPUT 1" hex switch
2	NOVA to spark timing computer least significant 8 bits
3	NOVA to spark timing computer most significant 4 bits
4	Console COMPUTER-LOCAL-ENTER switch
6	Interrupt flag word

OUTPUT	PORTS
0	Spark timing computer to NOVA and operator console display least significant 8 bits
1	Spark timing computer to NOVA most significant 8 bits and operator console display most significant four bits
2	Spark trigger
3	Interrupt flip-flops reset

Fig. I-9 Spark Timing Computer I/O Port Assignments

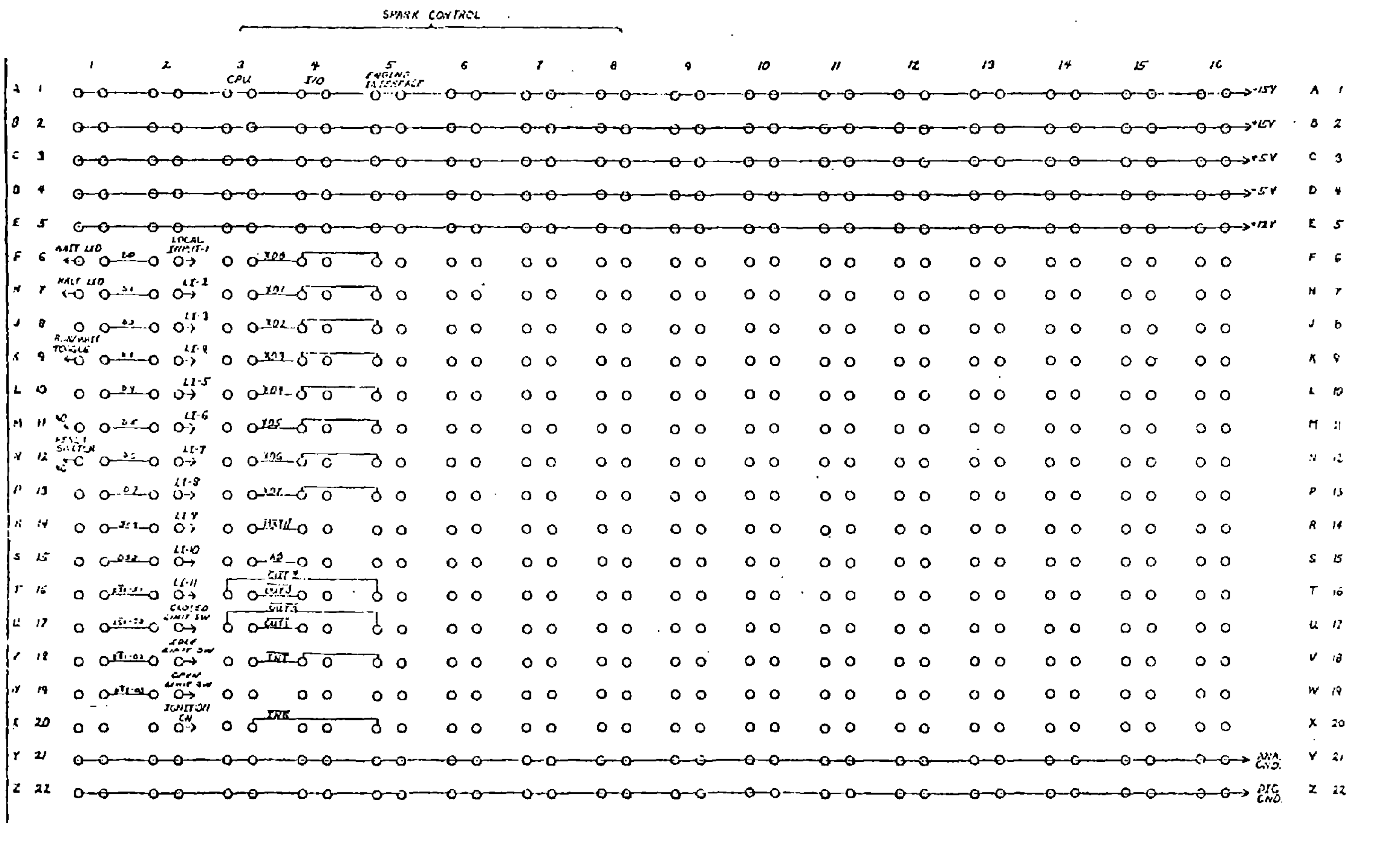

FIG.I-10A TEST ENGINE CONSOLE RACK WIRING

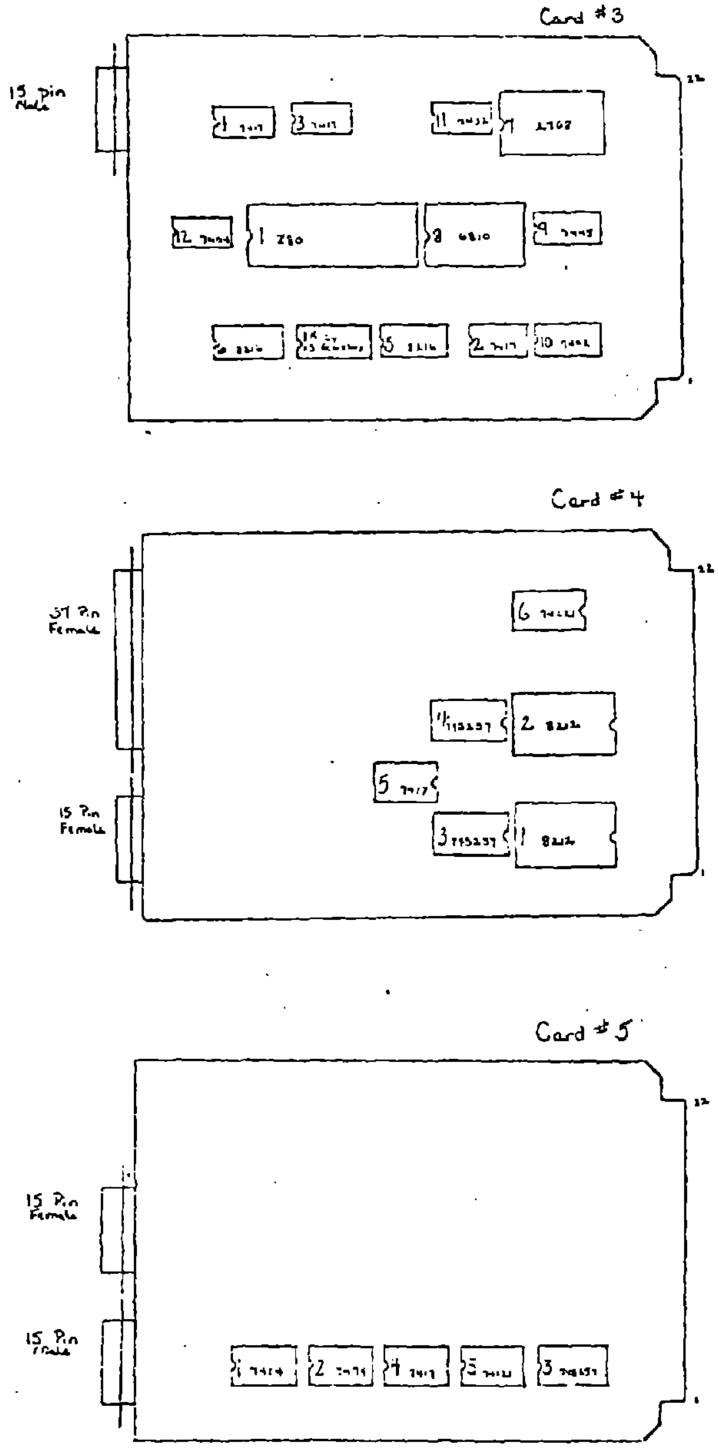

Fig. I-10B Test Engine Console Spark Controller Cards 3,4,5 Layout

3. Software

a. Outline

The software is organized as two interrupt driven programs: one program collects spark timing data when spark advance is controlled by the distributor; while the other program controls the spark timing to give a desired spark advance for engine mapping. The interrupts are generated by the crank angle reference optical pickoff at 60^{o}BTDC and 120^{o}ATDC and by spark discharge on the #1 cylinder. One of these two programs is selected during software initialization.

Both programs work on the basis of correspondence between time and engine cycle position at constant or slowly changing engine speeds as illustrated in Fig. I-11. In this figure it can be seen that the ratio of time-to-go 40^{o} to time-to-go 180^{o} is equal to the ratio of 40^{o} to 180^{o}; i.e., 1.3 msec/6msec = $40^{o}/180^{o}$ = .222. In the software provided with the spark timing computer, counters are used as timers. An LDIR instruction is used for counting which gives a count or "tick" of 21 T-states of the Z80 CPU; so a tick is 8.4 microseconds with the 2.5 megahertz clock. At 5000 RPM a tick corresponds to .25 degrees of crankshaft rotation.

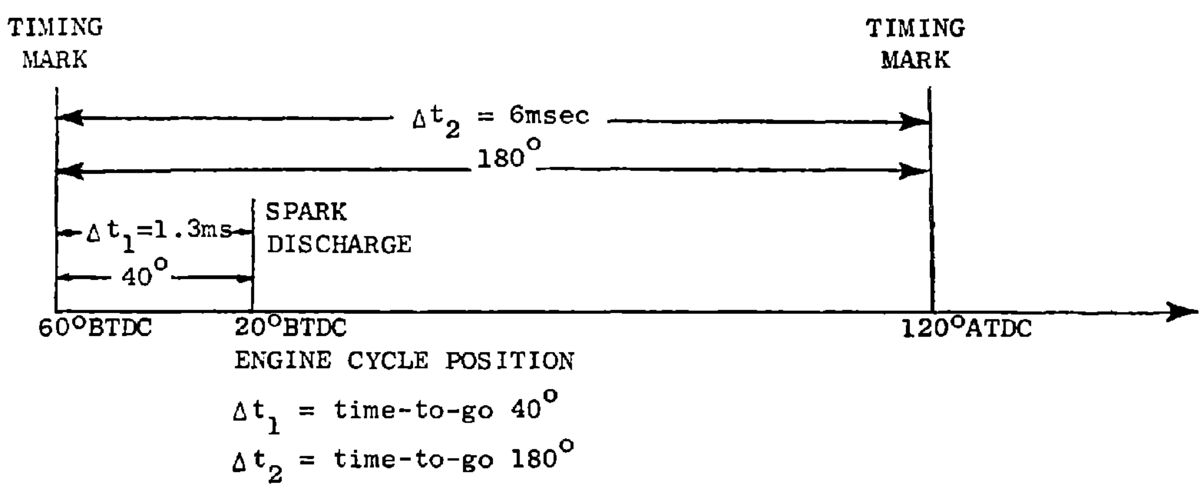

Fig. I-11 Correspondence between time and engine cycle position at 5000 RPM.

The following abbreviations are used for the various timers:

CTOSPK = counts from 60^{o}BTDC to #1 cylinder spark discharge;

CYISPT = counts from 60^{o}BTDC to spark trigger command for spark timing control;

CSPTRF = counts from spark discharge to 120^{o}ATDC reference;

C180 = counts for 180^{o} crankshaft rotation from 60^{o}BTDC to 120^{o}ATDC.

When the computer is used for acquisition of spark timing data, the following sequence is used for calculation of spark timing:

1) the time from the 60^{o}BTDC timing mark to the detection of the spark discharge (CTOSPK) is stored;
2) the time from spark discharge to the 120^{o}ATDC timing mark (CSPTRF) is added to CTOSPK to give the time for 180^{o} of crankshaft rotation (C180);
3) spark advance (SA) is calculated using the equation:

$$SA = 60^{o} - 180^{o}*(CTOSPK/C180) \quad . \qquad (I-1)$$

When the spark timing computer is used for control of spark advance, the software produces the following sequence:

1) the desired spark advance is input either through the console switches or from the digital input port from the NOVA;
2) A spark timing ratio (CYISPR) is calculated from the desired spark advance (DESSA):

$$CYISPR = (60^{o}-DESSA)/180^{o} \quad ; \qquad (I-2)$$

3) The time for 180^{o} of crankshaft rotation is measured; then the spark timing ratio is used to calculate the number of timer ticks (CYISPT) which is required to give the desired spark advances:

$$CYISPT = CYISPR*C180 \quad ; \qquad (I-3)$$

4) When the 60^{o}BTDC interrupt occurs, the timer is decremented to 0 at which time the spark trigger command is output. The 60^{o}BTDC timing mark is used for timing the #1 and #4 cylinders. The #2 and #3 cylinders are timed by starting the timer at 120^{o}ATDC which is also 60^{o}BBDC. Distribution of the spark is determined by distributor rotor position.

Initialization Software

Figure I-12 is a block diagram of the initialization software. After the stack register is initialized, the hexadecimal switches (LEFTSW) on the console front panel are input. If the operator has entered "FF," then the computer will run the spark advance data collection program. This program is selected by storing the address of the interrupt service routine for the data collection program into index register IY. All interrupts are serviced with a jump indirect through index register IY.

Similarly, if the operator has entered any number except "FF" into the switches, the spark advance control program is selected by storing the address of the interrupt service routine for spark timing control into index register IY. In order to change from data collection to control or vice versa, the software must be reinitialized.

For spark advance control, the number entered by the operator is used by the software as the desired spark advance (DES.SA) for calculation of the spark ratio (SPKRAT) for initial engine timing. Initialization for spark timing control is completed by the interrupt driven routine which is block diagrammed in Fig. I-13. This routine times for half of a crankshaft rotation to get a value for C180, then calculates initial values for the counts required to give the desired spark advance (CYISPT, etc.). Control is then passed to the spark timing control interrupt servicing software by setting register pair IY equal to RSPCON.

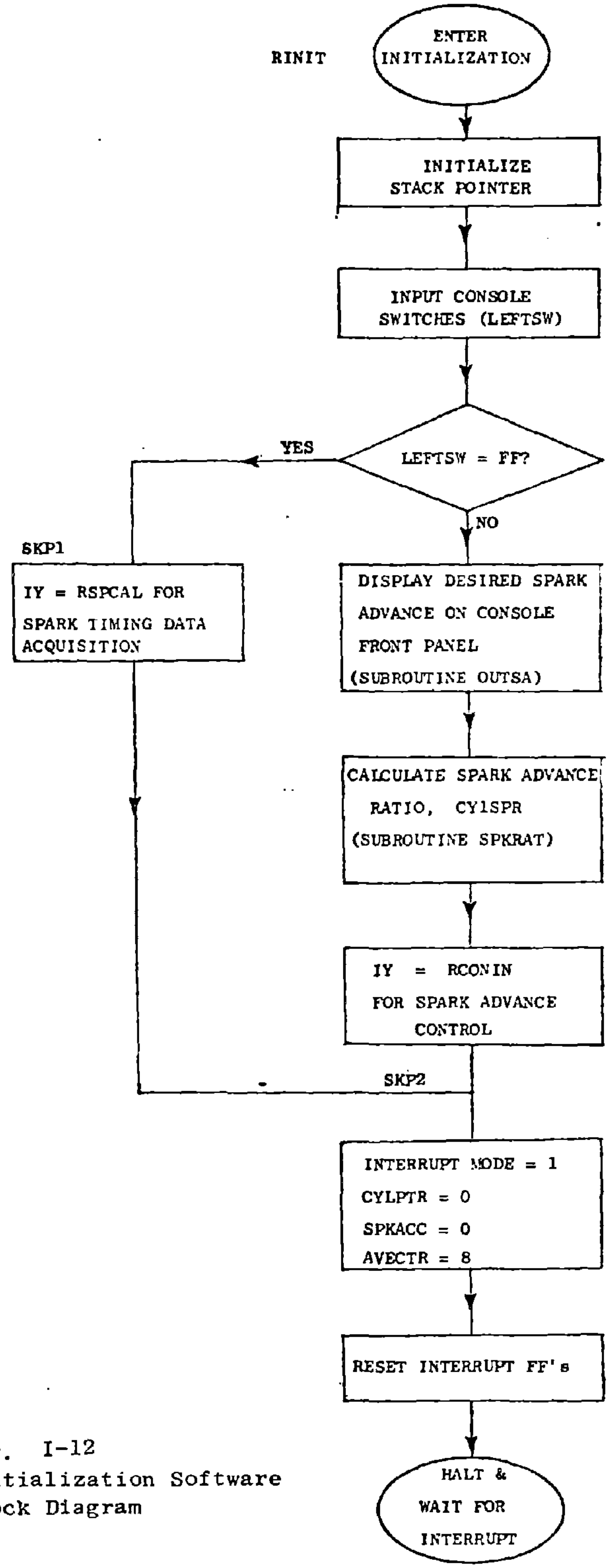

Fig. I-12
Initialization Software
Block Diagram

Fig. I-13 SPARK CONTROLLER INITIALIZATION

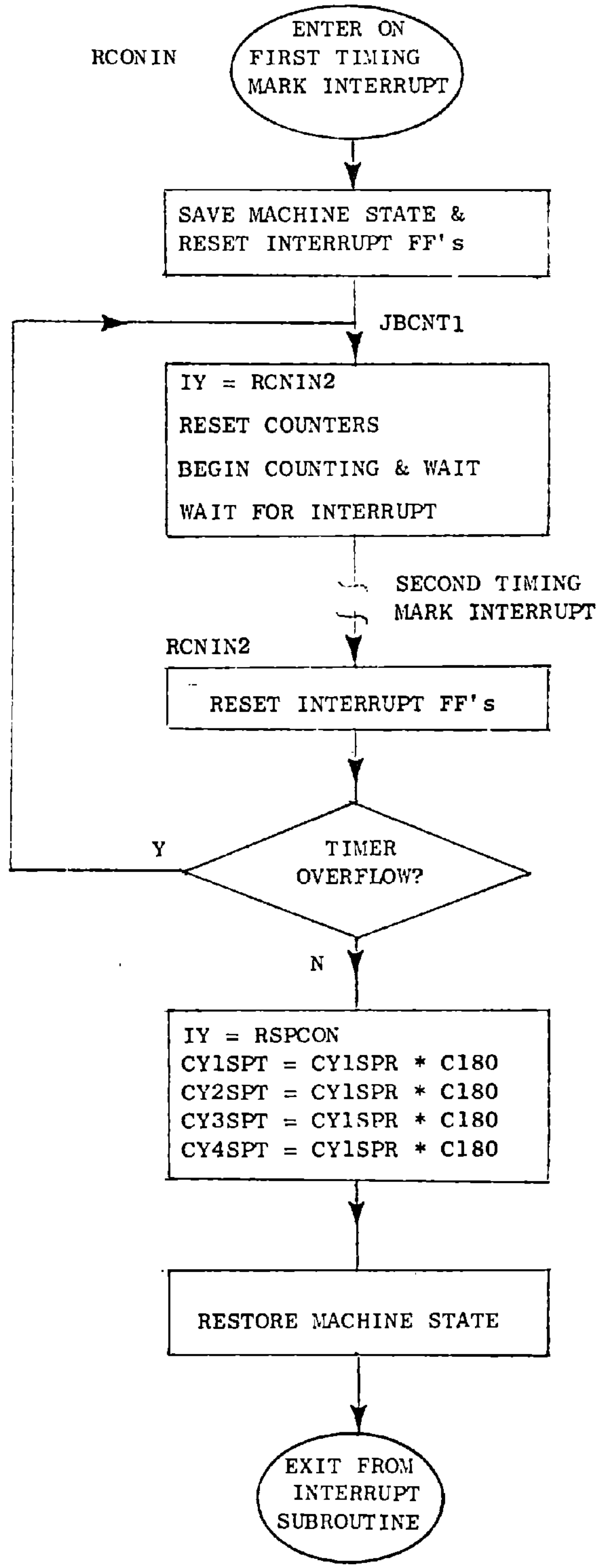

b. Spark Timing Control Software

Figure I-14 is a block diagram of the spark timing control interrupt service software. When the interrupt is generated by a timing mark, the computer counts down the spark advance timer to zero, at which time the spark trigger is output. A spark advance timer is maintained for each cylinder (CY1SPT, CY2SPT, etc.) to facilitate the implementation of spark advance control for individual cylinders; although this feature has not been implemented in the current software. Additionally a cylinder pointer (CYLPTR) is maintained by the software. This pointer is initialized to 1 by detection of the #1 cylinder spark plug discharge. The pointer is incremented each time a timing mark interrupt occurs; so the pointer may be used by the software to keep track of the spark timers for individual cylinders. Additionally this pointer may be used to relate peak cylinder pressure timing data to individual cylinders.

After the spark is triggered, the machine state is restored except for register pair BC which is set equal to one. If an LDIR counting loop has been interrupted by the timing mark detection, then setting BC equal to one will pop the program out of the counting loop upon the return from the interrupt.

If the #1 cylinder spark plug discharges (distribution of the spark is determined by the distributor rotor position) then a spark discharge interrupt will be generated. The cylinder pointer is reset to one, and an LDIR counting loop is started. The LDIR counting loop is interrupted by the next timing mark interrupt, at which time register pair HL will contain the counts from spark output to the timing mark (CSPTRF). After outputting the spark trigger to the next cylinder, the timing mark interrupt routine pops the spark routine out of the LDIR timing loop by loading register pair BC = 1. If the timer count is greater than 2^{15}, then the initialization routine is repeated. This provides a recovery capability should engine speed drop below 100 RPM. If there is no timer overflow, spark timing counts for each cylinder are calculated. Finally desired spark advance is input, spark ratio for the next cycle is calculated, the machine state is restored and a return from interrupt subroutine is implemented.

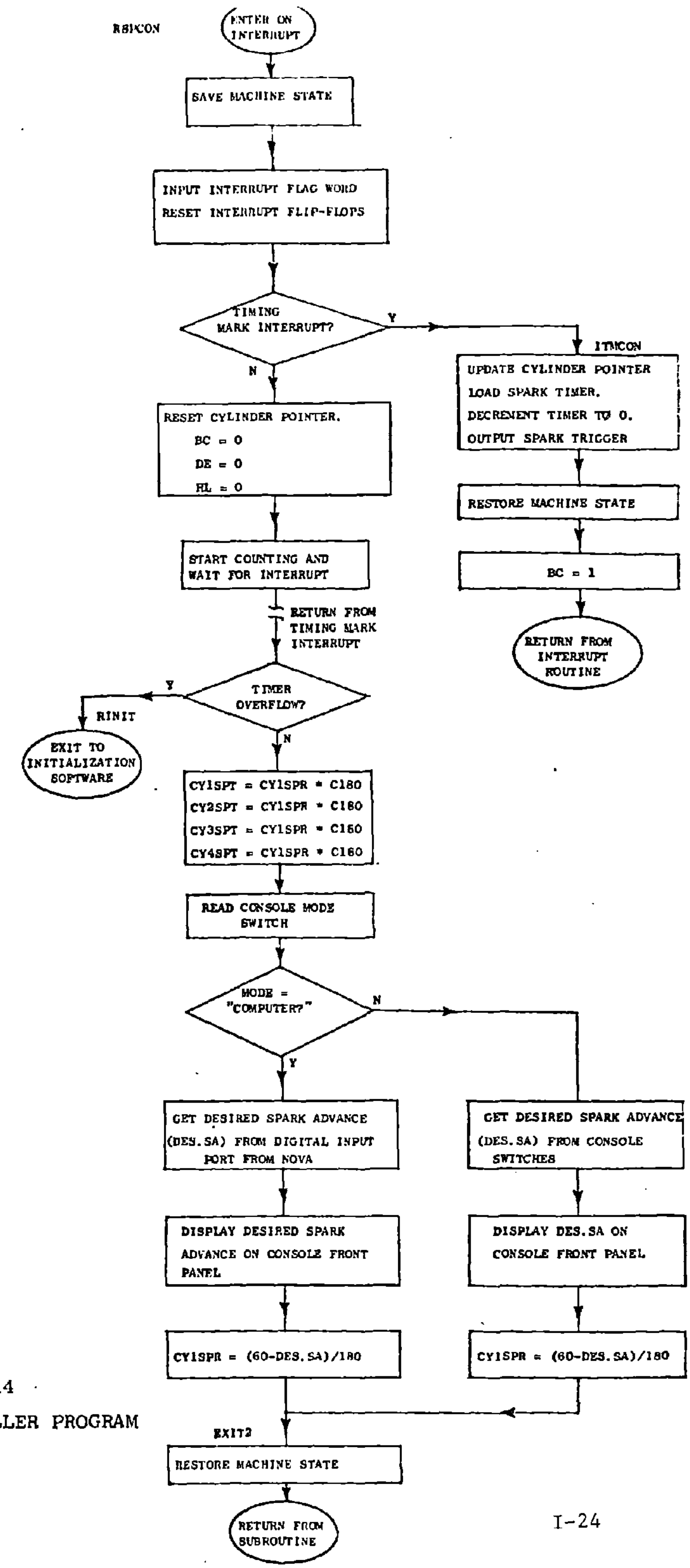

Fig. I-14

SPARK CONTROLLER PROGRAM

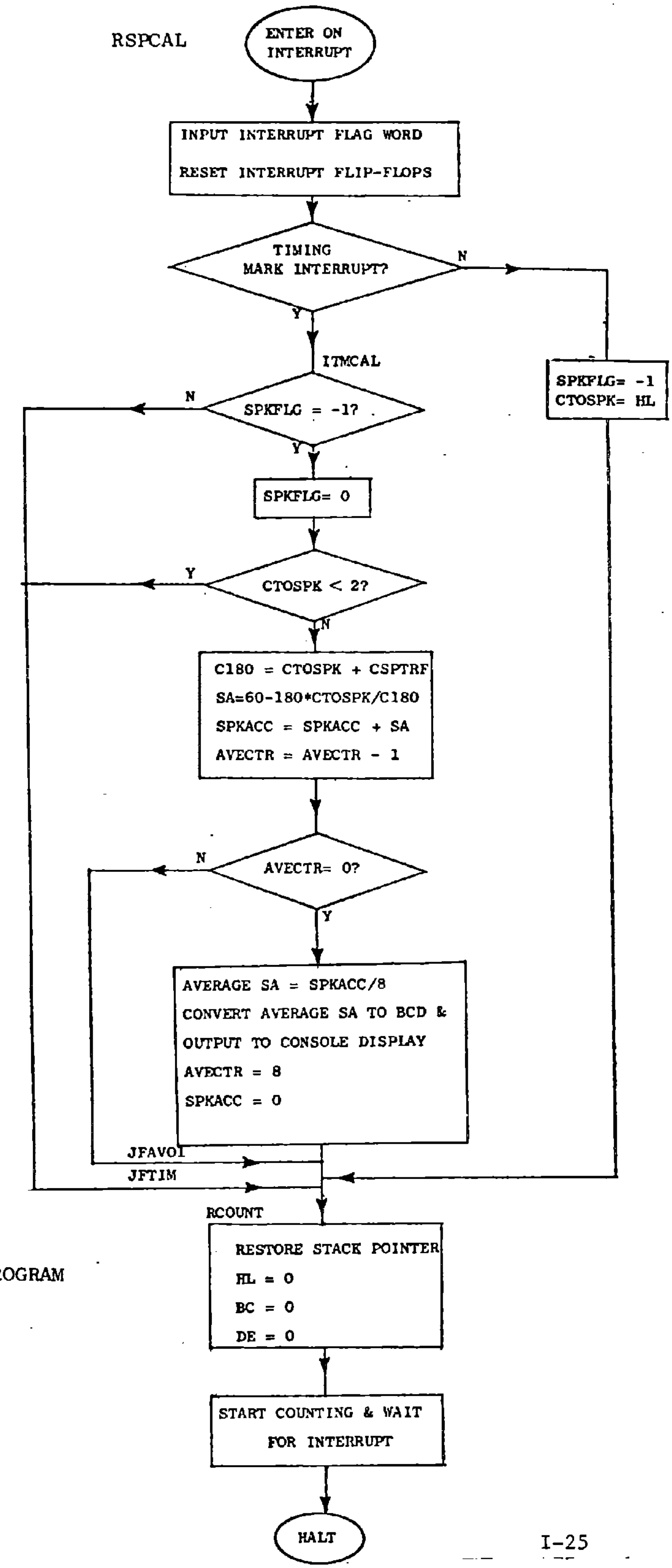

Fig. I-15

SPARK CALCS PROGRAM

c. Spark Timing Data Acquisition Software

Figure I-15 is a block diagram of the spark timing data collection software. The interrupt flag word is input, then the the interrupt flip-flops are reset. The interrupt flag word is tested to determine whether the interrupt was generated by a timing mark or by the #1 cylinder spark discharge. If the interrupt was generated by the spark discharge, a spark discharge flag (SPKFLG) is set, the counts from the 60^{o} BTDC timing mark to the spark discharge (CTOSPK) are saved, then the timers are reinitialized and restarted.

If the interrupt is generated by a timing mark, then SPKFLG is tested. If SPKFLG is set, then CTOSPK has just been updated and the timer contains the counts from spark discharge to the 120^{o}ATDC timing mark (CSPTRF); so spark advance may be calculated. Occasionally the spark discharge generates two digital pulses which are transmitted to the computer, and CTOSPK contains the time between these pulses. In order to prevent calculation of erroneous spark advances, CTOSPK is tested for a minimum value indicating that it contains good data. If CTOSPK contains good data then spark advance is calculated. In order to smooth the operator console display, spark advance is averaged over eight engine cycles. The counter AVECTR is used to count eight engine cycles and the spark advances for eight cycles are accumulated in SPKACC. After eight cycles, the average spark advance is output to the NOVA and to the operator console and AVECTR and SPKACC are reinitialized.

Appendix J

DIGITAL CONTROL OF AN ENGINE ON A DYNAMOMETER TEST STAND

I. DYNAMOMETER CONTROL

1. Introduction

As described in various other sections of this report, the automated, engine-test system was intended to reduce the operator workload while enabling smoother data to be taken. In a completely manual system each data point may take from 30 to 45 minutes while the operator must first establish a steady operating condition in terms of engine torque, RPM, spark advance, EGR, and fuel/air (F/A) ratio, then reads each measurement once with "eye-ball" smoothing. The cost of obtaining enough data points with sufficient accuracy to generate meaningful regression curve-fits should be apparent.

In the system described in this report the engine power point was automatically held to within ± 1 RPM and ± 1 Ft-lb torque over the entire operating range, independent of other external operating parameters (e.g., spark advance, EGR, F/A ratio and temperatures). Once temperatures stabilized, the desired measurements were automatically sampled many times and averaged, generating statistically smoother, more usable data.

A variety of automated, engine-test systems have been developed for reciprocating and turbine engines, for data collection and endurance testing. Several very general overviews exist in the literature which describe the makeup of systems in use at several major manufacturer laboratories: Ford [L-1], Detroit Diesel [W-1], GM Research [C-2,C-3].

This section of the report will present that portion of the engine-test system associated with the control of torque and RPM. The discussion will present the reader with the major aspects of component dynamics and control strategies. A more detailed discussion of the hardware, software and control analysis along with a full discussion of the "Servo Application of a Microprocessor-Based Stepper Motor Controller" will be available in the form of an Engineer Thesis later this year by Richard Boucher.

2. Background

The system to be controlled (as shown in Fig. J-1 consisted of the 4 cylinder Ford Pinto engine with two outputs: torque and RPM; the analog speed controlled dynamometer; the throttle servo (described in detail in Sec. J.II) and the main control computer (a NOVA minicomputer).

For purposes of control, the engine and dynomometer are treated together. They are coupled through fourth gear of a standard transmission giving a 1:1 speed ratio. The dynamometer speed is measured by a digital tachometer/counter using a 0.5 sec update rate. The output is converted to a four digit BCD value for local display and transmission to the NOVA minicomputer, and converted to a voltage level for use by the speed controller.

The engine torque is not measured directly but rather as a reaction torque measurement on the dynomometer casing. Thus the relation between measured torque, T_M, and actual engine torque, T_E, is a dynamic one:

$$T_E - T_M = J\dot{\omega} \quad . \qquad \text{(J-1)}$$

J represents the total moment of inertia of all coupled, rotating parts in the engine, drive train and dynomometer, while $\dot{\omega}$ is the rotational (angular) acceleration. In the static state

$$\dot{\omega} = 0 \Rightarrow T_M = T_E \quad , \qquad \text{(J-2)}$$

but in the dynamic state where the engine/dynomometer is accelerating or decelerating

$$TM = T_E - J\dot{\omega} \quad . \qquad \text{(J-3)}$$

Here T_E may remain fairly constant while T_M varies wildly (as will be seen in the transient response (Figs. J-15 to J-22).

There are several parasitic loads placed on the engine which are functions of the rotational velocity and not the field voltage. One of these is termed the dynomometer "windage," which is actually the bearing friction. The reaction to this torque is mechanically summed with the field torque in the torque measurement, T_M, made at dynomometer casing. Other loads include drive-train friction, and dynomometer cooling-air pumping-torque from the armature fan, neither of which is measured and both of which are assumed to be small. The torque measurement is made by use of a linear, strain-guage type load-cell measuring the reaction force on the casing of the dynomometer. The signal is boosted yielding a 0-10v output which is equivalent to 0-130 ft-lb. Calibration is effected in the computer.

Engine torque measurement is inherently noisy. Induced engine vibration due to imbalance and mechanical linkages is seen but the primary contributor is the impulsive torque caused by each cylinder event. This noise cannot be completely damped by the mechanical damping as shown in Fig. J-2.. The analog torque signal conditioning included a single pole filter at 200 Hz to eliminate the higher frequency structural modes. Low frequency digital filtering is to be discussed later.

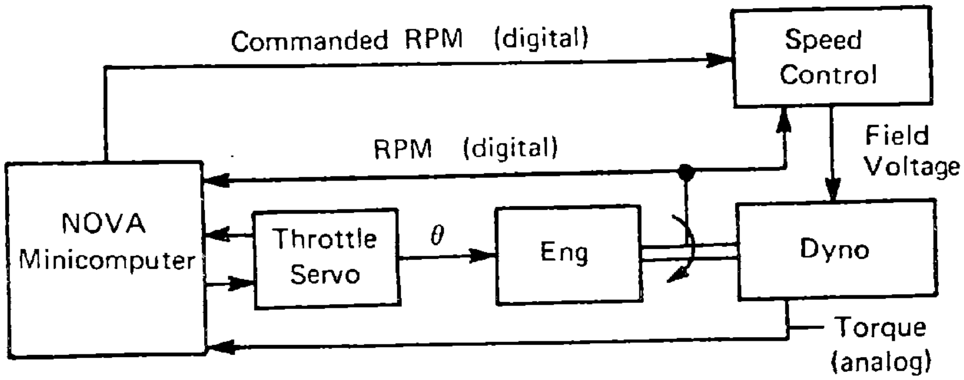

Eng/Dyno Control

Figure J-1

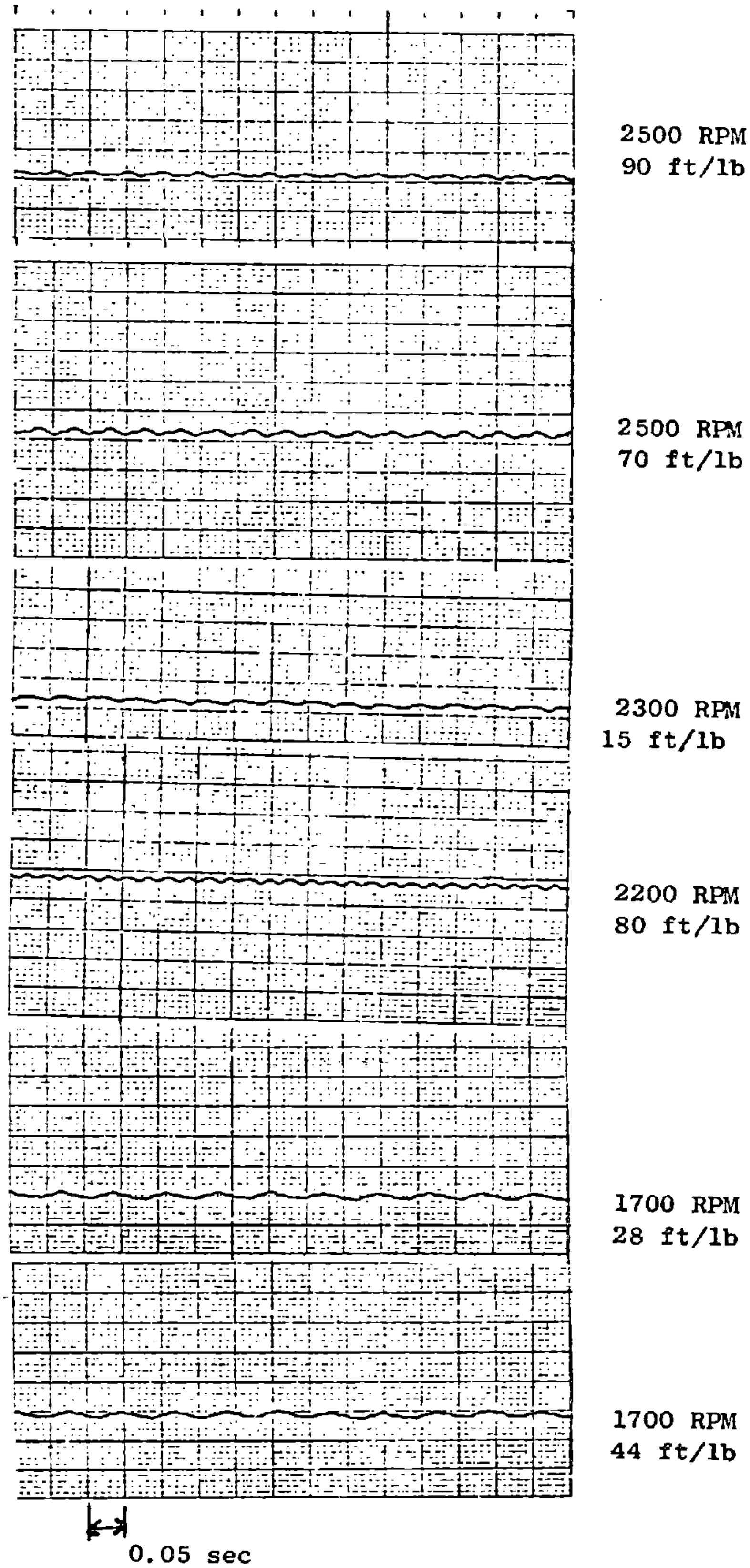

Fig. J-2 Recordings of Torque at Various Resonant Engine Speeds

T versus θ at RPM

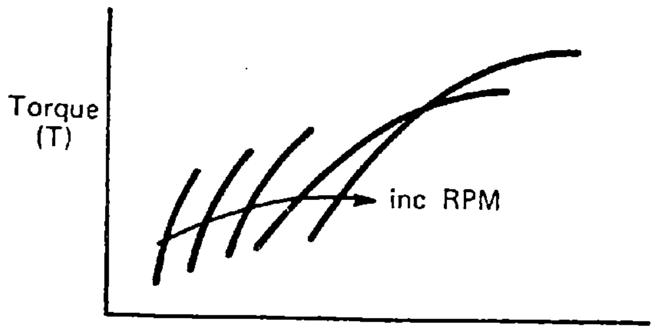

$$\left.\frac{dT}{d\theta}\right)_{\text{low power}} \approx 30 \text{ ft-lb/degree}$$

Figure J-3 T vs θ at Constant RPM

The engine/dynomometer speed is controlled by modulating the field voltage of the dynomometer while maintaining constant armature voltage. Increased field voltage yields increased load torque, resulting in reduced engine speed for a constant throttle setting. An analog speed controller was used which fedback the 0.5 sec. updated speed to implement integral compensation of the field voltage, yielding zero steady state speed error, regardless of other operating conditions. The speed controller accepts local operator inputs at the front panel, or computer inputs via transmission cable. RPM commands range from 0 to 5000 RPM with 1 RPM increments for front panel inputs and 10 RPM increments for computer inputs (12 bits, encoded BCD). Speed is displayed on the front panel in four digits with 1 RPM resolution and is available at the computer in 16 bits, encoded inverted BCD, with 1 RPM resolution.

3. Program Structure

The control programming was constructed in a multi-tasking environment using FORTRAN under the Data General Realtime Disk Operating System (RDOS) on a NOVA 3 minicomputer. A display of critical system variables was updated at the computer terminal every second. All command inputs were issued through the terminal keyboard. Commands of throttle position and RPM setpoint could be made in the open-loop mode, or engine torque and RPM in the closed loop mode. Output of various parameters may be made through D/A conversion to a stripchart recorder at a 10 Hz rate for a continuous recording of system dynamics.

Tasks in order of relative priority:

1. CLOCK - Time base generation for 10 Hz sample rate.
2. RBxCON- (x = version no.) - Control Logic.
3. GAIN 1- implements function
   GAIN = F(TORQUE,RPM): Compensation for normalization of nonlinear feedforward engine gain.
4. CONxIO- (x = version no.) - Command input acceptance, checking and conversion to a format usable by RBxCON.
5. DPYT - Terminal display of critical operating parameters made up of the following subroutines:
   - BCDTH - conversion of inverted BCD throttle position to decimal for display;
   - DSPLY - display of operating parameters.
6. DACOUT - Output of selected parameter through one of two D/A converters, with scaling and zero suppression.

4. Static and Dynamic Response of Hardware

A series of static engine runs were made to determine the open-loop torque of the engine as a function of RPM and throttle setting in degrees from fully closed. The general result of these runs is shown without scaling in Fig. J-3. These curves are a predominent result of the non-linear nature of the butterfly valve used in the automotive carburetor. The low power section of the curves (lower left corner) shows the high throttle sensitivity:

$$\left.\frac{\partial T}{\partial \theta}\right)_{RPM} \approx 30 \text{ ft-lb/deg} \quad , \qquad (J\text{-}4)$$

which generated the step resolution requirement for the throttle servo. The wide range of values for

$$\frac{\partial T}{\partial \theta} = F(RPM,\theta)$$

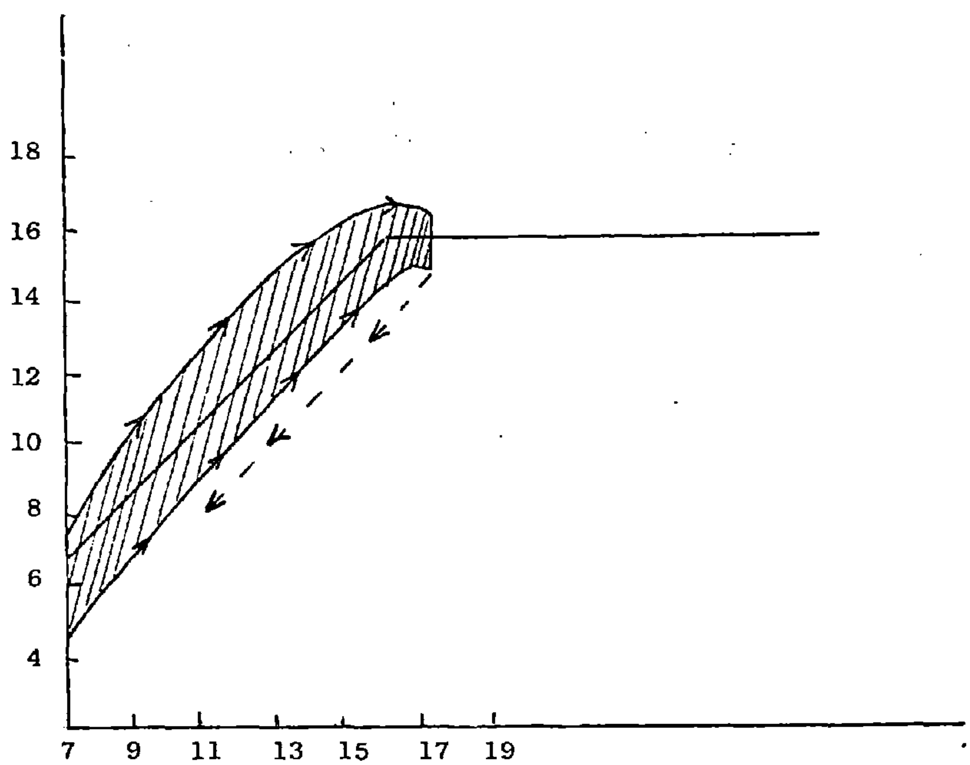

Fig. J-4 Windage Torque vs RPM with No Field Voltage demonstrate the need for linearization of the plant feed-forward gain in the control compensation. This was implemented as a look-up table composed of a 4 x 6 matrix of constants used to normalize the plant gain (Table J-1).

The upper left corner of the figure shows the low RPM curves stopping before full throttle which records the onset of engine knock or lugging. The lowest point of all curves represents that point at which the engine torque was equal to the dynomometer windage torque and the point at which the dynomometer field voltage went to zero with the engine no longer able to sustain the desired speed. A more accurate measurement of dynomometer windage was required to compensate for speed controller "drop-out" (as will be discussed), and so a FORTRAN program was written which would construct a table of torque vs. RPM from 700 RPM to 2500 RPM averaging a large number of torque readings after the RPM had settled to a steady state value. In this test the throttle was indexed manually with the speed controller defeated. The result of this table is represented by the band in Fig. J-4.

The droop in the curve at 1600 RPM is accounted for by reduced bearing friction with frictional heating at higher RPM. There is, in fact, hysteresis in the curve, as represented by the dotted line, when reducing RPM after several minutes at sustained high RPM. A functional representation of this data was approximated as:

$$T(RPM) = \frac{RPM}{100} ; \quad 0 \leq RPM \leq 1600 \qquad \text{(J-5)}$$

$$T(RPM) = 16 ; \quad 1600 < RPM .$$

The analog speed controller implemented a high gain, integral compensation to obtain accurate regulation with zero steady state error and rapid disturbance recovery. The controller exhibited nonlinearity and saturation resulting in instability for large step inputs or operation at low torque. Loop gain increased with RPM: a nonlinear characteristic of the dynomometer. A simple dynamic model for the dynomometer with the speed controller is shown in Fig. J-5. A brief discussion of the speed

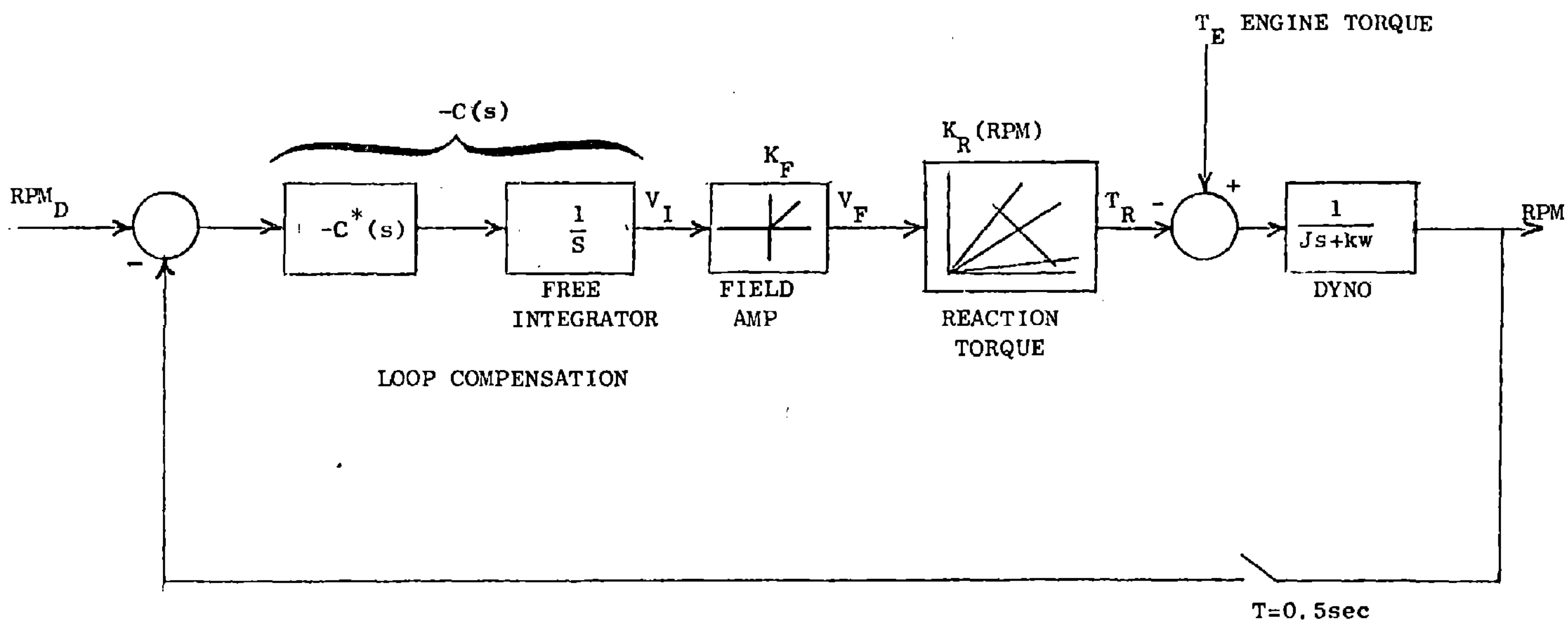

Fig. J-5 Nonlinear Dynamic Model of Speed Controlled Dynomometer controller will aid in understanding important total system nonlinearities which must be compensated in the final controller.

In Fig. J-5, $C^*(s)$ and the integral term, 1/s, represent the dynamic compensation. The minus sign emphasizes the sense of the loop gain while the integral term is to emphasize the free integrator in the loop with V_I as the output voltage of the integrator. K_F represents the gain of the field voltage amplifier for which the output is constrained to positive values (this is because the dynomometer cannot be switched from generating to motoring while in motion). As discussed earlier, the stable response of reaction torque, T_R, to the field voltage, V_F, is a positive function. The factor which relates these, K_R, varies with RPM. The engine torque, T_E, may be modeled as biased process noise in a simple, dynamically uncoupled model. The dynomometer here is modeled as a single pole. The tachometer update rate, T = 0.5sec, is the limiting factor in maximum system bandwidth.

The combined effect of integral control and the positively constrained field voltage results in controller "drop-out," and sustained oscillation in low torque operation. Figure J-6 shows the dynamic effect of controller drop-out, which is attributable to the unclamped, negative-voltage output of the integrator. Digital compensation of the above behavior will be discussed in the section on nonlinear compensation.

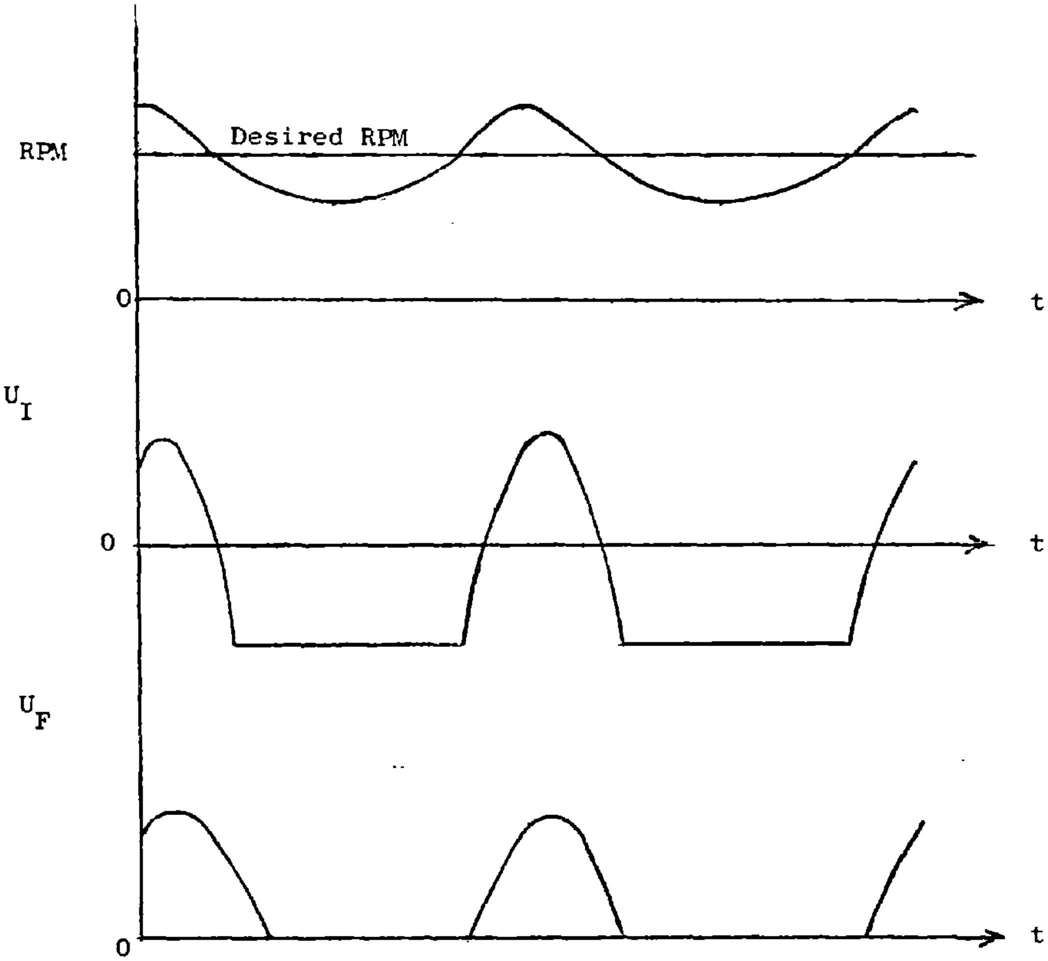

Fig. J-6 SPEED Controller Drop-Out

5. Simple Controller

a. Model

It should be apparent from the previous discussion that within a certain operational envelope the engine/dynomometer system, with speed controller, is essentially open loop stable. That is to say, with bounded inputs,, the outputs will remain bounded, although the static and dynamic relationship between input and output will be nonlinear.

A primary requirement of the torque controller is that the steady state error between measured engine torque and command torque be zero. To do this requires a controller which adds a pure integrator in the feed forward path, making the open loop system unstable, then adding appropriate compensation with feedback to obtain desired dynamics.

As a real and physical system, this was not one that lent itself to analytical, dynamic analysis. A wide variety of dynamic models could be constructed to approximate the system dynamics. These might range from a paired linear, first order, uncoupled plant to a nonlinear, high order, multi-input, multi-output plant.

The selection of a model is dependent upon the specifications of the controller, primarily bandwidth and damping factor. Generally we need not be overzealous in selecting a complex model if the specifications are relatively loose. Additionally, until some form of system response data has been obtained, it cannot be known in advance if the effort to obtain the data will be warranted, given that a controller based on the simplest model might suffice.*

Since the specifications for control were loose, the controller based on the simplest model, once "tuned" to the system, provided adequate controlled response for all engine tests. This controller will be discussed only briefly. Because this relatively complex dynamic system provided the opportunity to apply some innovative digital compensation, a multivariable controller based on a nonlinear, high order, coupled model

---

*As an aside: a substantial benefit of digital control is that to go from a simple controller to a complex one requires only a change in software; additionally, the computer enables one to obtain the system response data.

was developed which would seek to obtain higher bandwidth and compensate for the undesirable features of the dynomometer speed controller.

b. Control

In the analysis for the simple controller, the plant is trans ferred from the linear, first order continuous model

$$\frac{T_E(s)}{\theta_t(s)} = \frac{K_E}{s+a} \tag{J-6}$$

to the discrete representation

$$\frac{T_E(Z)}{\theta_t(Z)} = \frac{K_E'}{Z-e^{-aT}} \tag{J-7}$$

by means of the zero-order hold and Z transform. In the above, "a" represents the plant time constant which will be only roughly estimated. The gains K_E and K_E' are related by a constant and are both functions of torque and RPM. The analysis to find C(Z), the digital compensation, is most easily done in the Z plane. Note that system time constants have not yet been determined and that all values will be rough estimates. The break frequency for the digital torque filter is based on the knowledge that aliasing will occur in the torque measurement, yielding an apparent subharmonic of the torque impulses which were to be filtered. As the engine RPM varies, the apparent pulse frequency will vary from 0 to 5 Hz with a maximum amplitude of approximately 2 ft-lb. It was felt that a digital filter with a 1 Hz break-frequency would be effective at reducing the amplitude of the torque impulses as the subharmonic frequencies of the dominant structural modes were all greater than 4 Hz (see Fig. J-2.

In Fig. J-7 the plant is represented by a single pole. It is conceivable that the location of this pole could migrate as a function of torque or RPM. Thus, in running tests to determine the appropriate location for the compensation zero, the data must be taken as a function of torque and RPM.

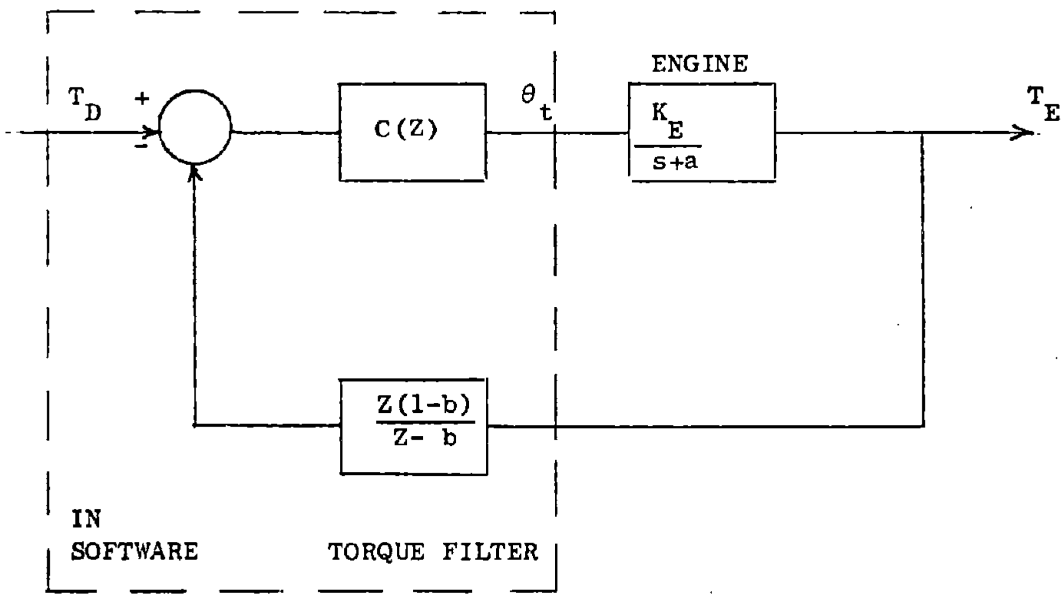

Fig. J-7 Simple Model Used for Torque Control

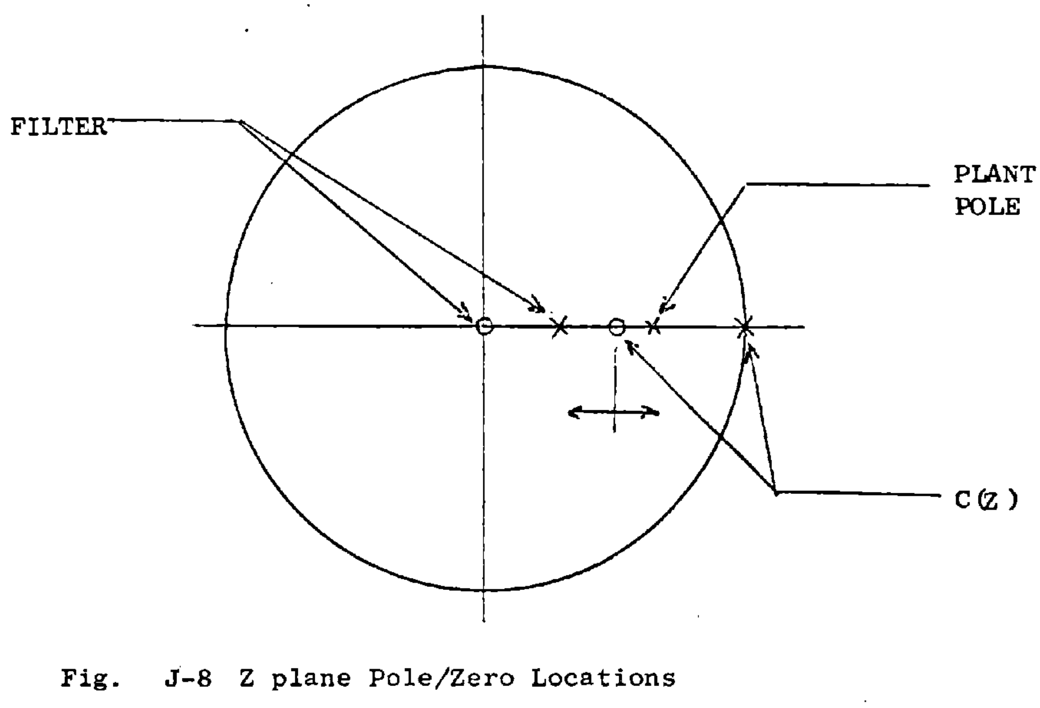

Fig. J-8 Z plane Pole/Zero Locations

Figure J-8 shows the open loop pole/zero locations of the plant, filter and compensation. A representative Z plane root locus based on the simple model is illustrated in Fig. J-9. The reader should note there is no scale with Fig. J-8 nor Fig. J-9, as they are intended to generate a feeling for the dynamics rather than represent an analysis.

Fig. J-9

Z-Plane Root Locus for Simple Controller (estimate for non-linear system)

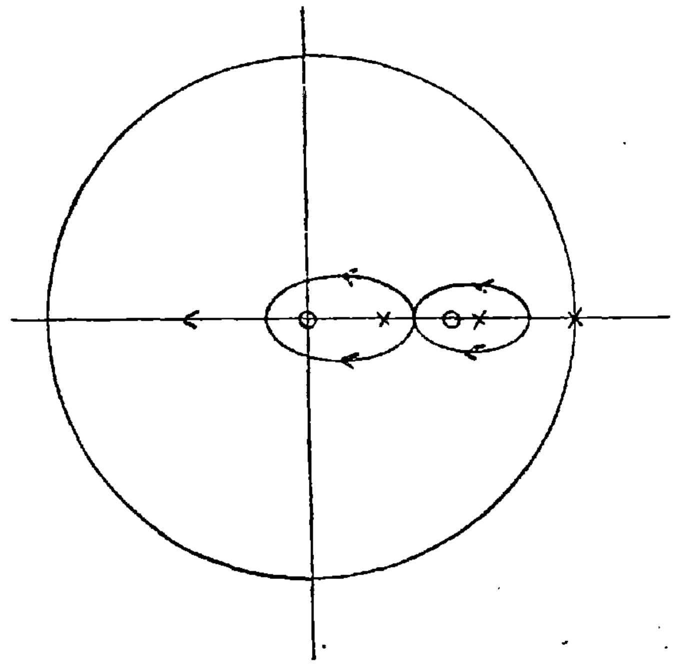

A FORTRAN program was written which accepted inputs of variable loop gain and compensation zero location. Using this program the controller was fine tuned at nine operating points to obtain the fastest torque response to a step input while maintaining an equivalent minimum damping ratio of 0.3 for small ($\leq$ 10 ft-lb) steps. It was found that a constant compensation zero location was adequate over the entire range while a look-up table of loop gains was necessary.

The actual speed of response of the controller depended to some extent on the operating point but typical was a 15-20 sec rise-time to a step. Loop gains which might lead to faster response either created a totally unstable response to steps of greater than 10 ft-lb or would not settle out in steady state. Using this controller in the torque loop, control of RPM was left completely to the analog speed controller, with the computer issuing static speed commands. Commands for slower speed were responded to rapidly with a large increase of field voltage.

Commands for higher speeds were slow: as the field was removed, measured torque goes to windage level and the engine slowly increases in speed. To complete this controller and enable an operator to issue large torque and RPM commands, a subroutine was implemented which converted step inputs from the terminal into ramp commands, with limiting slope, for the controller.

The final form of the torque control was:

$$C(Z) = \frac{P_{GAIN}(Z-.9)}{(Z-1)} \quad , \qquad (J-8)$$

yielding a control algorithm of

CONT = CONT + GAIN*(1.1*ERROR - OERROR)

where "CONT" is the control output (throttle position in degrees), "ERROR" is the present measured error (torque in ft-lb), and "OERROR" is the past error. The look-up table used for the gain compensation is shown in Table J-1.

RPM \ TORQUE (ft-lb)	0	20	30	50	70	90
0	.0413	.0596	.0456	.0304	.0304	.0304
1000	.0388	.0456	.0337	.0456	.0517	.0775
1500	.0272	.0310	.0408	.0470	.0517	.0775
2000	.0155	.0235	.0250	.0258	.0554	.0775

TABLE J.1 Look-up Table for Nonlinear Gain Compensation.

6. Multivariable Controller

a. Theory

To improve the speed response while increasing the system stability it was necessary to study in greater detail the dynamic coupling of the torque and RPM loops. Additionally, greater effort was to be made in compensating for the system nonlinearities while improving the "large step" response of the speed controller.

A model of the open-loop, coupled system is shown in Fig. J-10. This model displays the relative dynamic interaction of the system components based solely on known physical interconnections, but assumes no knowledge of time constants, delay times or feed forward gains.

Conceivably a somplete linear multivariable controller with state feedback, which would decouple the torque and RPM modes, could be constructed if an adequate linear model, as a function of operating point, could be generated over the entire operating range. In this controller, the dynomometer speed controller is viewed as a servo, much the same as the throttle servo.

Certain hardware limitations and system nonlinearities prevent the implementation of a linear, multivariable controller with state feedback from a practical standpoint:

1. The RPM command input to the speed controller was limited to an incremental resolution of 10 RPM. Depending on the operating point, a step of +10 RPM could result in a measured torque "impulse" of 30-60 ft-lb. Time modulation of the RPM command input would reduce this effect, but would be costly in CPU time.
2. Storage of the state transition and control gain matrices as a function of torque and RPM would require matrices of 4 and 3 dimensions respectively to attempt linearization about appropriately spaced operating points. Given the real complexities and dubious results, this procedure seemed ill-advised.

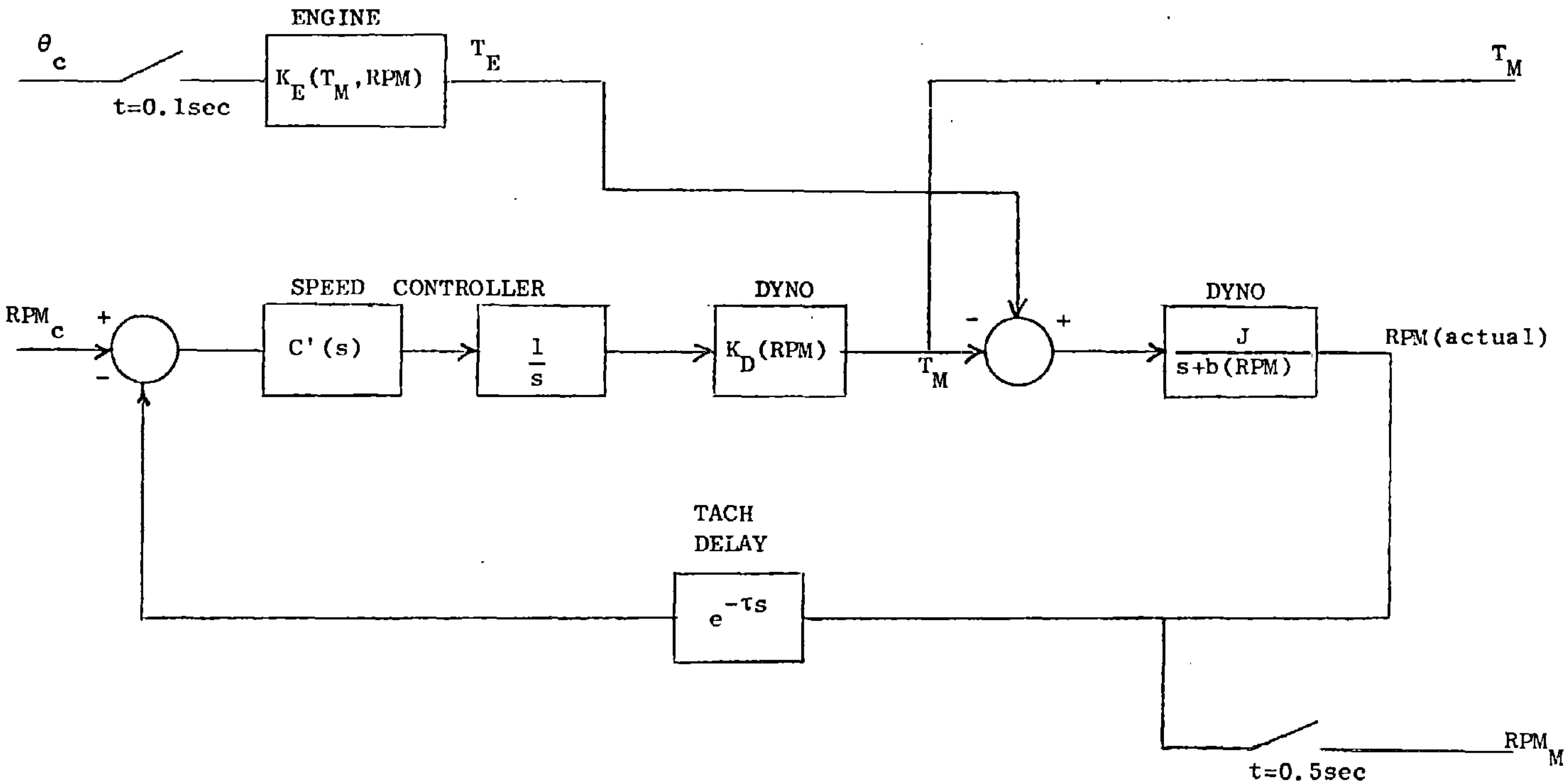

Fig. J-10 Open-Loop, Coupled System-Engine/Speed Controlled Dynomometer

What remains useful for control are the following:

$$T_M(s) = H_E(s) \cdot \theta_c(s) \quad , \qquad (J.9)$$

$$RPM_M(s) = H_1(s) \cdot \theta_c(s) \quad , \qquad (J.10)$$

$$RPM_M(s) = H_2(s) \cdot RPM_c(s) \quad . \qquad (J.11)$$

The control objective is now to find $H_E(s)$, $H_1(s)$, and $H_2(s)$, and to construct three linearized controllers which can be superposed to approximate a linear multivariable controller. The controller will minimize undesirable coupling of system modes while increasing damping and bandwidth. The objective is left general in that the real objective was to determine to what degree both damping and bandwidth could be increased while consuming a minimum of CPU time.

b. Control Analysis: Step and Frequency Response

Using the open-loop system of Fig. J-10, a sinewave was injected onto a constant throttle setting, θ_c. The sinewave was synthesized in software and added to θ_c. The torque response, $T_M(s)$, was recorded on a strip chart recorder and the test was repeated for a range of operating points, thereby generating the necessary frequency response data.

Tests for the response of $T_M(s)$ vs $\theta_c(s)$ were made at low power (1400 RPM and 25 ft-lb), and at high power (2000 RPM and 65 ft-lb). The delay time taken from step response tests, was the same for each, $\tau = 0.5$ sec. The delay was modeled by the bilinear, Pade approximation:

$$\frac{(1-\tau s)}{(1+\tau s)} \quad .$$

The magnitude portion of the frequency response yielded, in the low power case:

$$\frac{7.54}{(s^2+0.583s + 0.973)} \quad ,$$

and in the high power case:

$$\frac{4.61}{(s^2 + 0.5s + 1.5s)} \quad .$$

Thus, with delay:

$$H_E(s)\Big|_{Low\ Power} = \frac{-7.54(s-2)}{(s^2 + 0.583s + 0.973)(s+2)} \qquad (J.12)$$

$$H_E(s)\Big|_{High\ Power} = \frac{-4.61(s-2)}{(s^2 + 0.5s + 1.54)(s+2)} \quad . \qquad (J.13)$$

Each of these transfer functions was transformed to the Z plane by the zero-order-hold, Z-transform:

$$H(Z) = \left(\frac{Z-1}{Z}\right)\mathcal{Z}\left\{\frac{H(s)}{s}\right\} \quad . \qquad (J.14)$$

Applying partial fraction expansion to reduce each of the s-plane transfer functions to sums of lower order elements, and a table of common Z-transforms, the following Z-plane transfer functions were obtained.

(Normalized with respect to K_E)

$$H_E(Z)\Big|_{Low\ Power} = \frac{-0.0053K_E(Z-1.2175)(Z+.8604)}{(Z-.8187)(Z^2-1.9342Z+.9434)} \qquad (J.15)$$

$$H_E(Z)\Big|_{High\ Power} = \frac{-0.0066K_E(Z-1.210)(Z+.884)}{(Z-.8187)(Z^2-1.93642+.9512)} \quad . \qquad (J.16)$$

Because the two resulting Z plane transfer functions were so similar, only one of them was used as the basis for compensation analysis.

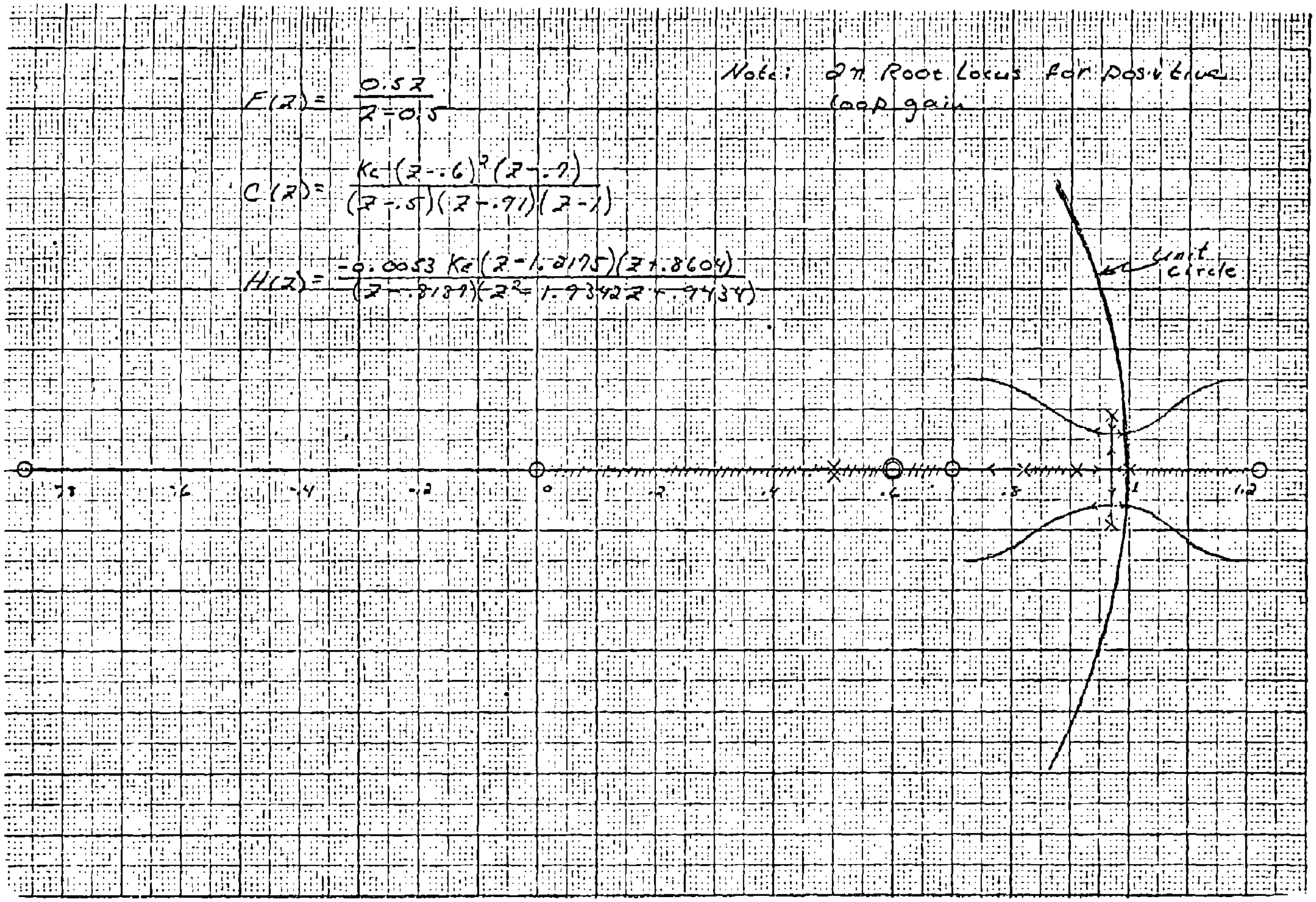

Fig. J-11 Root Locus for Torque Loop of Multivariable Controller

Figure J-12 shows the completed root-locus used for the compensation analysis.

$$\text{PLANT:} \quad H_E(Z) = \frac{-0.0053K_E(Z-1.2175)(Z+.86)}{(Z-.8187)(Z^2-1.9342+.7434)} \tag{J.17}$$

$$\text{FILTER:} \quad F(Z) = \frac{0.5Z}{Z-0.5} \tag{J.18}$$

$$\text{CONTROL:} \quad C(Z) = \frac{K_c(Z-0.6)^2(Z-.7)}{(Z-.5)(Z-.91)(Z-1)} . \tag{J.19}$$

$H_E(Z)$ is represented having a negative feed forward gain. This is a result of the non-minimum phase element used to model the delay. To stabilize this system using root-locus methods, the 360° locus is required. Thus, the reader should note this fact in reading Fig. J-12. The gain was chosen such that the closed-loop roots could be near the point where the loci meet and depart. Certainly, that the loci actually meet and depart, or deflect within some given range, as shown in Fig. J-11, is academic. The intent is that the closed loop roots will remain within a desired minimum area for the expected shift of the open loop poles, zeroes and loop gain, over the range of operation.

In determination of $RPM_M(s)$ vs $\theta_c(s)$, both the analog speed controller and the torque control loop discussed above, were active. A block diagram of the system is shown in Fig. J-12.

The frequency response test was made at a variety of operating points over the complete operating range and for various values of torque loop gain. Generally, the response changed little over the operating range, and more significantly for various values of torque loop gain. It is important to note the two different sample periods used: $t = 0.1$ sec for the torque loop, and $t = 0.5$ sec (result of tachometer update rate) for RPM loop.

The response of RPM_M to θ_c was most pronounced with PGAIN = 5 (where PGAIN is the total torque loop gain in units of DEG Throttle/ft-lb Torque), and so this value of torque loop gain was used in the following analysis.

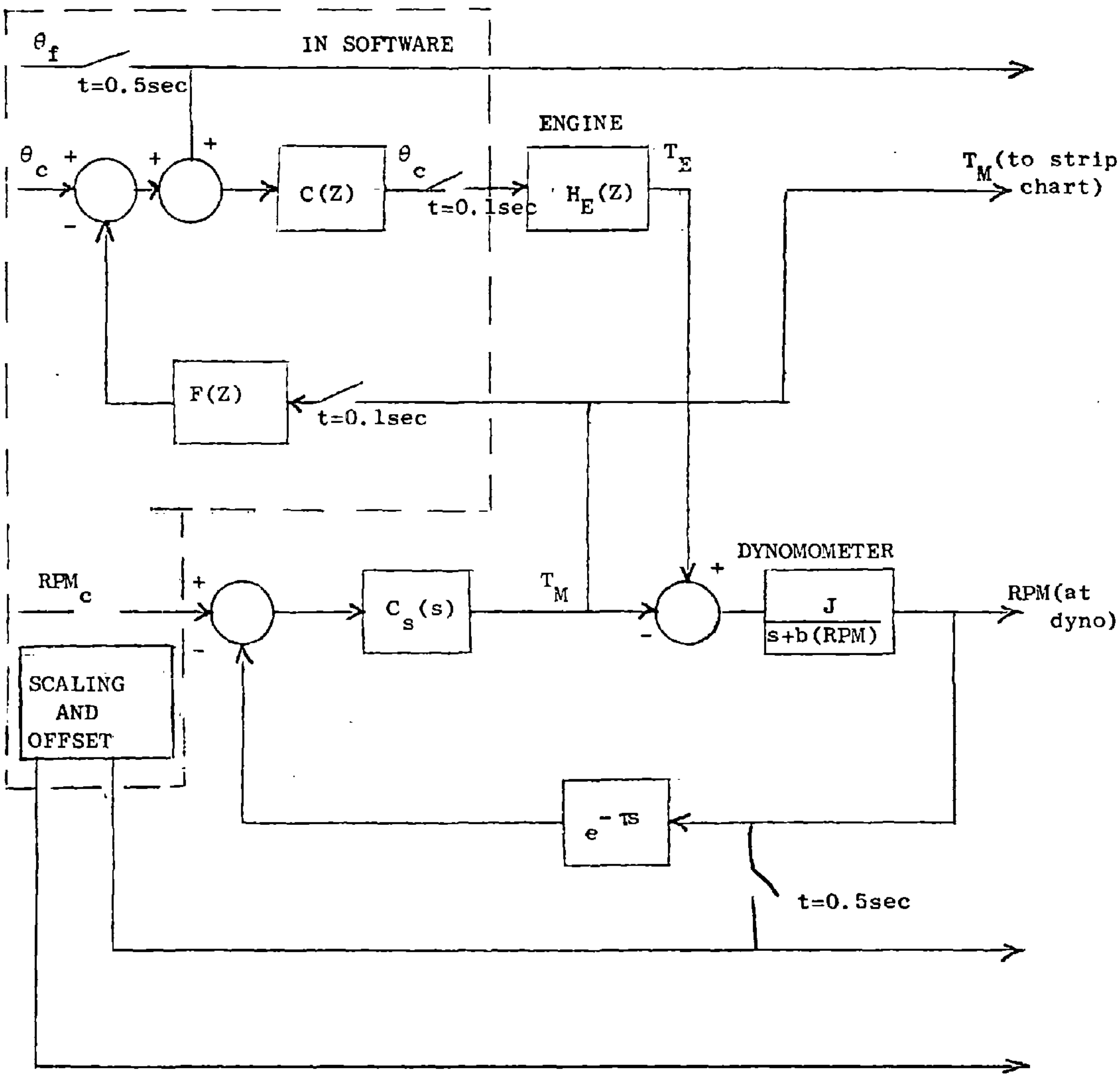

Fig. J-12 System Used to Find Frequency Response of RPM_M vs θ_c

It is of interest to note that the zero gain at DC (free differentiator) in the RPM response confirms the presence of integral control in the speed controller, but because of this it is impossible to determine the feed forward gain of the resulting transfer function. Thus, the final loop gain to be used will be determined empirically as actual response begins to match analytical data.

The step response tests showed a delay of $\tau = 1.5$ seconds. This behavior was modeled with the following bilinear Pade approximation.

$$\frac{1 - \frac{\tau s}{2}}{1 + \frac{\tau s}{2}} = \frac{-(s-1.33)}{(s+1.33)} \quad . \tag{J.20}$$

The gain response of the system yielded

$$\frac{s}{(s+.57)(s^2+.75+.77)} \quad ; \tag{J.21}$$

resulting in

$$H(s) = \frac{-s(s-1.33)}{(s+.57)(s+1.33)(s^2+.75+.77)} \quad . \tag{J.22}$$

Again using the zero-order-hold, Z-transform method of transformation to the Z plane, H(s) became

$$H(Z) = \frac{-0.05743(Z-1)(Z-1.963)(Z+.568)}{(Z-.752)(Z-.514)(Z^2-1.5462+.705)} \quad . \tag{J.23}$$

$t = 0.5$ was used as the sample period or conversion time base.

As was seen in the torque loop analysis, the delay period led to a non-minimum phase transfer function in both the continuous and discrete transfer functions, and, as before, a 360^o root locus was necessary to achieve stability. The root locus from the final compensation analysis is shown in Fig. J-13. The final compensation used was:

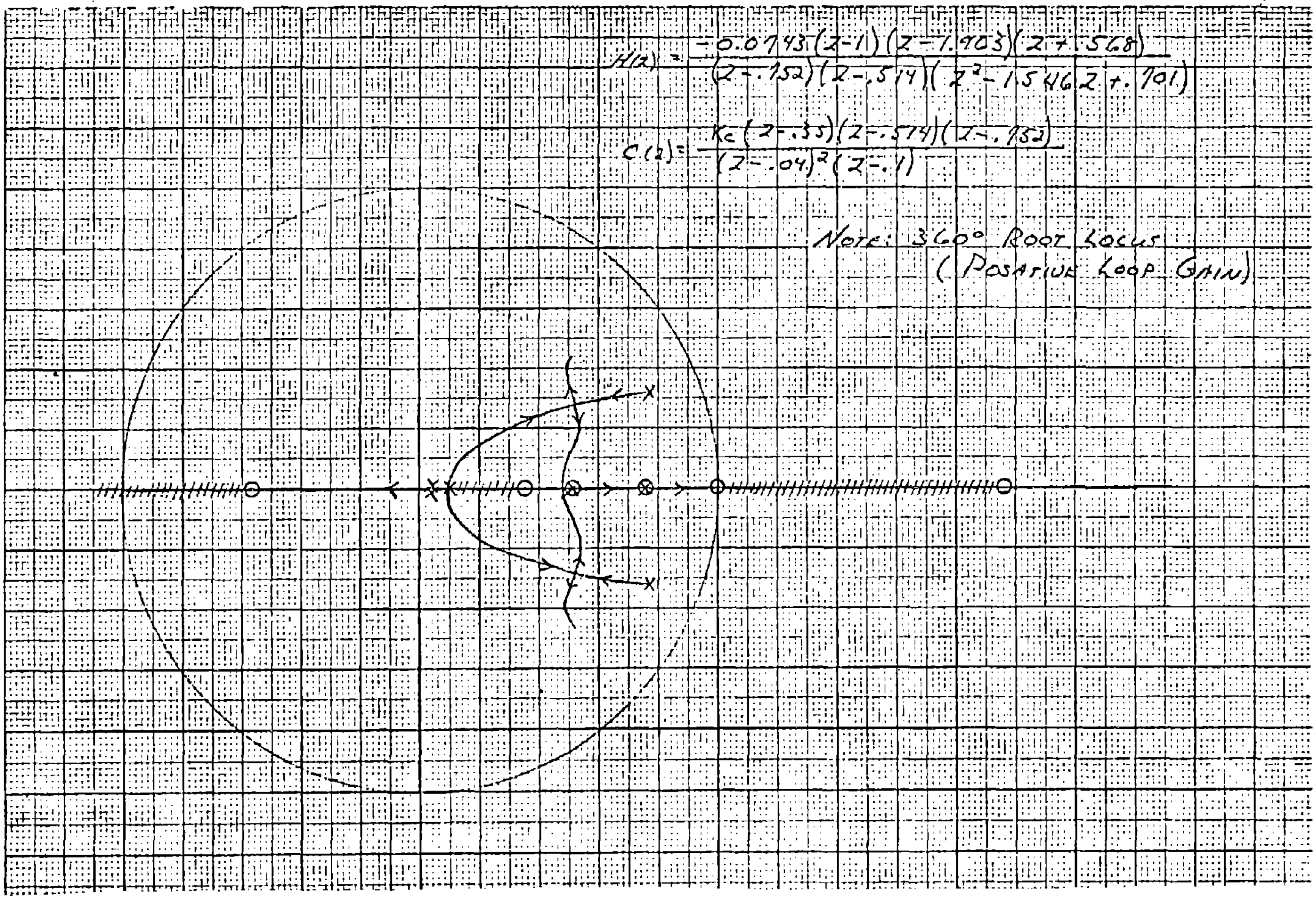

Fig. J-13 Root Locus for RPM vs θ_c in Multivariable Controller

$$C(Z) = \frac{K_c(Z-.35)(Z-.514)(Z-.752)}{(Z-.04)^2(Z-.1)} \quad . \qquad (J.24)$$

The control design intended that the closed-loop roots be located in the area of meeting/departure points of the loci. When the system is tested, the loop gain is to be increased until the expected behavior results.

c. Additional Nonlinear and Linear Compensation Required

Several solutions to the nonlinearities of the system defy analysis, falling into a class of empirical solutions. Mentioned earlier was the problem of speed controller "drop-out" when the field voltage went to zero, and T_M went to the windage value for the present speed. The cure was to ensure that the field voltage never went to zero. A simple, approximate function of windage torque vs RPM was used (see Fig. J-4) as a minimum value for T_M, and when T_M fell below this value, the throttle was opened in increments until T_M exceeded the minimum value.

As mentioned previously, the extremely high gain of the speed controller was desirable in recovering from disturbances, but was unacceptable in its step response to steps greater than 100 RPM. To make use of the first result and diminish the negative effect of the latter engine speed was effectively controlled by the throttle, using the speed controller merely as a final trim to obtain zero state speed error. This was accomplished by implementation of the multivariable controller and by delaying the issuance of RPM commands to the speed controller by 1.5 sec.

As a result of the significant lead compensation used on both the torque and RPM controllers, there was a tendency to overreact initially to step commands. While this was a stable response, it was clearly unacceptable. As a remedy, input prefilters were used for both controllers as shown in Fig. J-14.

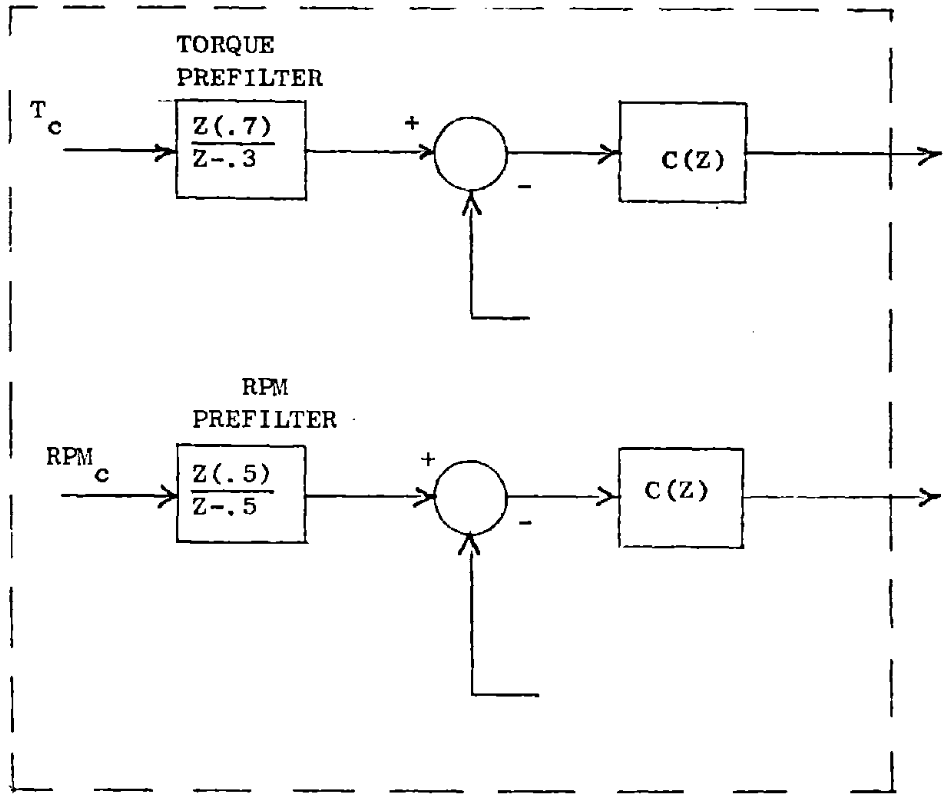

Fig. J-14 Controller Input Prefilters (Software Synthesis)

d. Controlled Response of Multivariable Controller

The following figures show the torque and RPM responses for step inputs to the controller. The traces were obtained by a multichannel strip chart recorder. The torque trace was obtained directly from the boosted output of the loadcell amplifier which was also being read by the A/D converter. The RPM trace was obtained through the computer with scaling and zero suppression, and output through the D/A converter.

The series, Figs. J-15 to J-18 show the medium power response of the controller to RPM step commands of ± 100 RPM, ± 200 RPM, ± 400 RPM and ± 600 RPM respectively. In studying these traces, it must be remembered that dynomometer torque is the control input used by the analog speed controller, thus, to increase speed the analog speed controller reduces dynomometer torque and vice versa. In Fig. J-15 when the step command is received the throttle opens, while the speed controller reduces the dynomometer torque, resulting in the initial dip in torque.

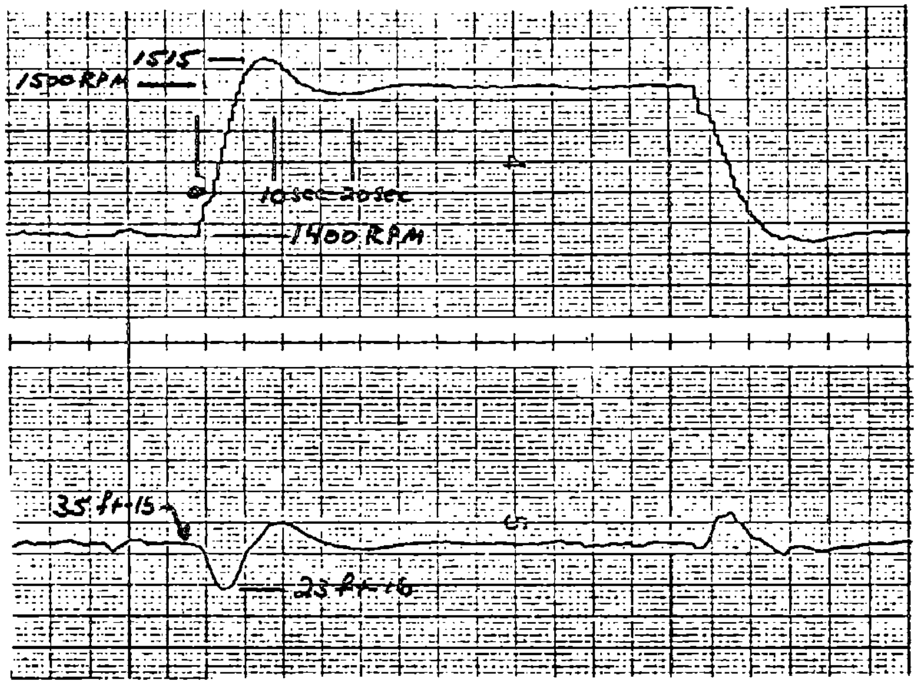

Fig. J-15 Medium Power RPM Step Response
a) + 100 RPM Step
b) - 100 RPM Step

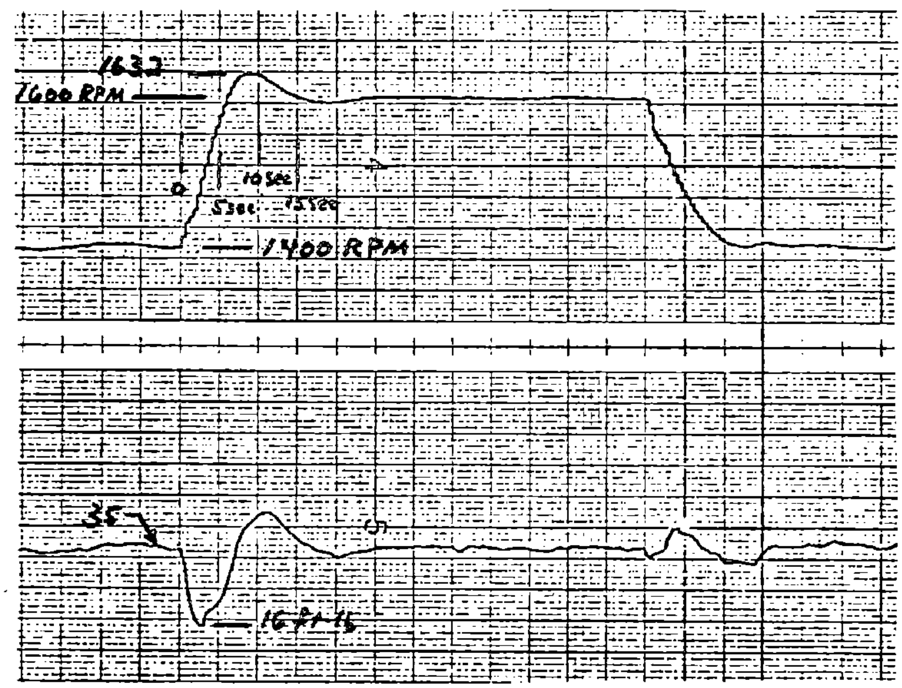

Fig. J-16 Medium Power RPM Step Response
a) + 200 RPM Step
b) - 200 RPM Step

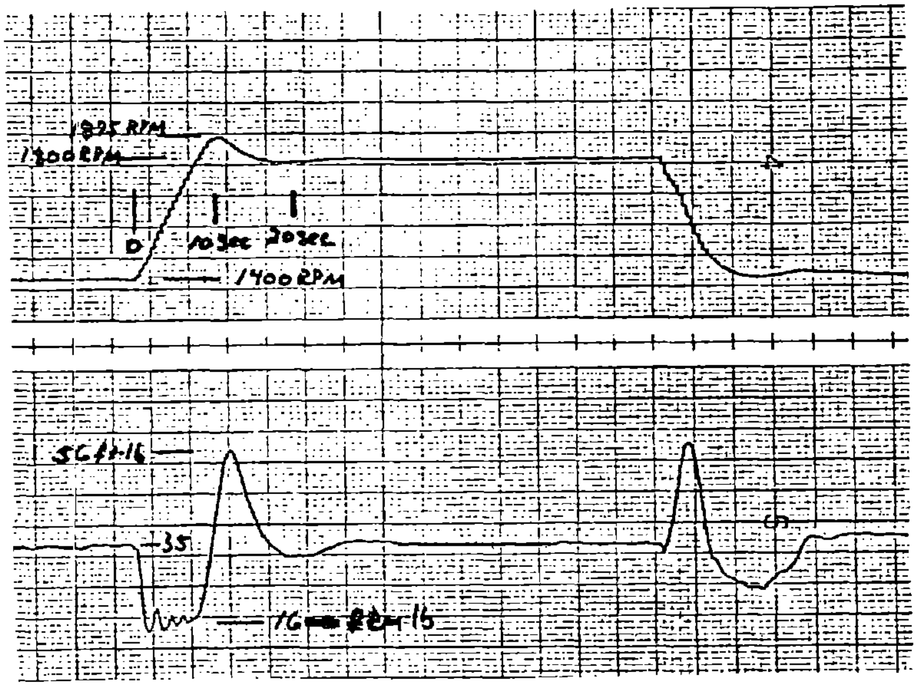

Fig. J-17 Medium Power RPM Step Response
a) + 400 RPM Step
b) - 400 RPM Step

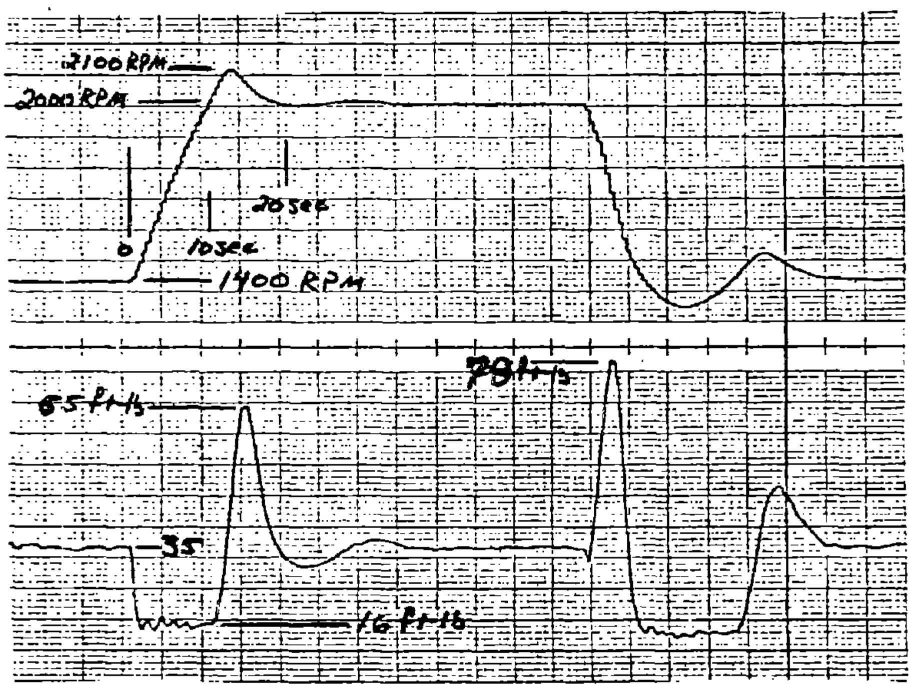

Fig. J-18 Medium Power RPM Step Response
a) + 600 RPM Step
b) - 600 RPM Step

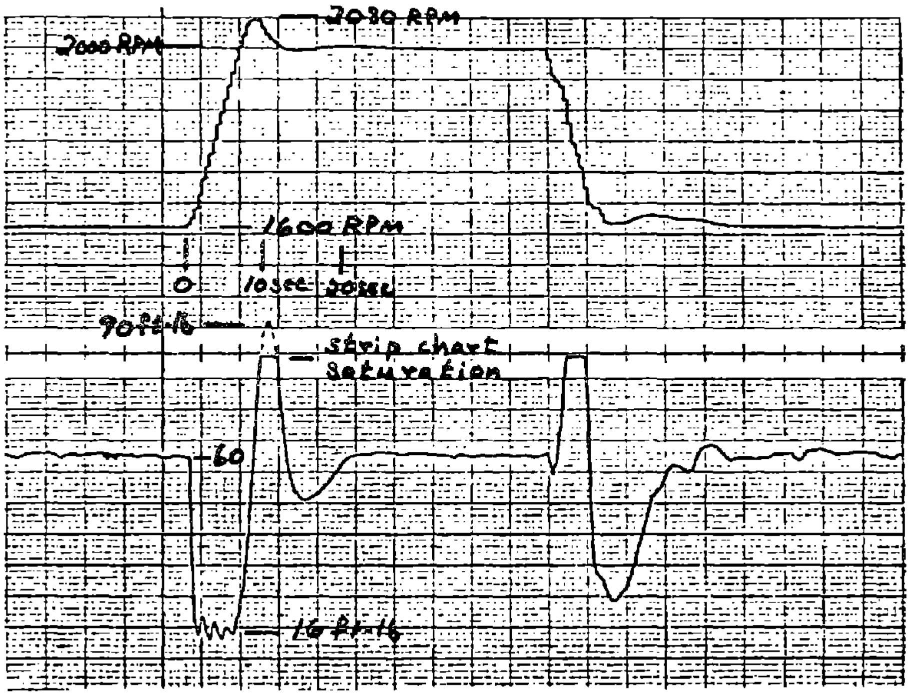

Fig. J-19 High Power RPM Step Response
a) + 400 RPM Step
b) - 400 RPM Step

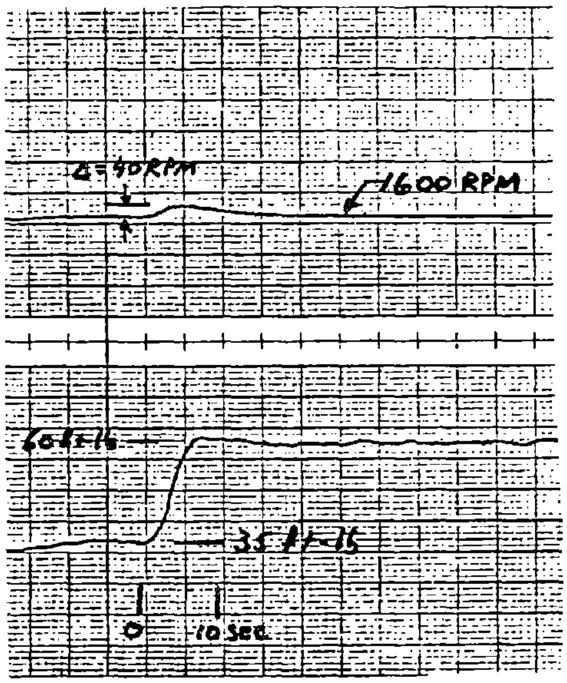

Fig. J-20 Medium Power Torque Step Response
+ 25 ft/lb Step

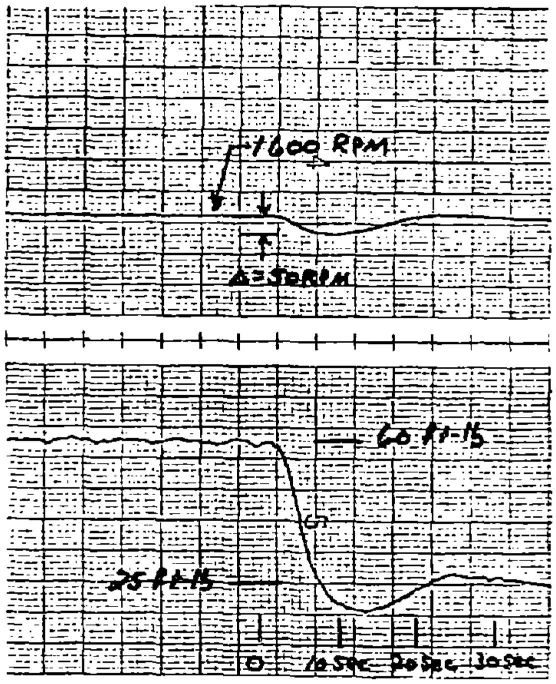

Fig. J-21 Medium Power Torque Step Response
- 35 ft/lb Step

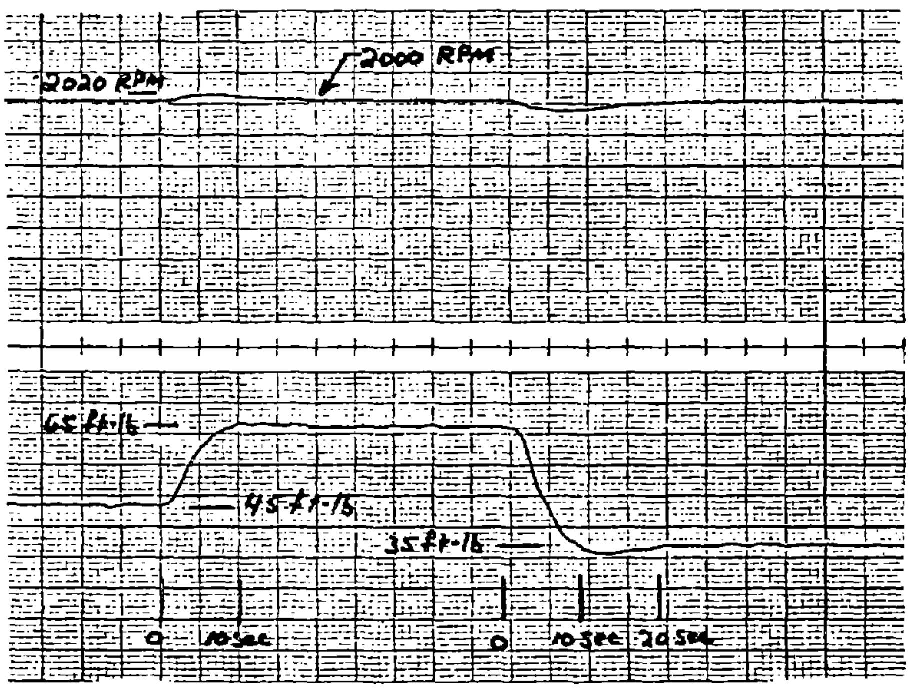

Fig. J-22 High Power Torque Step Response
a) + 20 ft/lb Step
b) - 30 ft/lb Step

As the RPM begins to overshoot, the torque correction goes positive. In Fig. J-16 the torque dip and peak became more pronounced. In Figs. J-17 and J-18 the response is substantially nonlinear. The RPM appears to have reached a slew rate limit while the measured torque has been reduced to the windage torque value. Note the pulses on the torque measurement at the windage value. These are the result of the analog speed controller "drop-out: compensation discussed in the section on Additional Nonlinear Compensation. It may be seen that the speed controller does not saturate and that the torque rises immediately to correct the overshoot.

Figure J-19 gives the response for the high power response to $\pm$ 400 RPM step commands. The result is again very nonlinear, yet stable.

Figures J-20 through J-22 display the multivariable controller response to torque step commands. Generally these figures show the very highly damped response of the system to torque commands. The system behavior for any torque step in an operating envelope defined roughly by 20 ft-lb $\leq$ Torque $\leq$ 80 ft-lb, 1000 $\leq$ RPM $\leq$ 2500 and 0.016*RPM $\leq$ Torque $\leq$ 0.045*RPM, remained quite stable and similar to that of Fig. J-20 through Fig. J-22.

7. Conclusion

As stated in general terms it was an objective of this work to attempt to increase the bandwidth and damping factor of the system while minimizing computer time and storage dedicated to control. Actual improvement factors are elusive due to system nonlinearities. Comparisons of the simple controller using ramped inputs for large and the multivariable controller give the following:

	TYPE OF CONTROLLER	
	Simple (Ramped Inputs)	Multivariable (Pure step input)
1. RPM Step Response 600 RPM step		
a) settling time	1 min	20 sec
b) rise time	1 min	10 sec
c) damping factor for equivalent 2nd order system.	0.05-0.2	0.3-0.8
2. Torque Step Response 50 ft-lb step		
a) settling time	50 sec	10-15 sec
b) rise time	50 sec	10 sec
c) damping factor for equivalent 2nd order system	0.3 - 0.5	0.3-0.7

3. CPU Storage: ~ factor of 1.5 increase for multivariable controller.
4. CPU Time: ~ factor of 1.25 increase for multivariable controller.

It is believed that the next escalation in controller complexity, using full state feedback, would result in a significant increase in computer time and storage when compared to the multivariable controller described above.

II. SERVO APPLICATION OF A MICROPROCESSOR-BASED STEPPER MOTOR CONTROLLER

1. Introduction

Frequently in industrial control problems rectilinear and angular positioning elements constitute the necessary output. In systems which use a digital computer as the central logic element, it is convenient, while not necessary, to use a digital servo.

Stepper motors, being incremental motion devices, are inherently suited to function with digital systems. A characteristic unique to stepper motors is that they may be reliably operated in an open-loop servo mode as well as the more common closed-loop mode. This inherent capability of the stepper motor is discussed in the open literature [P-2, F-2] and in the sales literature supplied by the various stepper motor manufacturers. It is a result of the finite number of magnetically detented positions available in the motor. In a servo application, elimination of the position feedback loop is a desirable simplification resulting in a substantial decrease in hardware and accompanying sensor alignment problems, But, open-loop control is not always possible: a microprocessor servo which adapts to wide variations in load by the use of position feedback around a stepper motor is discussed by Hunts, et al., [H-5].

The following system description discusses the hardware and software of an open-loop angular position servo, with a brief mention of possible modifications which can serve to generalize it to a wider variety of industrial applications. This development is an outgrowth of an academic effort on the part of the authors to maximize the use of software, exploiting the inherent value of the microprocessor in a control system application.

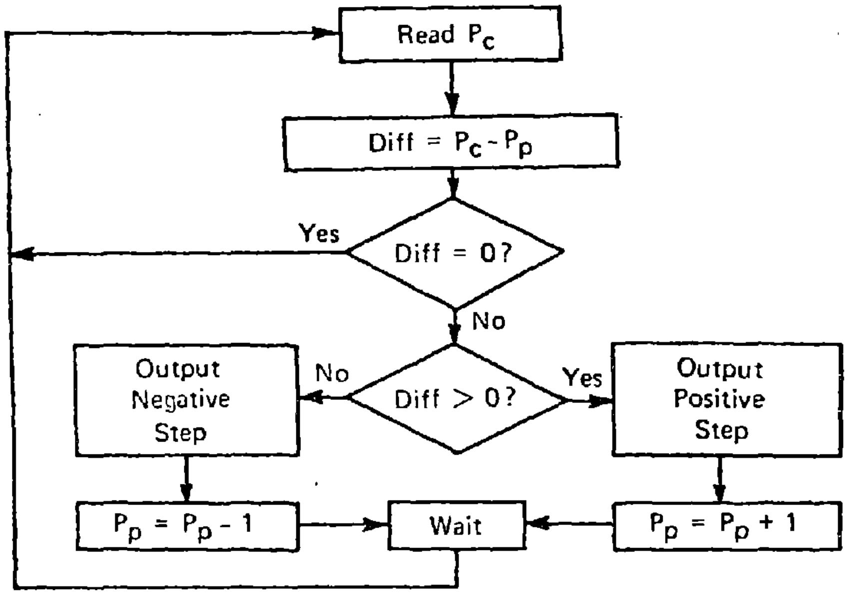

Conceptual servo flow chart

Fig. J-23

2. Tutorial

Figure J-23 is a flow diagram of the essential servo logic. READ requires the input and storing of a binary or BCD word, P_c, representing the commanded position, whose bit size is compatible with the required position range. DIFF is the differencing of P_p, a stored word which represents the present shaft position, with P_c. If the result is zero, we are there, if not, test for positive difference. If positive, command one positive step and increment P_p, otherwise command one negative step and decrement P_p. All electromechanical dynamics are compensated by the WAIT loop.

Stepper motors are available in a variety of step resolutions, e.g., 24 step/rev, 200 step/rev, 1000 step/rev, etc., maximum holding torques, rotor inertias, winding resistances and inductances. Several stepper motor manufacturers can supply a range of driver circuits matched to their motors, or the user may choose to design and build his own. The circuit (Fig. J-24 can be a simple series resistance, current limiting circuit from which one applies the motor ratings and a desired current rise time to determine the remaining circuit values. Neglecting back emf, the current obeys the simple exponential relation:

$$I(t) = \frac{V}{(R_m+R)}\left(1-e^{-\left(\frac{R_m+R}{L_m}\right)t}\right) \quad (J.25)$$

from which the following are obtained

$$V = I_{max}(R_m + R) \quad (J.26)$$

$$\tau_r = \frac{L_m}{R_m + R} \quad . \quad (J.27)$$

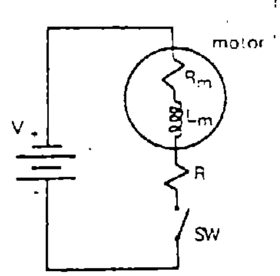

Fig. J-24 A stepper motor driver circuit.

Equally important is the current fall time which is controlled by the addition of a voltage limiter to the above circuit. Actually the switch is a solid state switch (transistor) which has a limiting open-circuit voltage (Vceo). The following equations apply:

$$\tau_f = \frac{L_m}{R_m + R + R_r} \tag{J.28}$$

$$V_{s,max} = I_{max}(R+R_r) \tag{J.29}$$

We can achieve $\tau_f < \tau_r$ easily by making $R_r > 0$, subject to $V_{s,max} <$ Vceo.

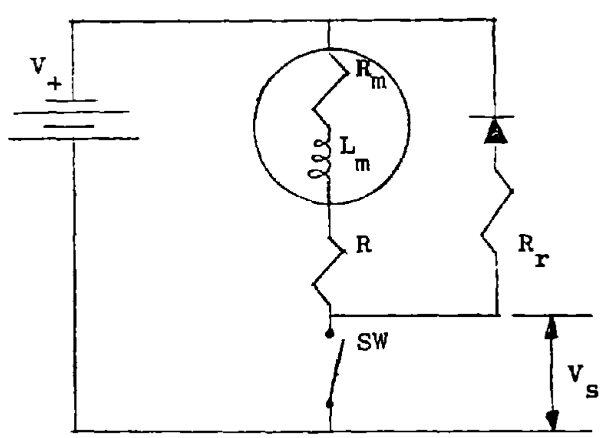

Fig. J-25 A Driver Circuit with Voltage Limiting

In systems requiring high stepping rates, L_m is chosen as small possible for the given torque requirement. Once L_m is known, R (typically a power resistor) is chosen to achieve the desired rise time and V is then chosen to obtain the steady state current. In circuits requiring fast rise times, V and R will be large and a great deal of heat will be dissipated in the series resistor R. To avoid this, slightly more complex circuits, e.g., bi-level and chopper, are a wise choice.

For the four phase stepper motor, Fig. J-26 shows the required current phasing in the motor windings for full steps and half steps. A DC level of current in one or more windings creates a significant holding torque at one position. The order in which windings are activated determines the direction of rotation.

The foregoing is offered merely as an introduction. Obviously, there is great room for creativity to efficiently achieve the desired result.

3. Servo Hardware Development

Once the servo functions are defined the major decision to be made is the trade-off between hardware and software. This is determined by the designer's relative skill level in each of these areas, development time available for design iterations, reliability requirements and flexibility desired for future modifications.

In its present application, the servo is the throttle actuator in an automated engine test system located in the Engine Laboratory of the Mechanical Engineering Department of Stanford University. During operation, it is necessary to precisely control engine torque and RPM while a variety of engine data are automatically sampled. A NOVA minicomputer is used as the master control and data acquisition computer

A desire to reduce the deadband oscillation in final engine torque output lead to a stringent angular resolution requirement.

PHASE

POSITION	A	B	C	D
1	1	0	1	0
2	1	0	0	1
3	0	1	0	1
4	0	1	1	0
1	1	0	1	0

(a) FULL STEP

PHASE

POSITION	A	B	C	D
1	1	0	1	0
2	1	0	0	0
3	1	0	0	1
4	0	0	0	1
5	0	1	0	1
6	0	1	0	0
7	0	1	1	0
8	0	0	1	0
1	1	0	1	0

(b) HALF-STEP

Fig. J-26 Stepper Motor Truth Tables of a Four-Phase Motor

The speed/resolution trade-off was made by selecting a 200 step/sec motor; incorporating a 20:1 anti-backlash, reduction gear; designing driver circuits for a low torque maximum speed of 2,000 step/sec and acceleration rate of 10,000-15,000 step/sec^2, yielding (with half steps available) a resolution of 0.045 degrees at the throttle and less than 1 sec for full throttle travel (80 degrees).

The position storage requirement came from the resolution and travel specifications, thus:

Storage = 80 deg. travel/(0.09 deg. per step)
= 889 steps 10 bits
Additional half steps + 1 bit .

Position storage with half steps required 11 bits, which in turn required 11 bits of input data. Output requirements included 4 BCD digits (16 bits) and four bits for motor step control. (Actually, 8 bits were used for motor step control as will be seen later.)

There is now enough information to design the system hardware. Figure J-27 is the essential system block diagram. The simple design (or with minor variations) might conceivably be used for a wide variety of applications. As will become more evident, it is the software and the interface which give this collection of hardware its unique personality, making it a position servo.

The Z-80 microprocessor was used by default because the development system which was available (Cromemco Z1) was applicable to the Z-80. With its speed and large number of internal registers, the Z-80 became also a fortunate choice at the time of this development (July 1977). By the end of the software development period a full 1k-bytes of PROM was required for program storage. Each I/O port was a single chip, 8 bit register and tristate outputs and internal control logic.

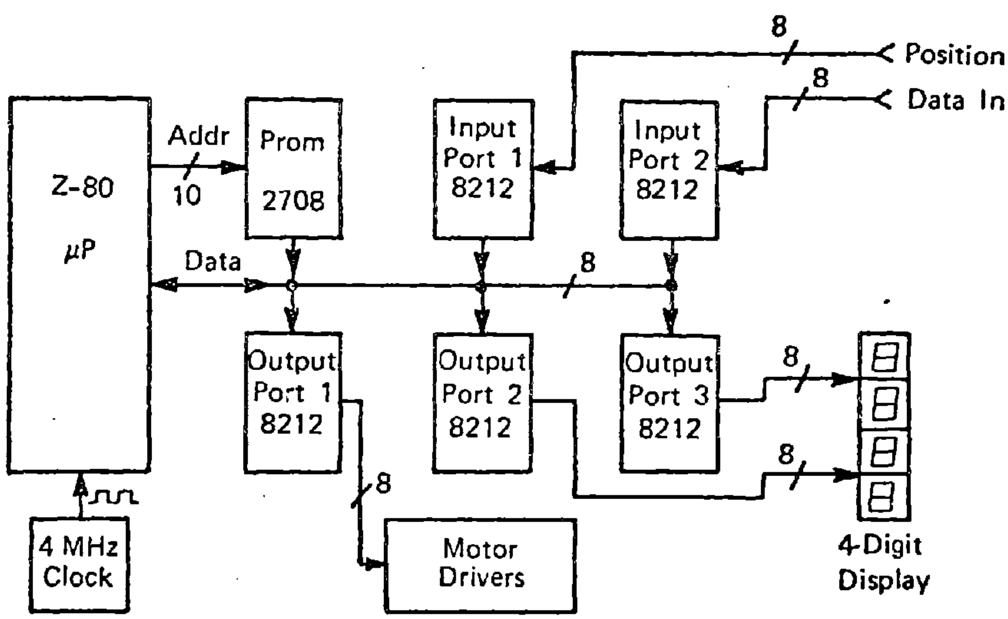

Fig. J-27 Essential Microprocessor Hardware

The input to this simple hardware from the world outside was very function dependent: (note b0 = LSB)

Position Input Data	10 bits	I port 1: b0-b7 I port 2: b0-b1
IDLE LIMIT bypass	1 bit	I port 2: b2
HALF STEP	1 bit	I port 2: b3
CLOSED LIMIT Switch	1 bit	I port 2: b4
IDLE LIMIT switch	1 bit	I port 2: b5
OPEN LIMIT switch	1 bit	I port 2: b6
IGNITION OFF	1 bit	I port 2: b7

Position limit switches were used at the carburetor as an indication of throttle open and closed limits plus an idle limit position. The mechanical idle stop was removed in favor of a software idle limit which may be bypassed if desired. The limit switches were used as reference positions to initialize the servo at start-up and also as software stops to prevent over travel.

There was also an IGNITION ON indication. This was used to prevent movement of the throttle at power-on of the servo, in the event that the ignition was on (engine running).

The only unique quality of the driver circuits was a high and low current level capability. Because the holding torque requirement was minimal, the holding current and consequently power, may be greatly reduced. This reduced heat dissipation in the driver circuits and heat build-up in the motor. Figure J-28 shows the simple interface of units: output port, driver circuits and motor, as well as the convenient use of all 8 bits to achieve the lower holding current.

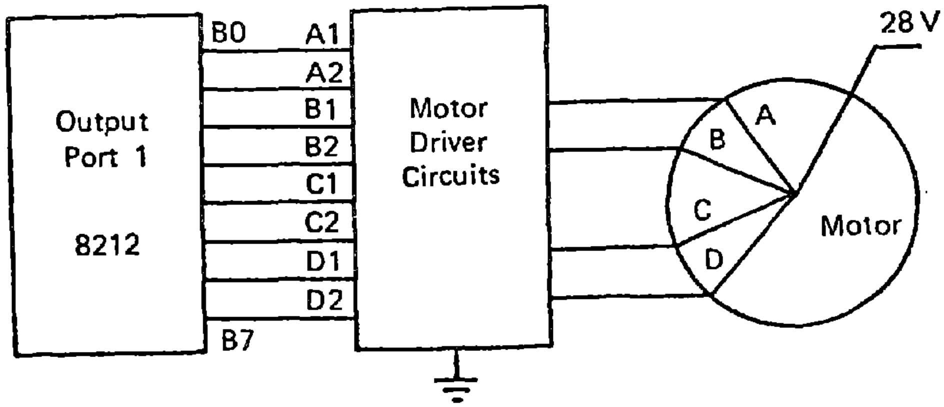

Fig. J-28 Driver Circuit Interface

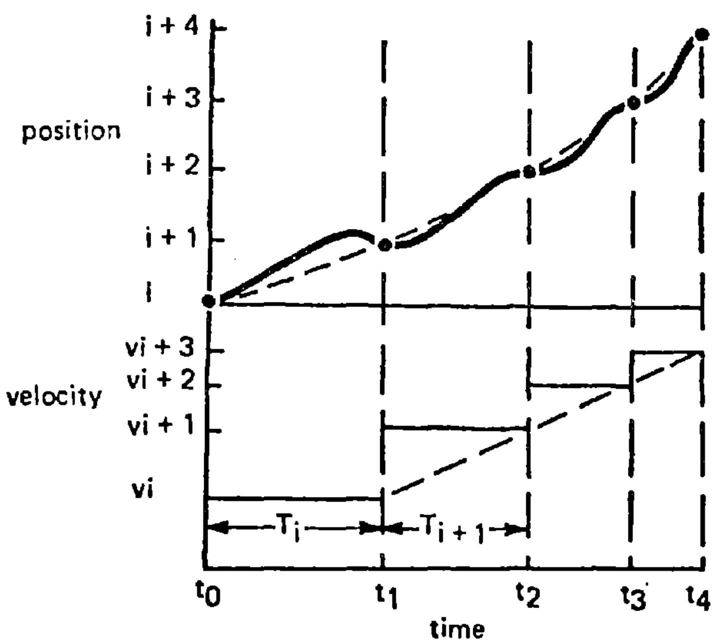

Fig. J-29 Position and Velocity for Accelerating Motor

4. Software

Figure J-29 shows an abbreviated version of the flow diagram of the servo indexing routine. Upon completion of this routing (approximatelty 10 sec) the servo position is known relative to a closed reference position; all limit switches have been tested; the throttle has been tested for binding and clutch slippage; and the motor is in low power hold, having entered the main stepping routing, ready for normal input commands. During indexing, output codes are displayed (and sent to the NOVA) to aid the operator in diagnosing possible troubles.

Before discussing the details of the main stepping routine, a brief discussion of the logic necessary to accelerate the motor is required. One should be very careful to note that due to the discrete-time nature of the issuance of step commands, determination of step timing during acceleration or decelleration is not as simple as generating a linear frequency ramp. The frequency may be incremented only at unique instants and by finite amounts. In effect, position, not time, is the independent variable.

In the plot of position vs. time in Fig. J-29 the dots represent the step positions, the dashed line is the hypothetical shaft position and the solid line represents a more probable behavior displaying the oscillatory response of the motor shaft to slewing commands. In the plot of velocity vs. time, the solid lines represent the final velocity levels and the dotted line represents an average velocity during each time interval. From the above, the following expression may be derived for the determination of the delay interval (T_{i+1}) based on the previous interval (T_i) and the step-wise acceleration (a).

$a \doteq$ stepwise acceleration (step/sec^2)

$V \doteq$ stepwise velocity (step/sec)

$$V_i = \frac{1}{T_i} \doteq \frac{1}{t_1 - t_0} , \tag{J.30}$$

$$V_{i+1} = \frac{1}{T_{i+1}} \doteq \frac{1}{t_2 - t_1} , \tag{J.31}$$

$$V_{i+1} - V_i = \frac{1}{T_{i+1}} - \frac{1}{T_i} = aT_{i+1} , \tag{J.32}$$

thus solving:

$$T_{i+1} = \frac{-1+\sqrt{1+4a(T_i)^2}}{2aT_i} . \tag{J.33}$$

These delay times would suffice for the loop times in the main stepping routine were it not for the finite cycle time of the Z-80. The CPU was driven at its maximum rate of 4MHz using a crystal oscillator. Additionally, at the time of the design, the lowest access time of any available PROM was 450 ns. Timing requirements of the Z-80, thus, required one additional clock cycle on each memory read cycle to ensure reliable data. The step timing delay was implemented by a two instruction loop:

```
TIME:  INC A        ; 4+1 clock cycles
       JP NZ,TIME   ;10+3 clock cycles
```

where the accumulator, A, was initialized by a predetermined value and incremented until overflow occurred. The INC instruction required 4 cycles and 1 memory read cycle. The JP instruction required 10 cycles and 3 memory read cycles. Thus, a total of 18 clock cycles of 4.5 μsec were needed to execute the loop. The final result was that the smallest elemental change in delay timing was 4.5 μsec.

Examples of the impact of this finite delay time on the stepwise acceleration are:

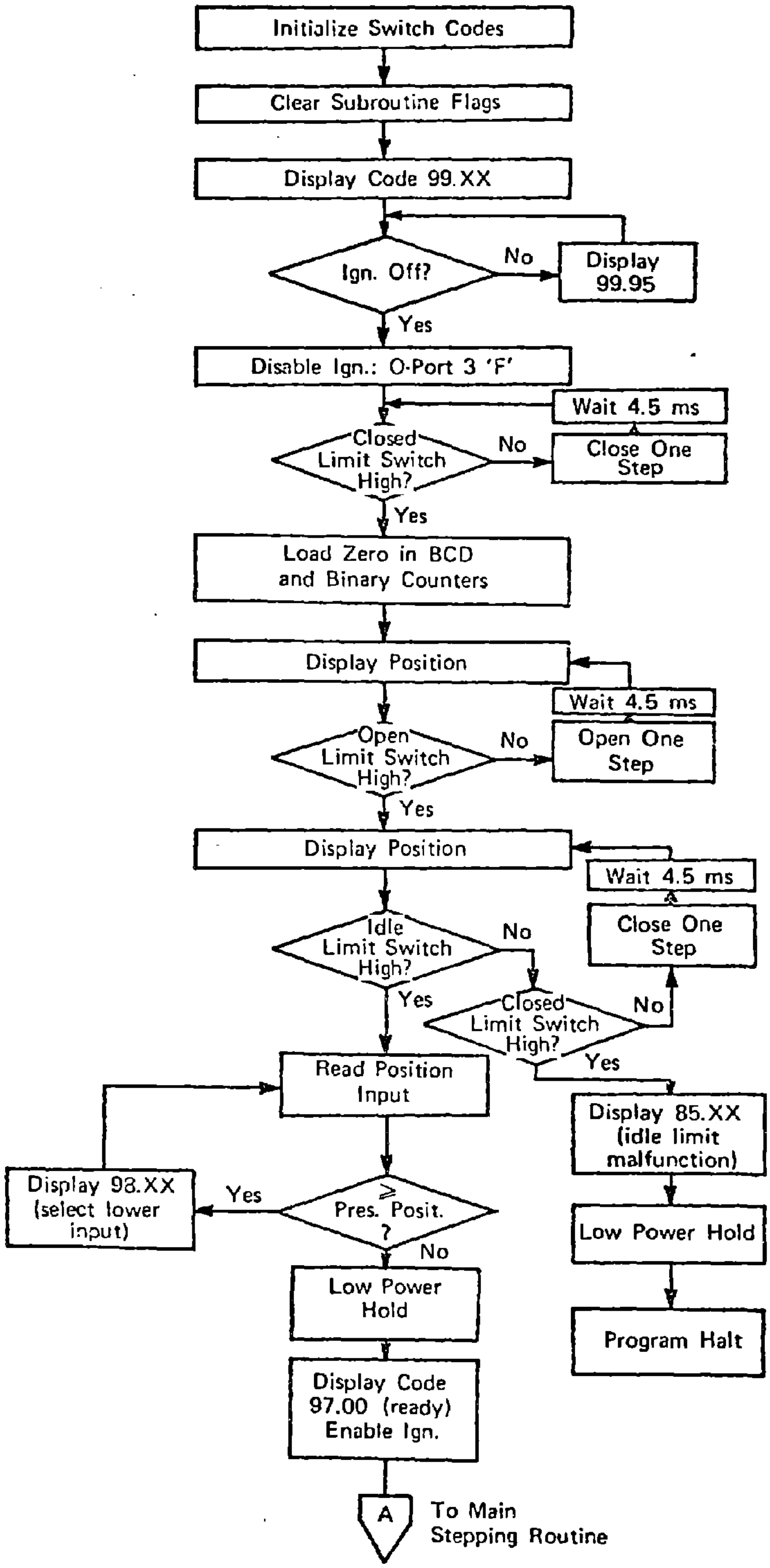

Fig. J-30 Flow Chart of Servo Indexing Routine

$$\text{step rate} = 2000 \text{ step/sec}$$
$$T = 500 \ \mu\text{sec}$$
$$\text{yields: } a = 36{,}337 \text{ step/sec}^2$$

$$\text{step rate} = 1500 \text{ step/sec}$$
$$T = 667 \ \mu\text{sec}$$
$$\text{yields: } a = 15{,}291 \text{ step/sec}^2$$

$$\text{step rate} = 1000 \text{ step/sec}$$
$$T = 1000 \ \mu\text{sec}$$
$$\text{yields: } a = 4{,}520 \text{ step/sec}^2$$

A FORTRAN program was written which made use of equation (J.33). Starting from a desired acceleration rate, initial step time, and main stepping routine execute time, it generated the stored values for the loop count, based on the 4.5 μsec interval, which would preclude an acceleration rate more than 10% above the desired value.

Figure J-31 is a portion of the three dimentional state diagram representing the structure of the states of the motor at unique instants of time. Represented are displacement and its first two discrete time derivatives.

Acceleration (A) is limited to three states. It has a magnitude of zero or the full value of acceleration in either direction. The sign of the acceleration is not that of the actual motor shaft angular acceleration but rather:

$$\text{sgn}(A) = \text{sgn}(\alpha) \cdot \text{sgn}(\omega) \quad ; \qquad \text{(J.34)}$$

where α = motor shaft angular acceleration and ω = motor shaft angular velocity.

Acceleration is represented in the main stepping routine by two bits of one register:

	b1	b0
A = -1	1	0
A = 0	0	0
A = +1	0	1

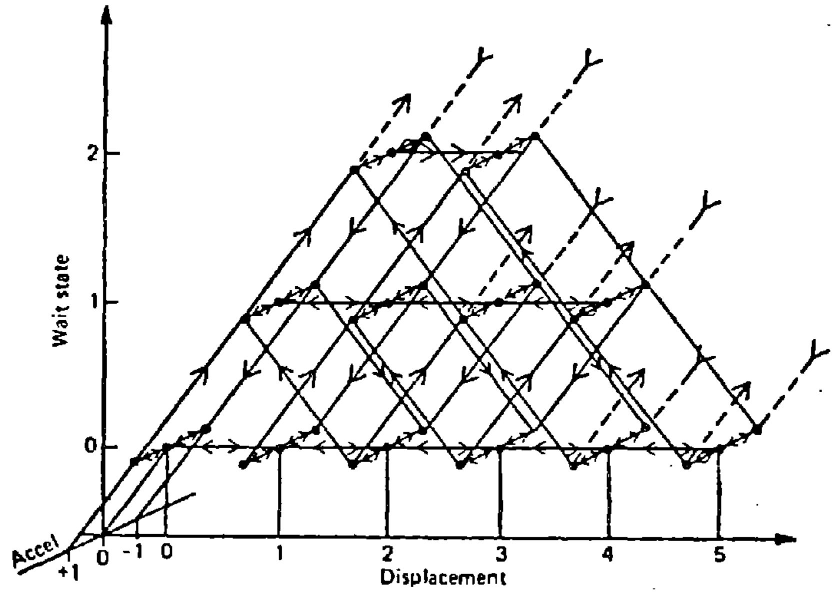

Fig. J-31 Three-dimensional State Diagram

Acceleration implies that for the next step the wait state will move to the succeedingly shorter or longer delay period corresponding to positive or negative acceleration respectively. To avoid a double value of acceleration, "A" is not allowed to go from +1 to -1, or vice-versa, without going through the zero value for at least one step period.

Shaft direction is stored independently as a distinct, one bit value.

5. <u>Main Stepping Routine</u>

A condensed flow diagram of the main stepping routine is shown in Fig. J-32 and is briefly explained here.

<u>Position Read:</u> Input data is stored in two bytes, read consecutively. The servo reads data asynchronously through its interface, thus it is conceivable that data may change during a read operation. To avoid the possibility of spurious data, input data is read twice, compared, and read again if they do not compare.

Limit Switches: A series of checks are made of the limit switches to prevent motor over-travel. The IDLE LIMIT switch is checked as well as the IDLE LIMIT ENABLE bit to create the software idle stop.

Subtract: A Desired Direction Flag (DDF) is set as a result of the value of "DIF." "A" is determined from "DIF" and the value of the present wait-state "WS." Acceleration is always based on new information. Because a finite time is involved in a transit between two positions, it is possible for the commanded position to change prior to completing a move. The servo can readily accept a command on any cycle through the main stepping routine which will take it from any state defined generally by position, "WS," and "A," to a state defined by position, with "WS" and "A" both equal to zero.

Half-Step: All stepping is accomplished by motor full steps. To double the position resolution, one motor half-step may or may not be added at the end of a move.

Direction: When "WS" is zero, Present Direction (PD) is equated to "DDF", thus this is the only time a direction change is effected.

Timing: The total loop time is composed of the execution time of the main stepping routine and the added, variable period controlled by "WS," as discussed earlier. This poses a strict timing constraint on the entire program, requiring that all paths through the program be of exactly the same number of clock cycles.

Subroutines: The subroutine call instructions of the Z-80 require the existence of RAM. It would have been impossible to confine the total program to 1K bytes of PROM without some semblance of subroutines. Three frequently used subroutines were simulated. When a call is made, a register bit is set which will be decoded by the called subroutine and associated with a unique return address. The bit is reset upon return. This technique possesses the program advantages of the Z-80 subroutine call but not its ease of use. Here the programmer is required to ensure proper decoding of the return address.

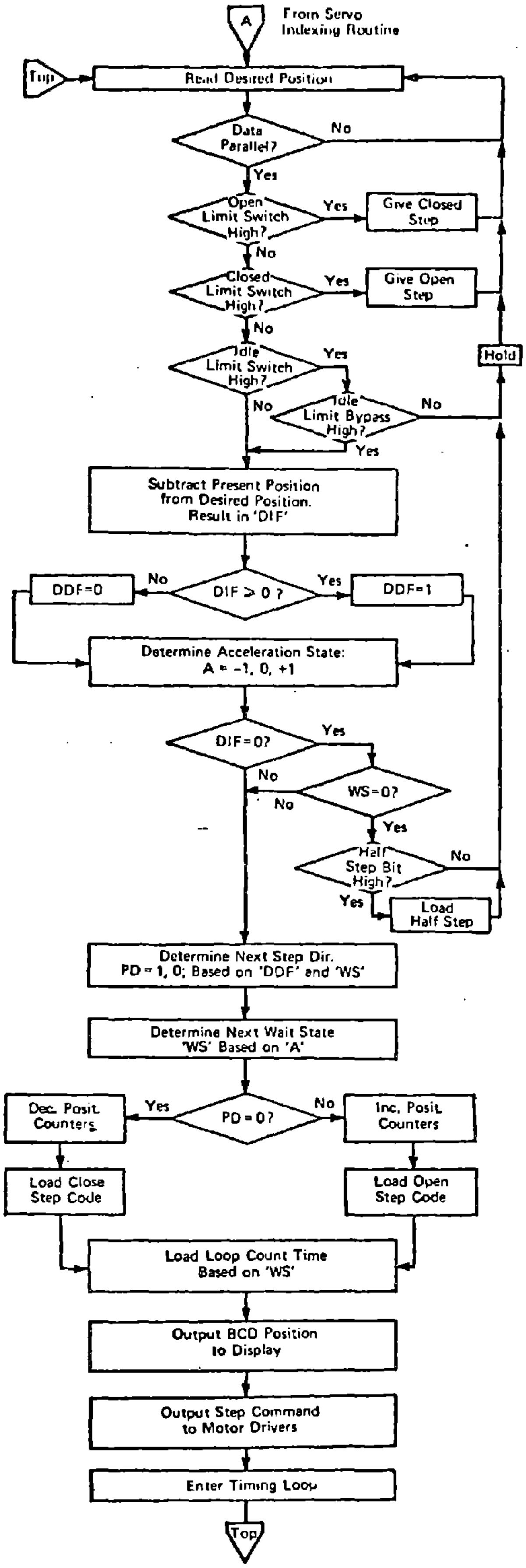

Fig. J-32

Flow Chart of Main Stepping Routine.

6. Generalizations

The above design was optimized for the intended application. It was speed limited by the combination of the storage available for the wait period data in the 1K PROM, and the discrete time element of 4.5 μsec available to create the delay periods. It was acceleration limited by the design of the motor drivers. It was position limited by the availability of internal registers and the lack of external RAM.

The maximum stepping rate limited by storage is 1,273 step/sec. with a maximum momentary acceleration of 10,949 step/sec^2. If the storage limitation were eliminated the maximum stepping rate would increase to 1,351 step/sec with an acceleration of 11,027 step/sec^2. Redesigning the driver circuits for higher acceleration would yield slightly higher maximum stepping rates, e.g., for an acceleration of 20,000 step/sec^2 the maximum stepping rate would be only 1,652 step/sec.

In systems requiring higher stepping rates, the discrete time element could be reduced to 1.25 μsec by using an external timer to generate a nonmaskable interrupt (NMI) after a HALT instruction when the delay time had elapsed. This would additionally eliminate the strict timing requirement on the main stepping routine. Increasingly shorter discrete time elements may be generated by using an external high frequency timer and external motor phasing logic to command the motor drivers, leaving the remaining tasks to the software.

To extend the servo position availability beyond 2 bytes (2^{16} positions) would require compromises in the use of the internal registers of the addition of external RAM as well as an additional input port or input multiplexing.

7. Conclusion

Hopefully the reader will agree that for a variety of applications the servo hardware can remain minimal and quite simple. Replacement of the microprocessor by MSI and SSI components would significantly increase chip count while replacing only the essential functions. Reliability and flexibility, as well as increased minor functions leading to the SMART controller, are the motivating reasons to choose software over hardware.

APPENDIX K

REPORT OF NEW TECHNOLOGY

No patents on inventions or applications for patent rights resulted from this work. However, new technologies are an outcome and are summarized in the conclusions (Chapter 6).

REFERENCES

[A-1] Auiler, J.E., J.D. Zbrozek, P.N. Blumberg, "Optimization of Automotive Engine Calibration for Better Fuel Economy Methods and Applications," SAE Paper No. 770076, Feb. 28, 1977.

[A-2] Austin, J.C., R.B. Michael and G.R. Service, "Passenger Car Economy Trends Through 1976," SAE Paper No. 750957, October 1975.

[B-1] Bailey, R.L., "An HEC-2 Low Emission Concept Car," SAE Paper No. 780206, February 1978.

[B-2] Baker, R.E., and E.E. Daby, "Engine Mapping Methodology," SAE Paper No. 770077, Feb. 28, 1977.

[B-3] BMDP - Biomedical Computer Programs - P Series 1977. Health Science Computing Facility - UCLA. University of California Press.

[B-4] Bayler, T. and L. Eder, "Impact of Diagnostic Inspection on Automotive Fuel Economy and Emissions," SAE Paper No. 780028, Feb. 1978.

[B-5] Baruah, P.C., et al., "Performance and Emission Predictions of a Multicylinder Spark Ignition Engine with Exhaust Gas Recirculation," SAE Paper No. 780663, Feb. 1978.

[BR-1] Bryson, A.E. and Y.C. Ho, Applied Optimal Control, John Wiley & Sons, 1975.

[C-1] Cassidy, J.F., "A Computerized On-line Approach to Calculating Optimum Engine Calibrations," SAE Paper No. 770078, Feb. 28, 1977.

[C-2] Currie, J.H., D.S. Grossman, J.J. Gumbleton, "Energy Conservation with Increased Compression Ratio and Electronic Knock Control," SAE Paper 790173, Feb. 1979.

[C-3] Cackette, T., P. Lorang and D. Hughes, "The Need for Inspection and Maintainance for Current and Future Motor Vehicles," SAE No. 790782, Aug. 1979.

[C-4] J.F. Cassidy, Jr., J.H. Rillings, "Transient Engine Testing by Computer Control," SAE Paper No. 720454, Society of Automotive Engineers, Inc., N.Y. 1972.

[C-5] J.F. Cassidy, Jr., "On the Use of a Computer Controlled Engine Dynomometer for the Development of Automotive Electronics," GMR-1425, General Motors Corporation, Warren, Michigan, 1973.

[D-1] Daby, E.E., private communications, March 2, 1978.

[D-2] Dohner, A.R., "Transient System Optimization of an Experimental Engine Control System Over the Federal Emissions Driving Schedule," SAE Paper No. 780286, Feb. 1978.

[DR-1] Draper, C.S., and Y.T. Li, "Principles of Optimalizing Control Systems and an Application to the Internal Combustion Engine," ASME Publication, Sept. 1951.

[E-1] EPA Report, "Advanced Emission Control Program Status Report," December 1975. Submitted by Ford Motor Co.

[F-1] Federal Register, Vol. 37, No. 221, November 15, 1972.

[F-2] Fredriksen, T.R. "Design of Digital Control Systems with Step Motors," Proc. of the Symposium on Incremental Motion Control Systems and Devices, pp.479-523, Univ. of Illinois, 1972.

[G-1] Gill, P.E. and W. Murray, "Two Methods for the Solution of Linearly Constrained and Unconstrained Optimization Problems," National Physical Laboratory, NAC 25, Nov. 1972.

[H-1] Heywood, J.B., "Cycle Simulation to Predict Spark Ignition Efficiency and NOx," SAE Paper No. 790291, Feb., 1979.

[H-2] Patterson, D.J. and N.H. Henein, "Emissions from Combustion Engine and Their Controls," Ann Arbor Science Publishers, Inc. 1972.

[H-3] Hubbard, Mont, "Application of Automatic Control to Internal Combustion Engine," Ph.D. Dissertation, Stanford University, May, 1975.

[H-4] Hosey, R.J., J.D. Powell, "Closed-Loop Knock Adaptive Spark Timing Control Based on Cylinder Pressure," Transaction of the ASME; J. Dynamic Sys., Meas. & Contr., Vol. 101, pp. 64-70, March 1979.

[H-5] B.D. Hunts, W. Kahan and J.B.S. Waugh, "An Adaptive Stepper Motor Control System," Proc. of the 20th Midwest Symposium on Circuits and Systems, pp.675-661, Texas Tech. Univ., 1977.

[L-1] Leshner, M.D., J.W. Stuart and E. Leshner, "Closed-Loop Control for Adaptive Lean Limit Operation," SAE Paper No. 780039, Feb., 1978.

[L-2] L.S. Leonard and F.E. LaVerghetta, "Dynamometer Testing under Computer Control," SAE 680131, Society of Automotive Engineers, Inc., N.Y. 1968.

[M-1] Meier, R.C., "Development of a Lean Burn/Lean Reactor through the Application of Engine Dynamometer Mapping Techniques," SAE Paper No. 770300, Feb. 1977.

[M-2] Maisel, Louis, "Probability, Statistic and Random Processes," Simon and Schuster Tech. Outlines, 1971.

[M-3] McDonald, W.R., "Feedback Carburetor Control Electronic Design for Improved System Performance," SAE Paper No. 780654, 1978.

[O-1] Ostrouchov, Nicolas, "Effect of Cold Weather on Motor Vehicle Emissions and Fuel Consumption-II," SAE Paper No. 790229, Feb., 1979.

[P-2] J.D. Pawletka, "Approaches to Stepping Motor Controls," Proc. of the Symposium on Incremental Motion Control Systems and Devices, pp.431-463, Univ. of Illinois, 1972.

[PO-2] Powell, J.D., K.W. Randall and R. Hosey, "Closed Loop Control of Automotive Engines," SUDAAR Rept. No. 509, Feb. 1978, Final Report.

[PO-3] Powell, J.D., and K.W. Randall, "Closed Loop Control of Internal Combustion Engine Efficiency and Exhaust Emissions," SUDAAR No. 503, May 1976, Final Report.

[PO-4] Hubbard, M. and J.D. Powell, "Closed-Loop Control of Internal Combustion Engine Exhaust Emissions," Final Rept. for Dept. of Transportation, DOT-TST-75-62 (also published as SUDAAR #473, Aero/Astro Dept., Stanford Univ., 1974)

[PO-5] Hubbard, M., P.D. Dobson and J.D. Powell, "Closed-Loop Control of Internal Combustion Engine Efficiency and Exhaust Emissions," SUDAAR #493, Final Report, 1975.

[R-1] Rishavy, E.A. and S.C. Hamilton, "Engine Control Optimization for Best Fuel Economy with Emission Constraints," SAE Paper No. 770075, Feb. 1977.

[R-2] Rao, H.S., et al., "Engine Control Optimization via Nonlinear Programming," SAE Paper No. 790177, Feb. 1979.

[R-3] Rao, H.S., J.D. Powell, et al., "Development and Validation of Engine Models via Automated Dynamometer Tests," SAE Paper No. 790178, Feb. 1978.

[R-4] Randall, K.W., "A Cylinder Pressure Sensor for Spark Advance Control and Knock Detection," SAE Paper No. 790139, Feb. 1979.

[S-1] Spindt, R.S., "Air/Fuel Ratio from Exhaust Gas Analysis," SAE Paper No. 650507, 1965.

[S-2] Stivender, D.L., "Development of a Fuel Based Mass Emission Measurement Procedure," SAE Paper No. 710604, 1971.

[S-3] Singh, T., "Mathematical Modelling of Combustion Process in a Spark Ignition Engine," SAE Paper No. 790354, Feb. 1979.

[SC-1] Schweitzer, P.H., C. Volz and F. DeLuca, "Control System to Optimize Engine Power," SAE Paper 660022.

[SC-2] Schweitzer, P.H., C. Volz and F. DeLuca, "Adaptive Control for Prime Movers," ASME Winter Annual Meeting, Nov., 1967.

[SC-3] Schweitzer, P.H., "Control of Exhaust Pollution Through a Mixture Optimizer," SAE Paper 720254.

[SC-4] Schweitzer, P.H., "Electronic Optimizer Control for I.C. Engine-Most MPG for any MPH," SAE Paper No. 750370.

[T-1] Taylor, C.F. & E.S.Taylor, Internal Combustion Engines., Int. Textbook Co., Scranton, Pa., revised ed., 1956.

[T-2] Trella, T., "Spark Ignition Engine Fuel Economy Control Optimization Techniques and Procedures," SAE Paper No. 790179, Feb., 1979.

[V-1] Vora, L.S., "Computerized Five Parameter Engine Mapping," SAE Paper No. 770079, Feb. 1977.

[WR-1] Wrausmann, R.C. and R.J. Smith, "An Approach to Altitude Compensation of the Carburetor," SAE Paper 760286, Feb. 1976.

[W-1] Walker, D.L., et al., "How Passenger Car Maintainance Affects Fuel Economy and Emissions - A Nationwide Survey," SAE Paper No. 780032, Feb., 1978.

[W-2] Walpole, R.E. and R.H. Myers, Probability and Statistics for Engineers and Scientists, 2nd ed., Macmillan 1978.

[W-3] R. Wellington, "Applications of Automatic Process Control to Engine Development Testing," SAE Paper No. 690227, Society of Automotive Engineers, Inc., N.Y. 1969.

[Z-1] Zeleznik, F.J. and B.J. McBride, "Modeling the Complete Otto Cycle-Preliminary Version," SAE Paper No. 770223, Feb. 1977.

185 copies